Uniwersytet Warszawski
Wydział Biologii

Rafał Piechowski
Nr albumu: 251917

Functional anatomy of *Silesaurus opolensis*

Rozprawa doktorska
w dziedzinie nauk biologicznych
w zakresie dyscypliny: biologia

Praca wykonana pod kierunkiem
prof. dr hab. Jerzego Dzika
Instytut Biologii Ewolucyjnej

Warszawa, wrzesień 2020

Oświadczenie kierującego pracą

Oświadczam, że niniejsza praca została przygotowana pod moim kierunkiem i stwierdzam, że spełnia ona warunki do przedstawienia jej w postępowaniu o nadanie stopnia doktora nauk biologicznych w zakresie biologii.

Data Podpis kierującego pracą

Oświadczenie autora pracy

Świadom odpowiedzialności prawnej oświadczam, że niniejsza rozprawa doktorska została napisana przeze mnie samodzielnie i nie zawiera treści uzyskanych w sposób niezgodny z obowiązującymi przepisami.

Oświadczam również, że przedstawiona praca nie była wcześniej przedmiotem procedur związanych z uzyskaniem stopnia doktora w innej jednostce.

Oświadczam ponadto, że niniejsza wersja pracy jest identyczna z załączoną wersją elektroniczną.

Data Podpis autora pracy

Słowa kluczowe (key words)

Silesaurus, Dinosauromorpha, archosauria, functional anatomy, Late Triassic

Tytuł pracy w języku polskim

Anatomia funkcjonalna *Silesaurus opolensis*

Streszczenie

Silesaurus opolensis Dzik, 2003 z późnego triasu (późny karnik) Polski jest gatunkiem kluczowym dla zrozumienia ewolucji wczesnych dinozaurów. Okazy *Silesaurus* dostarczają przełomowych danych na temat genezy budowy ciała dinozaurów (Smith i in., 2007; Langer i in., 2009; Martinez i Alcober, 2009; Nesbitt i in., 2010, 2017; Martinez i in., 2011, 2013; Langer, 2014), co ma szczególnie znaczenie w sporze o parafiletyczność (Langer i Ferigolo, 2013) bądź monofiletyczność (Kammerer i in., 2012) rodziny Silesauridae i o jej związek z dinozaurami ptasiomiednicznymi Ornithischia (Dzik, 2003; Dzik i Sulej, 2007; Ferigolo i Langer, 2007; Niedźwiedzki i in., 2009; Cabreira i in., 2016). Celem niniejszego opracowania jest szczegółowe zbadanie materiału *Silesaurus* i wykorzystanie zdobytej wiedzy do oceny stopnia podobieństwa z wczesnymi dinozaurami. W pracy przedstawiłem szczegółową anatomię szkieletu pozaczaszkowego i niektóre aspekty anatomii czaszki *Silesaurus*. Otrzymane rezultaty pozwalają na rekonstrukcję morfologiczną i oszacowanie zakresu zmienności cech szkieletowych.

Znalezisko częściowo artykułowanego szkieletu *Silesaurus* z czaszką, szyją, pasem barkowym i klatką piersiową, uzupełnione danymi z izolowanych okazów, umożliwiło pełne odtworzenie kręgosłupa i związanych z nim części szkieletu. Żebra szyjne *Silesaurus*, zachowane w pierwotnym położeniu, układają się równolegle do szyi i rozciągają do tyłu na kilka długości kręgów. Za siódmym kręgiem następuje nagła zmiana ich morfologii, pomimo że zmiana pokroju kręgów w odcinku szyjno-grzbietowym jest stopniowa. Parafizy stopniowo migrują w górę wzdłuż przedniej krawędzi trzonów kręgowych i opuszczają je na szóstym lub siódmym kręgu tułowiowym. Zwężenie grzbietowych końców wyrostków kolczystych czwartego i sąsiednich kręgów sugeruje zdolność tego regionu kręgosłupa do zginania się w górę. Istnieje zatem różnica między strukturalnym a funkcjonalnym przejściem szyi w klatkę piersiową. Obecność trzech kręgów krzyżowych, mocno zespolonych żebrami z kośćmi biodrowymi, a także długi ogon *Silesaurus* stanowiący przeciwwagę dla ciężaru przedmiednicznej części ciała, sugeruje zdolność do szybkiego, dwunożnego biegu. Długie, choć delikatne, kończyny przednie *Silesaurus* wskazują jednak na postawę czworonożną.

Powszechnie przyjmuje się, że ornithodiry (gałąź ptasia) i niektórzy przedstawiciele pseudosuchów (gałąź krokodylowa) osiągnęli w pełni wyprostowaną postawę kończyn w odmienny sposób. Ornithodiry mają tylne kończyny podciągnięte pod tułów wskutek zgięcia kości udowej tak, że wchodzi ona bocznie w pionowo ustawioną panewkę stawu biodrowego,

podczas gdy niektóre zaawansowane pseudosuchy mają tylne kończyny ustawione pionowo pod obróconą w dół panewką tego stawu, bez zgięcia kości udowej. Analiza aparatu mięśniowo-szkieletowego *Silesaurus* podważa ten pogląd. Ten ornitodir miał kończyny tylne ustawione pionowo pod skierowaną w dół panewką stawu biodrowego, jak niektóre pseudosuchy. Można to traktować albo jako cechę pierwotną (plezjomorfię), albo jako stan przejściowy między kończyną wczesnych dinozauromorfów kontrolowaną przez mięśnie przywodziciele, a podciągniętymi pod tułów tylnymi kończynami dinozaurów z zagiętą kością udową. Taka właśnie sekwencja zmian jest wspierana przez tropy zwierząt z linii dinozaurów, pochodzące z okresu triasowego. Zmiany te były powiązane z silnym rozwojem zginaczy i prostowników kolan. Ponadto przednie kończyny *Silesaurus* również były w pełni wyprostowane, analogicznie do przednich kończyn wczesnych zauropodów. U członków obydwu linii zmniejszeniu podległy mięśnie związane z wysuwaniem, cofaniem i zginaniem kończyn. Używali oni kończyn przednich raczej jako podparcia ciała, mniej jako napędu. Podobną konstrukcję łopatki i kości ramieniowej można znaleźć u Lagerpetidae i *Lewisuchus*, co sugeruje, że długie, smukłe, w pełni spionizowane kończyny przednie są wyjściowe dla wszystkich Dinosauromorpha, a nie tylko dla Silesauridae. U wczesnych dinozaurów doszło do przebudowy kilku przyczepów mięśniowych na kończynie przedniej, prawdopodobnie w związku z dwunożnością.

Analiza składników głównych (PCA), przeprowadzona dla zestawu 24 pomiarów na 33 kościach udowych i 15 pomiarów na 20 kościach biodrowych *Silesaurus* wykazała, że próba ta jest wysoce zmienna, ale prawdopodobnie jednorodna, a więc monospecyficzna. Większość zmian morfologicznych koncentruje się w przyczepach mięśniowych i proporcjach kości, które znacznie zmieniają zarówno rozmiar, jak i pozycję podczas ontogenezy. Pomimo małej wielkości próby, wynika z niej, że kości udowe mniejszych osobników są mniej spłaszczone i mają bardziej sinusoidalny wygląd. W wielu dużych okazach bliższe części ścięgien mięśniowych są skostniałe w miejscu ich mocowania na kości udowej i pozostają przyczepione do kości w największych okazach. Okazy z dodatkowymi skostnieniami są interpretowane jako dojrzałe samice, które były statystycznie większe, niż proponowane samce. Sugeruje się, że kostnienie rozwija się u samic pod kontrolą kalcytoniny. Zmienność wewnątrzpopulacyjna kości biodrowych jest również wysoka, ale mniej zależna od ontogenezy.

Duża zmienność wewnątrzpopulacyjna obserwowana w puszce mózgowej *Silesaurus* nakłania do ostrożności w badaniach taksonomii i różnorodności wczesnych dinozauromorfów. Zewnętrzna i wewnętrzna osteologia trzech prawie kompletnych

mózgoczaszek *Silesaurus* ukazuje kilka podobieństw z innymi wczesnymi dinozaurami, co potwierdza ścisły związek między tymi formami. Jednakże wyrostki paroccipitalne *Silesaurus* są skierowane brzusznie, jak u ptaków, osiągając dolny poziom kłykcia potylicznego. U dinozauromorfów wyrostki te mają zwykle orientację prawie poziomą (przypuszczalnie jest to stan plezjomorficzny). Modyfikacje zaobserwowane u ptaków i *Silesaurus* są spowodowane ekspansją grzbietowo-brzuszną mięśni *musculus complexus* i *m. depressor mandibulae*, które przyczepiają się grzbietowo-bocznie do tyłu czaszki. U dorosłych ptaków mięśnie te są silnie zaangażowane w początkowe uniesienie głowy podczas picia. Dlatego wywnioskowane rozmieszczenie tych mięśni u *Silesaurus* może sugerować, że Silesauridae ewoluowały w kierunku karmienia młodych.

Uzyskane w wyniku badań dane osteologiczne i ich funkcjonalna interpretacja potwierdziły kluczową pozycję *Silesaurus opolensis* we wczesnej ewolucji dinozaurów.

Contents

Summary

Silesaurus opolensis Dzik, 2003 from the Late Triassic (late Carnian) of Poland is a key species for understanding the evolution of early dinosaurs. Specimens of *Silesaurus* offered rich evidence about the origin of the dinosaur body plan (Smith et al., 2007; Langer et al., 2009; Martinez & Alcober, 2009; Nesbitt et al., 2010, 2017; Martinez et al., 2011, 2013; Langer, 2014), which becomes especially important in the dispute of paraphyly (Langer & Ferigolo, 2013) or monophyly (Kammerer et al., 2012) of the Silesauridae and its relationship to the Ornithischia (Dzik, 2003; Dzik & Sulej, 2007; Ferigolo & Langer, 2007; Niedźwiedzki et al., 2009; Cabreira et al., 2016). This study presents postcranial anatomy and some aspects of the skull of *Silesaurus* that permit myological reconstructions and estimation of the range of its skeletal variability. The objective of the present contribution is to use of this knowledge to evaluate similarities of *Silesaurus* with early dinosaurs.

A find of partially articulated skeleton of *Silesaurus*, with the skull, neck, pectoral girdle and thorax, supplemented by additional specimens, enabled complete restoration of the vertebral column and associated skeletal parts. Cervical ribs of *Silesaurus*, well preserved in their original disposition, are parallel to the neck and extend backward for a few vertebral lengths. There is a sudden change in their morphology behind the seventh vertebra, although otherwise the transition from the cervical to the dorsal vertebrae is very gradual. Parapophyses slowly migrate upward along the anterior margin of the centrum and leave the centrum at the sixth or seventh dorsal vertebra. Narrowing of the dorsal extremities of the neural spines of the fourth and neighboring vertebrae suggests the ability of this region of the vertebral column to bent upward. There is thus a disparity between the structural and functional neck–thorax transition. The presence of three sacrals firmly connected by their ribs with the ilia and the long tail of *Silesaurus*, providing a counterbalance to the weight of the body in front of the pelvis, suggest the ability for fast bipedal running. However, unusually long but gracile forelimbs of *Silesaurus* indicate quadrupedal stance.

It is widely accepted that ornithodirans (bird lineage) and some pseudosuchians (crocodilian lineage) achieved fully erect limb posture in different ways. Ornithodirans have buttress-erected hindlimbs, while some advanced pseudosuchians have pillar-erected hindlimbs. Analysis of the musculoskeletal apparatus of the early dinosauriform *Silesaurus* challenges this view. This ornithodiran had pillar-erected hindlimbs like some pseudosuchians. This condition could be plesiomorphic or represents a transitional state

between adductor-controlled limb posture of early dinosauromorphs and the buttress-erected hindlimbs of dinosaurs. This sequence of changes is supported by Triassic tracks left by animals of the dinosaurian lineage. It was associated with the strong development of knee flexors and extensors. Furthermore, the forelimbs of *Silesaurus* were fully erect analogously to those of early sauropods. Members of both lineages had reduced muscles related to the protraction, retraction, and bending of the limb. They used forelimbs more as a body support and less for propulsion. A similar scapula and humerus construction can be found in the Lagerpetidae and *Lewisuchus* suggesting that long, slender, fully erected forelimbs are primitive for all Dinosauromorpha, not just the Silesauridae. Early dinosaurs redeveloped several muscle attachments on the forelimb probably in relation with bipedality.

A principal component analysis (PCA) performed for a set of 24 measurements on 33 femora and 15 measurements on 20 ilia of *Silesaurus*, shows that this sample is highly variable but probably monospecific. Most of the morphological variation is concentrated in the muscle attachments and proportions of bones, which significantly change in both size and position during ontogeny. Despite the small sample size, femora of smaller individuals have less flattened shafts and a more sinusoidal appearance. In many large specimens, proximal parts of muscle tendons are ossified at their attachment site on femora and remain attached to the bone in the largest specimens. The specimens with attached ossifications are interpreted as mature females that were statistically larger than proposed males. It is suggested that ossifications developed in females under the calcitonin control. The intrapopulation variability of ilia is high, but less dependent on ontogeny.

High intraspecific variation observed in the *Silesaurus* braincase calls for caution in taxonomy and diversity studies of early dinosauromorphs. The osteology of three almost complete braincases of *Silesaurus* shows that this taxon shares several similarities with other early dinosauriforms, which supports a close relationship among them. However, the paroccipital processes of *Silesaurus* are directed ventrally, like in birds, reaching the level of the ventral margin of the basioccipital condyle. In dinosauromorphs, these processes usually have an almost horizontal orientation (presumed to be the plesiomorphic condition). Modifications observed in birds and *Silesaurus* have resulted in the dorsoventral expansion of Musculus complexus and M. depressor mandibulae, which occupy the dorsolateral part of the posterior side of the skull. In adult birds, these muscles act strongly on the initial upstroke of the head during drinking. Therefore, the inferred condition of these muscles in *Silesaurus* may imply that Silesauridae evolved toward bird-like feeding behaviour.

The obtained osteological data and their functional interpretation have demonstrated the crucial position of *Silesaurus opolensis* in early evolution of dinosaurs.

Introduction

The Late Triassic was a time of rapid evolution and diversification of archosaurs that resulted in their diversification into numerous lineages of dinosaurs and dinosaur-like forms (Parker et al., 2005; Nesbitt, 2007; Irmis et al., 2007a; Brusatte et al., 2008). However, the ichnological evidence suggests that dinosauromorphs originated already by the Early Triassic (Niedźwiedzki et al., 2013). Dinosauromorphs are defined as archosaurs more closely related to birds than to pterosaurs and crocodiles (Langer et al., 2013). They encompass small gracile Lagerpetidae (Müller et al., 2018), proto-dinosaurs like *Marasuchus* (Sereno & Arcucci, 1994) and *Lewisuchus* (Bittencourt et al., 2015), beaked Silesauridae (Langer et al., 2010; Nesbitt et al., 2010), and dinosaurs (Figure 1). The Lagerpetidae is the first known branch of dinosauromorphs. Until now, basal dinosauromorphs were characterized as having shortened forelimbs and primitive morphology of the pelvis and femur, but highly asymmetric foot. They are considered quadrupedal, with some ability to run bipedally (Fechner, 2009).

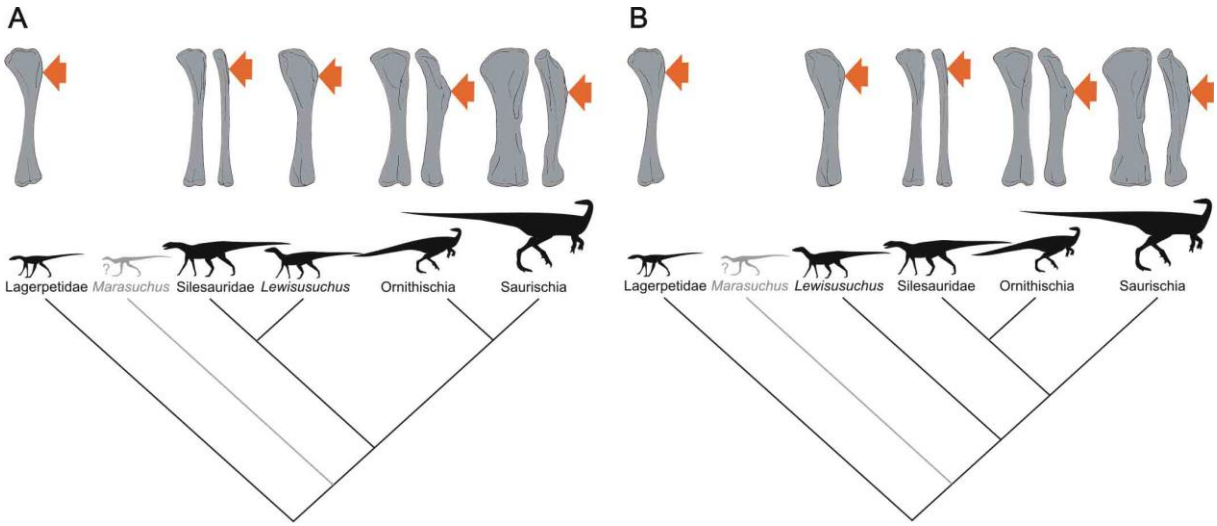

Figure 1. Phylogenetic framework of the Dinosauromorpha used in this study with illustrations of humeri. **A**, phylogeny based on Cabreira et al. 2016; **B**, phylogeny based on Nesbitt et al. 2017.

The main difficulty with deciphering the actual course of the evolutionary transformations and pattern of relationships is the scarcity of data. Especially for the early Late Triassic, knowledge of the anatomy of possible early dinosaurs and their close relatives is very limited. There are few reports on articulated skeletons, isolated in time and separated by great geographic distances. Among Triassic archosaurs closely related to the dinosaur clade, those in the family Silesauridae, which show quadrupedal adaptations in their locomotion and a

horny beak in the lower jaw, seem to be geographically most widespread (Ezcurra, 2006; Ferigolo & Langer, 2006; Nesbitt et al., 2010; Kammerer et al., 2012). All silesaurids are known from incomplete, usually highly disarticulated material except for *Silesaurus opolensis* Dzik, 2003, from the Late Triassic (late Carnian) deposits exposed at Krasiejów in southern Poland. Thus, detailed information on its anatomy is crucial in understanding the mode of life, relationships and evolution of the whole group.

The discovery of *Silesaurus* helped to identify other problematic dinosauriform remains from the Late Triassic of Pangea (i.e., Ezcurra, 2006; Nesbitt et al., 2007, 2010, 2013, 2017; Kammerer et al., 2012; Niedźwiedzki et al., 2016; Barrett et al., 2015; Skawiński et al., 2017) and demonstrated that the dinosaur lineage diversified earlier than had previously been thought (Brusatte et al., 2011; Langer et al., 2013; Niedźwiedzki et al., 2013; Cabreira et al., 2016).

Silesaurus is the first described member of Silesauridae represented by rich material collected from a single locality (Dzik, 2001, 2003; Dzik & Sulej, 2007), that makes it probably the largest available sample of a member of the dinosaur stem group. The locality is biostratigraphically dated as late Carnian, according to conchostracan finds, although its age continues to be a matter of discussion (Olempska, 2004; Kozur & Weems, 2010; Nawrocki et al., 2015; Szulc et al., 2015; Dzik & Sulej, 2016; Geyer & Kelber, 2018).

The most unusual aspect of its anatomy, apart from its beaked dentary, is the elongation and gracile appearance of its forelimbs. This morphology may be interpreted either as a stage in the transition from the plesiomorphic quadrupedality of its archosaurian ancestor or, conversely, as incipient secondary quadrupedality at the beginning of the dinosauromorph radiation. The relatively long trunk of *Silesaurus* (0.79 hindlimb/trunk length ratio), closed acetabulum, and untwisted femoral head (Dzik, 2003) can be used to argue for the first interpretation. *Silesaurus* apparently walked mainly on four limbs. The second interpretation is supported by the relatively narrow pelvis and functionally tridactyl foot. The presented below detailed restoration of locomotory muscles is expected to improve our understanding of the problem.

Several aspects of the anatomy and life history of *Silesaurus* have already been considered, including its probable environment (i.e., Zatoń & Piechota, 2003; Zatoń et al., 2005; Bodzioch & Kowal-Linka, 2012; Dzik & Sulej, 2007; Gruszka & Zieliński, 2008; Jewuła et al., 2019; Pacyna, 2014; 2019), skull anatomy (Dzik & Sulej, 2007; Piechowski et al., 2015), phylogenetic position (i.e., Dzik, 2003; Ezcurra, 2006; Dzik & Sulej, 2007; Butler et al., 2007; Ferigolo & Langer, 2007; Irmis et al., 2007; 2008; Niedźwiedzki et al., 2009; Nesbitt et

al., 2010; Nesbitt, 2011; Bittencourt et al., 2015; Cabreira et al., 2016), bone histology (Fostowicz-Frelik & Sulej, 2010), dental microwear (Kubo & Kubo, 2014), and diet (Qvarnström et al., 2018).

Among Triassic dinosauromorphs only *Coelophysis* (Colbert, 1989; Rinehart et al., 2009; Griffin, 2016), *Dromomeron* (Nesbitt et al., 2009; Griffin et al., 2019), and *Asilisaurus* (Griffin & Nesbitt, 2016) were analyzed for variability. The present study attempts to explore the unique opportunity of having insight into variability and ontogeny of such a phylogenetically important animal as is *Silesaurus*. In comparison with other archosaurs from the same period, the *Silesaurus* specimens are extremely numerous, and the bones are often preserved in the original anatomical alignment. In addition, the bones remained in good condition. It gives a unique opportunity to precise measurements of specimens and skeletal reconstruction.

Until now, detailed muscle anatomy of *Silesaurus* remained unknown. Well preserved muscle attachments on the bone surface and increasing knowledge about musculature of other Dinosauromorpha give unique opportunity to fill this gap. Throughout this paper, Dinosauromorpha and Dinosauriformes are used in the sense of Nesbitt (2011 and discussion therein) and Nesbitt et al. (2017).

Chapter 1. Material and Methods[1]

Material

The material of *Silesaurus* is represented by several hundred bones, most of which were collected from the upper (fluvial) fossiliferous horizon in the Krasiejów locality, which is dated biostratigraphically as the late Carnian (Dzik, 2001; Olempska, 2004; Dzik & Sulej, 2007; Lucas, 2015; Nawrocki et al., 2015). They represent over a dozen individuals, some of which were found in articulation (Dzik, 2003). At least one individual (in addition to the sacral illustrated by Dzik, 2001) has been found in lower (lacustrine) fossiliferous horizon in Krasiejów (Dzik & Sulej, 2007; Piechowski & Dzik, 2010). The material is housed at the Institute of Paleobiology, Polish Academy of Sciences (Warsaw) and catalogued as ZPAL Ab III (see figures and tables).

Three braincases were found in the probably isochronous *Silesaurus* bone accumulation, named as the upper bone-bearing horizon (Dzik, 2003; Dzik & Sulej, 2007). They were not found widely spread, but in local accumulations of bones from several individuals of the same species, all with partly articulated skeletons (see Dzik, 2003). The bones comprising this accumulation are preserved in a similar manner, not sorted, and are without any mechanical or bioerosional damage. This condition implies a local and short transport, and perhaps rapid burial. Thus, the braincases are almost certainly from a single temporal horizon and possibly even from individuals of one social group. I can therefore exclude temporal differences (e.g., different stages of evolution) or differences between populations as the source of anatomical variation among the braincases. The analyzed specimens have braincases of very similar sizes and all vertebral sutures on the entire length of the axial skeleton are closed. The histological data suggest that these animals were mature or close to maturity (Fostowicz-Frelik & Sulej, 2010), so large ontogenetic differences among them should not be expected.

[1] Part of this chapter was published in:
Piechowski, R. & Dzik, J. 2010. The axial skeleton of *Silesaurus opolensis*. *Journal of Vertebrate Paleontology* **30**, 1127–1141.
Piechowski, R., Tałanda, M. & Dzik, J. 2014. Skeletal variation and ontogeny of the Late Triassic dinosauriform *Silesaurus opolensis*. *Journal of Vertebrate Paleontology* **34**, 1383–1393.

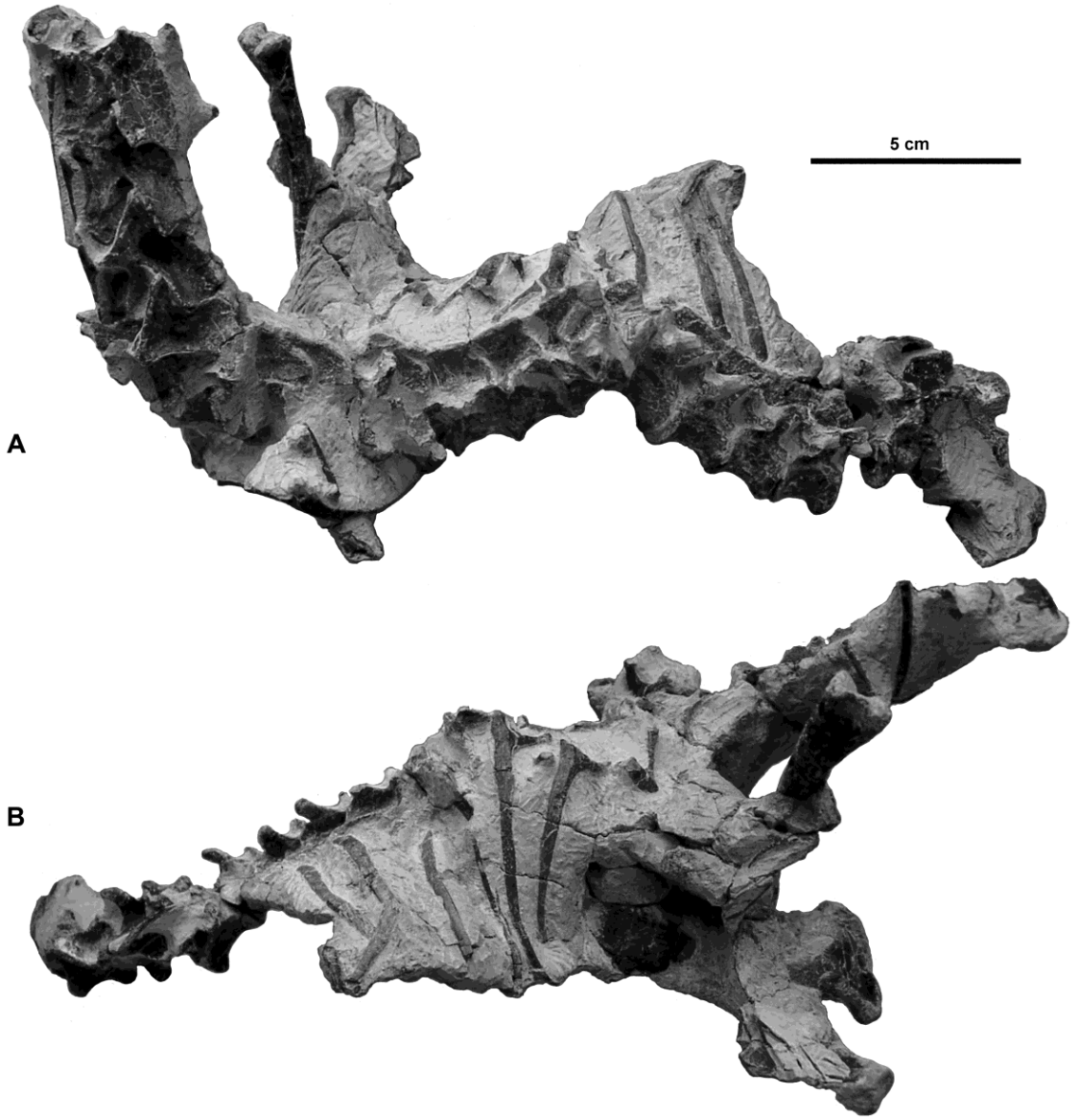

Figure 2. Articulated partial skeleton ZPAL AbIII/1930 of *Silesaurus opolensis* Dzik, 2003 from the early Late Triassic lacustrine horizon in Krasiejów near Opole, Poland. **A**, left lateral side; **B**, right dorsolateral side.

The braincase ZPAL AbIII/361 was found among semi-articulated bones of single almost complete skeleton. ZPAL AbIII/364 represents a braincase articulated with vertebrate column and associated with limb bones of a single individual. Only ZPAL AbIII/362 was found in loose association of cranial and postcranial bones, which probably belongs to one individual, although it is less clear. All three specimens were illustrated in situ by Dzik (2003).

The braincases were prepared mechanically or cleaned with weak formic acid. The general proportions of the neurocranium are best preserved in ZPAL Ab III/362/1, which is embedded in a limestone concretion. The braincase ZPAL Ab III/361 is split into three parts (numbered 35, 36, 38), with the parasphenoid and ophisthotic separated from the rest of the braincase.

The braincase wall ZPAL Ab III/361/35 was imbedded in claystone, helping the exposure of the interior of the endocranial cavity. The cavity was also prepared chemically in ZPAL Ab III/364/1 (after Dzik 2003).

The braincase terminology used in this study follows that used by Gower & Weber (1998), Nesbitt (2011), Martinez et al. (2013), and Sobral et al. (2016).

Table 1. Measurements of *Silesaurus opolensis* braincases and associated long bones (in mm).

Specimen	**Braincase height**	**Braincase length**	**Humerus length**	**Femur length**	**Angle between basal tubera (°)**
Ab III/361	27.6	24	134.5	199	110
Ab III/362	29.1	20.5	116	160	120
Ab III/364	28.5	21.5	?	?	95

Most of the new information on the axial skeleton presented here is derived from the specimen ZPAL AblII/1930 (Dzik & Sulej, 2007), which preserves a partial skull articulated with the anterior part of the postcranial skeleton (Figures 2, 3). The specimen was found in the lacustrine lower fossiliferous horizon, from which earlier a few isolated bones of *Silesaurus* had been collected, including the first known specimen of this species (Dzik, 2001). The axial skeleton of specimen ZPAL AblII/1930 shows well preserved and articulated presacral vertebrae (including the atlas) of proximal part of the column with their ribs and gastralia, mostly in original disposition, although in places some sets of bones are displaced. Proximal elements of the pectoral girdle are also preserved. The tail is represented by a few articulated caudal vertebrae found in proximity.

All other specimens of *Silesaurus* were collected from the fluviatile upper fossiliferous horizon at Krasiejów (Dzik, 2003; Dzik & Sulej, 2007). Except for the proatlas and a few distal caudals, elements of the entire vertebral column are represented in the studied material. Despite some difference in size, all specimens show complete co-ossification of the neural arches with the centra. The morphological sequence and number of the vertebrae in particular subdivisions of the column not represented in specimen ZPAL AblII/1930 is inferred from previously described, partially articulated specimens ZPAL Ab III/361, 362, and 363 (Dzik, 2003).

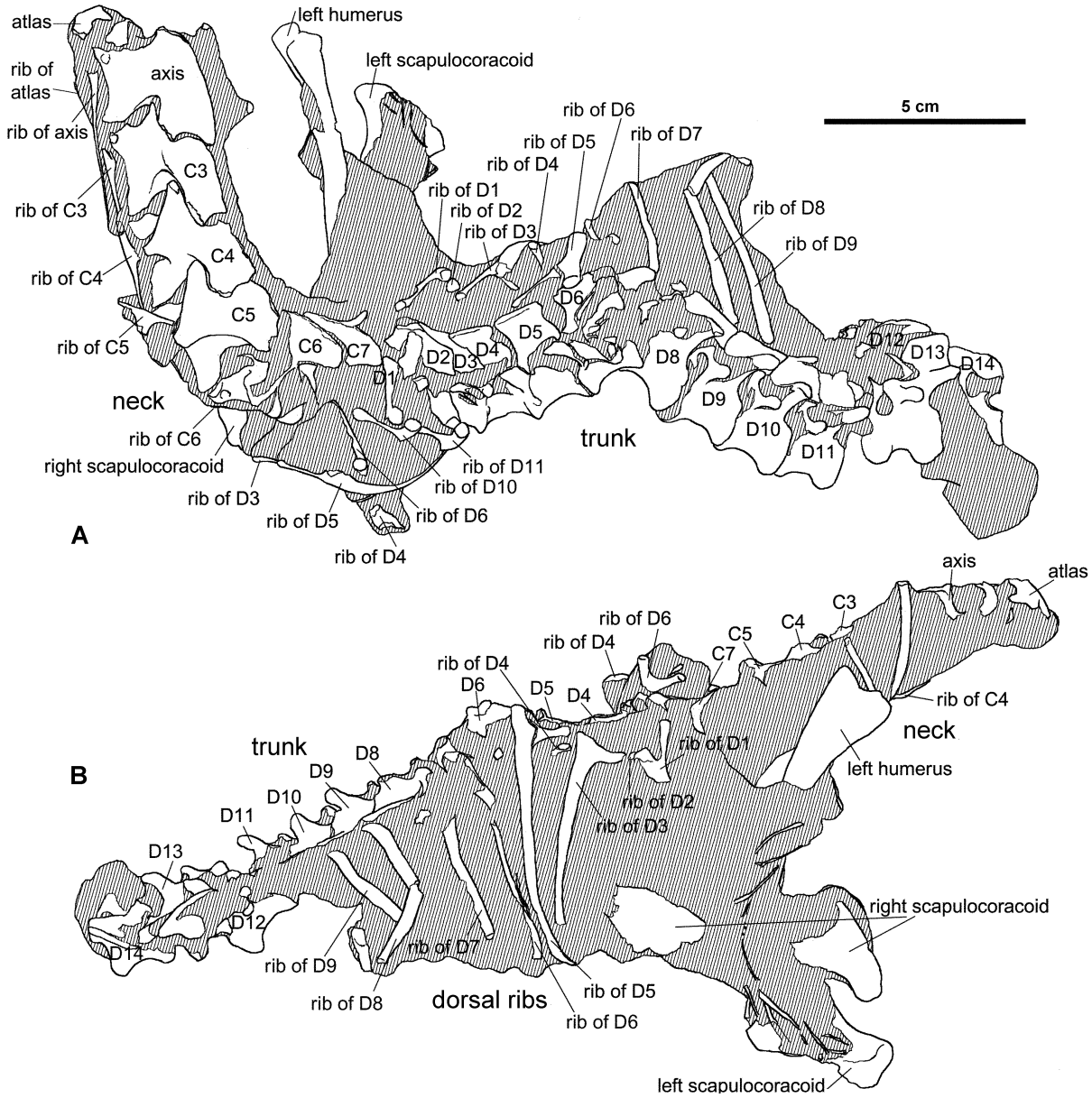

Figure 3. Identification of *Silesaurus opolensis* bones in specimen ZPAL AbIII/1930 (see also Figure 2). **A**, left lateral side; **B**, right dorsolateral side.

The holotype of *Silesaurus* (ZPAL Ab III/361) includes all presacral vertebrae except for the atlas. The sacrum is associated. Only 15 caudals of the proximal part of the tail are present, including a few crushed chevrons. The ribs are more or less displaced from their original articulation. The vertebral column is broken in few places with its bones dispersed over some area, but it is possible to determine the morphological sequence of the vertebrae within the column.

The vertebral column of the skeleton ZPAL Ab III/364 includes 16 presacral vertebrae of the proximal part of the column (including atlas) with most of their ribs. These bones are preserved mostly in articulation. In specimen ZPAL Ab III/362, the vertebral column is

represented by the well preserved sacrum and fragmentary cervical, dorsal, and caudal series. Specimen ZPAL Ab III/363 includes only the sacrum. Numerous isolated vertebrae were collected in addition to the articulated specimens within the same lenticular rock unit, probably representing a single depositional episode (Dzik & Sulej, 2007).

The available ilio-femoral material is generally well preserved, although shafts of long bones are usually crushed and some degree of deformation may alter the original proportions of the bones. Therefore, I did not use landmark-based shape analysis, restricting this analysis to simple measurements taken with a caliper. This allowed better control of deformational artifacts (especially in case of displacement or rotation of crushed bone segments) and to omit areas where deformation affected the dimensions of particular bone structures.

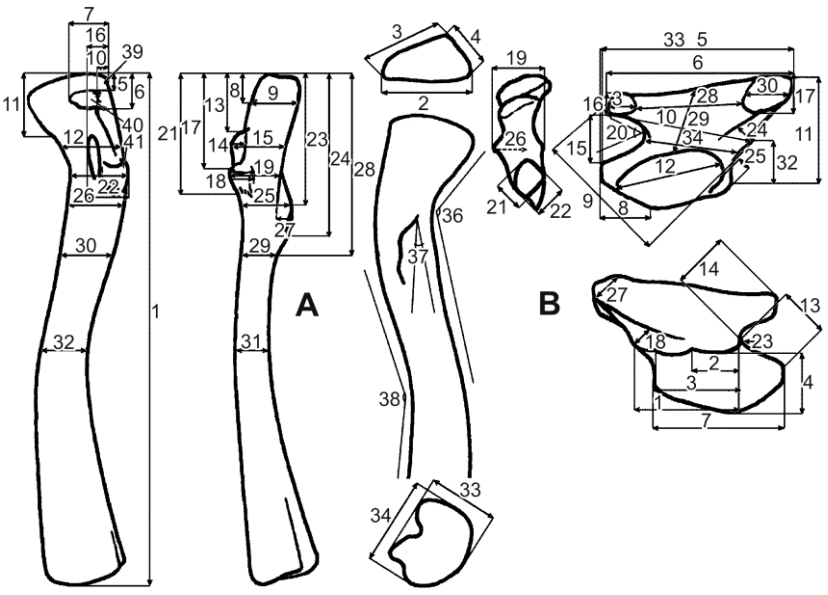

Figure 4. Characters measured on femora (1–38, **A**) and ilia (1–34, **B**) used in the first factor analysis. Characters 39–41 (**A**) mark ossifications on the femur that were not included in the factor analysis

Thirty-three more-or-less complete femora were used in this study: ZPAL AbIII/361/23L, 361/21R, 1930L, 460/1L, 411/4R, 563/7R, 405L, 362R, 362L, 363L, 1914R, 457L, 2498L, 407/1L, 2514L?, 1266R, 403/5L, 1272R, 1263R, 1884L, 2063R, 2068R, 1155/1R, 458/1L, 2515R, 458/6L, 1269R, 2516R, 907/10R, 2380R, 907/11L, 907/9R, and 2534R. Their morphology has been quantified by measuring 38 linear traits (Figure 4A). Twenty ilia were available for measurement: ZPAL AbIII/404/2L, 2517L, 404/1R, 907/8L, 907R, 362R, 362L, 2518L, 400R, 2519R, 2520L, 1202L, 2521R, 1835R, 439/1L, 363R, 363L, 2522R, 361R, and 361L, and 34 linear traits have been measured (Figures 4B, 6).

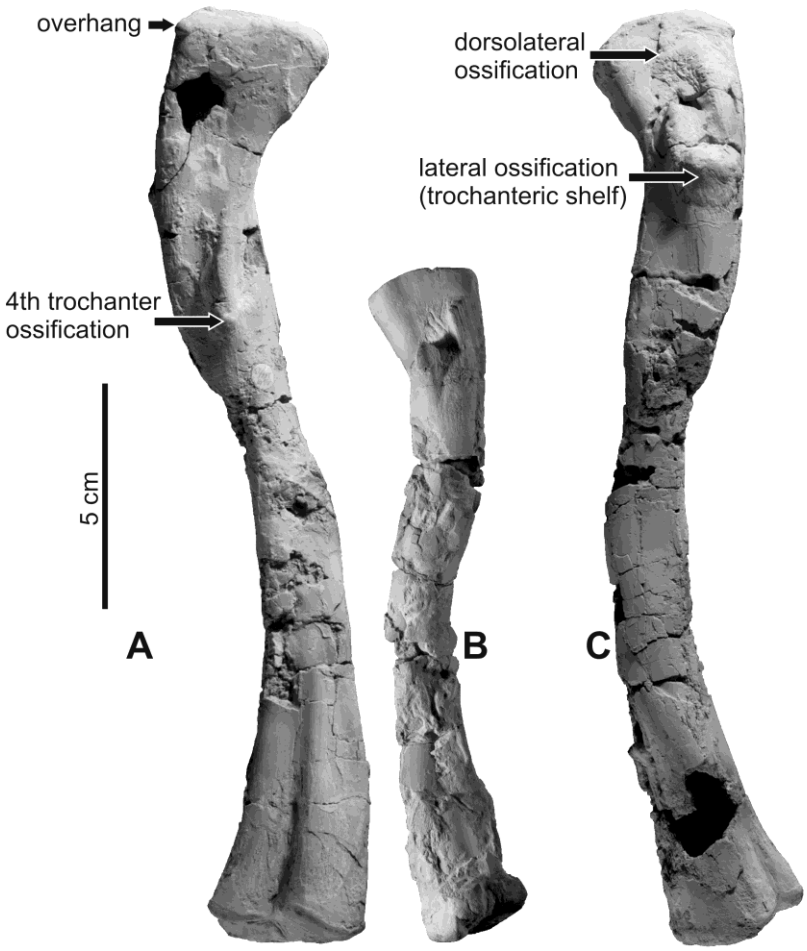

Figure 5. Femora of *Silesaurus opolensis* Dzik, 2003 from the late Carnian of Krasiejów. **A**, ZPAL AbIII/361/23 left femur of a large individual in posteromedial view; **B**, ZPAL AbIII/457L left femur of a small individual in anterolateral view; **C**, ZPAL AbIII/361/21 right femur of a large individual in lateral view (note that the proximal part of bone is a little twisted in relation to the distal part).

Methods

The objective of quantitative studies on the skeletal material of *Silesaurus* was to estimate the range of variation in the sample and identify its possible multimodal distribution or discrete groups of specimens. To determine this, I used principal component analysis (PCA). Due to incompleteness of the bones, the data matrix includes many missing measurements. There are many ways of replacing missing data. The simplest is to substitute missing values with the mean of the available data. However, if the amount of missing data is great, then their substitution requires a more sophisticated approach (Jackson, 1991). Most of the morphological characters I measured depend on size of the individual being measured. Therefore, I created a method of substituting a missing measurement by multiplying the arithmetic mean of a character by a coefficient of relative specimen size. The coefficient was based on characters 1, 2, 34, 33, 11, 25, 26, 9, 20, 15, 12, 31, and 32 (femur) and 5, 6, 13, 14, 34, 4, 19, 11, 1, 25, 16, and 17 (ilium) (Figure 4). Bones of the same individual were analyzed together, so the same coefficient value was applied to each of them. Although this has introduced an artificial clustering of points in the center of the PCA plots, such procedure

makes interpretation of incomplete specimens possible, although one has to be aware of resulting distortion of data.

For bivariate plots, I estimated relative specimen size for each individual by comparing available measurements of particular bones with those of more completely preserved specimens. The inferred specimen size was then standardized with respect to the mean.

I performed several Student's t-tests to check if the differences between observed groups of femora (e.g., with overhang structure or without it) are statistically significant.

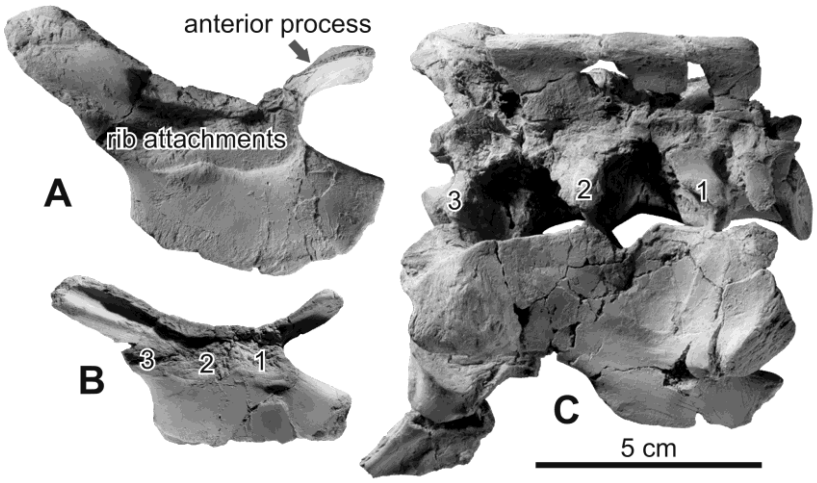

Figure 6. Ilia of *Silesaurus opolensis* Dzik, 2003 from the late Carnian of Krasiejów. **A**, ilium of a large individual ZPAL AbIII/404/2 in medial view; **B**, ilium of a small individual ZPAL AbIII/907/8 in medial view; **C**, pelvis of a large individual ZPAL AbIII/362R in lateral view.

Factor Analysis

Factor analysis is a technique of data exploration, which finds the hidden structure of the latent variables responsible for the observed relationships between the data. The analysis is limited to such factors that can be expressed as a sum of the weighted variables.

TABLE 2. Measurements used to calculate the morphological distance between femora.

No.	Name
1	Upper edge of femoral head compression (ratio of 2 and 9 in Fig. 1A)
2	Lower edge of femoral head compression (ratio of 15 minus 14 and 12 in Fig. 1A)
3	Femoral neck compression (ratio of 20 and 19 in Fig. 1A)
4	Compression below first ridge of fourth trochanter region (ratio of 25 and 26 in Fig. 1A)
5	Proximal part of femoral shaftcompression (ratio of 29 and 30 in Fig. 1A)
6	Middle part of femoral shaft compression (ratio of 31 and 32 in Fig. 1A)
7	Distal end compression (ratio of 33 and 34 in Fig. 1A)
8	Femoral head curvature angle (measurement 36 in Fig. 1A)
9	Femoral shaft curvature angle (38 in Fig. 1A)

10	Distance between dorsolateral trochanter to proximal end (8 in Fig. 1A)
11	Anterior dorsolateral trochanter location (10 in Fig. 1A)
12	Dorsolateral tuber area (40 in Fig. 1A)
13	Anterior trochanter size (14 in Fig. 1A)
14	Distance between the anterior trochanter to proximal end (13 in Fig. 1A)
15	Anterior trochanter location (16 in Fig. 1A)
16	Lateral ossification size (18 in Fig. 1A)
17	Distance between proximal edge of lateral ossification to proximal end (17 in Fig. 1A)
18	Distance between distal edge of lateral ossification to proximal end (21 in Fig. 1A)
19	Anteroposterior muscle attachment of anterior trochanter and lateral ossification extent (22 in Fig. 1A)
20	Fourth trochanter size (27 in Fig. 1A)
21	Distance between first ridge of fourth trochanter to proximal end (23 in Fig. 1A)
22	Distance between second ridge of fourth trochanter to proximal end (24 in Fig. 1A)
23	Fourth trochanter angle (37 in Fig. 1A)
24	Overhang presence (39 in Fig. 1A)

Each of the measurements was standardized.

I used this method to reveal factors engaged in observed variation. I tried to check if factors are linked to ontogeny, intraspecific variation, or the presence of two separate species.

Factor analysis was performed for 38 femoral variables and 34 iliac variables (Figure 4), as well as 24 (femoral) and 15 (iliac) variables (Tables 2 and 3) belonging to the values standardized and normalized in respect to the means of particular features. Main factors were identified by PCA. I created scree plots and applied the Kaiser criterion to determine the number of factors necessary to describe adequately the distribution: eight for the femur and five for the ilium.

I applied multidimensional scaling for 24 variables of the femur and 15 of the ilium (Tables 2 and 3). The distance matrix of standardized measurements was figured for each animal. As the measure of the distance between each two animals, I used the root of the sum of squared differences in each individual variable (in Euclidean distance).

Student's t-Test

I performed 26 Student's t-tests for the whole femoral sample. The independent binary variable (grouping) was the presence of the 'overhang structure': (1) exists or (0) does not exist. I chose this character, because it is possible to trace its presence (or absence) on almost all specimens and it defines two distinct classes in the sample. The null hypothesis was the assumption that the average values of the dependent variable in both groups are the same. All

26 tests were performed at the significance level of 5%. Means and standard deviations were rounded to two figures and the standard error of the mean was estimated.

I also prepared several bivariate plots to display possible trends in the ontogeny of *Silesaurus*. The lack of histological data for each specimen forced us to choose total bone length as an age indicator. This seems defensible as the length of the bones engaged in locomotion is usually linked with body length mass (Klein & Sander, 2008). I am aware that this assumption may have resulted in introducing error into interpretations of the plots. Therefore, I figured and discussed only the most apparent trends. I use linear correlation and Spearman rank correlation tests to check the statistical significance. Unfortunately, the number of specimens is too small to reveal significant results in some cases.

TABLE 3. Measurements used to calculate the morphological distance between ilia.

No.	Name
1	Anterior process length (measurement 14 in Fig. 1B)
2	Postacetabular process length
3	Preacetabular process length (13 in Fig. 1B)
4	Ischiatic process length (32 in Fig. 1B)
5	Distances between muscle attachments ratio (28 in Fig. 1B)
6	Angle between anterior and preacetabular processes (20 in Fig. 1B)
7	Distances from lower ridge to medial ridge and to brevis shelf ratio (24 in Fig. 1B)
8	Anteroposterior iliac blade extent (6 in Fig. 1B)
9	Lateromedial bone thickness (19 in Fig. 1B)
10	Lateromedial ischiatic process thickness (25 in Fig. 1B)
11	Distances from the anterior process to the preacetabular process and from the postacetabular process to ischatic process ratio (11 to 15 in Fig. 1B)
12	Acetabulum depth (26 in Fig. 1B)
13	Acetabulum width (12 in Fig. 1B)
14	Iliac median width (34 in Fig. 1B)
15	Area above attachment

Each of the measurements was standardized.

Muscle attachments examination

To examination of limb muscle attachments and reconstruction of the locomotor musculature of *Silesaurus*, all partially articulated skeletons (ZPAL Ab/361, ZPAL Ab/362, 363, 364, and 1930), as well as numerous isolated or semiarticulated bones of the fore- and

hind limbs were used. The available material is generally well preserved, and shows clear muscle attachment features.

Information about homology and myological arrangement in selected extant phylogenetically relevant taxa was derived largely from the literature (see description of locomotor musculature). For comparative purposes, bones and muscles of *Caiman niger*, *Crocodylus niloticus*, *Alligator mississippiensis*, *Sphenodon punctatus*, *Struthio camelus*, *Rhea americana*, *Ciconia nigra*, *Anser anser*, *Gallus gallus*, *Tribolonotus novaeguineae*, and *Neophron percnopteus* from the collection of the Faculty of Biology, University of Warsaw were examined.

I adopted the Extant Phylogenetic Bracket method (Witmer, 1995) for the soft tissue inference. Witmer recognized three levels of phylogenetic inferences based on absence, presence of soft tissue in closely related extant taxa. Obtained levels of inference are provided in tables 7–8 and 11–12.

Chapter 2. Braincase[2]

The braincase anatomy is well known in several basal dinosaurs (mostly sauropodomorphs), including *Panphagia* (Martinez et al., 2013), *Thecodontosaurus* (Benton et al., 2000), *Massospondylus* (Gow, 1990), *Eoraptor* (Sereno et al., 2012), and the Late Triassic dinosauriform *Lewisuchus* (Bittencourt et al., 2015). However, information on the braincase morphology in the earliest and most basal theropods and ornithischians is limited (see Martinez et al., 2013 and references cited therein).

The objective of the present contribution is to describe in detail the braincase material of *Silesaurus* and to use these characters to evaluate its phylogenetic affinities to, and similarities with, *Lewisuchus* and early dinosaurs. In the construction of the neck muscles, which left the muscle attachments on the posterior part of the skull, it was recognized as an intermediate state between crocodiles and birds. In the chapter on myology all these aspects are described and illustrated in detail.

Three examined braincases of *Silesaurus* are of very similar sizes (Table 1), with heights (the lower surface of the occipital condyle to the tip of the supraoccipital) close to 3 cm ± 1 mm. This does not necessary mean that the animals were of the same size; for example, in *Coelophysis* the skull grows faster in length than in height during ontogeny (Rinehart et al., 2009). In order to determine overall size differences, I measured the braincase from the distal surface of the occipital condyle to the anterior end of the parabasisphenoid recess and compared that length to the length of the humeri and femora. I also measured the angle between the basal tubera on the basioccipital (Table 1).

Comparative data on the braincase morphology are primarily available for proterosuchids and erythrosuchids (Gower & Sennikov, 1996a, 1996b; Gower, 1997), *Euparkeria* (Gower & Weber, 1998; Sobral et al., 2016), *Lewisuchus* (Bittencourt et al., 2015), *Eoraptor* (Sereno et al., 2012), *Herrerasaurus* (Sereno & Arcucci, 1994), *Panphagia* (Martinez et al., 2013), *Thecodontosaurus* (Benton et al., 2000), and *Lesothosaurus* (Sereno, 1991).

The braincase of *Silesaurus* was described for the first time by Dzik (2003) based on three specimens ZPAL Ab III/361/35, 36, 38 (Figure 7), ZPAL Ab III/362/1 (Figure 8), and ZPAL Ab III/364/1 (Figure 9). Subsequently, additional information about the *Silesaurus* braincase has been offered by Nesbitt (2011), Piechowski et al. (2015), and Sobral et al. (2016). I

[2] Part of this chapter was published in:
Piechowski, R., Niedźwiedzki, G. & Tałanda, M. 2015. New data on skull anatomy of *Silesaurus opolensis*. *13th Annual Meeting of the European Association of Vertebrate Palaeontologists, Opole, Poland; Jul 8–12. Abstracts*, p. 143.

studied mainly the braincase elements that are visible externally (supraoccipital, exoccipital, basioccipital, otoccipital = opisthotic + part of exoccipital, prootic, parabasisphenoid and cultriform process). The basisphenoid will be described together with the parasphenoid (parabasisphenoid), as it is not possible to discern any suture between them (Figures 10–12).

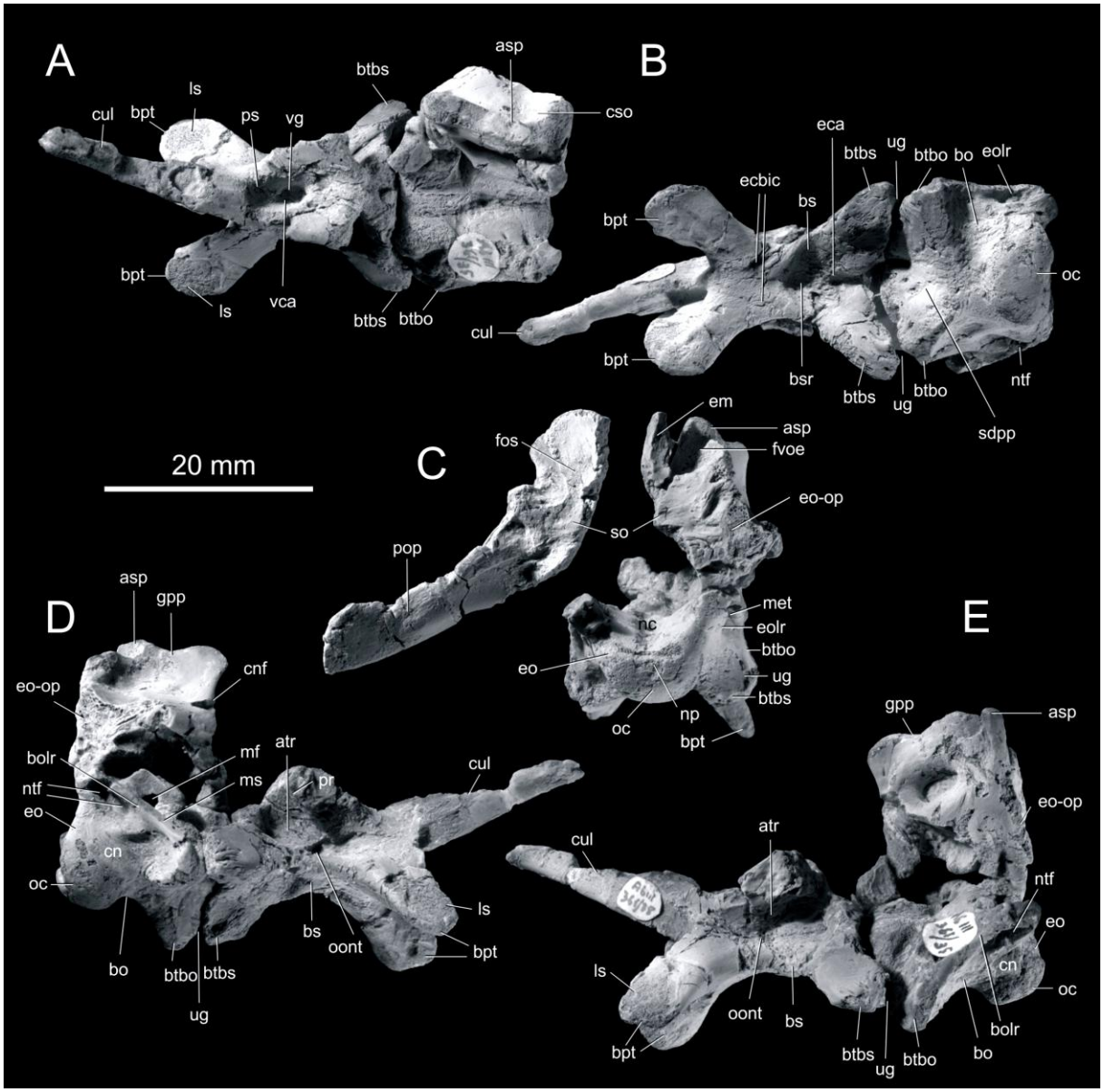

Figure 7. Photographs of the braincase ZPAL Ab III/361/35, 36, 38 of *Silesaurus opolensis* in dorsal (**A**),– ventral (**B**), posterior (**C**), right lateral (**D**), and left (**E**) views.

Abbreviations: asp – articular surfaces for parietal, atr – anterior tympanic recess, bo – basioccipital, bolr – lateral ridge on basioccipital, bpt – basipterygoid process, bs – parabasisphenoid, bsr – parabasisphenoid recess, btbo – basal tuber of basioccipital, btbs – basal tuber of parabasisphenoid, cn – condylar neck/stalk, cnf – notch for the cranial nerve V, cso – contact between the supraoccipital and otoccipital, cul – cultriform process of parabasisphenoid, eca – Eustachian canal, ecbic – entrances of cerebral branches of internal carotid artery, em –

eminence, eo – exoccipital, eolr – lateral ridge on exoccipital, eo-op – exoccipital-opisthotic, fvoe – foramen for the vena occipitalis externa, gpp – groove from posterodorsal margin of prootic, met – metotic foramen, mf – metotic fenestra, ms – metotic strut, np – notochordal pit, ntf – nerve XII foramina, oc – occipital condyle, oont – openings of oculomotor nerve III, pop – paroccipital process, pr – prootic, ls – surface for articulation with laterosphenoid, sdpp – subtriangular depression from the posteroventral surface of the parabasisphenoid, so – supraoccipital, vca – Vidian canal, vg – ventral groove, ug – unossified gap.

Supraoccipital

It is a relatively broad and flat element that forms the posterodorsal part of the braincase roof. Lateroventrally and posterolaterally, the supraoccipital contacts the otoccipital and anterolaterally contacts the prootic. The contact suture is clear in dorsal, lateral and posterior views. The supraoccipital angles posteroventrally to anterodorsally and contacts the parietal dorsally and exoccipital-opistotic lateroventrally. The principal external surface is facing posterodorsally. In posterior and posterodorsal views, the supraoccipital has a semi-elliptical shape that is broader transversely than dorsoventrally high (Figure 9).

The laterodorsal portions of the supraoccipital bear relatively large deep and pocket-like notches, possibly for the vena occipitalis externa (dorsal head vein; see Dzik, 2003). The notches open dorsolaterally and contain groove which turns in the ventromedial region of the fossa. They are limited anterolaterally by oblique oriented crests, as seen in posterior view. Deeply excavated fossae are present dorsolateral to the crests. However, the depth is variable among different specimens. The fossae are elliptical and oriented at 45° in dorsal view to the long axis of the skull. The notches separate relatively large processes from the main body of the supraoccipital. These processes expand dorsolaterally. They are blunt, and the lateral surfaces are flat (ZPAL Ab III/364/1) or rounded (ZPAL Ab III/361/35, 36, 38 and 362/1). The processes are anteroposteriorly compressed, having a subtriangular outline in dorsal view.

The dorsomedial or nuchal region is shallow and develops only a low median eminence (nuchal or sagittal crest). Shallow fossae are present on either side of the median eminence. In posterodorsal view, the anterodorsal contour of the supraoccipital between the vena occipitalis externa notches is smoothly arched. In dorsal view, the supraoccipital has four articular surfaces for the parietal, two of them localised laterally and aligned horizontally. Another two form an angle medially of about 107° and are aligned less horizontally.

The contact between the supraoccipital and otoccipital (= opisthotic-exoccipital) is visible in dorsal view. The suture with the prootic is subvertical, whereas the suture with the opisthotic is subhorizontal. Thus, the supraoccipital is subrectangular in lateral view.

The posteroventral border of the supraoccipital fuses with the exoccipitals and enters the foramen magnum. It forms a quarter of the lateromedial width of the foramen.

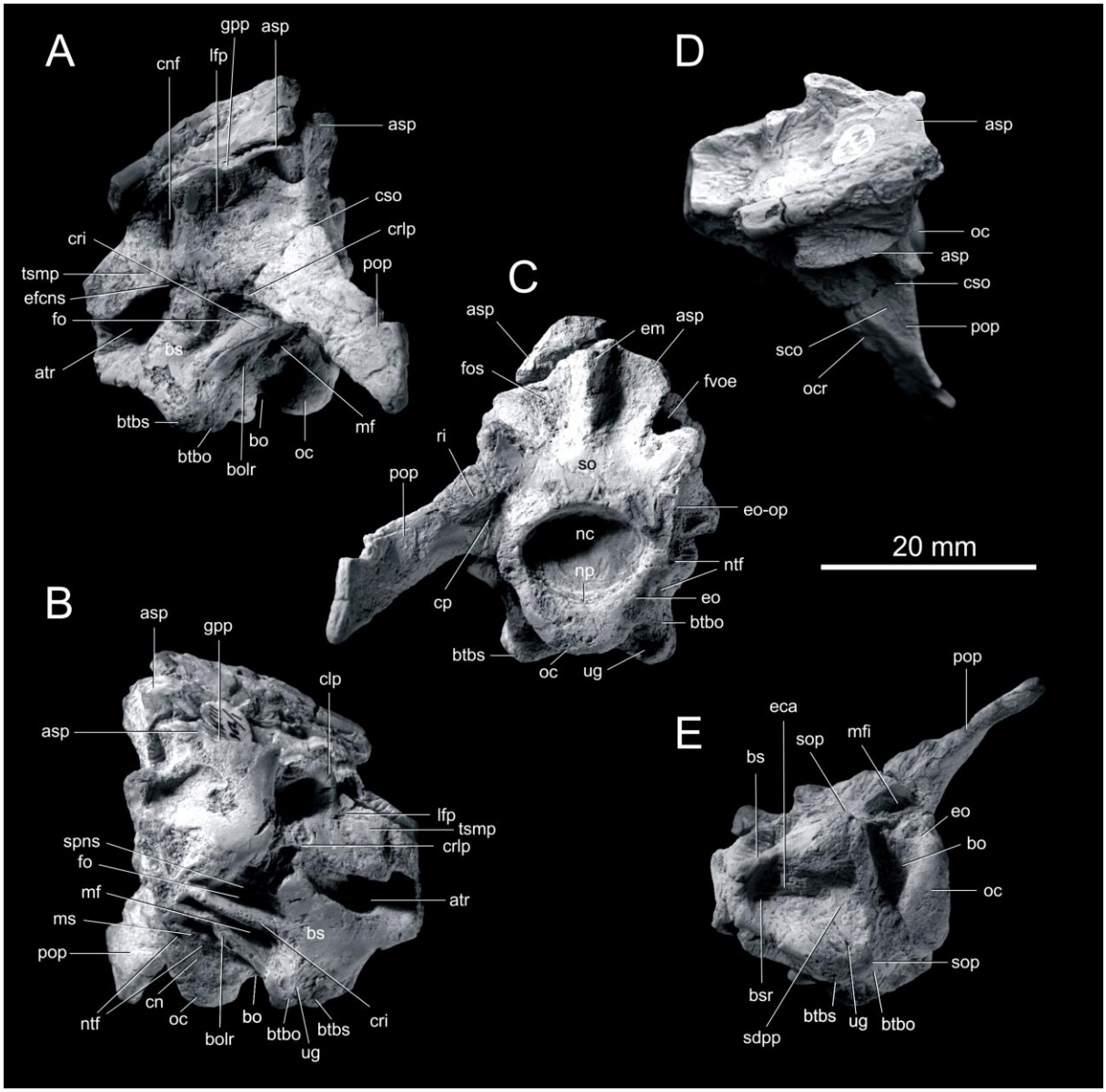

Figure 8. Photographs of the braincase ZPAL Ab III/362/1 of *Silesaurus opolensis* in left lateral (**A**), right lateral (**B**), posterior (**C**), dorsal (**D**), and ventral (**E**) views.

Abbreviations: asp – articular surfaces for parietal, atr – anterior tympanic recess, bo – basioccipital, bolr – lateral ridge on basioccipital, bs – parabasisphenoid, bsr – parabasisphenoid recess, btbo – basal tuber of basioccipital, btbs – basal tuber of parabasisphenoid, clp – clinoid process, cn – condylar neck/stalk, cnf – notch for the cranial nerve V, cp – concavity for proatlas, cri – crista interfenestralis, crlp – curved ridge from lateral surface of the dorsal region of prootic, cso – contact between the supraoccipital and otoccipital, eca – Eustachian

canal, efcns – external foramen for cranial nerve VII, em – eminence, eo – exoccipital, eo-op – exoccipital-opisthotic, fo – fenestra ovalis, fos – fossa, fvoe – foramen for the vena occipitalis externa, gpp – groove from posterodorsal margin of prootic, lfp – large fossae of prootic, mf – metotic fenestra, mfi – metotic fissure, ms – metotic strut, nc – neural canal (=foramen magnum); np – notochordal pit, ntf – nerve XII foramina, oc – occipital condyle, ocr – otosphenoidal crest, pop – paroccipital process, ri – ridge, sco – shallow concavity in opisthotic, sdpp – subtriangular depression from the posteroventral surface of the parabasisphenoid, so – supraoccipital, sop – small openings (?nutrient foramina), spns – single opening (cranial nerve VI?), tsmp – trapeizodal surface for the origin of the M. protractor pterygoidei et quadrati, ug – unossified gap.

In medial view, the anterodorsal part of the supraoccipital and posterodorsal part of the prootic share almost equally the fossa auriculae cerebelli (flocullar lobe of cerebellum; see Dzik 2003). The supraoccipital portion of the fossa auriculae cerebelli is broad, deep, and approximately semielliptical in medial view, with its longer axis positioned approximately 55° to the horizontal plane. The fossa is dorsally limited by the eminentia canalis semicircularis, and by the ventrally oriented medial wall of the auditory bulla (Oelrich, 1956 after Martinez et al., 2013). The medial cerebral vein is positioned posterodorsal to the fossa auriculae cerebelli, just below the suturnal contact with the parietal. The fossa auriculae cerebelli is located posterior to the auditory bulla on the inner side of the supraoccipital and housed the sinus occipitalis and cerebellum.

Basioccipital

The basioccipital participates in the floor of the foramen magnum and forms the central portion of the occipital condyle (Figures 7–9). The condyle is wider than high in posterior view. In ventral view, the condyle is transversely wider at the posterior end, and forms a subtriangular bulge. This bulge is limited by a transversely narrow condylar neck.

In posterior view, the condyle is subcrescentic and is convex both dorsoventrally and transversely. It has a short neck, which projects directly posteriorly, probably extending almost parallel to the long axis of the skull. The dorsal surface of the basioccipital condyle is strongly concave. The basal tubera (basioccipital tubera) emerge immediately anteroventral to the neck of the condyle.

The basioccipital processes that form the basal tubera expand anteroventrally as divergent processes, with an almost right angle between them. The processes are transversely broad due to the lateral contribution of the ventral projections of the opistotical/exoccipital portion.

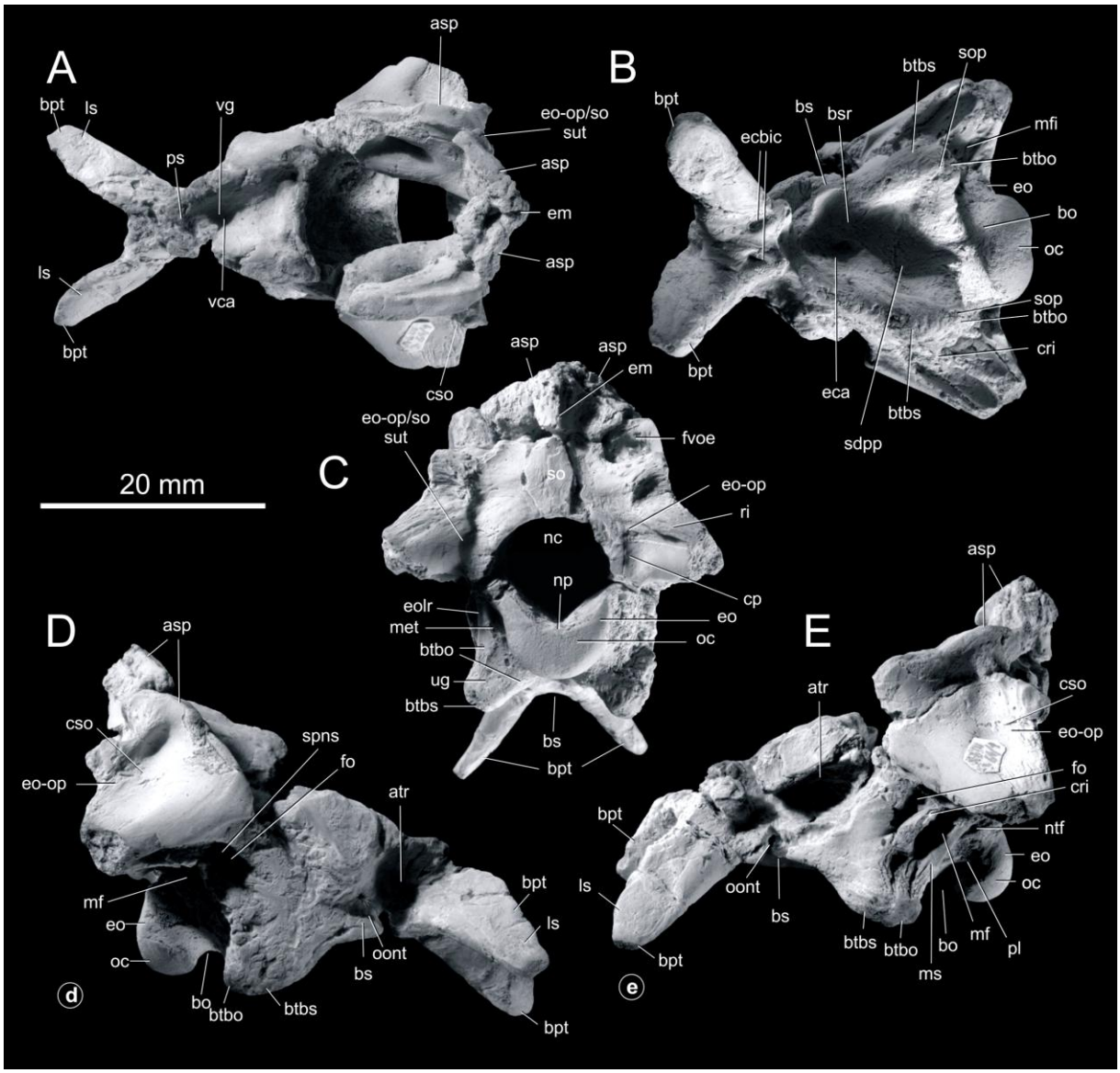

Figure 9. Photographs of the braincase ZPAL Ab III/364/1 of *Silesaurus opolensis* in dorsal (**A**), ventral (**B**), posterior (**C**), right lateral (**D**), and left lateral (**E**) views.

Abbreviations: asp – articular surfaces for parietal, atr – anterior tympanic recess, bo – basioccipital, bpt – basipterygoid process, bs – parabasisphenoid, bsr – parabasisphenoid recess, btbo – basal tuber of basioccipital, btbs – basal tuber of parabasisphenoid, cp – concavity for proatlas, cri – crista interfenestralis, cso – contact between the supraoccipital and otoccipital, eca – Eustachian canal, ecbic – entrances of cerebral branches of internal carotid artery, em – eminence, eo – exoccipital, eolr – lateral ridge on exoccipital, eo-op – exoccipital-opisthotic, eo op/so sut – exoccipital-opisthotic/supraoccipital suture, fo – fenestra ovalis, fvoe – foramen for the vena occipitalis externa, met – metotic foramen, mf – metotic fenestra, mfi – metotic fissure, ms – metotic strut, nc – neural canal (= foramen magnum); np – notochordal pit, ntf – nerve XII foramina, oc – occipital condyle, oont – openings of oculomotor nerve III, pl – posterior lamina, ps – pituitary (hypophyseal) fossa; ri – ridge, ls – surface for articulation with laterosphenoid, sdpp – subtriangular depression from the posteroventral surface of the parabasisphenoid, so – supraoccipital, sop – small openings (?nutrient foramina), spns – single opening (cranial nerve VI?), vca – Vidian canal, vg – ventral groove, ug – unossified gap.

Otoccipital (= opisthotic-exoccipital)

The opisthotic and the exoccipital are fused (Figures 7–9), forming the otoccipital (*sensu* Sampson & Witmer, 2007 after Bittencourt et al., 2015). The otoccipital articulates anteriorly with the prootic, anterodorsally with the parietal, mediodorsally with the supraoccipital, posteroventrally with the basioccipital, and anteroventrally with the parabasisphenoid. The contact with the parietal, squamosal and quadrate is visible due to disarticulation of specimens. Only a left complete otoccipital is preserved in specimens ZPAL Ab III/361/35, 36, 38, and 362/1. In the latter, it is separated from the rest of the braincase. The sutural articulation for the exoccipital opisthotic is composed of two rugose lines, one facing anteroventrally and the other ventrolaterally. Another suture continues from the anteroventral point of the supraoccipital towards the distal end of the paroccipital process and connects the otoccipital with the opisthotical part of the prootic.

The paroccipital process is elongated and projects posterolaterally and ventrally from its base. The process has slightly a concave dorsal margin in posterior view, in contrast to the ventral margin, which is straight and forms an angle 45° to the distal margin in posterior view. In dorsal view, the paroccipital processes form an angle of about 120°.

In posterior view (Figures 7–9), the region of the opisthotic immediately dorsolateral to the border of the foramen magnum shares the concavity for the proatlas with the exoccipital, which diminishes along the paroccipital process. A distinct ridge is located just above this concavity. It begins at the contact between the supraoccipital and the exoccipital, and continues towards the distal end of the opisthotic. It has a variable length. The opisthotic bears a shallow concavity surrounded anteriorly by the opisthotical and the posterodorsal portions of the prootic. A ridge (otosphenoidal crest) continues from the anterior aspect of the mid-length of the paroccipital process onto the laterodorsal portion of the prootic in anterodorsal view.

In ventrolateral view, three laminae appear on the ventral portion of the opisthotic and continue on the exoccipital as described above. The most anterior of them is the crista interfenestralis that separates the fenestra ovalis from the metotic fissure. The intermediate lamina is entirely on the exoccipital lateral surface, and has been described above as the metotic strut. The metotic strut projects ventrally and connects the opisthotic to the basal tubera. The metotic fissure has been referred to as the metotic fenestra (Nesbitt, 2011), jugular foramen (Dzik, 2003) or homologous to the fenestra cochleae (Gower & Weber, 1998; Sampson & Witmer, 2007; Bittencourt et al., 2015). The posterior lamina, which is limited by

a short transverse crest at the mid-height of the foramen magnum, is also restricted to the exoccipital.

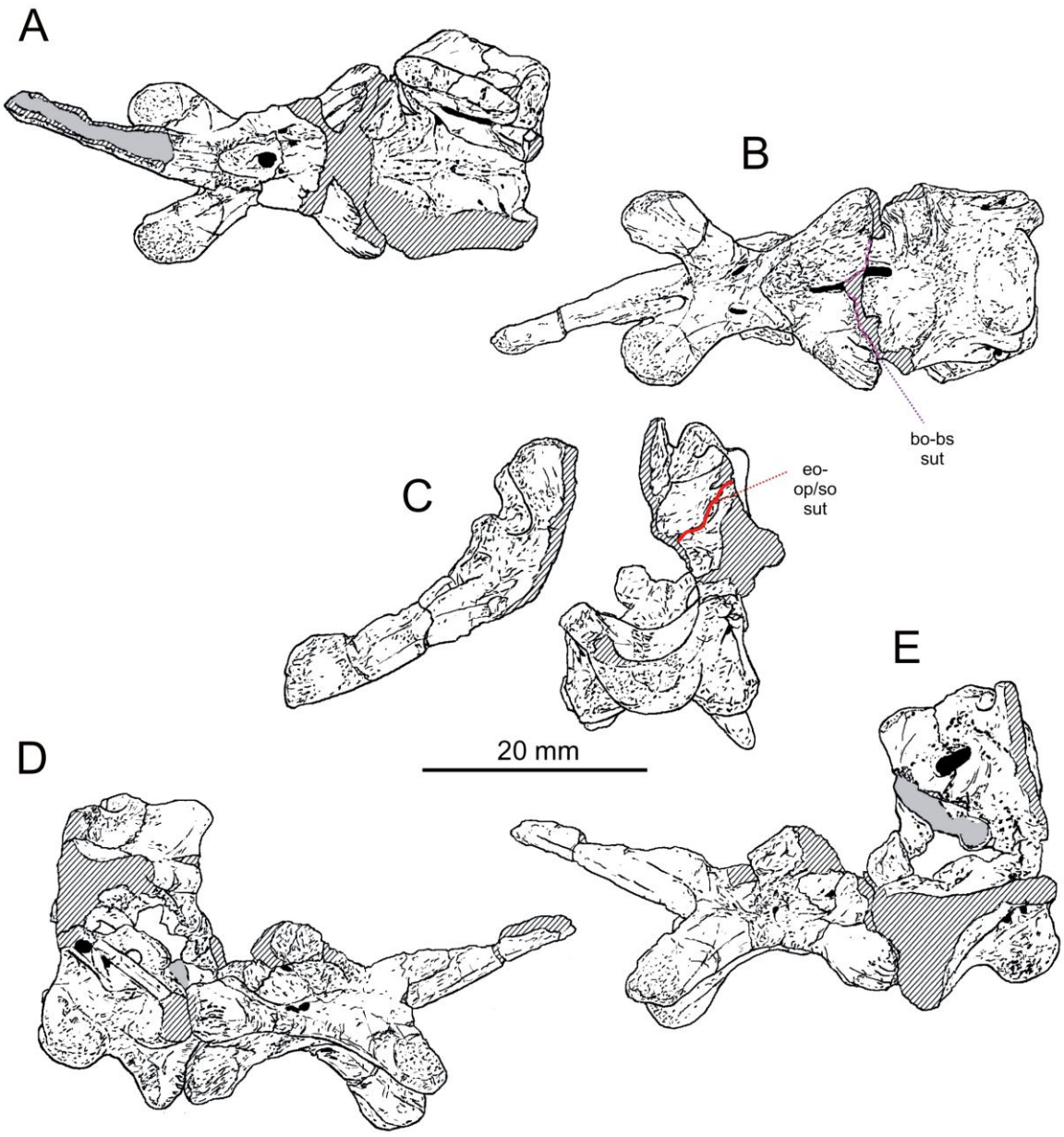

Figure 10. Interpretive drawings of braincase elements of ZPAL Ab III/361/35, 36, 38 from Figure 7. **A,** dorsal; **B**, ventral; **C**, posterior; **D**, right lateral; **E**, left lateral view. Cross-shading denotes areas with fracture surface, matrix infill or artificial material.

Abbreviations: bo-bs sut – basioccipital-parabasisphenoid suture, eo op/so sut – exoccipital-opisthotic/supraoccipital suture.

Both exoccipitals are preserved in all *Silesaurus* braincases (Figures 7–9), but in specimen ZPAL Ab III/361/35, 36, 38 the left-side is incomplete. The exoccipital is fused with the

opisthotic and forms the lateral and ventral wall of the foramen magnum. Its posterior surface shows concavities for the proatlas articulation dorsolateral to the foramen magnum.

Laterally, the exoccipital is pierced by the metotic fenestra and more posteriorly located hypoglossal nerve XII foramina, which are separated by the metotic strut. The strut extends from the lateroventral surface of the exoccipital down to the basal tubera, and forms the posterior wall of the metotic fenestra.

In medial view, the exoccipital is almost vertically corrugated and shows two inner openings for the hypoglossal nerve XII, and more anterior opening of the jugular foramen enclosed in the bone. Both exoccipitals meet along the midline endocranial cavity (see ZPAL Ab III/361/35, 36, 38; ZPAL Ab III/364/1). Thus, the basioccipital does not participate in this part of the braincase (Nesbitt, 2011).

Prootic

Both prootics are complete in specimen ZPAL Ab III/362/1, but are covered internally by a limestone concretion. The medial morphology of the prootic is exposed in specimens ZPAL Ab III/364/1 and 361/35, 36, 38 (Figures 7–9). The prootic forms most of the lateral portion of the braincase. Its long axis forming an angle of approximately 55° to the horizontal. Two large fossae are visible in lateral view. The first one is posterodorsally and the second one anteroventrally positioned to the notch for the cranial nerve V. The anteroventral fossa continues on the parabasisphenoid, and in dinosaurs is either considered the recessus tympanicus dorsalis (Baumel & Witmer, 1993; Witmer, 1997) or a surface for attachment of M. adductor mandibularis externus profundus (Vanden Berge & Zweers, 1993; Holliday, 2009). The lateral surface of the dorsal region of the prootic (below the foramen for cranial nerve V) is flat and ventrally bears with a thick and curved ridge.

The posterodorsal margin of the prootic, which originally contacted the parietal, is slightly convex and limited by a small groove posteriorly and cranial nerve V notch anteriorly. The notch is located between the posterior part of the prootic and the clinoid process. The notch for cranial nerve V is very deep and dorsolaterally directed. The upper borders of the notch slightly converge anterodorsally. The clinoid process has a distinctive subtriangular shape in anterior view and a subtriangular contact with the parietal. A very gentle vertical ridge is visible on the lateral surface of the clinoid process. However, it is only preserved on the right side of the specimen ZPAL Ab III/362/1. Anteroventral to the trigeminal notch is a smooth, trapezoidal surface for the origin of the M. protractor pterygoidei et quadrati (Vanden Berge

& Zweers, 1993). The sharp posteroventral border of the bone forms the posterodorsal border of the external foramen for cranial nerve VII (nervus facialis), which is located ventral to the opening for cranial nerve V.

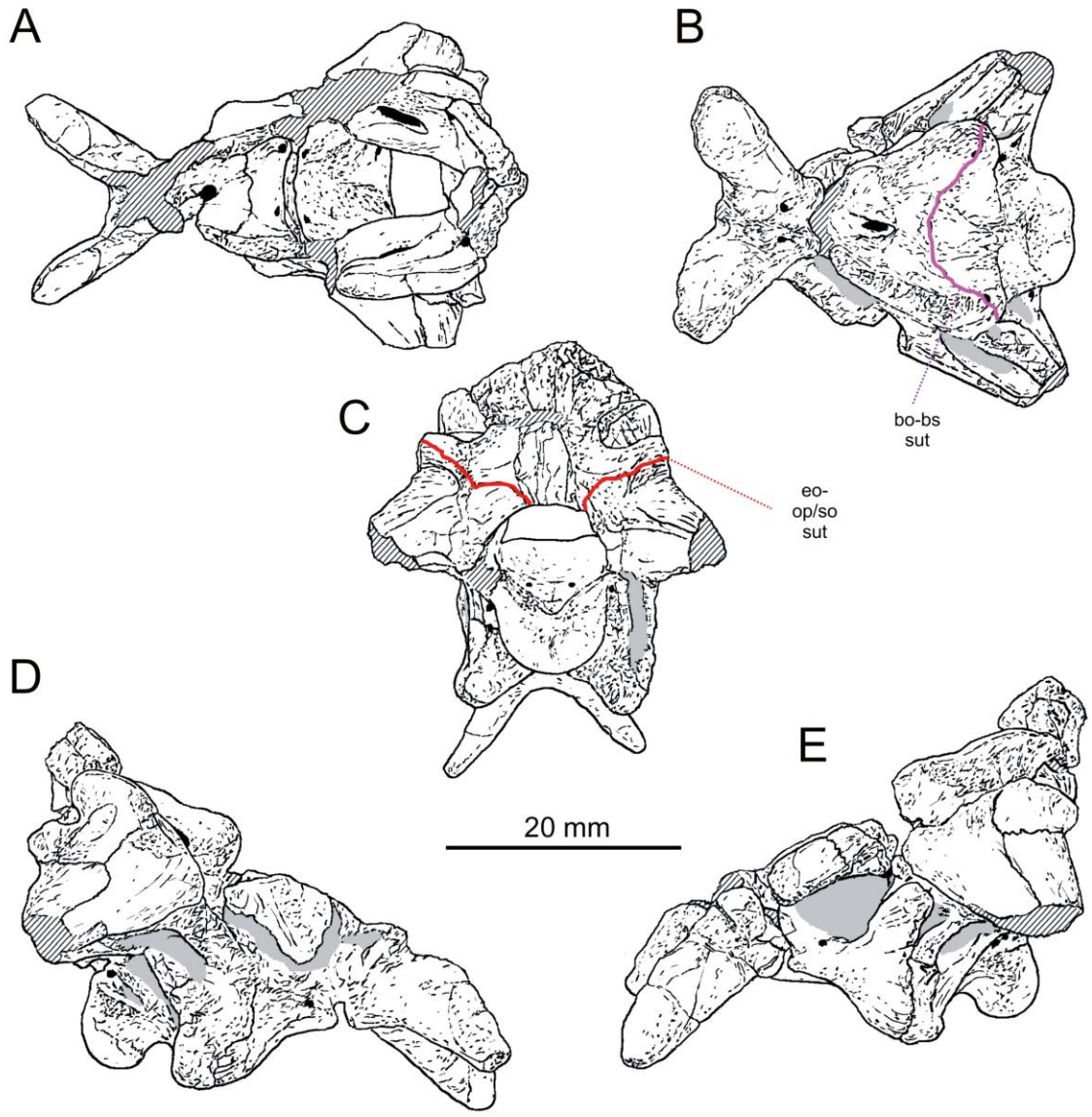

Figure 11. Interpretive drawings of braincase elements of ZPAL Ab III/362/1 from Figure 9. **A**, left lateral; **B**, right lateral; **C**, posterior; **D**, dorsal; **E**, ventral view.

Abbreviations: bo-bs sut – basioccipital-parabasisphenoid suture, eo op/so sut – exoccipital-opisthotic/supraoccipital suture.

Note: Cross-shading denotes areas with fracture surface, matrix infill or artificial material.

The attachment area for the protractor pterygoidei et quadrati is short. In dorsal view (Figures 7–9), the elongate posterior articular surface of the prootic and the clinoid process

form an angle approximately of 120° and face dorsomedially. This surface is semirectangular and has several narrow sulci.

In medial view, the posterodorsal part of the prootic and anterodorsal part of the supraoccipital share almost equally the fossa auriculare cerebella. The prootic portion of the fossa is anterodorsally limited by the eminentia canalis semicircularis and ventrally by the medial wall of the auditory bulla. The auditory bulla surrounds the vestibular recess and inflates towards the cavum crani. Immediately anteroventral to the auditory bulla, there is the fossa acustica interna (Baumel & Witmer, 1993). Specimen ZPAL Ab III/364/1 shows two foramina, one above another. These are probably openings for undivided roots of nervus vestibulocochlearis (cranial nerve VIII) and nervus facialis (cranial nerve VII). The ventral extremity bears the foramen for the crus osseum commune and a notch.

Parabasisphenoid

Generally in archosauriforms (e.g., Ewer, 1965; Walker, 1990; Parrish, 1993; Yates, 2003; Bittencourt et al., 2015; Sobral et al., 2016), both the parasphenoid and basisphenoid are co-ossified and are referred as the parabasisphenoid. That forms the ventral part of the *Silesaurus* braincase and is positioned ventral to the prootics (Figures 7–9). The ventral surface of the parabasisphenoid was aligned more horizontally than vertically in *Silesaurus*.

The parabasisphenoid contacts the basioccipital posteriorly and the pterygoids anteriorly *via* the basipterygoid articulation. The junction between the basioccipital and the parabasisphenoid can be traced in all studied specimens. A rather deep fissure separates the parabasisphenoid from the basioccipital in ventral view. This suture is expressed as a gently meandering line and projects anteriorly, forming a triangular outline (Figures 10–12). Two small openings (?nutrient foramina) are located inside that suture, on the apex of the basal tubera.

The basal tubera equally contribute to the parabasisphenoid and the anterior part of the basioccipital. In addition, the parabasisphenoid contribution to the basal tubera extends posteroventrally and laterally from near the posteroventral margin of the fenestra ovalis. The tubera are relatively short, subtriangular processes that project ventrolaterally. A very deep subtriangular depression separates the basal tubera anteriorly and covers a major part of the posteroventral surface of the parabasisphenoid. A longitudinal opening of the median Eustachian canal is present at the deepest point of the depression, where the right-left

basioccipital-parabasisphenoid sutures converge obliquely. The anterior part of the basal tubera are connected to each other and form the elevated anterior border of the depression.

Anterior to this depression, *Silesaurus* has two entrances of the cerebral branches of the internal carotid artery between the posterior margins of the bases of the basipterygoid processes.

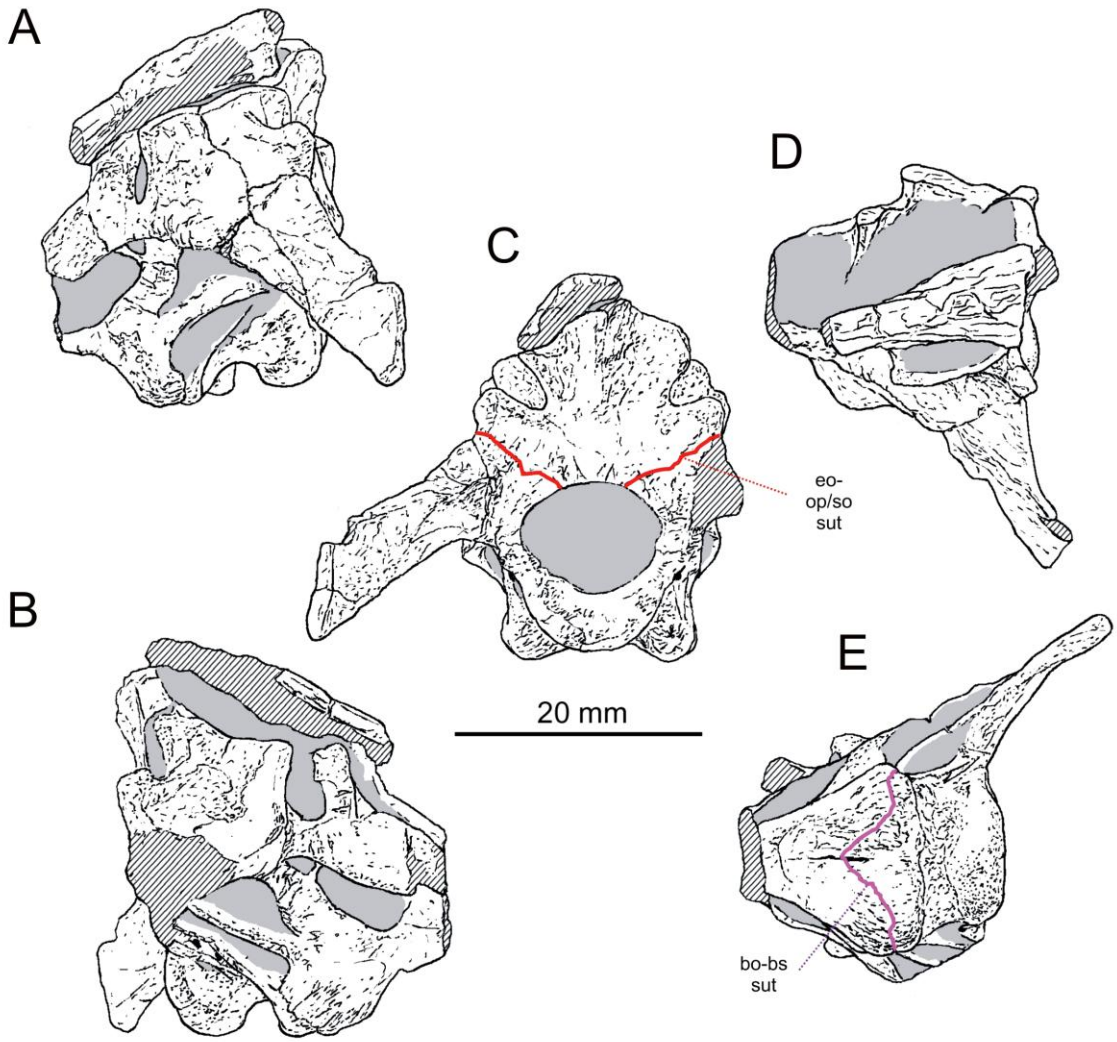

Figure 12. Interpretive drawings of braincase ZPAL Ab III/364/1 elements from Figure 8. **A**, dorsal; **B**, ventral; **C**, posterior; **D**, right lateral; **E**, left lateral view.

Abbreviations: bo-bs sut – basioccipital-parabasisphenoid suture, eo op/so sut – exoccipital-opisthotic/supraoccipital suture.

Note: Cross-shading denotes areas with fracture surface, matrix infill or artificial material.

In lateral view (Figures 7–9), the main body of the parabasisphenoid has a triangular shape, narrowing anteriorly. Its dorsolateral surface has a subrectangular shape. The sharp border of

this surface is delimited by the posteroventrally to anterodorsally oriented anterior tympanic recess. This recess is deep and is located just anteroventral to the fenestra ovalis. A single opening (cranial nerve VI?) is visible at the base of the tympanic recess in specimen ZPAL Ab III/364/1.

The basipterygoid processes are almost twice as long as the basal tubera. They are oriented anteroventrally in lateral view. In ventral view, they diverge ventrolaterally arising from the base of the basisphenoid close to its junction with the parasphenoid. In specimen ZPAL Ab III/361/35, 36, 38 they are subcircular in lateral view (contrasting with ZPAL Ab III/364/1, in which they become narrower towards their distal ends), and their distal tips bear distinct articular facets for the pterygoids.

The parabasisphenoid is concave internally, probably housing the optic lobe. Five openings for cranial nerves are visible internally on the floor of the braincase. Two of them are localized on the base of the parabasisphenoid and are recognised as cranial nerve VI (abduces) foramina VI. Another two exist on the anterior cerebral part of the braincase; they are cranial nerve III (oculomotor) openings. Finally, the fifth single opening is the Vidian canal, which is located anterior to the oculomotor foramina and is the largest of them.

A tall posterior ascending process of the parabasisphenoid was illustrated by Dzik (2003; Figure 13). However additional examination of all specimens shows that it is difficult to exactly verify the correlations of the parabasisphenoid to the fenestra ovalis. In ZPAL Ab III/364/1 this process seems robust and tall, but is only visible on the left side of braincase. There are no signs of the processes on a second braincase (ZPAL Ab III/361).

Cultriform process

Only specimen ZPAL Ab III/361/38 preserved the cultriform process of the parabasisphenoid (Figure 7). It is sub-triangular in cross section, and becomes narrower at its anterior part. Dorsally, it houses a relatively deep longitudinal groove. The cultriform process seems to be horizontally oriented and situated ventrally relative to the occipital condyle. Between the cultriform and the basipterygoid processes, two very deep longitudinal, vertical pockets are seen.

Pneumatization of the parabasisphenoid

Examination of all braincase specimens suggests the lack of true pneumatic cavities in *Silesaurus*. Some broken surfaces expose trabeculate bone, which suggests the presence of

less dense internal spaces within a compact bone, but there is no evidence that such areas were connected to external spaces *via* a foramen. However, according to some authors (see Sobral et al., 2016 and references cited therein) the pneumatic system of the archosauromorph braincase also included relatively shallow recesses that did not necessarily perforate the adjacent bones. If one accepts this assumption, some recesses observed in the braincase of *Silesaurus* (Figures 7–9) could be described as pneumatic structures, including the parabasisphenoid recess (= ventral median pharyngeal recess; *sensu* Sobral et al., 2016) and the lateral depression of the parabasisphenoid.

The parabasisphenoid recess is known in basal archosauriforms (e.g., *Euparkeria*), some pseudosuchians (e.g., *Saurosuchus*), dinosauriforms (e.g., *Lewisuchus*), and basal dinosaurs (e.g., *Herrerasaurus*, *Eoraptor*). It is worth adding that a similar parabasisphenoid depression is present in several non-archosauriform reptiles (see Heaton, 1979; Evans, 1986; Gardner et al., 2010), but it is well-developed (extremely deep and broad) only in the large Late Triassic archosaur *Smok wawelski* (Niedźwiedzki et al., 2012) and in neotheropod dinosaurs (Rauhut, 2003; Nesbitt et al., 2009; Witmer & Ridgely, 2009; Nesbitt, 2011; Xing, 2012) while absent or poorly developed in ornithischians (e.g., *Lesothosaurus*) and sauropodomorphs (e.g., *Thecodontosaurus*, *Massospondylus*, *Plateosaurus*), indicating that this trait is common to the earliest dinosaurs and their direct ancestors and was modified later in the evolution of early dinosaurs.

Silesaurus braincase bears a deep depression located on the lateral surface of the parabasisphenoid, posterodorsal to the basipterygoid process (Figures 7–9), the presence of which among archosaur, according to Nesbitt (2011), is restricted to dinosauromorphs. According to Gower & Weber (1998) the deep lateral depression of the parabasisphenoid is present in *Euparkeria*, but contra Welman (1995), they suggest that it is not homologous to the anterior tympanic recess of dinosaurs and birds. However, Sobral et al. (2016) suggested that the lateral depression in *Euparkeria* corresponds topologically to the anterior tympanic recess of dinosaurs and birds. I confirm that the anterior tympanic recess of *Silesaurus* lacks pneumatic sinuses (see Nesbitt, 2011), but I agree also with the observation of Sobral et al. (2016) that it is extremely similar both in terms of morphology and topology to the lateral depression of *Euparkeria*. The anterior tympanic recess of *Silesaurus* is deeper and larger than that of *Euparkeria*, with a lateral expansion of the parabasisphenoid marking its anterior limit (Sobral et al., 2016).

Structures very similar to the lateral depression or anterior tympanic recess are visible in the braincases of some non-crocodylomorph pseudosuchians (Sobral et al., 2016 and

references cited therein), so the presence of such a recess does not necessarily suggest ornithodiran or dinosauriform affinities. This issue requires further research and some new discoveries clearly demonstrate that early avemetatarsalians had rather complex evolutionary histories (see Nesbitt et al., 2017).

Variability of the braincase

As it is in some postcranial skeletal elements (see Piechowski et al., 2014), the specimens of *Silesaurus* differ from one another in several aspects of the braincase proportions (Figures 13, 14, Table 4).

The supraoccipital of ZPAL Ab III/362/1 is broader than that of ZPAL Ab III/364/1 (the former height is 20.5 mm and width is 16 mm, the latter 21 mm and 14 mm respectively). The most notable difference between them is the shape and extent of the longitudinal eminence (nuchal or sagittal crest) on the posterior surface of the supraoccipital. In ZPAL Ab III/362/1 this structure is high but limited to the upper half of the bone. It is wedgeshaped and smoothly merges with the rest of the supraoccipital. In contrast, in ZPAL Ab III/364/1 the longitudinal eminence is robust and reaches the foramen magnum, continuing across the whole bone. In this specimen the structure is flat ventrally and is slightly expanded laterally, especially just below the notches for the vena occipitalis externa. Compared to ZPAL Ab III/362/1, the longitudinal eminence in ZPAL Ab III/364/1 has distinct lateral edges. The supraoccipital processes lateral to the notch for of the vena occipitalis externa differ in a similar manner. In ZPAL Ab III/362/1, these structures are smooth and rounded but distinct, whereas in ZPAL Ab III/361/35, 36, 38 and ZPAL Ab III/364/1 they are angular, more integrated with the braincase and have a ridge along the whole posterior surface. There are distinct fossae of variable depth lateroventrally to them, which are visible on the lateral surface of the braincase. These are deeper than the fossa for vena occipitalis externa in ZPAL Ab III/364/1 and ZPAL Ab III/362/1 but not in ZPAL Ab III/361/35, 36, 38. Another ridge is visible on the proximal part of the paroccipital process of all specimens, but is robust only in ZPAL Ab III/364/1.

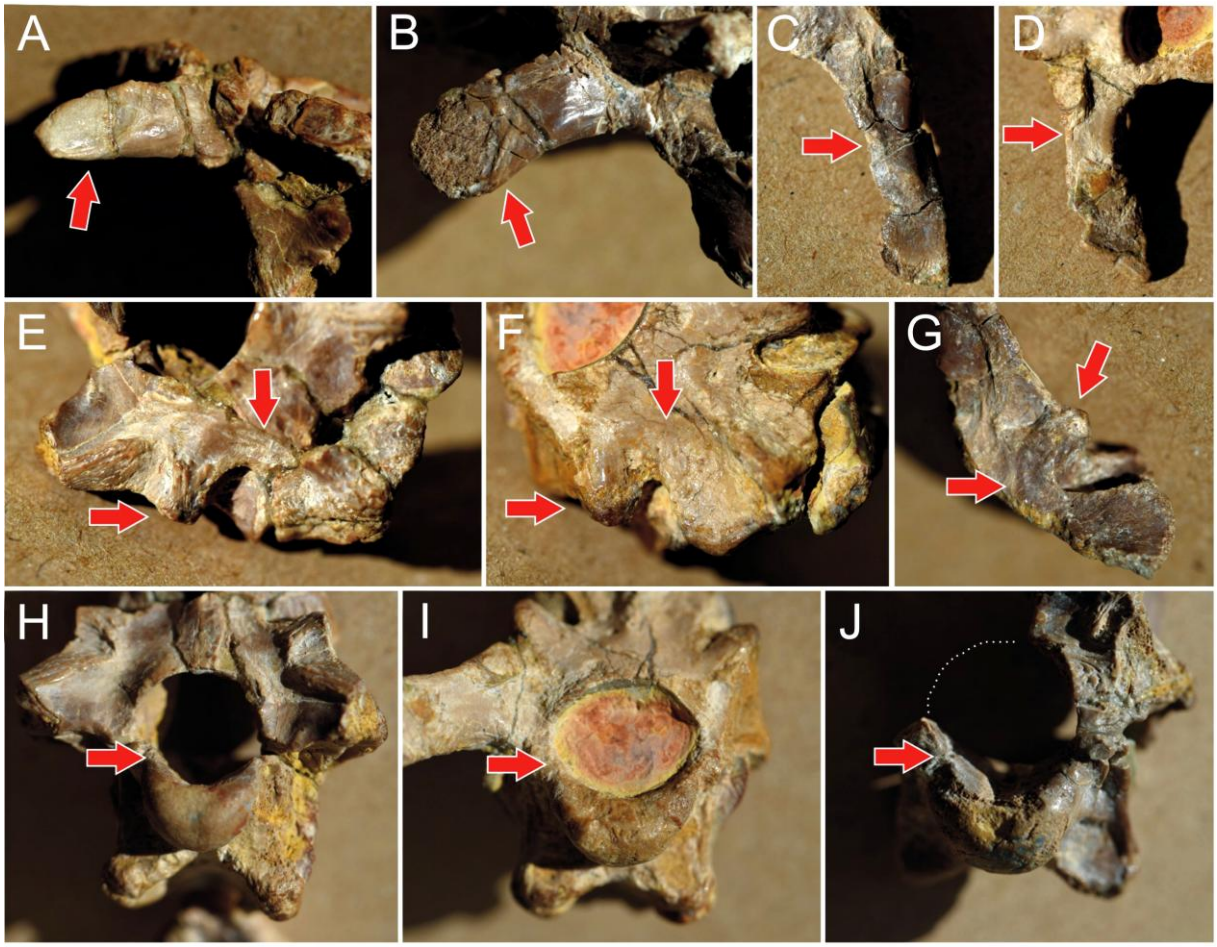

Figure 13. Comparison of *Silesaurus opolensis* braincase specimens. **A**, **B**, basipterygoid process in ZPAL Ab III/364/1 and 362/1. **C**, **D**, paroccipital process in ZPAL Ab III/361/35, 36, 38 and 362/1. **E**–**G**, supraoccipital process and ridge on supraoccipital process below dorsal head vein in ZPAL Ab III/364/1, 362/1, and 361/35, 36, 38. **H**–**J**, foramen magnum and occipital condyle in ZPAL Ab III/364/1, 362/1, and 361/35, 36, 38. Red arrow indicates the differences between specimens.

One of the most striking differences of the specimens is the shape of the foramen magnum and occipital condyle. These are subcircular and narrow in ZPAL Ab III/364/1 and ZPAL Ab III/361/35, 36, 38, but much wider and oval in ZPAL Ab III/362/1 (the foramina magna have there almost the same height – about 9 mm, but the width is about 10, 10 and 11.5 mm respectively). In addition, ZPAL Ab III/364/1 and ZPAL Ab III/361/35, 36, 38 have both longer basal tubera than ZPAL Ab III/362/1. The angle between the basal tubera on the basioccipital is 95° in ZPAL Ab III/364/1, 110° in ZPAL Ab III/361/35, 36, 38 and 120° in ZPAL Ab III/362/1. Consequently, the fossa on the ventral side of parabasisphenoid-basioccipital is narrowest in ZPAL Ab III/364/1 and widest in ZPAL Ab III/362/1. The longitudinal opening of the medial Eustachian canal (the groove at the bottom of the fossa) is different in all specimens. In ZPAL Ab III/362/1 it starts from the parabasisphenoid-

basioccipital suture and ends shortly posterior (about 3 mm in total length). In ZPAL Ab III/364/1 it starts about 4 mm anterior to the suture. It is even shorter (about 2 mm) but wider in this specimen than in ZPAL Ab III/362/1. The third specimen (ZPAL Ab III/361/35, 36, 38) has this groove on both sides of the suture. It is the widest and the longest one (7 mm).

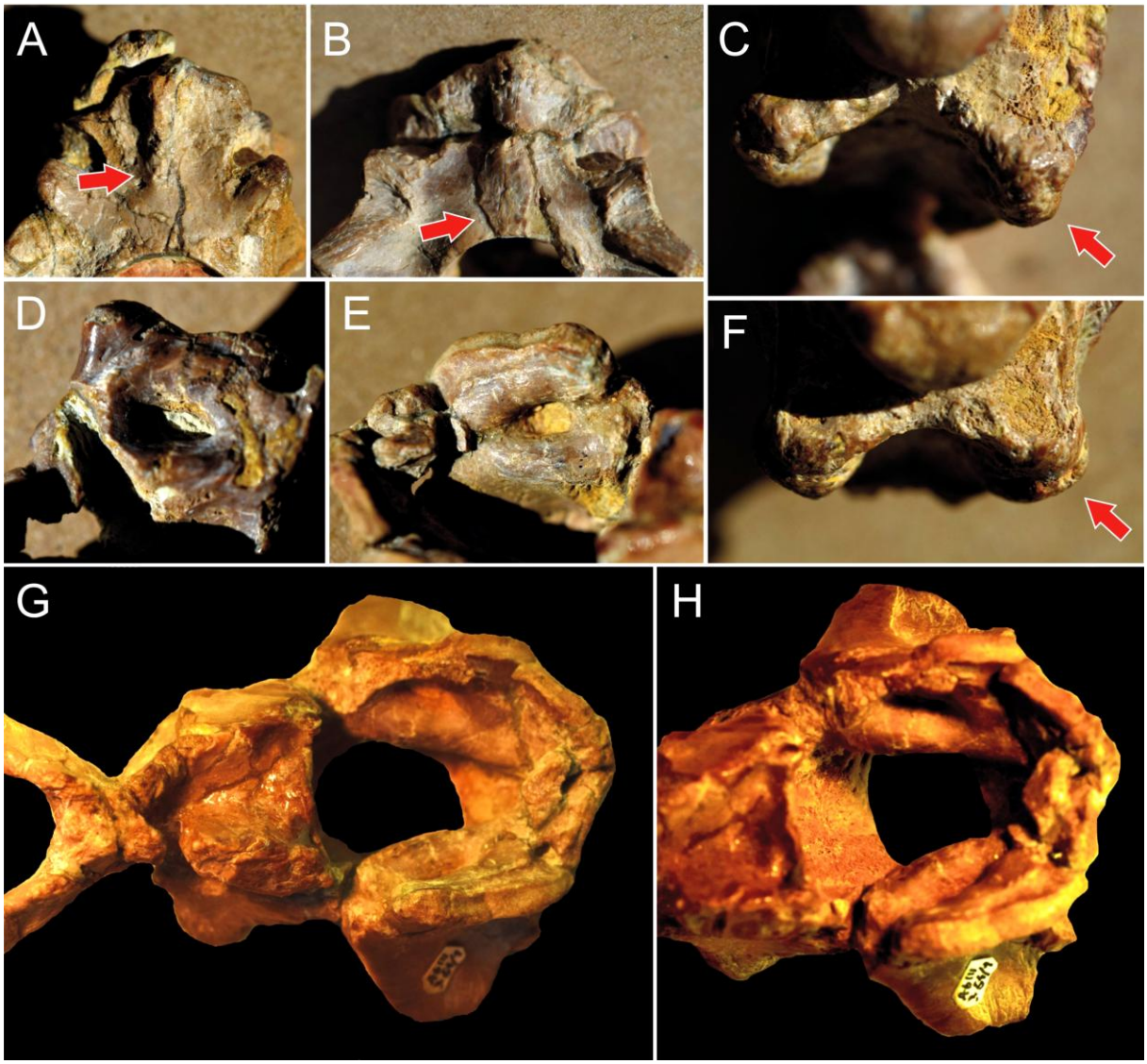

Figure 14. Comparison of *Silesaurus opolensis* braincase specimens. **A**, **B**, longitudinal ridge on paroccipital (ZPAL Ab III/364/1 and 362/1. **C**, **D**, flocullar lobe of cerebellum (fossa auriculare cerebelli) and the auditory bulla (ZPAL Ab III/364/1 and 362/1). **E**, **F**, shows robustness and size of basal tubera (ZPAL Ab III/364/1 and 362/1). **G**, **H**, internal surface of the braincase ZPAL Ab III/364/1. Red arrow indicates the differences between specimens.

One of the most distinct differences among the braincases of *Silesaurus* is the shape of the basipterygoid process, preserved only in ZPAL Ab III/361/35, 36, 38 and ZPAL Ab III/364/1. In the former, the processes taper distally, but are rounded and broader at the distal end in the

latter. Additionally, the latter have these processes enhanced by a longitudinal ridge on their ventromedial side. These differences obviously determine different shapes of the articulation surfaces.

Another aspect of variability is visible on the medial side of the prootic-supraoccipital contact in ZPAL Ab III/361/35, 36, 38 and ZPAL Ab III/364/1 (ZPAL Ab III/364/1 is filled with sediment). The former has a relatively large flocullar lobe of the cerebellum (fossa auriculare cerebelli) and the auditory bulla is just below and slender, with an additional ridge. In contrast, the lobe in the latter braincase is much smaller and the bulla is robust and smooth.

The observed variability in the braincases of *Silesaurus* is apparently linked to its musculature. While ZPAL Ab III/362/1 has a relatively smooth posterior surface, with only a minor sagittal eminence of the supraoccipital and a ridge on the paroccipital process, ZPAL AbIII/361/35, 36, 38 and ZPAL Ab III/364/1 have more robust structures and an additional ridge below the notch for vena occipitalis externa. These structures mark the attachment of the neck muscles M. biventer cervicis (and other) and M. splenius capitis (medial part), (see Table 5 and Tsuihiji, 2005). Similarly, ZPAL Ab III/362/1 has shorter and more obtuse basal tubera than the others, where the M. rectus capitis dorsalis and M. rectus capitis ventralis attach (see Table 5 and Tsuihiji 2007). These differences suggest a better developed musculature in ZPAL Ab III/361/35, 36, 38 and ZPAL Ab III/364/1.

A similar division into robust and gracile forms has been observed in braincases of the Late Jurassic macronarian sauropod *Europasaurus* (Marpmann et al., 2014). Sexual dimorphism was proposed to explain different femoral forms of *Silesaurus* (Piechowski et al., 2014), but sexual dimorphism is probably not the case here as the ‘gracile’ ZPAL Ab III/362/1 and the ‘robust’ ZPAL Ab III/364/1 both have additional ossifications on femora, indicating that they are likely female. However, the long bones of the two discussed specimens have markedly different lengths (see Table 1), and clearly belong to animals of different sizes, even if the differences in braincase size are only moderate. Such allometric shifts have been observed in several tetrapods and *Coelophysis* (e.g., Rinehart et al., 2009) and possibly means that variation in muscle attachments to braincases was probably size dependent in *Silesaurus* and *Coelophysis*, and developed throughout growth.

Allometric differences probably also account for the different shapes of the foramen magnum and occipital condyle in *Silesaurus*. In at least some reptiles, the relative size of the foramen magnum is reduced due to negative allometric growth of the brain (Monteiro & Abe, 1997). The narrowing of the foramen is correlated with an expansion of the exo- and

supraoccipitals where the neck muscles attach, a condition also correlated with size increase in some reptilian taxa (Monteiro & Abe, 1997).

Other differences between the braincases can be observed, which do not fit the distinction of 'robust' and 'gracile' specimens. Each specimen (in which the condition can be observed) has a different geometry of the fossa on the ventral side of the parabasisphenoid-basioccipital, the basipterygoid processes, and the auditory bulla, the size of the flocullar lobe of the cerebellum, and the length and position of the longitudinal opening of the median Eustachian canal. The differences are especially visible in the two 'robust' braincases ZPAL Ab III/364/1 and ZPAL Ab III/361/35, 36, 38. I interpret these differences as intraspecific (probably within the population) variability, as this is known also in other archosauromorphs (e.g., Borsuk-Białynicka & Evans, 2009; Gold et al., 2014; Gower et al., 2014).

Table 4. Variability of the braincase of *Silesaurus opolensis*.

Character\number of specimens	**ZPAL Ab III/362/1**	**ZPAL Ab III/361/35, 36, 38**	**ZPAL Ab III/364/1**
Supraoccipital (width/height in mm)	205/160	?	210/140
Longitudinal eminence on posterior side of supraoccipital	Appears in the middle part of the bone	?	Reaches the edge of the foramen magnum
Supraoccipital process (below dorsal head vein)	Robust	Delicate	Intermediate
Ridge on supraoccipital process (below dorsal head vein)	Absence	Indistinct	Distinct
Foramen magnum/occipital condyle	Semi-oval and wide	Round and narrow	Round and narrow
Longitudinal ridge on paroccipital	Distinct	Indistinct	Indistinct
Distal end of paroccipital	Tapering tightly	Slightly expanded and blunt	?
Fossa on ventral side of supraoccipital	Deep	Shallow	Deep
Basal tubera	Short	Short	Long
Robustness of basal	Robust	?	More slender

tubera			
Groove in fossa on ventral side of basisphenoid	More behind and short	Centrally located and long	More in front and short
Fossa on ventral side of basisphenoid	Deep and narrow	Deep and narrow	Wide and shallow
Basipterygoid process	?	Wide and flat at the distal end	Tapering tightly
Flocullar lobe of cerebellum between prootic and epiootic/auditory bulla	?	Large/delicate with small ridge	Clearly smaller/massive and smooth
Lateral surface of the supraoccipital lateral process	Rounded	Rounded	Flat

Significance of braincase osteology

The braincase morphology of *Silesaurs* shows some similarities to that of *Euparkeria capensis*, the dinosauriform *Lewisuchus*, basal sauropodomorphs (e.g., *Thecodontosaurus*) and early ornithischians (e.g., *Lesothosaurus*). It lacks the deep and expanded parabasisphenoid recess that is characteristic of neotheropod dinosaurs. The first stage in formation of such recess can be seen in *Lewisuchus*, a small carnivorous dinosauriform from the late Ladinian/early Carnian of Argentina. *Lewisuchus* has previously been considered either a member of Silesauridae (Nesbitt, 2011) or a dinosauriform predating the Siliesauridae-Dinosauria split (Bittencourt et al., 2015). The relatively shallow parabasisphenoid recess in *Silesaurus* resembles that of basal sauropodomorphs and ornithischians, but this condition is most probably plesiomorphic along early dinosauriform braincase evolution. The supraoccipital of *Silesaurus* (Figures 7–9) is almost identical to that of *Panphagia* in posterior view (Martinez et al., 2013). However, the bone differs from that of *Panphagia* because it forms a larger part of the dorsal border of the foramen magnum. The passage for vena occipitalis externa through the supraoccipital is oblique to the occipital surface, as has been described for *Panphagia* (Martinez et al., 2013), the juvenile *Massospondylus* (Gow, 1990), and *Lewisuchus* (Bittencourt et al., 2015). The notches are elliptical and deeply incised in the supraoccipital body, and because of that they are presumed to be homologous to the posttemporal opening of dinosaurs (Langer & Benton, 2006; Nesbitt, 2011; Bittencourt et al., 2015). The processes laterally restricting the notches resemble more

those of *Adeopapposaurus* than those of *Panphagia* (Martinez et al., 2013) in posterior view. The supraoccipital possesses an elevated rugose contact with the otoccipital, resembling the condition in *Euparkeria*, *Herrerasaurus*, and some other dinosauriforms (Nesbitt et al., 2010; Nesbitt, 2011; Bittencourt et al., 2015). The lateral and posteroventral articular surfaces for the exoccipital-ophistotic are angled at nearly 90° to one another in posterior view, as in *Panphagia* (Martinez et al., 2013). Meanwhile, the posterior groove of the prootic may represent the ventral border of the opening for the vena parietalis, as in *Plateosaurus* (von Huene, 1926; Galton & Kermack, 2010), or a pneumatic opening, as suggested for *Coelophysis kayentakatae* (Tykoski, 1998). The ratio between its length along the long axis of the prootic to the length along its orthogonal axis in the sagittal plane is similar to that in *Lesothosaurus*, and some sauropodomorphs (e.g., *Plateosaurus*), but shorter than in *Panphagia* (Martinez et al., 2013).

There are several other anatomical similarities between the *Silesaurus* braincase and that of other early dinosauriforms. The supraoccipital margin of the foramen is proportionally narrow lateromedially compared with the rest of the ventral contour of the bone, similar to the condition of early dinosauriforms (Smith et al., 2007). In *Silesaurus*, the otosphenoidal crest extends from the posterior margin of the otoccipital, spanning anteriorly onto the lateral surface of the prootic, as observed in *Lewisuchus* and *Marasuchus* (Bittencourt et al., 2015). In the braincases of both *Silesaurus* and *Lewisuchus* the position of the hypoglossal nerve foramina is posterior to the metotic strut (Nesbitt et al., 2010; Nesbitt, 2011; Bittencourt et al., 2015) and I confirm that the same configuration can be seen in a partially preserved braincase of *Marasuchus* (Sereno & Arcucci, 1994; Bittencourt et al., 2015; Piechowski et al., 2015). According to Bittencourt et al. (2015), this configuration strongly suggests that the exit of cranial nerve XII occupied a similar position amongst non-dinosaur dinosauriforms. In addition, in both *Silesaurus* and *Lewisuchus*, the basipterygoid process is as long as the basal tuber, distally rounded, and there is no web of bone between the two processes (Bittencourt et al., 2015).

However, the braincase of *Silesaurus* is quite derived in that the paroccipital processes are directed ventrally, reaching the level of the ventral margin of the basioccipital condyle. In contrast, in *Euparkeria* and early ornithischians, theropods, and sauropodomorphs, these processes have an almost horizontal orientation (Sereno, 1991; Benton et al., 2000; Munter & Clark, 2006; Prieto-Márquez & Norell, 2011; Bittencourt et al., 2015; Sobral et al., 2016), only *Lewisuchus* also showing some ventral inclination (Bittencourt et al., 2015). Admittedly the *Lewisuchus* braincase is very low and wide like in crocodilians, so only a slight downward

bending of these processes results in that they reach the level of the ventral margin of the basioccipital condyle. According to some analyses (e.g., Kammerer et al., 2012), this shift in orientation is synapomorphic for silesaurids. Yet, compared to *Lewisuchus*, the braincase of *Silesaurus* is higher and narrower, approaching the condition seen in birds.

From an evolutionary point of view, the braincase anatomy of *Silesaurus*, compared with the dinosauriform *Lewisuchus*, the sauropodomorphs *Saturnalia*, *Thecodontosaurus*, *Efraasia*, ornithischian *Lesothosaurus* and theropod dinosaurs (Rauhut, 2003) suggests a pattern of character acquisition that eventually resulted in the highly modified condition of the neotheropods and rather small modifications to the braincases of early herbivorous dinosaurs.

Chapter 3. Head muscles[3]

The reconstruction of the craniocervical muscle organization and function is increasingly important in palaeobiological studies on dinosaurs. Particular attention has been directed to large-headed theropods (e.g., Bakker, 2000; Snively & Russell, 2007a, 2007b; Tsuihiji, 2010) but little is known about the craniocervical muscles of small and early dinosaurs (Smith, 2015).

Here, I present a preliminary reconstruction of the major craniocervical muscles for *Silesaurus* (Figure 15), which may help in understanding the evolutionary changes in the posterior part of braincase of early dinosaurs. The position and size of each muscle was inferred from skeletal similarities to other reptiles (e.g., Tsuihiji, 2005, 2007; Snively & Russell, 2007a, 2007b; Smith, 2015). *Silesaurus* is an ornithodiran (bird-line of archosaurs) and its braincase closely resembles those of non-archosaur archosauriforms and basal dinosaurs, but the general bird terminology (Vanden Berge & Zweers, 1993) of craniocervical muscles will be used here (Table 5).

M. biventer cervicis

M. biventer cervicis was a dorsomedial muscle in the cervical region of *Silesaurus*. Its insertion is limited in modern archosaurs (Tsuihiji, 2005) due to a highly modified dorsoposterior side of the skull. In *Silesaurus*, this area retains the primitive condition, similar to that of lepidosaurs. The insertion is represented by a posterior eminence (nuchal crest/sagittal crest) in the supraoccipital and was restricted to that bone. It was limited laterally by the dorsal head vein notch (Dzik, 2003). The insertion probably expanded dorsolaterally together with the supraoccipital, but not so much ventrally (Figure 15). The muscle is responsible for the dorsiflexion of the head (Snively & Russell, 2007a, 2007b).

[3] Part of this chapter was published in:
Piechowski, R., Niedźwiedzki, G. & Tałanda, M. 2015. New data on skull anatomy of *Silesaurus opolensis*. *13th Annual Meeting of the European Association of Vertebrate Palaeontologists, Opole, Poland; Jul 8–12. Abstracts*, p. 143.

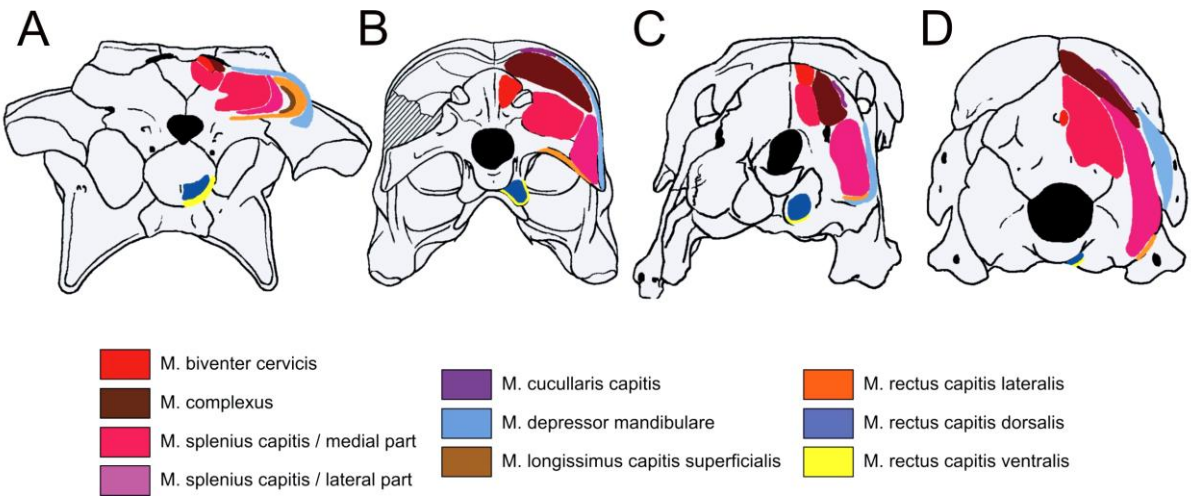

Figure 15. Attachments of muscles on the occipital region of archosaurs. **A**, Crocodilia (*Alligator mississippiensis*). **B**, Dinosauriform (*Silesaurus opolensis*). **C**, Theropoda, Oviraptorosauria (*Avimimus portentosus*). **D**, Aves (*Struthio camelus*, embryo). A, C, and D are based on the data presented by Tsuihiji (2007) and Tsuihiji et al. (2017).

M. cucullaris capitis

M. cucullaris capitis takes part in dorsiflexion of the head as well (Snively & Russell, 2007a, 2007b). It has various insertion areas in modern diapsids (Tsuihiji, 2007), but is usually located dorsolaterally. The muscle is covered by the depressor mandibulae externally in lepidosaurs and crocodilians. In birds, M. cucullaris capitis has an insertion above the depressor mandibulae. Accordingly, I reconstruct this muscle in a transitional position, on the posterodorsal edge of the parietal, where a distinct arched crista is present. This is just above M. complexus of *Sphenodon* and some birds (Tsuihiji, 2007).

M. complexus

M. complexus is a group of indistinct muscles taking part in the head dorsiflexion (Snively & Russell, 2007a, 2007b). They have common insertion and acts together in birds (Snively & Russell, 2007a, 2007b), but other diapsids have these muscles separated from one another. In *Silesaurus*, it is possible to see their separation on the posterior surface of the parietal. The dorsalmost portion of that bone has a clear depression, which corresponds to the insertion of M. transverse spinalis capitis lateralis in crocodiles. The parietal flattens ventrolaterally, creating an insertion for the M. splenius capitis, lateral part (Figure 15). It continues ventrally to meet the paroccipital process.

The ventral part of M. complexus is tentatively homologized with the crocodilian M. longissimus capitis superficialis (Snively & Russell, 2007a, 2007b), and inserted on the

distalmost portion of the paroccipital process, as in crocodiles (Snively & Russell, 2007a, 2007b). It is marked by a distinct scar with a rounded ventromedial border. The M. longissimus capitis superficialis is responsible for the lateral flexion of the head (Snively & Russell, 2007a, 2007b).

M. splenius capitis, medial part

The M. splenius capitis, medial part, inserts deep and medial to the M. complexus and homologous muscles in extant archosaurs (Snively & Russell, 2007a, 2007b). In *Silesaurus*, its insertion marks the third surface on the parietal. It is oriented more medially than the previous two insertion areas and forms a concavity for the muscle, in the lateral part of the supraoccipital and dorsal part of the paroccipital process. The two bones bear distinct ridges that delimit the insertion. The medial part of the M. splenius capitis was responsible for the dorsiflexion of the head (Snively & Russell, 2007a, 2007b).

M. rectus capitis lateralis

M. rectus capitis lateralis inserts on the ventrolateral end of the paroccipital process in birds, and in the distal and ventral edges of the same structure in crocodiles (Tsuihiji, 2007). In *Silesaurus* a slightly concave surface occurs ventrally on the paroccipital process. It fades distally, but a low longitudinal ridge emerges and continues to the end of the bone. All these elements probably represent the insertion sites for this muscle. The M. rectus capitis lateralis works in the ventrolateral flexion of the head (Snively & Russell, 2007a, 2007b).

M. depressor mandibulae

M. depressor mandibulae arises typically at the dorsolateral edge of the posterior face of the skull. This usually involves the parietal, squamosal and/or distal edge of the paroccipital process (Tsuihiji, 2007). I reconstruct this muscle insertion at the posterolateral edge of the parietal and the distalmost edge of the paroccipital process in *Silesaurus*. The action of this muscle is to open the jaws.

M. rectus capitis dorsalis

M. rectus capitis dorsalis has a very conservative insertion along the posteroventral margin on the basal tubera of the basioccipital of *Silesaurus*. The muscle arises from the posterior concavity on these structures. It is marked by a distinct edge and resembles the condition in

crocodiles (Snively & Russell, 2007a, 2007b; Tsuihiji, 2007). M. rectus capitis dorsalis was responsible for the lateral flexion of the head (Snively & Russell, 2007a, 2007b).

The ventral orientation of the paroccipital processes of *Silesaurus* resulted in the dorsoventral expansion of the M. complexus and M. depressor mandibulae, which occupied the dorsolateral part of the posterior side of the skull. The development of the M. complexus in birds is related to shell-breaking during hatching (Gross & Oppenheim, 1985) and begging behavior (Ashmore et al., 1973; Schwabl & Lipar, 2007). In adults, the muscle acts strongly on the initial upstroke of the head during drinking (Snively & Russell, 2007a, 2007b). As such these dorsolateral muscle expansions may imply that silesaurids evolved in the Late Triassic toward bird-like feeding behaviors.

Table 5. Synopsis of the occipital musculature in *Silesaurus opolensis*, listing the muscle names, insertions, and actions. Names in bold are those used in this study.

Homologies of muscles attaching to the occiput in extant archosaurs, bases on Tsuihiji (2005, 2007, 2010)		**Attachment side on the occiput of *Silesaurus opolensis***	**Action, based on Snively and Russell Crocodilia, Aves (2007a, 2007b)**
Crocodilia	Aves		
Epaxial musculature			
M. transversospinalis capitis, medial part	M. biventer cervicis (+ m. longus coli dorsalis, pars caudalis inserting on cervical vertebrae)	Dorsomedial part of the supraoccipital along the posterior eminence	Head dorsiflexion
M. cucullaris derivatives: **• m. dorsoscapularis** **• m. capitisternalis**	M. cucullaris capitis	Posterior edge of the parietal	Head dorsiflexion
M. transverso spinalis capitis, lateral part	M. complexus	Posterior, dorsomedial part of the parietal	Head dorsiflexion
M. epistropheo-capitis	M. splenius capitis, lateral part	Posterior, dorsolateral part of the parietal	Head dorsiflexion
M. altoido-capitis	M. splenius capitis, medial part	Posterior, medial part of the parietal	Head dorsiflexion
Part of m. iliocostalis capitis	M. rectus capitis lateralis	Ventrolateral part of the paroccipital process	Head ventro/-lateral flexion
M. rectus capitis dorsalis derivatives:	M. rectus capitis dorsalis	Posterior surface of the basal tubera	Head dorsiflexion

• m. longissimus capitis profundus **• part of m. iliocostalis capitis**			
Hypaxial musculature			
M. rectus capitis antiqus major	M. rectus capitis ventralis	Posteroventral margin of the basal tubera	Head ventroflexion
Other muscles attaching to the occiput			
M. longissimus capitis superficialis	(Absent)	Distal end of the paroccipital process	Head lateral flexion
M. depressor mandibulare	M. depressor mandibulare	Posterior dorsolateral edge of the parietal; distalmost end of the paroccipital process	Opening the jaws

Chapter 4. Axial skeleton[4]

Vertebral column

The vertebral column of *Silesaurus* (Figures 2, 3 and 16–22) was described for the first time by Dzik (2003) based mostly on articulated specimens ZPAL Ab III/361, 362, and 364. Subsequently, additional information about the *Silesaurus* vertebral column was offered by Piechowski & Dzik (2010), Nesbitt (2011), and Langer et al. (2013). There seems to be some individual variation in the gradation from the cervical to the dorsal vertebrae, as the morphology of particular vertebrae differs slightly between particular articulated specimens (Dzik, 2003). A sudden change in morphology of the ribs in specimen ZPAL AblII/1930 shows that the junction between the neck and trunk is located between the seventh and eighth presacral vertebrae, although migration of the parapophyses from the centrum to the neural arch continues to the middle of the dorsal series. The vertebral formula in *Silesaurus*, with 23 presacral vertebrae, of which 16 are dorsals, probably represents a primitive condition for dinosauriforms, as suggested by the same vertebral formula in *Coelophysis* and other theropod dinosaurs, especially coelurosaurs. Four fused sacrals are represented by several specimens (Dzik, 2003); their modified restoration was published in Dzik & Sulej (2007). The number of caudal vertebrae seems to vary from about 35 to perhaps 40.

No evidence of pneumaticity was found on the vertebrae of *Silesaurus*.

[4] Part of this chapter was published in:
Piechowski, R. & Dzik, J. 2010. The axial skeleton of *Silesaurus opolensis*. *Journal of Vertebrate Paleontology* **30**, 1127–1141.
Piechowski, R., Tałanda, M. & Dzik, J. 2014. Skeletal variation and ontogeny of the Late Triassic dinosauriform *Silesaurus opolensis*. *Journal of Vertebrate Paleontology* **34**, 1383–1393.

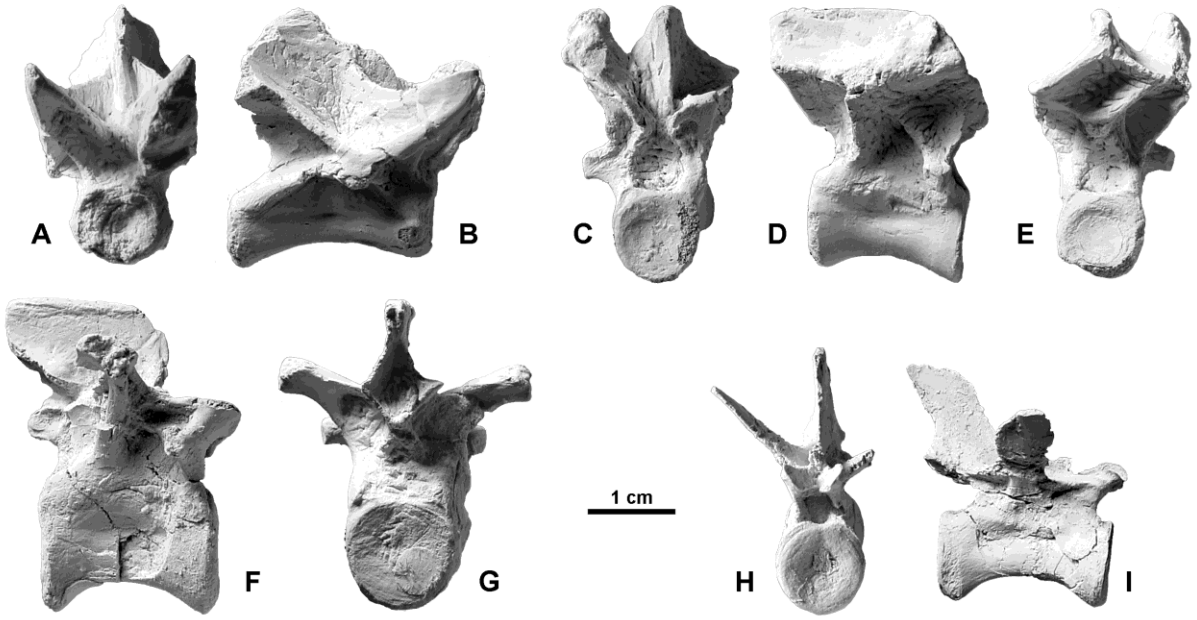

Figure 16. Individual vertebrae of *Silesaurus opolensis*. **A**, **B**, 4th cervical ZPAL AbIII/411/7 in anterior and right lateral views; **C-E**, 7th dorsal ZPAL AbIII/433/1 in anterior, right lateral, and posterior views; **F**, 14th dorsal ZPAL AbIII/1991 in right lateral view; **G**, 13th dorsal ZPAL AbIII/362/11 in posterior view; **H**, **I**, caudal ZPAL AbIII/923 in anterior and right lateral view.

Cervical vertebrae and ribs

The atlas is partially preserved in ZPAL Ab III/364 and 1930 (Figure 16A, B). As typical of reptiles, the atlas is composed of three elements — the intercentrum and paired neural arches, occupying a restricted space between the occiput and second cervical vertebra. The intercentrum is a rectangular, thin strip of bone. The atlantal intercentrum is U-shaped in anterior view. The articular surface for the occipital condyle faces anterodorsally. The occipital condyle articulates posteriorly against this trough-shaped surface, which permitted wide movement of the skull in many planes. The articular surface for the odontoid faces posterodorsally. The articular surface for the axial intercentrum is also U-shaped and faces posteroventrally.

Description of the axis is based on specimens ZPAL Ab III 361, 364, and 1930 (Figure 16C). The axis shows considerable elongation, and each next vertebra in the cervical series shows gradational decrease in length. The axial centrum is almost twice as long as deep. The axial intercentrum is fused with the anterior end of the axis. The anterior surface of the centrum is very broad and deeply concave (cup-shaped), to receive atlantal intercentrum. A strong ventral keel is present. The parapophysis is positioned low on the anterior rim of the centrum. The axis lacks diapophyses, which are represented by low prominences on the third

cervical vertebra and are fully developed only in the presacral vertebrae following it. The neural arch of the axis is completely co-ossified with the centrum. Small, eliptical prezygapophyses are projected anterolaterally. The articular surface of prezygapophysis is gently convex along its long axis. The neural spine is projected anteriorly between the prezygapophyses. At its posterodorsal extremity, the neural spine divides into two ventrolaterally oriented laminae, which terminate ventrally as structures resembling incipient epipophyses that are located posterior to the well developed postzygapophyses (they do not have recognizable serial homologues behind). In posterior view, a deep postspinal fossa, which is delimited by the spinopostzygapophyseal lamina is developed between the neural spine and the postzygapophyses. A thin lamina connects the medial edges of the postzygapophyses and floors the postspinal fossa at the base of the neural arch. When looking at the fossa, one gets an impression that its posterior outline is rhomboidal but the interior is actually pentagonal. In the following vertebrae, the postspinal fossa gradually decreases in size, until it almost disappears in the posterior dorsals.

The postaxial cervical vertebrae are best preserved in the articulated specimens ZPAL Ab III 361 and 1930 (Figure 16D–H). The neck of *Silesaurus* consists of somewhat elongated vertebrae (except for the atlas). These vertebrae are amphicoelous, the centra being concave a little more at their anterior face. The postaxial cervical centra are parallelogram-shaped in lateral view, with slight skewing and elevation of the anterior centrum face. The centra are compressed from sides. In contrast to the posterior cervical and all dorsal and sacral vertebrae, articulation surfaces of centra of the anterior cervical vertebrae are circular in outline. As on the axis, a strong ventral keel is present on third cervical centrum but it is reduced in depth in more posterior cervicals. Oval parapophyses occupy the low anterior rim of the centrum in all cervical vertebrae. They keep their ventral position up to the last cervical vertebra. The diapophyses, which are developed as low prominences just above the neurocentral suture in the third cervical vertebra, project from the succeeding cervical vertebrae as ventrolaterally directed flanges. In fourth cervical vertebra, the diapophyses are anteroposteriorly shortened and oriented anterolaterally.

Four laminae extend from the diapophyses to the prezygapophyses (prezygodiapophyseal lamina) and postzygapophyses (postzygodiapophyseal lamina) and to the anteroventral (anterior centrodiapophyseal lamina) and posteroventral corners (posterior centrodiapophyseal lamina) of each neural arch behind third cervical vertebra. The laminae merge centrally into a low cross-shaped structure. A fifth lamina (middle centrodiapophyseal lamina) may be present below the diapophysis between the anterior and posterior centrodiapophyseal lamina.

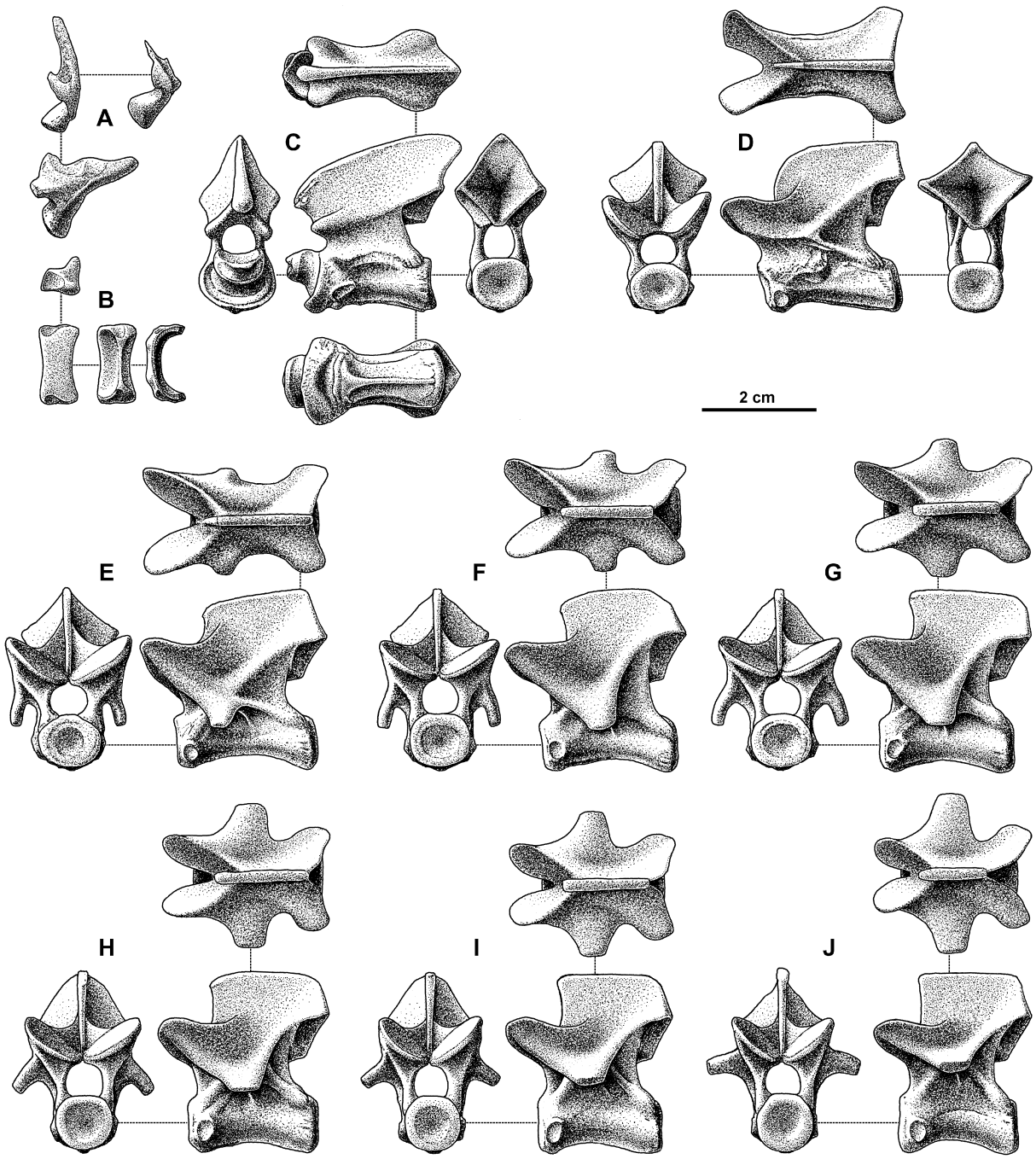

Figure 17. Restoration of presacral vertebrae of *Silesaurus opolensis*; dorsal, anterior and left lateral views (except for A, B, C, where also posterior view is given); based mostly on ZPAL AbIII/1930 and 361. **A**, **B**, neural arch and intercentrum of atlas; **C**, axis; **D,** 3rd cervical; **E**, 4th cervical; **F**, 5th cervical; **G**, 6th cervical; **H**, 7th cervical; **I**, 1st dorsal; **J**, 2nd dorsal.

As a result, the infradiapophyseal fossa is divided into anterior and posterior parts. The transverse processes appear broadly triangular in dorsal view because the lamina between the diapophyses and prezygapophyses that forms the external surface of the anterior portion of the neural arch is especially strong.

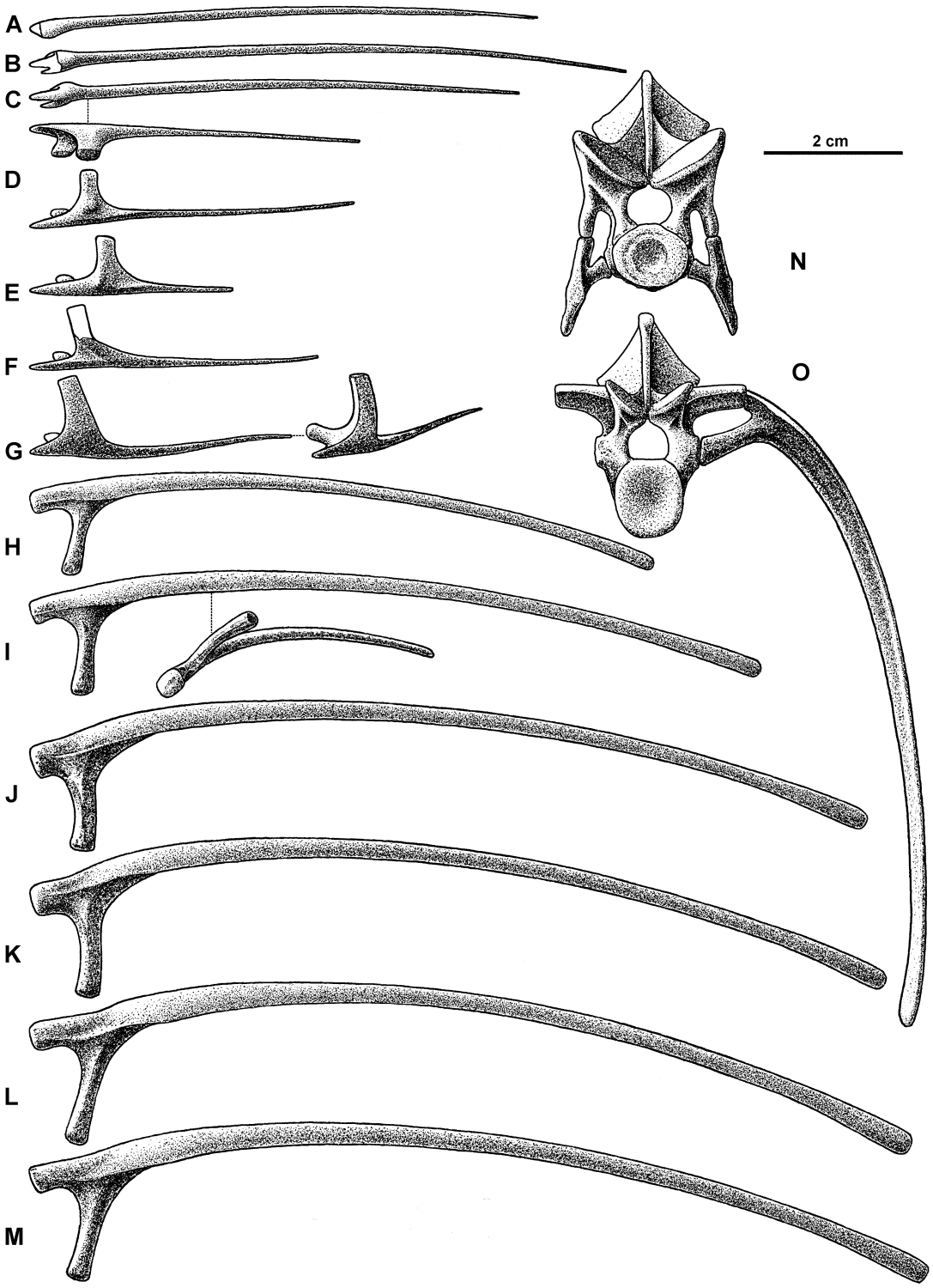

Figure 18. Restoration of ribs of *Silesaurus opolensis*; left lateral viev (except for D, G, I, where also dorsal view is given, and N, O shown in anterior view); based mostly on ZPAL AbIII/1930 and 361. **A**, 1st cervical; **B**, 2nd cervical; **C**, 3rd cervical; **D**, **N**, 4th cervical; **E**, 5th cervical; **F**, 6th cervical; **G**, 7th cervical; **H**, 1st dorsal; **I**, 2nd dorsal; **J**, **O**, 3rd dorsal; **K**, 4th dorsal; **L**, 5th dorsal; **M**, 6th dorsal.

The prezygapophyses project beyond the anterior face of the centrum in the third and succeeding cervical vertebrae. A distinct ridge extends posteriorly behind the parapophyses

over most of the length of the centrum in proximal cervicals (except for the atlas). The semioval articular surfaces are flat and face dorsomedially. A narrow spinozygapophyseal fossa demarcated by spinoprezygapophyseal laminae is present at the base of the neural spine between the prezygapophyses. In contrast to the axis, the postzygapophyses of the postaxial cervical vertebrae do not project behind the posterior centrum face, and the neural spines become there less pointed posteriorly.

Each neural arch of the atlas has a prominent neural spine. The plate-shaped neural spine of the third cervical vertebra is subquadrate in lateral view and inclined posterodorsally. In subsequent cervical vertebrae, posterodorsal corners of the neural spines are blunt. As in the axis, a deep posterior chonos is present at the base of the neural spine between the postzygapophyses.

The cervical ribs (Figure 17A–G, N) are well preserved in specimen ZPAL Ab III/1930 and relatively well recognizable in the specimens ZPAL Ab III/361 and 362. Each cervical vertebra, including atlas, bears a rib on either side. Each cervical rib is slender and delicate. The most robust are anteriorly located ribs that extend for more than three lengths of the supporting vertebra. The posterior ribs are much shorter and narrower and cover distance of only two vertebral lengths. The atlantal, axial, and third cervical ribs lack a tuberculum. Other cervical ribs are prominent and doubleheaded. The capitulum articulates with a parapophysis on the centrum and the tuberculum with a diapophysis located on the deep lateral lamina of the neural arch. Each cervical rib, except for the atlantal rib, has a prominent anterior process in front of its articulation, this process extending anteriorly to terminate acutely. Anteriorly, the cervical ribs are very long, each one extending back along the length of its vertebra and along more than three succeeding vertebrae. Backward their length and thickness decreases but tuberculum becomes more prominent. External surface of the rib, together with its anterior process, is flat.

Dorsal vertebrae

The series of dorsal vertebrae in ZPAL AbIII/362 and 1930 (Figures 16I, J, 17A–H, 18A–F) well shows details of their structure. The anterior dorsal vertebrae are similar to posterior cervical vertebrae, except for they are shorter than the last cervical vertebra (as well as the posterior dorsal vertebrae). Posteriorly, the dorsal vertebrae increase in their length and even more in height.

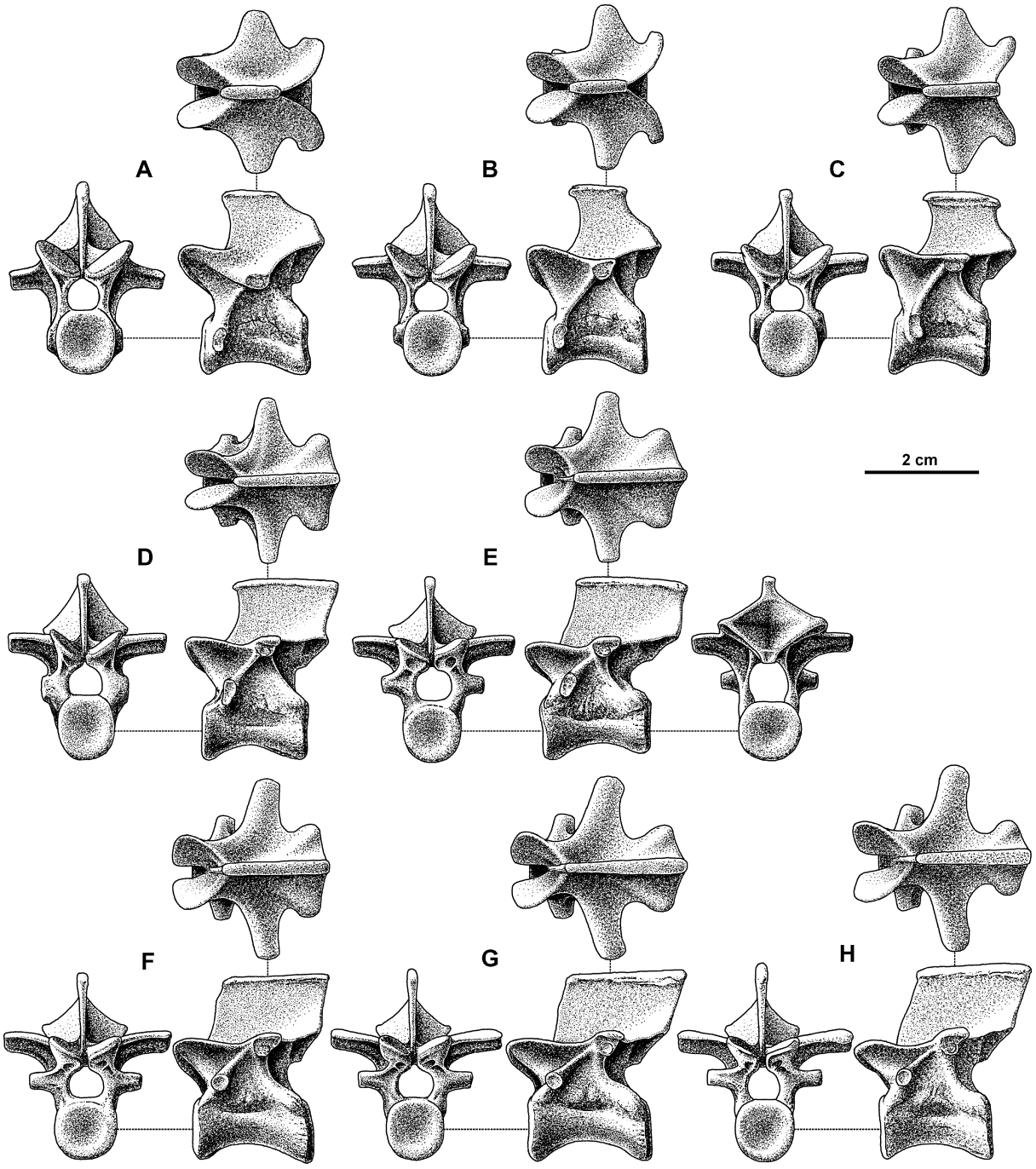

Figure 19. Restoration of presacral vertebrae of *Silesaurus opolensis*; dorsal, anterior and left lateral views (except for E, where also posterior view is given); based mostly on ZPAL AbIII/1930 and 361. **A**, 3rd dorsal; **B**, 4th dorsal; **C**, 5th dorsal; **D**, 6th dorsal; **E**, 7th dorsal; **F**, 8th dorsal; **G**, 9th dorsal; **H**, 10th dorsal.

The dorsal centra have wide, slightly concave, intercentral articulation surfaces, larger than in the cervical vertebrae. Each is strongly constricted at the mid-length of the centrum, which gives an hourglass shape, so characteristic of many early archosaurs. A shallow elliptical depression is present on the lateral face of the centrum, the upper rim of which exhibits a semicircular prominence. It does not seem to be a pneumatic feature. In contrast to cervical

vertebrae, the amphicoelous articular surfaces of the dorsal vertebrae are at right angle to the median axis of the centrum in both lateral and ventral views. In the cervical region, the articular surfaces are inclined dorsoventrally to the vertebral axis. This reflects the difference in the attitudes between the S-shaped neck posture and slightly arched disposition of the thoracic region.

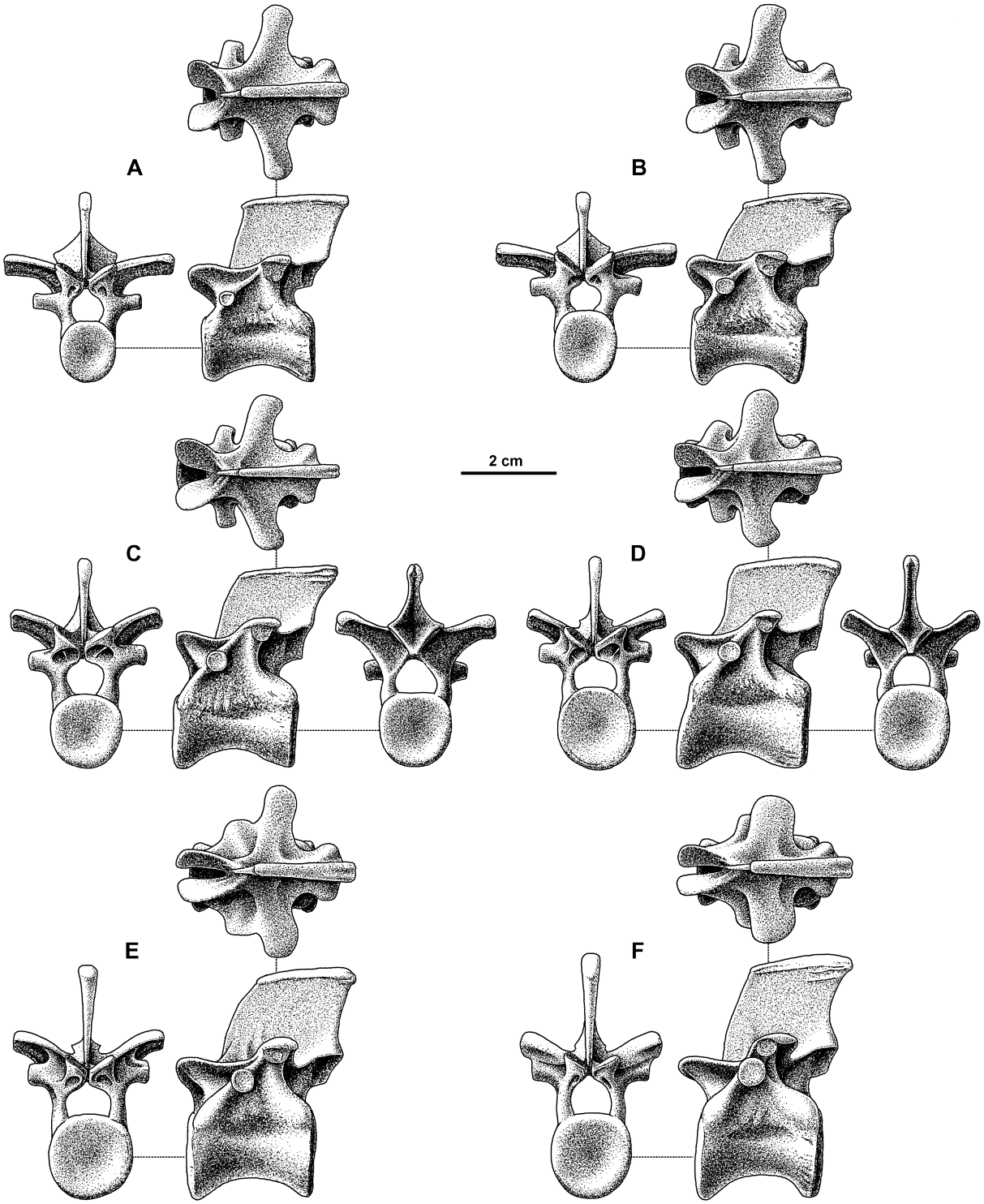

Figure 20. Restoration of presacral vertebrae of *Silesaurus opolensis*; dorsal, anterior and left lateral views (except for C, D, where also posterior view is given); based mostly on ZPAL AbIII/1930 and 361. **A**, 11th dorsal; **B**, 12th dorsal; **C**, 13 th dorsal; **D**, 14th dorsal; **E**, 15th dorsal; **F**, 16th dorsal.

The parapophyses are prominent at the base of the neural arch of first two dorsal vertebrae. From the third dorsal vertebrae backward, the parapophyses gradually shift dorsally and posteriorly, from their position at the level of the neurocentral suture to the level of the prezygapophysis. At the same time, the parapophyses become more elongated laterally. Near the eleventh dorsal vertebra, the parapophyses raise to reach nearly the same position with the diapophyses on fourteenth dorsal. The parapophyses of dorsal vertebrae are oriented obliquely posteriorward except for the last dorsals. The parapophyses of the third to sixth dorsals are anteroposteriorly compressed, in contrast to a circular articulation surface for the capitulum of the following dorsal vertebrae. The transverse processes are strong due to their remarkable anteroposterior width. They extend basally towards the pre- and postzygapophyses as the prezygodiapophyseal and postzygodiapophyseal laminae and are essentially horizontal.

The neural arches of the dorsal vertebrae are strong and carry long, neural spines elongated anteroposteriorly. Pronounced lateral ridges (laminae?) developed at the co-ossification of the neural arches with the centra. The neural spines change in shape along the dorsal series. In the first two dorsal vertebrae the neural spines are plate-shaped, similar to those in posterior cervicals. The next three neural spines of dorsal vertebrae have anteroposteriorly narrowed dorsal ends, being inclined somewhat forward. Evidently, this reflects the upward curvature of the neck. Each of the remaining dorsal vertebrae has an anteroposteriorly widened, subquadrate spine. The last five of them show the neural spine slightly curved. The neural spines of the anterior and middle part of the dorsal series are almost equal in height, but they become gradually higher posteriorly, with the dorsal extremity enlarged and strongly thickened. The diapophyses of dorsal vertebrae are supported by anterior and posterior laminae. The laminae have their common origin at the base of the transverse process to the parapophyses (paradiapophyseal lamina) and the posteroventral junction of the neural arch with the centrum (posterior centrodiapophyseal lamina), respectively, from where they run obliquely downward. This system of laminae demarcates three deep cavites below the transverse process: infraprezygapophyseal fossa, infradiapophyseal fossa, and infrapostzygapophyseal fossa. Consequently, the last dorsal vertebra has well-developed buttresses below the parapophyses. The transverse processes in the presacral series increase gradually gradually in length as far as to eleventh dorsal vertebra. They decrease in length

again from that point backward. Like the parapophyses, the diapophyses are oriented obliquely posteriorward except for the last dorsal vertebra, and in a few last dorsals the diapophyses are oriented obliquely dorsally. The diapophyses in the dorsal series form the articular surface of the tuberculum of the rib. In the more posterior region of the dorsal series, it consists of two elements, a short parapophysis for the capitulum and a diapophysis for the tuberculum of its rib.

The prezygapophyses extend beyond the anterior border of the centrum, they are inclined at a wide angle and face dorsomedially. The articular surfaces of prezygapophyses are anteroposteriorly elongated but decrease in length among the last dorsals. The postzygapophyses are short and inclined laterally. Accesory intervertebral articulations are present along the dorsal series. The hypantrum form a vertical medial articular surface of the prezygapophyses, and the hyposphene constitutes a distinct vertical articular surface below the postzygapophyses.

Dorsal ribs and gastralia

Ribs (Figures 17, 22) are best preserved in specimen ZPAL Ab III/1930 and relatively well recognizable in specimens ZPAL Ab III/361 and 362. The dorsal ribs are double-headed throughout the series. The first ten or eleven dorsal ribs are especially strong and long. Their slightly thickened distal ends suggest that in life they continued ventrally into cartilage. The remaining ribs narrow gradually towards their ends and become progresively shorter; fourteenth dorsal being the last and shortest. The capitulum of the anterior dorsal ribs articulates with a prominent articulation surfaces of the parapophyses. With the change in the position of parapophyses and diapophyses along the series, the capitulum becomes shorter and the capitular and tubercular facets are more and more closely spaced. The capitulum of the posterior ribs connects with a single transverse process of their vertebrae. The tuberculum of the anterior dorsal ribs articulates in each case with a diapophysis. The tuberculum forms a prominent process on first four ribs, but in the following dorsal vertebrae it is a small facet, dorsolateral to the long capitular process. The rib shafts are usually long and relatively slender and curve gently inward.

Gastralia consist of four rows of slender subparallel rods. Rods of the two admedial rows are alternately fused at the ventral midline at an approximately right angle in groups of up to six. Gastralia of the lateral rows are more slender in appearance, with acute tips. Their total

width seems to equal that of the proximal ends of pubes. The original arrangement of gastralia seems to be strictly horizontal.

Sacral vertebrae and ribs

The sacral vertebrae are preserved in partially articulated skeletons of *Silesaurus* and as isolated specimens. The sacrum of *Silesaurus* is composed of four fused vertebrae. Three posterior elements of the complex are broadly united to the ilia through robust ribs. The ribs are attached outwardly between the centra by two distinct structures, semioval in lateral aspects, broadly co-ossified with one another. The structure is homologous to the para- and diapophyses on the centrum and to corresponding capitula and tubercula in the ribs.

The first sacral vertebra is placed behind the tip of the anterior iliac spine. This bone is morphologically similar to the preceding presacrals, except that it is firmly co-ossified with the rest of the sacrum and its neural spine is higher and more stout, with the dorsal extremity greatly thickened. The transverse processes and sacral ribs diverge from each other. The transverse processes of first sacral vertebra are anteroposteriorly narrow and buttressed ventrally by delicate thin laminae. The processes project anterolaterally to contact the ilia close to the iliac spine. This vertebra lacks a rib and thus may be considered a dorsosacral rather than a true sacral.

The second sacral vertebra has its broad transverse processes modified into wing–like structures that project anterolaterally. Similar structures are present in next sacral vertebrae but they are broad and oriented transversely. In the last sacral vertebra, an additional wing-like process extends posterodorsally; its centrum and neural arch are similar to those in proximal caudal vertebrae. All specimens show an extensive fusion of transverse processes and corresponding sacral ribs. The second sacral vertebra bears fan-like ribs broadly attached to the ilia, forming an anterior vertical blade.

The anterior blade of the sacral ribs extends backward ventrally forming a floor that connects the ribs of consecutive vertebra. The transverse processes and ribs of the third and fourth sacrals form an almost continuous floor. In the third sacral, a vertical blade is present; in the last sacral, it connects directly to the wing-like process.

The neural spines of the sacral vertebrae are high, stout, with the dorsal extremities greatly thickened and fused with each other dorsally. In all specimens, the posterior surface of the centrum of the last sacral vertebra is oblique, facing upwards.

Caudal vertebrae

The holotype preserves 14 caudal vertebrae. The caudal vertebrae are in partial articulation in specimens ZPAL AbIII/361 and 1930, and are represented by many isolated specimens. The proposed restoration of the tail is based on articulated sections fit together and on size gradation among isolated vertebrae (Figures 21B,C, 22). The inferred number of caudal vertebrae is 33. The total number was probably closer to 35 or even 40, but remains conjectural.

The length of caudal vertebrae seems to be approximately uniform along the tail, slightly increasing only in the distal part of the tail. The vertebrae are amphicoelous, spool-shaped, and compressed transversely, as are all other vertebrae in *Silesaurus*. The articular surfaces of all caudal vertebrae are circular. An elliptical depression on the lateral surface of the centrum is present as far as to eighteenth caudal vertebra.

The neural spines of the anterior caudal vertebrae are oblique, very high with the dorsal extremity thickened in the first three caudals, they are widened anteroposteriorly. In the succeeding vertebrae, the slender, oblique neural spines progressively decrease in height distally along the series. They are reduced to low crests in caudals 26 to 31. The anterior process of the neural spines extends upward, reaching its maximum size in eight caudal vertebrae. Neural spines are absent on the last caudal vertebrae.

The transverse processes are broad, wing-like, and horizontally oriented in most caudal vertebrae, reaching maximum length in second caudal vertebra. Distal to this vertebra, the transverse processes gradually decrease in length and on caudal vertebra 22 they are positioned on the centrum. From caudal vertebra 11, the transverse processes project anterolaterally, in contrast to the preceding caudals, where then project posterolaterally. The transverse processes are reduced to rounded promontories on caudal vertebra 24 and are absent on more posterior caudals. They remain only as longitidinal ridges on lateral faces of their centra. The pre- and postzygodiapophyseal laminae are weakly developed in anterior and middle caudals, similarly as the ridge-like anterior and posterior centrodiapophyseal laminae.

The prezygapophyses lie well above the centrum, placed close to the midline; in the anterior four caudals far from the centrum and transverse processes. Short prezygapophyses extend upward just beyond the centrum faces as far as in caudal vertebra 27. The zygapophysal articulations are steeply inclined. In the following vertebrae the prezygapophyses significantly increase in their length, reaching maximum length at about caudal vertebra 27. Distal to this vertebra, their length slightly shortens again. Short

postzygapophyses are adjusted to the articular surface of prezygapophyses, fitting the changes in their length. Ventral facets on adjoining centra jointly support a single chevron.

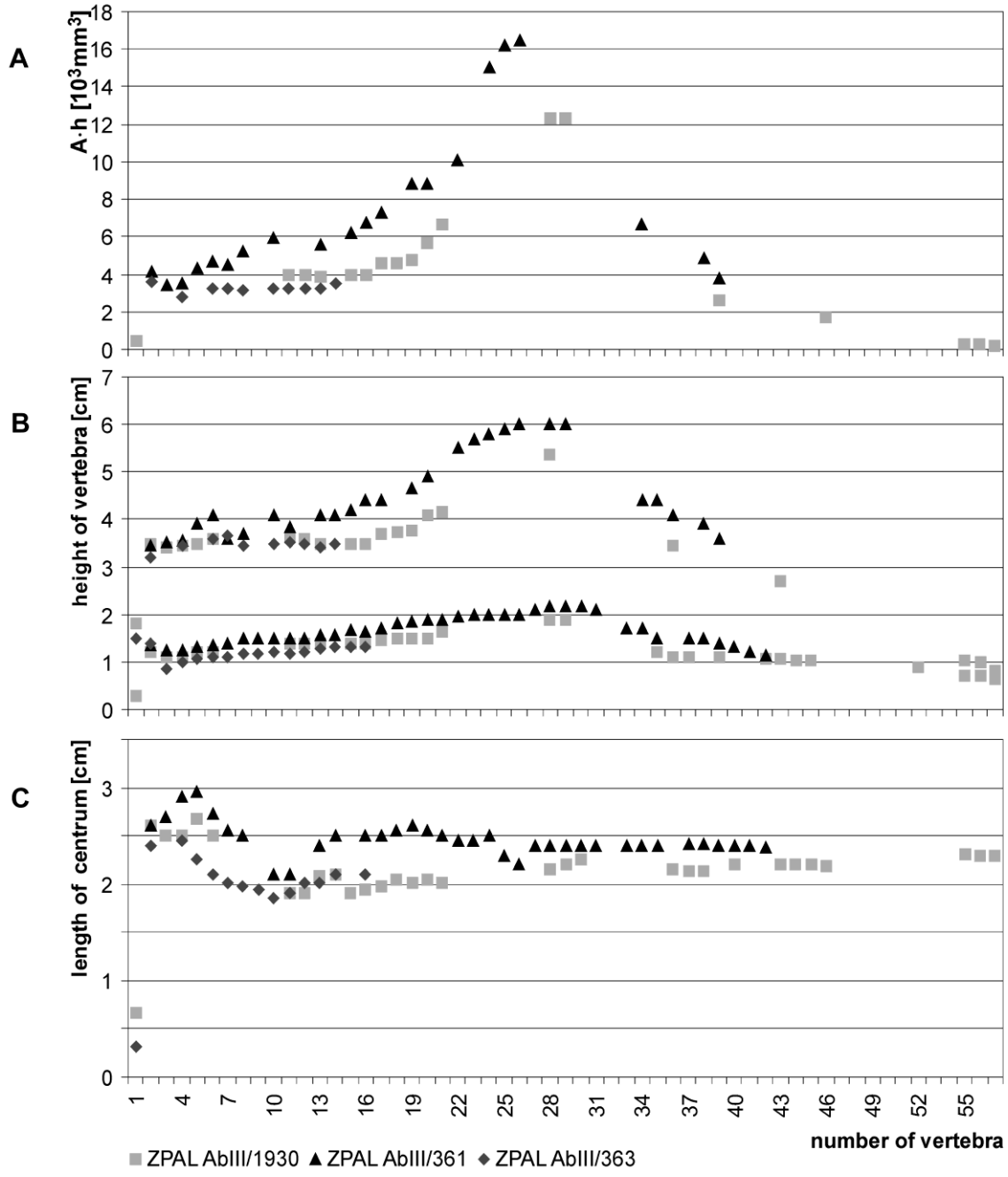

Figure 21. Measurements of vertebrae of *Silesaurus opolensis* from the early Late Triassic at Krasiejów near Opole, Poland; based on ZPAL AbIII/1930, 363, and 361. **A**, changes in functionally important ratio between the area of the frontal surface of the centrum (A) and height of the vertebra measured from the middle of centrum to the tip of the spinal process (h); **B**, changes in height of the centrum (lower series) and the complete height (upper series) along the vertebral column. Extent of the regions of vertebral column missing in some specimens was inferred from gradients in corresponding regions preserved in other articulated specimens; **C**, changes in vertebral centrum length along the vertebral column of *Silesaurus opolensis*; based on ZPAL AbIII/1930, 363, and 361.

Chevrons are incompletely preserved only in the holotype. The first chevron is borne between the second and third caudal vertebrae. Chevrons of the second to fourth caudal vertebrae increase in length, but distal to that point, the chevrons progressively decrease in length and disappear at about caudal 26 or 27.

Significance of axial osteology

There is some controversy regarding evolutionary meaning of buttressing apophyses of cervical vertebrae with prominent laminae, which is a feature of the vertebral column in *Silesaurus*. Wilson (1999) suggested that the distribution of vertebral laminae is generally restricted to saurischian dinosaurs because in the Ladinian *Marasuchu*s no laminae occur in cervicals and only in the ninth presacral vertebra two rudimentary laminae are present below the diapophysis (Sereno & Arcucci, 1994). However, well defined laminae below diapophyses of dorsal vertebrae were present already in the poposaurids *Postosuchus* and *Sillosuchu*s (Chatterjiee, 1985; Alcober & Parrish, 1997). The laminae may have developed earlier than in the Dinosauria and seem to be present (although often not described and variably developed) in many Triassic archosaurs (Gower, 2001; Nesbitt, 2005; Parker, 2008).

It is thus puzzling that vertebral laminae are absent on the vertebrae of ornithischian dinosaurs (Ostrom & McIntosh, 1966; Santa Luca, 1980; Norman, 1980; Brítt 1993). There is a rudimentary lamina below the transverse process of the dorsal vertebrae of some ornithischians, but this lamina does not reach the ventral margin of the neural arch (Norman, 1980; Galton & Powell, 1980). Probably the poor development of laminae in these dinosaurs is a secondary feature.

A deep postspinal fossa delimited by spinopostzygapophyseal laminae that extend between the postzygapophyses (Welles, 1984) in the cervical vertebrae in *Silesaurus*, occurs also in *Staurikosaurus*, *Herrerasaurus*, and prosauropods (Zhang, 1988; Bonaparte, 1999; Yates, 2003a; Langer & Benton, 2006). A similar excavation is present in theropods (Madsen, 1976; Colbert, 1989; Madsen & Welles, 2000; Langer & Benton, 2006; Martínez et al., 2008) and some non-dinosaurian archosaurs, for example *Polonosuchus* (Sulej, 2007). No comparable cavity occurs in the basal ornithischians (Ostrom & McIntosh, 1966; Galton, 1974), most non-dinosaurian archosaurs (Ewer, 1965; Bonaparte, 1972, 1999; Chatterjee, 1978; Fraser et al., 2002; Ferigolo & Langer, 2007) or *Marasuchus* (Bonaparte, 1975; Sereno & Arcucci, 1994). This seems thus to be a primitive trait of *Silesaurus*, lost by the ornithischians together with laminae.

The neck of *Silesaurus* was slightly sigmoidal, with curvature presumably similar to that restored in *Coelophysis*, as suggested by a similar disposition of the cervical ribs (Colbert, 1989). The slightly parallelogram-shaped cervical centra are present as far posteriorly as the ninth presacral. This character seems to be weakly expressed in *Herrerasaurus* (Sereno & Novas, 1994) and *Marasuchus* (Sereno & Arcucci, 1994). Unfortunately, the neck anatomy is unknown in *Lagerpeton* (Arcucci, 1986; Sereno & Arcucci, 1994). It must remain unsettled whether the relatively straight neck of *Silesaurus* is a primitive trait or it is rather connected with secondary quadrupedality.

Long sub-parallel cervical ribs, similar to those of *Silesaurus*, are present in *Eoraptor* (Sereno et al., 1993). Cervical ribs of the Late Triassic dinosaurs are generally poorly known because few fossil specimens are preserved well enough to show their morphology and distribution. Probably they are best known is the Norian or Rhaetian *Coelophysis bauri* from the Chinle Formation of New Mexico (Colbert, 1989). The cervicals of *Coelophysis* are longer anteriorly and diminish in length posteriorly. Unlike *Silesaurus*, where the acute anterior process suddenly disappears behind the seventh vertebra, they gradually change toward the dorsals and the change is parallel to the shortening of the vertebral centra of the ninth and tenth cervical, as interpreted by Colbert (1989, p. 83). That is, the vertebra change first, the ribs later, opposite to the condition in *Silesaurus*. Quite elongated cervical ribs are present also in prosauropods (Galton, 1976; He et al., 1988; Zhang, 1988; Langer & Benton, 2006; Galton, 2007) and basal theropods (Ostrom, 1978; Colbert, 1989; Rowe, 1989; Bonaparte et al., 1990; Harris, 1998; Martínez et al., 2008). In contrast, the cervical ribs of ornithischians (Galton, 1974; Santa Luca, 1980; Norman, 1986; Forster, 1990; Irmis et al., 2007b) are much shorter and protrude ventrally from the neck. Again, this may reflect change in flexibility of the neck in the evolution towards quadrupedality of ornithischians.

A sacrum comprising two vertebrae is the plesiomorphic condition for dinosaurs and other archosaurs (Walker, 1961; Ewer, 1965; Chatterjee, 1978; Bonaparte, 1984), including *Lagerpeton* and *Marasuchus*. In the evolution of the Dinosauria, the number of sacral vertebrae increased. In most dinosaurs, the sacrum is composed of three or more sacral vertebrae, as seen in basal ornithischians (Galton, 1974; Santa Luca, 1980; Langer & Benton, 2006; Nesbitt et al., 2007) and basal theropods (Raath, 1969; Welles, 1984; Colbert, 1989; Cuny & Galton, 1993; Langer & Benton, 2006). The sacrum of *Silesaurus* consists of four extensively fused vertebrae broadly attached to the ilia by three robust sacral ribs (Dzik & Sulej, 2007). Rather surprisingly, a similar condition is present in the Anisian *Bromsgroveia* (Galton, 1977; Galton & Walker, 1996; Benton & Gower, 1997); other poposaurid

rauisuchians, such as *Effigia*, *Poposaurus*, and *Shuvosaurus*, also have four sacrals (Nesbitt, 2007; Weinbaum & Hungerbühler, 2007; Long & Murry, 1995).

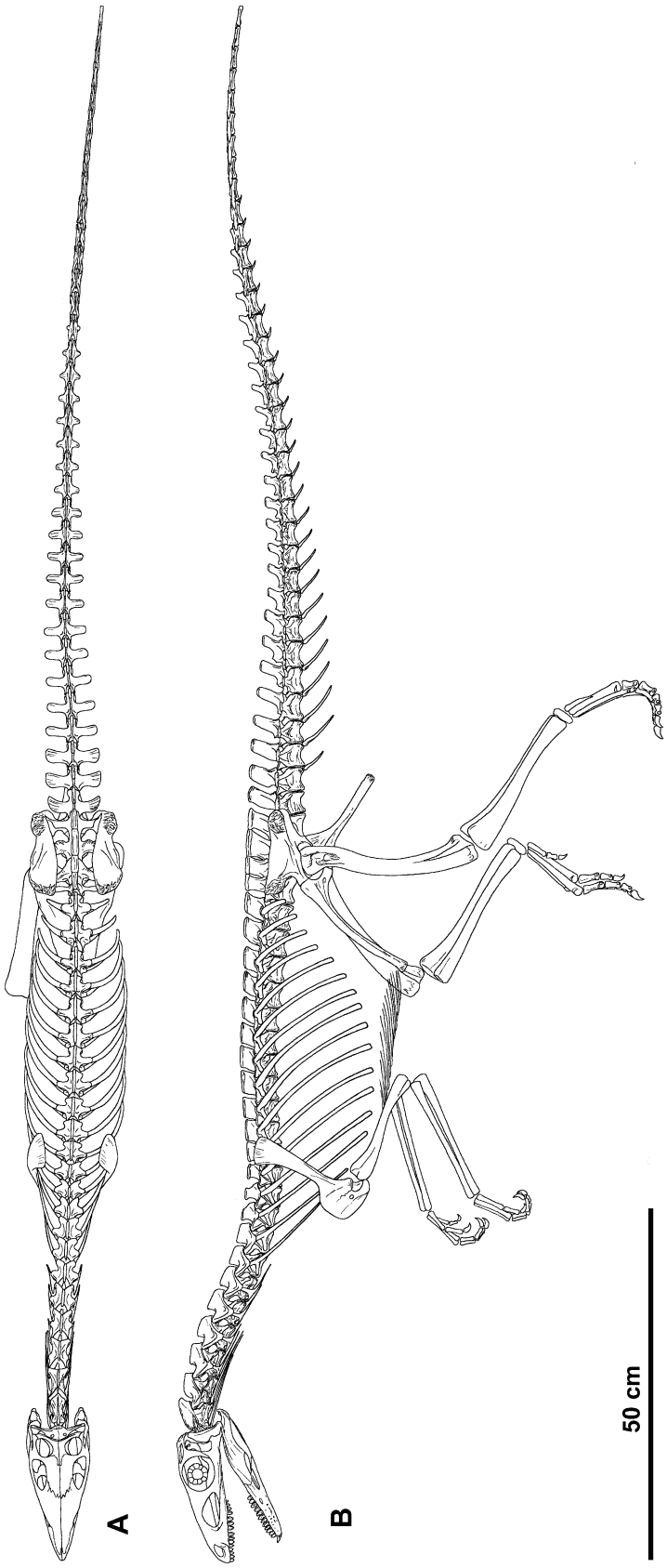

Figure 22. Restoration of the skeleton of *Silesaurus opolensis* from the early Late Triassic of Poland in facultative bipedal running pose; based mostly on ZPAL AbIII/1930 and 361.

In *Silesaurus,* three posterior elements of the fused complex of four vertebrae in the sacral region are broadly attached to the ilia by three robust sacral ribs. The ribs are attached outwardly between the centra (Dzik & Sulej, 2007). The first sacral vertebra is morphologically similar to the preceding presacrals. This similarity suggests that the last dorsal vertebra was incorporated into the sacrum. The last sacral vertebra shows an analogous condition: its centrum and neural arch are similar to those of the anterior caudal vertebrae. Perhaps the first caudal vertebra was incorporated into the sacrum.

The new morphological evidence presented here does not provide anything that could affect the numerous cladistic analyses, in which data for *Silesaurus* were included (e.g., Langer & Benton, 1991; Irmis et al., 2007; Martinez & Alcober, 2009).

Functional interpretation

The cervical vertebrae of *Silesaurus* bear prominent vertebral laminae, similar to those in long-necked dinosaurs (sauropodomorphs), although the neck of *Silesaurus* is relatively short. Comparable laminae are also present in short-necked theropods. Such laminae are usually interpreted as structural elements for resisting stress generated by movement of elongate neck or as osseous septa of pneumatic chambers (McIntosh, 1989; Wilson, 1999). The laminae are clearly aligned along principal axes of stress on the neural arches generated by muscle contraction (Herring, 1993; Carter et al., 1998). Ossification seems to be restricted to the laminae primarily as a measure to reduce weight of the skeleton. Schwarz et al. (2007) suggested that the laminae served to increase the attachment area of axial muscles. Some authors suggested that the prominent vertebral fossae housed an airsac system (e.g., O'Connor & Claessens, 2005; O'Connor, 2006) and in pneumatized vertebrae the laminae had a double function, separating the diverticulae and providing surfaces for attachment for axial muscles. The air-sac system has been reconstructed for the common ancestor of pterosaurs and dinosaurs (e.g., Wedel, 2007; Butler et al. 2009). However, there is no evidence of pneumatization in *Silesaurus* (Dzik, 2003; Butler et al. 2009). The posterior chonos formed by laminae probably served for insertion of interarticular vertebral ligaments (Baumel & Raikow, 1993).

The enlarged dorsal extremities of the neural spines of the dorsal, sacral, and anterior caudal vertebrae in *Silesaurus* suggest that they afforded considerable surfaces for muscle attachments. The morphology of neural spines of dorsals 3-5 of *Silesaurus* suggests a raised, S-shaped neck posture. Sereno (1991) and other authors consider parallelogram-shaped

cervical centra an adaptation for a flexed neck. Among the dinosaur vertebral columns measured by Christian and Preuschoft (1996) for proportions of vertebrae that are believed to be of functional importance in locomotion (Figure 21A), the one most similar to *Silesaurus* is that of *Iguanodon* (Christian & Preuschoft, 1996; Figure 19), which had both bipedal and quadrupedal gait. Somewhat unexpectedly, that of the sauropod *Dicraeosaurus* is also similar, although the tail of *Dicraeosaurus* was apparently shorter than that of *Silesaurus*.

Silesaurus had long, sub-parallel cervical ribs. Presumably, these ribs were flexible and their movement along the neck was possible to allow its bending, although at the same time they apparently served to strengthen the neck. Similarly, overlapping cervical ribs of sauropods are believed to have been connected with each other by intercostal ligaments that probably supported the neck (Martin et al., 1998; Schwarz et al., 2007). The gradual change in the morphology of the ribs and the position of the parapophyses at the neck-trunk transition corresponds to the change from the narrow neck to the broad thorax. It extends for several vertebrae, and there is no correspondence between the changes in the morphology of the vertebrae and the morphology of the ribs.

Gracile limbs similar to those in *Silesaurus* are typical of fast-running, quadrupedal animals (e.g., Schmidt & Fischer, 2009) but there is a remarkable disparity between its forelimbs and hind limbs. The forelimbs of *Silesaurus* are unusually gracile (despite their remarkable length), whereas the hind limbs are of proportions typical for the Triassic relatives of dinosaurs. This suggests a greater load on the pelvic girdle and the ability of *Silesaurus* to run bipedally on occasion. The relatively high spinal processes of vertebrae suggest well-developed musculature that enabled *Silesaurus* to carry all the body weight on its hind limbs (Christian & Preuschoft, 1996). Its long tail, considerably exceeding the length of the presacral series, probably formed a strong and flexible counterbalance to the weight of the body in front of the pelvis, although by itself it does not need to be connected functionally with facultative bipedality. In fact, the difference in skeletal proportions between quadrupedal and facultatively bipedal reptiles is usually minor (e.g., Snyder, 1954; Aerts et al., 2003).

Chapter 5. Skeleton of pectoral girdle and forelimb[5]

The appendicular skeleton of *Silesaurus* was described for the first time by Dzik (2003) based on articulated specimens ZPAL Ab III/361, 362, and 364, as well as some isolated, best preserved bones. Subsequently, additional information about the *Silesaurus* appendicular skeleton has been offered by Nesbitt (2011), Langer et al. (2013), and Piechowski & Tałanda (2020). I established limb proportions mostly from the holotype ZPAL Ab III/361, in which the scapulocoracoid, humerus, radius, ulna, pelvis, femur, tibia, fibula, and most elements of the pes are nearly complete (Dzik, 2003). Almost all of these bones occur in two other specimens: ZPAL Ab III/364 and ZPAL Ab III/1930 (Table 6). Unfortunately, most of the manus is unknown in *Silesaurus*.

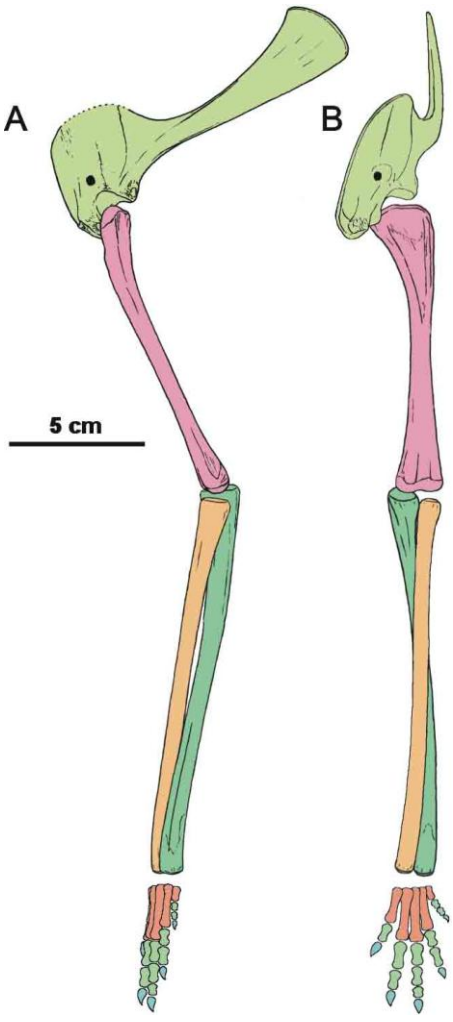

Figure 23. Restoration of the forelimb skeleton of *Silesaurus opolensis* Dzik, 2003 (late Carnian, Krasiejów locality) in lateral (A) and anterior (B) views.

[5] Part of this chapter was published in:
Piechowski, R. & Tałanda. M. 2020. The locomotor musculature and posture of the early dinosauriform *Silesaurus opolensis* provides a new look into the evolution of Dinosauromorpha. *Journal of Anatomy* DOI: 10.1111/joa.13155

Table 6. Length measurements of the most complete limb bones of *Silesaurus opolensis* (in mm).

Specimen	Scapulo-coracoid length	Humerus length	Ulna length	Radius length	Pubis length	Ischium length	Femur length	Tibia length	Fibula length	III metatarsal length
Ab III/361	145.6	136	151.8	146.5	157	122	200	160		85
Ab III/362		137					160			
Ab III/364								155.3	153.3	77
Ab III/1930		119					160	142		

Scapulocoracoid

Scapula and coracoids are firmly fused together. They form a paired lateromedially-flattened elements, which follow the contour of the rib cage (Figure 23). The scapulocoracoid of *Silesaurus* was oriented subvertically in previous reconstructions (Dzik, 2003; Piechowski & Dzik, 2010). My reexamination suggests a less vertical position in lateral view (possibly about 45°) which was probably intermediate between that of birds (subhorizontal) and crocodilians (subvertical), although the scapulocoracoid apparently rotated moderately with the forelimb movement (Baier & Gatesy, 2013; Figure 23). The bone orientation is due to the geometry of the chest and the length of the anterior dorsal ribs. The presence of clear striations and a distinct ridge on the dorsal edge of the scapular blade provides evidence to reconstruct the m. levator scapulae with the m. trapezius in *Silesaurus* (Figures 4A, 24A, C, Table 7). Because both muscles are hypothesized to have been lost due to the reorientation of the scapula into a subhorizontal position in birds (Jasinoski et al., 2006), they may be reconstructed in taxa lacking this scapular orientation (see also Burch, 2014).

The scapula is approximately equal in length to the humerus (Table 6). It forms a spatulate blade that becames thicker anteriorly but the posterodorsal projection is very thin. This is why its margin is broken in most specimens. The projection is wide and flares anterodorsally. Its anterodorsal corner is sharp whereas the posteroventral one is rounded and obtuse (Figures 23A, 24A, C). Between them, the posterodorsal margin is convex. The area is more porous and rough suggesting cartilagineous extension (Langer et al., 2007). The scapular blade bears subtle longitudinal striation. The thinnest part of the scapula is the anterodorsally expanded scapular prominence (= 'acromial process' of Nicholls & Russell, 1985). Its concave lateral surface forms the 'preglenoid fossa' (Welles, 1984; Madsen & Welles, 2000) or 'subacromial depression' (Currie & Zhao, 1993). A gentle ridge (= 'preglenoid ridge' of Madsen & Welles, 2000) extends ventrally, posterodorsal to that. The most massive part of the bone locates at

the basal portion (= caput scapulae of Baumel et al., 1993), near the glenoid. Ventrally, this thickened portion forms a subtriangular connection with the coracoid in the cross section. The glenoid surface can be divided into two planes. Thereby, the glenoid articular surface orients mainly ventrally, but its part is also directed somewhat laterally.

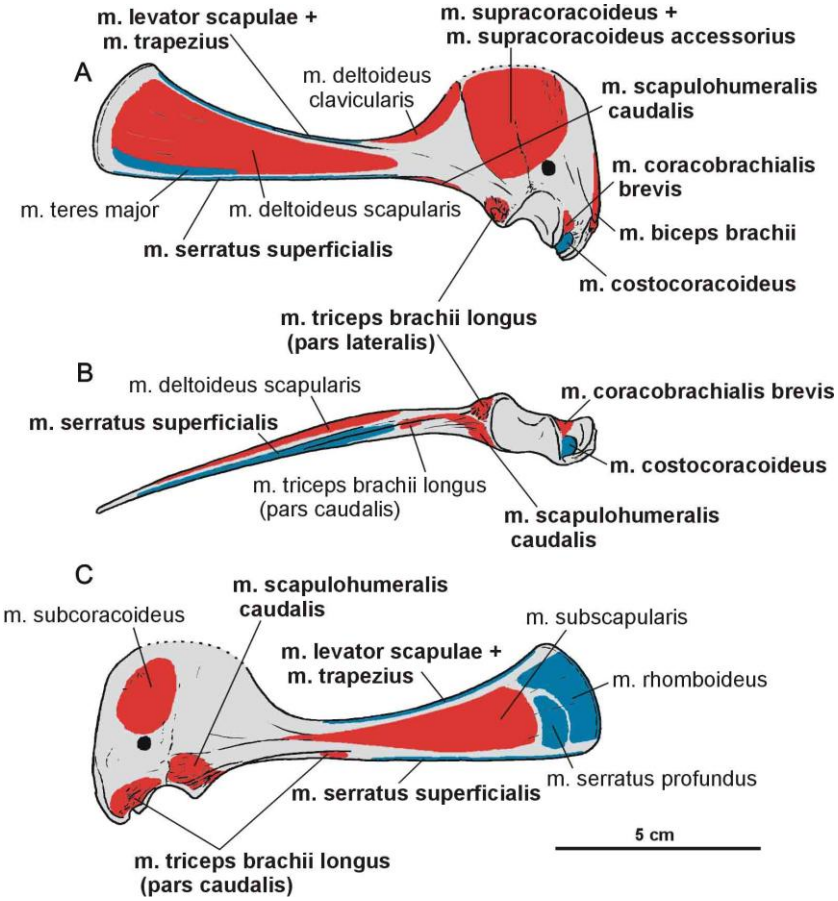

Figure 24. Attachments of muscles on the right scapulacoracoid of *Silesaurus opolensis*. Origins are in red, insertions are in blue. **A**, lateral view; **B**, ventral view; **C**. Medial view. Muscle attachments in bold are those that have visible osteological correlates.

The degree of fusion between the scapula and coracoid is similar in all more complete specimens. The suture is clear in its ventral part, near the glenoid, where the coracoid seems slightly overlap the scapula laterally. A marked tubercle locates on the basis of the scapula, just posteriorly to the glenoid. A similar structure also occurs in many dinosaurs (Walker, 1961; Ostrom, 1974; Butler, 2005; Figures 23A, 24A, B, 26)

The coracoid has a subrhomboidal outline in the lateral view, with a greatly expanded and rounded anterodorsal area. The bone is thin and plate-like anteriorly, in accordance with the development of the scapular acromion. The plate is enhanced by slight thickening that is parallel to the preglenoid ridge of the scapula. The coracoid thickens ventrally, where it contributes to the glenoid fossa. Thus, the scapulocoracoid is relatively massive only around

the glenoid. The coracoidal portion of the glenoid has tongue-like appearance in the postroventral view. The glenoid articular surface is subcircular in lateral view.

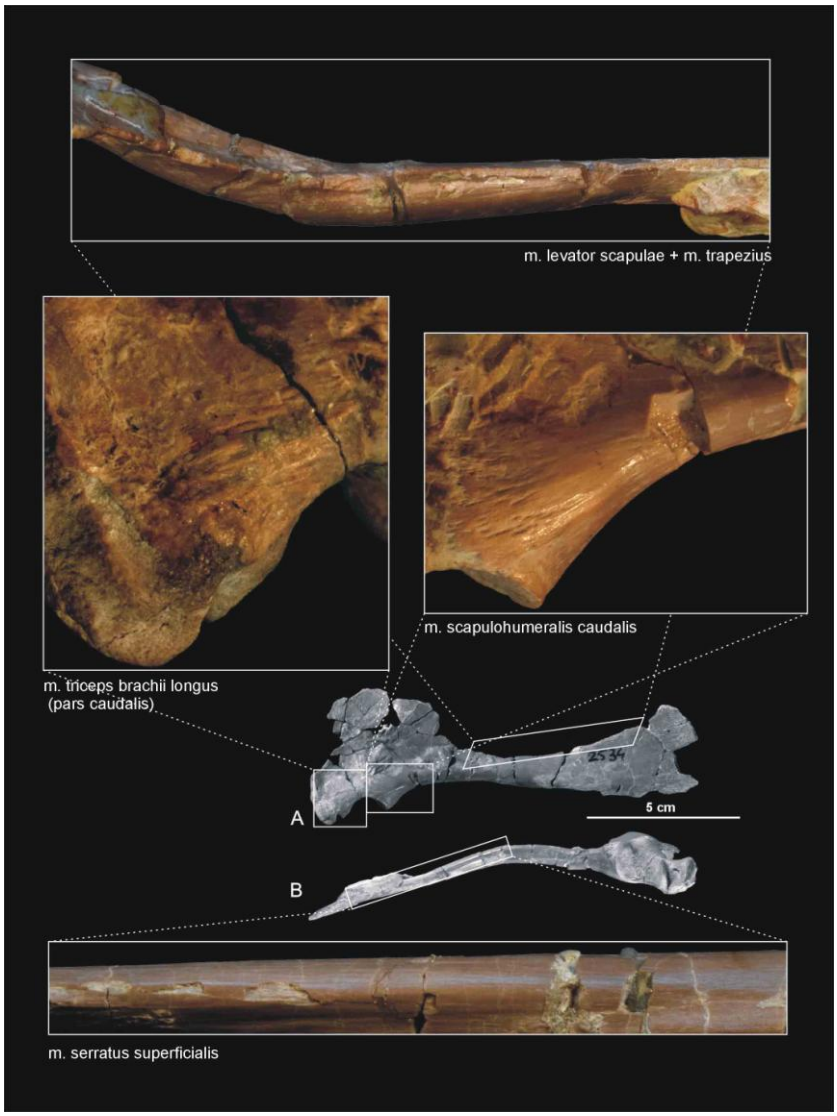

Figure 25. Muscle scars visible on the medial, dorsal, and ventral aspects of the right scapulocoracoid of *Silesaurus opolensis* specimen ZPAL AbIII/2530 except the lower one (ZPAL AbIII/404/8). The scars of m. levator scapulae and m. trapezius rotated 180°. **A**, medial view; **B**, ventral view.

A distinct coracoid foramen appears dorsal to the glenoid anterior to the coracoid-scapula suture on the lateral, slightly convex surface of the bone. A complex structure locates anteriorly to the glenoid (Figures 24A, B, 26). It resembles *Saturnalia* although the bone was described by Langer et al. (2007) in different orientation. The structure faces laterally and projects ventrally as a pointed, deflected process. From this point, it extends as a thickened embankment (= 'elongated tuber' of Langer et al. 2007; = 'biceps tubercle' of Nesbitt, 2011) dorsally on the anterior margin of the bone. It has a subtriangular outline in this view. A distinct semi-lunar groove separates the structure from the tongue-like lateroventral margin of the glenoid.

Figure 26. Muscle scars visible on the right scapulocoracoid of *Silesaurus opolensis* specimen ZPAL AbIII/2530.

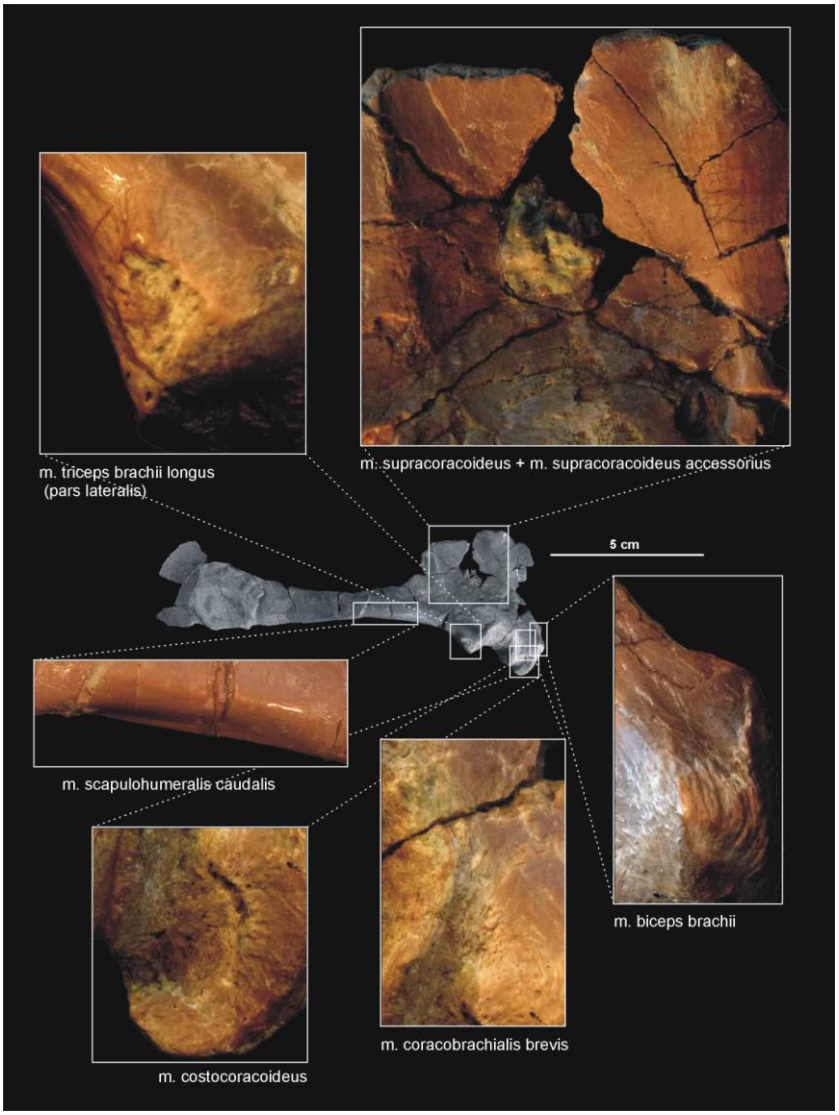

A distinct attachment for the clavicle is visible medially on the anteroventral edge of the coracoid (ZPAL Ab III 2534; Figures 24C, 25A). However, no ossified clavicles are in the material. They were probably cartilaginous or are not preserved.

The orientation of the articular surfaces of the humerus and scapulacoracoid suggests that the humerus could move slightly anteriorly and much farther posteriorly. The orientation of the scapulacoracoid implies a subvertical orientation of the humerus when the animal was standing still. The torsion of humeral heads was much weaker than in the first reconstruction (Dzik, 2003).

Humerus

The humerus (Figures 23 and 27) is a very slender and slightly curved bone. It is hollow but has fairly thick walls like the other long bones. Its moderately convex head (= ‘caput

articulare humeri' of Baumel et al., 1993) occupies most of the proximal end. In proximal view, the head is kidney-shaped, with the slightly concave border facing anteromedially. A slightly swollen medial tuberosity (= tuberculum ventrale of Baumel et al., 1993) forms the medial margin of the proximal humerus. The tuberosity projects dorsally, and its medial surface is convex. Originally it was probably capped by a thick cartilage (Dzik, 2003). Two ridges run longitudinally from the proximal head of the humerus, surrounding a shallow midline concavity on the anterior surface. The ridges are subvertical, low and they diminish before the midshaft. The deltopectoral crest is the smaller one located on the anterolateral side of bone (Figures 23, 27C, D, 28B).

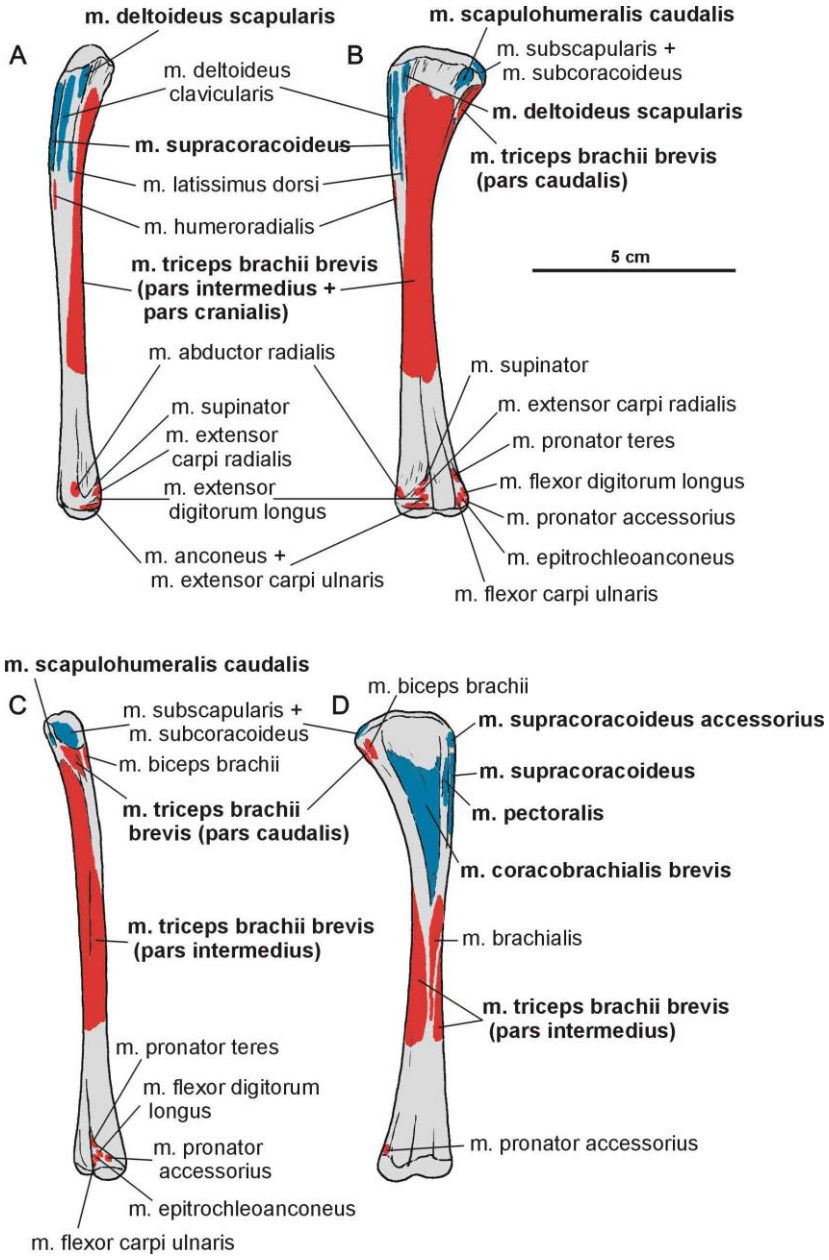

Figure 27. Attachments of muscles on the left humerus of *Silesaurus opolensis*. Origins are in red, insertions are in blue. Muscle attachments in bold are those that have visible osteological correlates. **A**, lateral view; **B**, posterior view; **C**. medial view; **D**, anterior view.

The shaft of the bone is almost straight in the anterior view. It is nearly circular in cross-section in mid-length, but increases its width lateromedially towards the heads. The distal expansion is about two thirds of the width of the proximal one. The distal end is sinuous in profile and is divided into two rounded convexities, the lateral (radial) condyle being slightly larger than the medial (ulnar) condyle. The condyles are separated from each other by a shallow trochlea. The radial condyle is trapezoidal in distal view. It is strongly convex anteroposteriorly and gently concave medially. The radial condyle projects directly distally. The articular surface of the ulnar condyle, in contrast, is oval (rounded) in distal view and reaches further distally. Epicondylar rugosites are well developed on both lateral and medial sides of the distal end of the humerus. The entepicondyle is present on the medial side of the bone just above the ulnar condyle. The ectepicondyle is localized above the radius condyle on the lateral side of the distal end. They are more widely separated, and expand towards the middle-shaft of the bone in larger specimens.

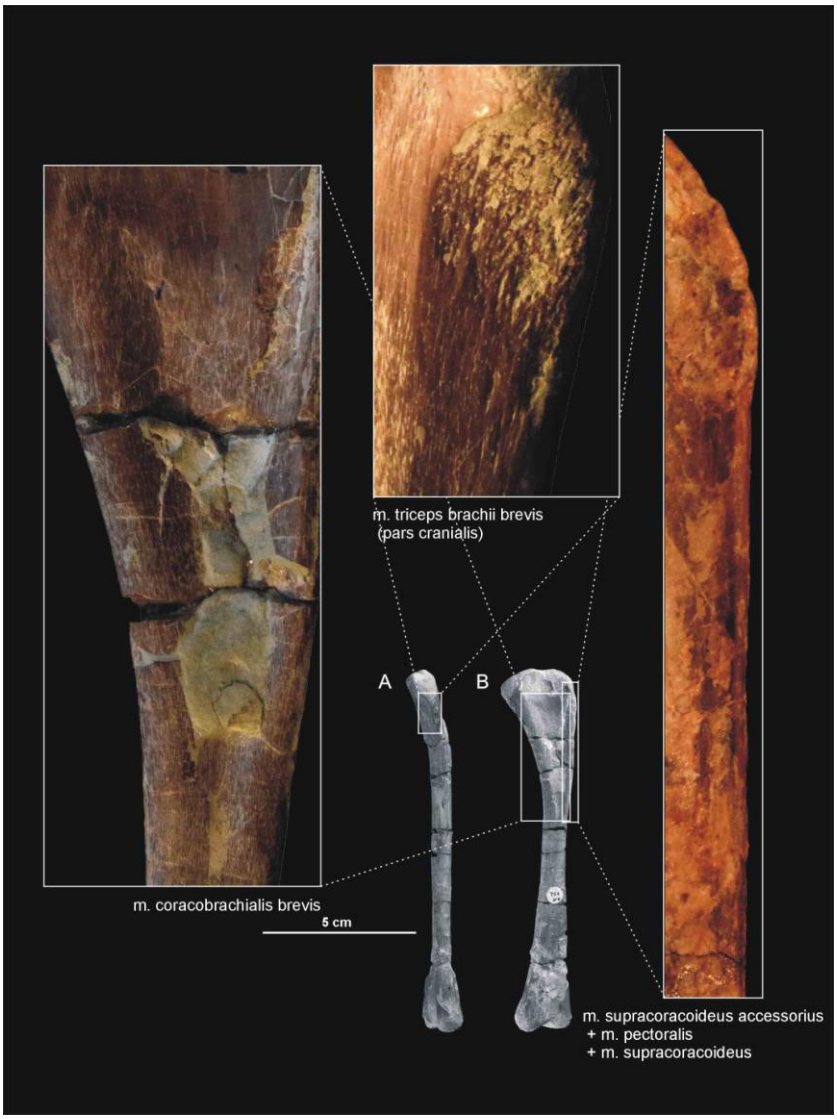

Figure 28. Muscle scars visible on the anterior and medial aspects of the left humerus of *Silesaurus opolensis*. All photographs of ZPAL AbIII/452 except the one on the right (ZPAL AbIII/1930). **A**, lateral view; **B**, posterior view.

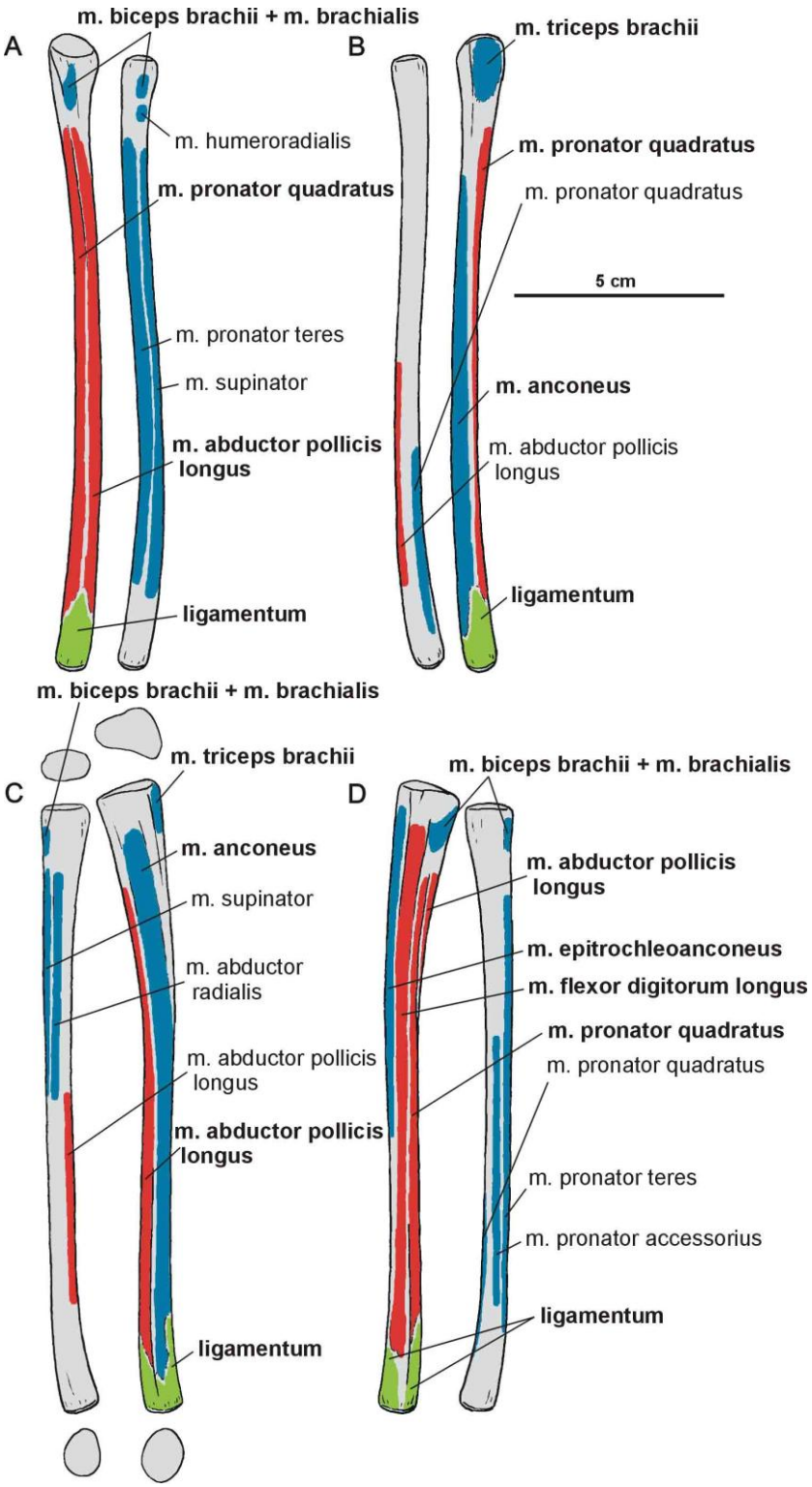

Figure 29. Attachments of muscles and ligaments on the left antebrachium of *Silesaurus opolensis*. Origins are in red, insertions are in blue, ligaments are in green. Muscle and ligament attachments in bold are those which have visible osteological correlates. **A**, anterior view; **B**, posterior view; **C**, lateral view; **D**, medial view.

Forearm

The forearm bones have articular surfaces directed proximally (Figure 23). This means that they were located exactly below the humerus, allowing a nearly vertical orientation. This was aided by the almost complete reduction of the olecranon process of the ulna. The ulna has a subtriangular outline, while the radius is semioval in dorsal view. Both radius and ulna

display a slight curvature, so they were not completely parallel to each other. This feature probably enabled some rotation of the forearm.

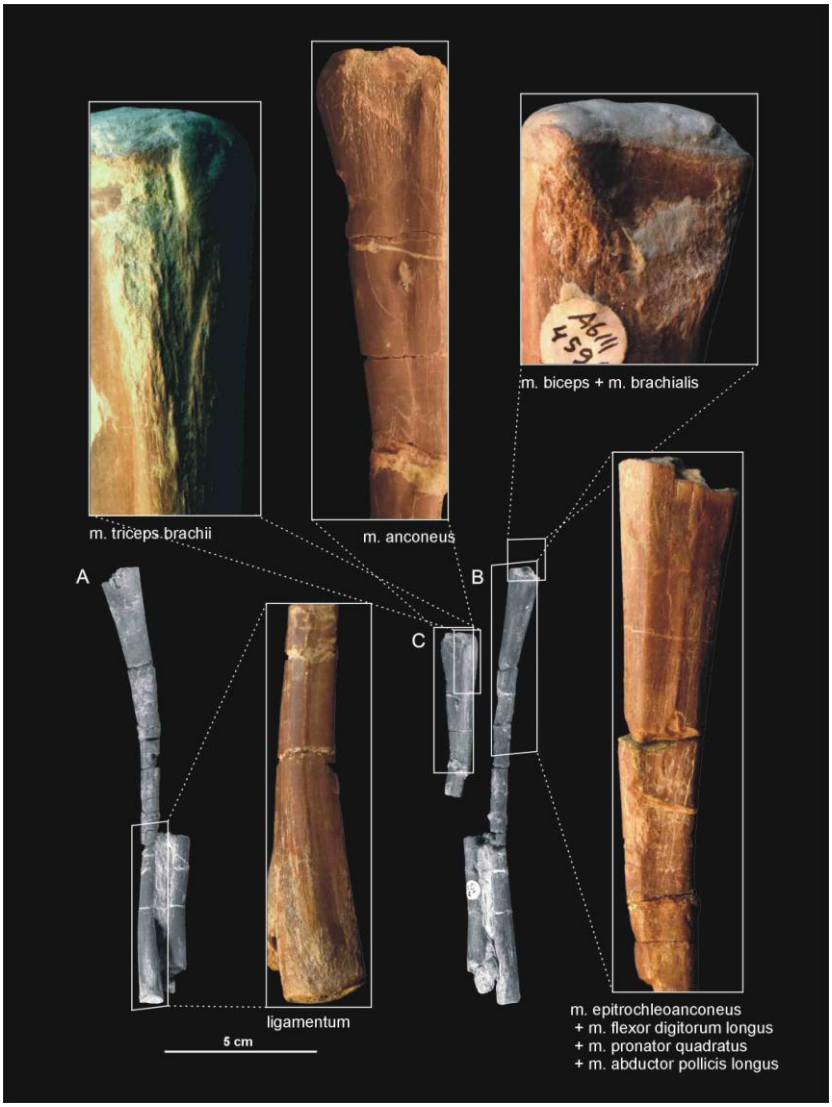

Figure 30. Muscle and ligament scars on the ulna and radius of *Silesaurus opolensis*. Upper left and right photographs of ZPAL AbIII/453/3, upper middle and C of ZPAL AbIII/407/3, remaining of ZPAL AbIII/453. **A**, partial left antebrachium in lateral view; **B**, same in medial view; **C**, incomplete left ulna in lateral view.

Despite some controversy (Hutson & Hutson, 2015; 2017), an active pronation of the manus may have been possible in *Silesaurus*, as lepidosaurs and crocodiles have such ability (Landsmeer, 1983; Baier & Gatesy, 2013). *Silesaurus* anatomy seems to allow semi-pronation by rearranging whole antebrachium *via* long-axis rotation at the elbow joint. This is suggested by the articular surfaces on the radius and ulna that indicate how these bones fit together (ZPAL Ab III 361, 453; Figures 23, 29C, 30A,C). Actually, in quadrupedal animals the muscle action depends more on the limb posture than on the bones morphology (Otero et al., 2017).

The ulna (Figures 23, 29, 30) is unusually slender and longer than the humerus. Its subtriangular proximal surface has a shallow depression. On the lateral side of the proximal

end, a slightly concave facet for articulation with the radius is present. Although the proximal end with its lateral portion is expanded, the distinct olecranon process is not visible. Anterior and posterior margins of the proximal end show indistinct ligament scars and ridges that pass along the length of the shaft.

The ulnar shaft is subtriangular proximally, but from the mid-shaft it becomes semicircular in cross-section (Figure 29C). The shaft curves slightly medially in its distal part. The ends of the bone are expanded and flattened, the proximal much more than the distal one. The convex distal lateral facet contacted a slight depression on the distal medial wall of the radius. The articular surface is semicircular in the distal view. The distinct ligament scars and a longitudinal ridge are visible just above them. This suggests that a strong ligaments may have bounded the distal ends of the ulna and radius.

The radius (Figures 23, 29) is an extremely slender bone, only slightly shorter than the ulna. Its proximal end is slightly concave and subtriangular in cross-section, but the bone becomes semicircular distally. The radius is a relatively simple bone with slightly expanded proximal and distal ends. The distal one is slightly depressed at its contact with the ulna.

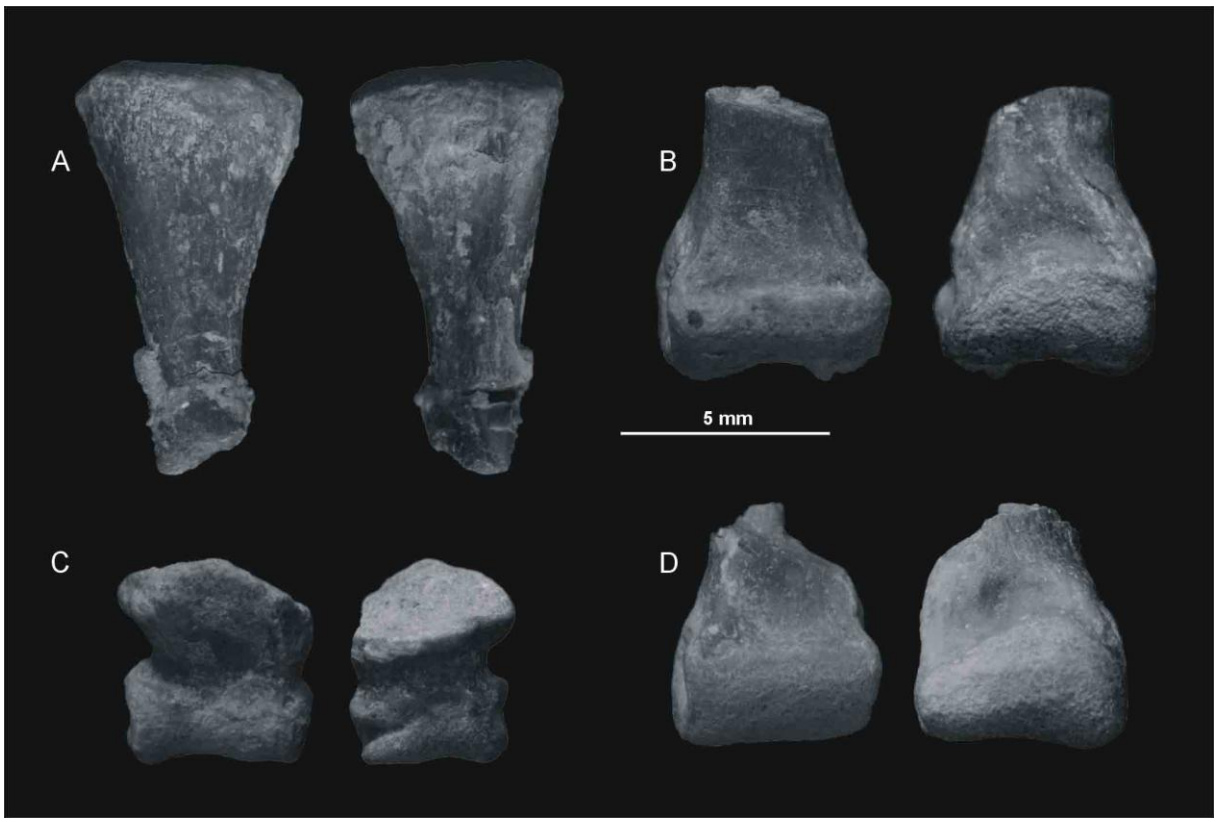

Figure 31. Elements of the manus ZPAL AbIII/455 of *Silesaurus opolensis*. **A**, proximal half of a metacarpal (probably third) in medial and lateral views; B, distal half of a metacarpal in ventral and dorsal views; **C**, distal phalanx in ventral and dorsal views; D, distal half of a metacarpal or phalanx in ventral and dorsal views

Manus

The manus of *Silesaurus* has never been described before. Dzik (2003) mentioned the existence of two possible carpals but I did not find them in the collection. However, I found four other bones that are probably from the manus of one individual ZPAL AbIII/455. In this material (Figure 31), the only complete bone is a distal phalanx. It is a small, short element with a slightly asymmetrical proximal articular facet. The shaft is wider mediolaterally than dorsoventrally and resembles a wedge in lateral view. The lateral and medial sides of the distal expansion bear a deep ligament pit that is bordered by rounded ridges. The sides are not of equal size. Another specimen represents the proximal half of a possible metacarpal IV. Its planar proximal end has a subtriangular, transversely elongated form. The shaft is slender and trapezoidal in cross section. Two incomplete specimens may represent asymmetric distal ends of metacarpals or phalanges. Both the lateral and medial sides of the distal expansion bear a ligament pit that is bordered by rounded ridges.

Chapter 6. Pectoral and brachial musculature[6]

The locomotor musculature of *Silesaurus* was described for the first time by Piechowski & Tałanda (2020), based on partially articulated skeletons (ZPAL Ab/361, ZPAL Ab/362, 363, 364, and 1930), as well as numerous isolated or semiarticulated bones of the fore- and hind limbs. The available material is generally well preserved, and shows clear muscle attachment features.

M. serratus superficialis

The origin of the m. serratus superficialis is tentatively reconstructed *in Silesaurus* based on other studies (Meers, 2003; Jasinoski et al., 2006; Remes, 2008; Burch, 2014) as arising from the lateral surfaces of several anteriormost dorsal ribs. The muscle inserts on the posterior part of the ventral edge of the scapular blade (compare with Fürbringer, 1900; Miner, 1925; Figure 24, Table 7). In *Silesaurus* material the insertion area can be recognized in specimens ZPAL Ab III/2534, 404/8, 406/7. The condition proposed here for *Silesaurus* resembles that in crocodilians (Meers, 2003) and lepidosaurs (Russell & Bauer, 2008) in having a single elongated insertion along the ventral edge of the scapula, as marked by longitudinal striations (Figure 25B). The m. serratus superficialis retracts and depresses the scapula (see Meers, 2003; Table 7).

Table 7. Synopsis of the pectoral and brachial musculature in *Silesaurus opolensis*, listing their names, origins, insertions, and actions. Muscle attachments in bold are those that have visible osteological correlates.

Muscle name	Origin	Insertion	Proposed function	Level of inference
M. serratus superficialis	Lateral surfaces probably of the ninth to twelfth ribs	**Posterior part of the ventral edge of the scapular blade**	Retracts and depresses the scapula	I
M. serratus profundus	Lateral surfaces probably of the ten to twelfth ribs	Distal part of the ventral aspect of the scapular blade	Protracts the scapula	II
M. costocoracoideus	Anterior edge	**Anteroventral**	Rotates, adducts and	III

[6] Part of this chapter was published in:
Piechowski, R. & Tałanda. M. 2020. The locomotor musculature and posture of the early dinosauriform *Silesaurus opolensis* provides a new look into the evolution of Dinosauromorpha. *Journal of Anatomy* DOI: 10.1111/joa.13155

	probably of the anteriormost dorsal ribs	**portion of the lateral surface of the coracoid**	protracts the forelimb	
M. rhomboideus	Neural spines probably of the anteriormost dorsal vertebrae	Distalmost end of the medial aspect of the scapular blade	Protracts the scapula	I
M. levator scapulae	Anterior cervical ribs	**Dorsal edge of the scapular blade**	Rotates the scapula, as well as lateral flexion of the neck	I
M. trapezius	Cervical and thoracodorsal fascia	**Dorsal edge of the scapular blade**	Rotates the scapular blade, likely assisting in protraction of the forelimb	I
M. latissimus dorsi	Neural spines or thoracodorsal fascia probably of the last cervical to the sixth or seventh dorsal vertebrae	Posterolateral side of the proximal humerus	Retracts the humerus	I
M. teres major	Posterior part of the lateral surface of the scapular blade?	Proximodorsal surface of the humerus?	Retracts the humerus	II
M. pectoralis	Gastral apparatus	**Posterolateral surface of the deltopectoral crest of the humerus**	Adducts and protracts the humerus	II
M. subscapularis	Medial side of the scapular blade	Medial tuberosity of the humerus	Retracts and rotates the humerus	II
M. subcoracoideus	Medial side of the coracoid	Medial tuberosity of the humerus	Adducts and laterally rotates the humerus	I
M. supracoracoideus	**Subacromial depression of the scapula, and adjacent lateral surface of the coracoid**	**Lateral surface of the deltopectoral crest of the humerus**	Protracts and abducts the humerus	II
M. supracoracoideus accessorius	**Subacromial depression of the scapula**	**Proximal part of the deltopectoral crest of the humerus**	Protracts and abducts the humerus	II

M. coracobrachialis brevis	**Anteroventral portion of the lateral surface of the coracoid**	**Broad, subtriangular depression on the anterior surface of the humerus**	Protracts the humerus	I
M. coracobrachialis longus	I refrained from reconstruction			II
M. scapulohumeralis caudalis	**Medial side of the scapula, next to the glenoid and the ridge on the ventral margin of the scapular blade**	**Medial tuberosity of the humerus**	Retracts the humerus	I
M. scapulohumeralis anterior	I refrained from reconstruction			I
M. deltoideus clavicularis	Acromion process of the scapula	Lateral surface of the deltopectoral crest of the humerus	Abducts and slightly protracts the humerus	II
M. deltoideus scapularis	Lateral blade of the scapula	**Posterolateral surface of the proximal humerus**	Abducts and retracts the humerus	II
M. triceps brachii longus and brevis	**Lateroventral surface of the scapula just posterior to the glenoid (triceps branchii longus, pars lateralis); medial surface of coracoid just anterior to the glenoid** and tentatively in the middle of the scapular blade ventrally **(triceps branchii longus, pars caudalis); oval rugose surface just below the medial**	**Olecranon process of the ulna**	Extends the antebranchium, as well as contributing to the extension of the humerus	I

	tuber of the humerus (triceps brachii brevis, pars caudalis); most of the posterior humeral shaft (triceps brachii brevis, pars intermedius)			
M. biceps brachii	**Anterior edge of the coracoid together with the biceps tubercle;** anteromedial aspect of the proximal humerus?	**Anterior sides of the proximal ulna and radius**	Flexes the antebrachium	I
M. humeroradialis	Lateral side of the deltopectoral crest of the humerus	Anterolateral side of the proximal radius	Flexes the antebrachium	II
M. brachialis	Lateral humeral midshaft, distal to the deltopectoral crest	**Anterior sides of the proximal ulna and radius**	Flexes the forearm	I

M. serratus profundus

In *Silesaurus*, the origin of the m. serratus profundus is similar to that in *Tawa* (Burch, 2014), where it arose from several anteriormost dorsal ribs (compare also with Fürbringer, 1900; Jasinoski et al., 2006; Remes, 2008). The insertion is not osteologically distinguishable on the scapula of *Silesaurus* but probably it lays behind the distal insertion of the m. subscapularis (compare with Jasinoski et al., 2006; Remes, 2008; Burch, 2014; Figure 24C, Table 7). The m. serratus profundus acted as a protractor of the scapula (see Burch, 2014; Table 7).

M. costocoracoideus

Phylogenetic bracketing suggests the presence of this muscle in *Silesaurus*. Because a large keeled sternum is a bird apomorphy, the origin of m. costocoracoideus in *Silesaurus* was presumably located on the ribs, as in crocodiles (compare Jasinoski et al., 2006; Remes, 2008). The insertion was probably located on the anteroventral portion of the lateral surface

of the coracoid (compare Meers, 2003; Remes, 2008; Figure 24A, B, Table 7), posteroventral to the origin of m. biceps brachii. The ventral (= posteroventral of Burch, 2014) process of the coracoid of *Silesaurus* (ZPAL Ab III/2534, and 1203) possesses a distinct rugose subglenoid fossa that is the likely insertion point (Figure 26). A similar fossa is visible in many dinosaurs (Santa-Luca, 1980; Jasinoski et al., 2006; Langer et al. 2007). The action of m. costocoracoideus is to rotate, adduct and protract the forelimb (Table 7).

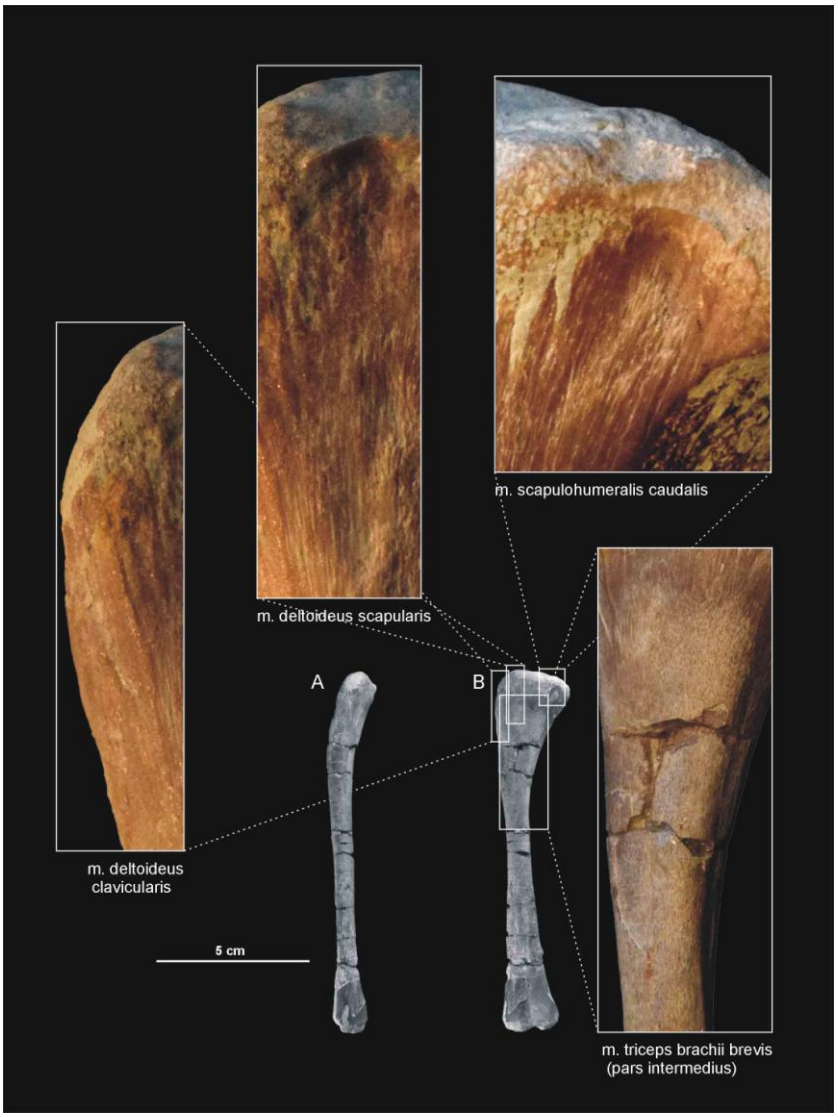

Figure 32. Muscle scars visible on the posterior side of humerus of *Silesaurus opolensis*. All photographs of the left humerus ZPAL AbIII/452 except the scar for m. latissimus dorsi that is on ZPAL AbIII/1930. **A**, lateral view; **B**, posterior view.

M. rhomboideus

Based on the scapula orientation in *Silesaurus*, which was probably intermediate between that of birds (subhorizontal) and crocodilians (subvertical), it is possible that the m. rhomboideus was transitional in its origin, arising from fascia and several anterior dorsal neural spines (compare with Fürbringer, 1876; Fürbringer, 1888; Fürbringer, 1902; Fitzgerald, 1969; Jasinoski et al., 2006; Remes, 2008; Burch, 2014). The muscle is reconstructed as

inserting on the distalmost end of the medial scapular blade as in *Tawa* (Burch, 2014; compare with Cong et al., 1998; Fürbringer, 1900; Meers, 2003; Remes, 2008; Figure 24C, Table 7), although the reconstruction of this muscle is tentative. What is clear is that the widening of the scapular blade provides a more extensive surface for the muscle. The m. rhomboideus acted as protractor of the scapula (see Burch, 2014; Table 7).

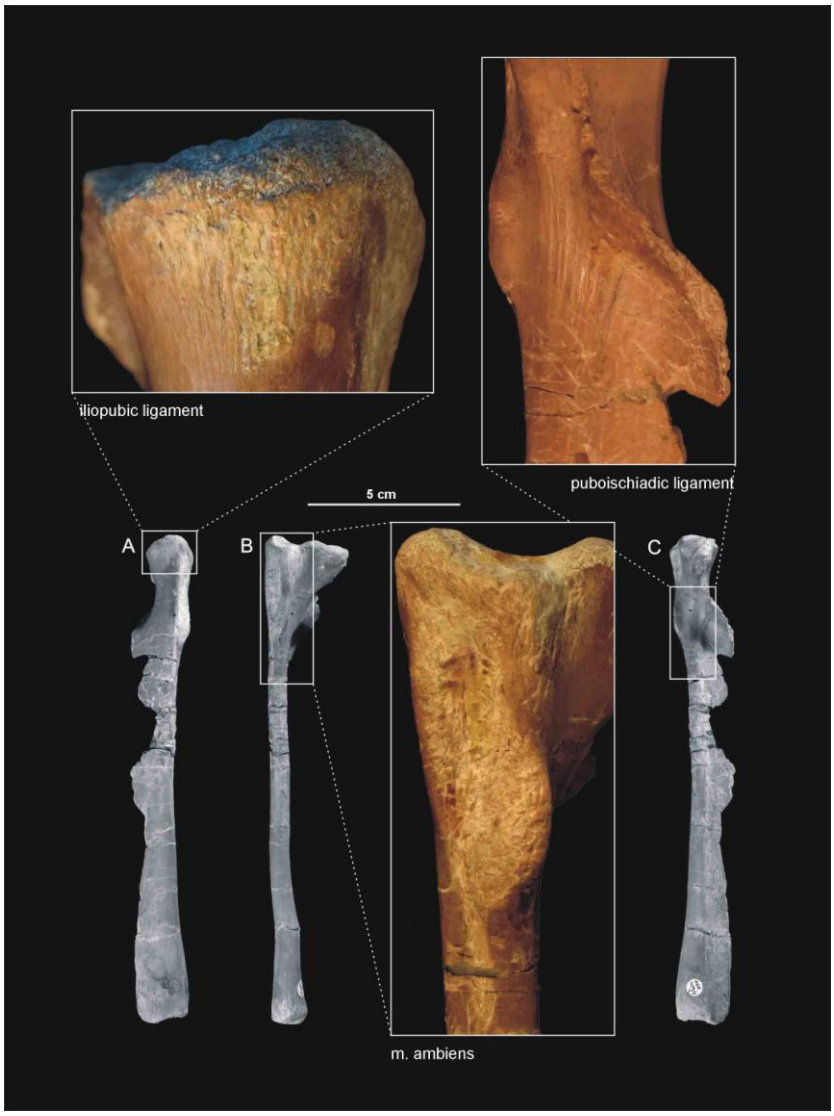

Figure 33. Muscle and ligament scars visible on the left pubis of *Silesaurus opolensis* specimen ZPAL AbIII/404/5. **A**, anterodorsal view; **B**, lateral view; **C**, posteroventral view.

M. levator scapulae

The m. levator scapulae is located on the lateral side of the neck, medial to the m. trapezius (Jasinoski et al., 2006; Remes, 2008). In *Silesaurus*, the anterior cervical ribs are parallel to the neck and extend backward for a few vertebral lengths (Piechowski & Dzik, 2010). Therefore, they could serve as a muscle attachment. The presence of clear striations and a distinct ridge (the latter only in the smaller specimen ZPAL AbIII/2534) on the dorsal edge of

the scapular blade provides evidence to reconstruct the m. levator scapulae with the m. trapezius in *Silesaurus* (compare with Fürbringer, 1876; Fürbringer, 1900; Romer, 1922; Remes, 2008; Meers, 2003; Burch, 2014; Figure 24A, C, Table 7). The insertion area can also be recognized in specimens ZPAL Ab III/404/8, 406/7, and 411/12 (compare with Meers, 2003; Jasinoski et al., 2006; Burch, 2014; Figure 25A). The m. levator scapulae acted as a rotator of the scapular blade, as well as a lateral flexor of the neck (see Burch, 2014; Table 7).

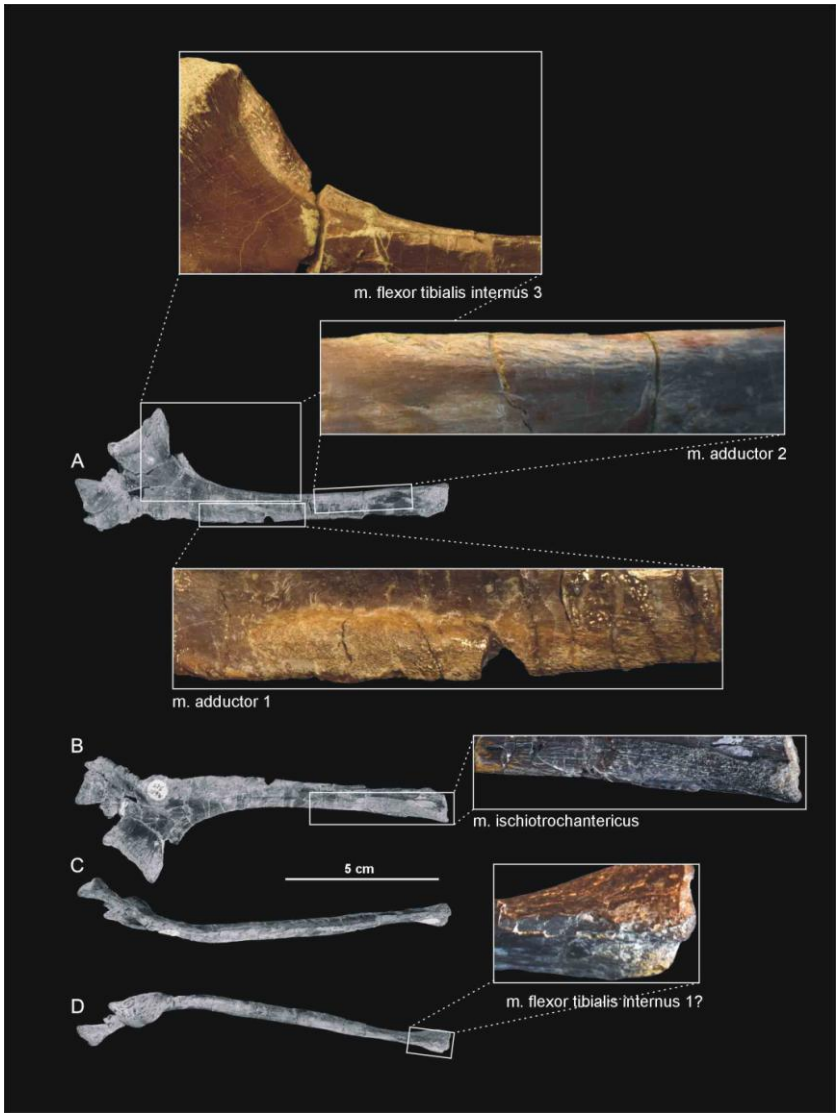

Figure 34. Muscle scars visible on the ischium of *Silesaurus opolensis*. The uppermost photograph is of ZPAL AbIII/3226, the first below ZPAL AbIII/404/7, the others from ZPAL AbIII/925. **A**, left ischium in lateral view; **B**, same in medial view; **C**, same in ventral view; **D**, same in dorsal view.

M. trapezius

In *Silesaurus*, as a result of sudden change in morphology of the ribs at the cervical to dorsal boundary, the first ten to eleven dorsal ribs are especially strong and long (Piechowski & Dzik, 2010). Therefore, the scapula of *Silesaurus* could not keep completely horizontal position. Given osteological evidence for the presence of the m. levator scapulae (see above), I include the m. trapezius in the reconstruction of musculature of *Silesaurus* (compare with

George & Berger, 1966; Meers, 2003; Russell & Bauer, 2008; Burch, 2014; Fearon & Varricchio, 2016; Figures 24A, B, 25A, Table 7). This superficial muscle acted as a rotator of the scapular blade, likely assisting in protraction of the forelimb (see Burch, 2014; Table 7).

M. latissimus dorsi

The m. latissimus dorsi is reconstructed here as a single muscle that originates on the neural spines or thoracodorsal fascia probably in the region from the last cervical to the sixth or seventh dorsal vertebrae (compare with Romer, 1922, 1944; Meers, 2003; Russell & Bauer, 2008; Burch, 2014; Figure 27A, B, Table 7). The insertion of the muscle is tentatively reconstructed on the proximal posterolateral side of the humerus (compare with Sullivan, 1962; George & Berger, 1966). The m. latissimus dorsi acted as a retractor of the humerus (see Burch, 2014; Table 7).

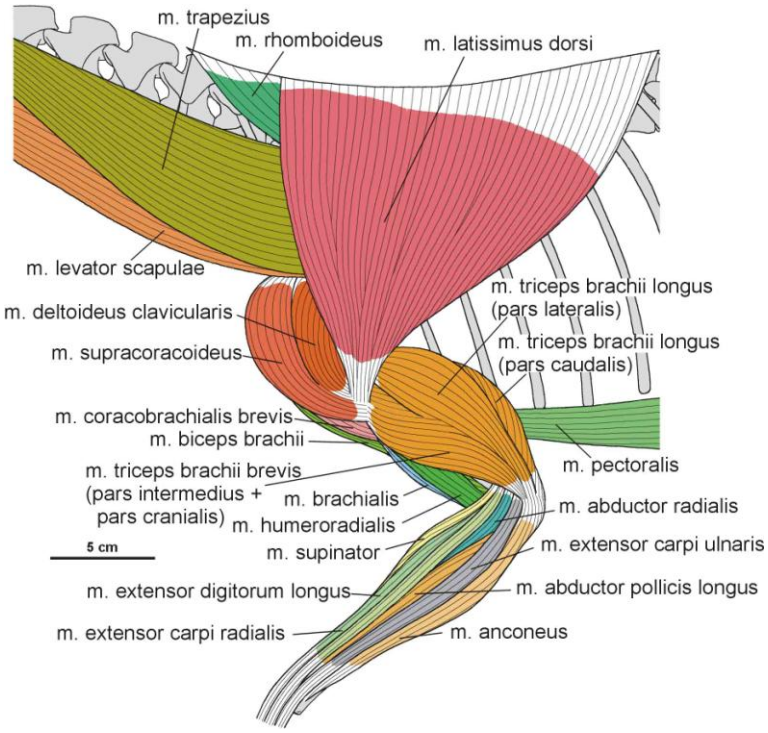

Figure 35. Muscle disposition on the forelimb of *Silesaurus opolensis* in lateral view.

M. teres major

Because no osteological correlates are present in *Silesaurus*, the m. teres major is shown tentatively in the reconstruction (Figure 24A, Table 7). Being a specialized part of the m. latissimus dorsi (Remes, 2008), the m. teres major retracted the humerus (see Butler, 2010; Table 7).

M. pectoralis

Due to the lack of ossified sternum of *Silesaurus*, it is difficult to determine the origin of m. pectoralis (see Remes, 2008; Burch, 2014; Padian, 2004; Fearon & Varricchio, 2016). Nevertheless, Fürbringer (1900) assumed that the well-development gastral apparatus found in many fossil amniotes might have served as an anchor for the m. pectoralis. Such a well-developed gastral apparatus is present in the skeleton of *Silesaurus* (Piechowski & Dzik, 2010). The insertion of m. pectoralis is located on the posterolateral surface of the low deltopectoral crest preserved in specimens ZPAL Ab III/1930, and 411/11 (Figures 27D, 28B, 9). The m. pectoralis would have adducted and protracted the humerus (see Burch, 2014; Table 7).

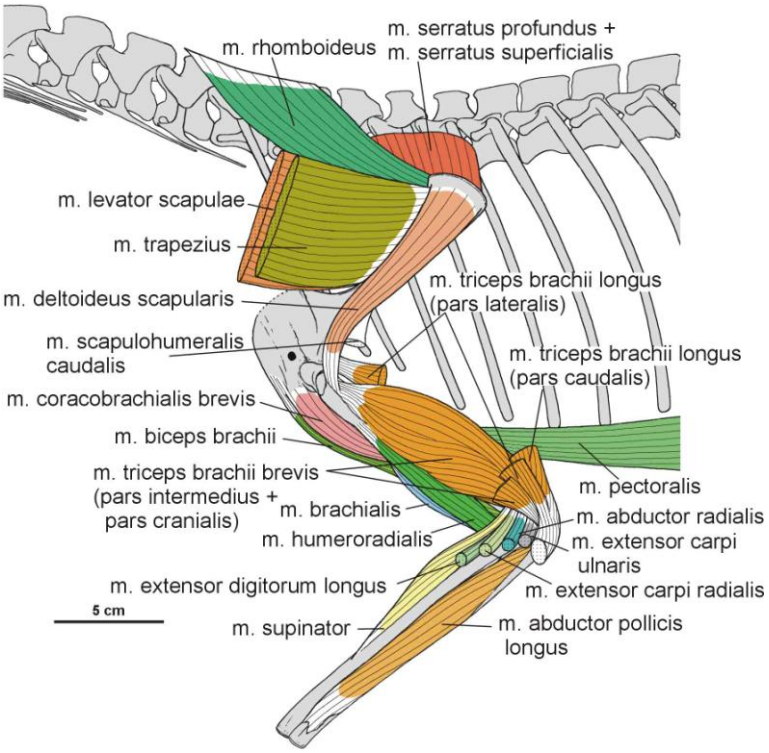

Figure 36. Muscle disposition on the forelimb of *Silesaurus opolensis* in lateral view. Some muscles are removed.

M. subscapularis

Phylogenetic inference suggests an origin of the m. subscapularis from the medial surface of the scapular blade in *Silesaurus*, as in crocodilians (compare with Romer, 1944; Sullivan, 1962; Meers, 2003; Maidment & Barrett, 2011; Figure 24C, Table 7). The insertion of the m. subscapularis is equivocally located on the medial tuberosity of the humerus (compare with Meers, 2003; Maidment & Barrett, 2011; Figure 27B–D, Table 7), sharing an insertion with the m. subcoracoideus. The m. subscapularis would have retracted and rotated the humerus (see Burch, 2014; Table 7).

M. subcoracoideus

Phylogenetic inference suggests the m. subcoracoideus originated on the medial side of the coracoid in *Silesaurus* (compare with Romer, 1944; Sullivan, 1962; Meers, 2003; Jasinoski et al., 2006; Maidment & Barrett, 2011; Burch, 2014; Fearon & Varricchio, 2016; Figure 24C, Table 7). The m. subcoracoideus equivocally shares a tendon insertion on the medial tuberosity of the humerus with the m. subscapularis (Figure 27B–D, Table 7). The m. subcoracoideus adducted and laterally rotated the humerus (see Burch, 2014; Table 7).

M. supracoracoideus

Because I cannot distinguish separate attachments on the surface of the coracoid, I reconstruct the m. supracoracoideus of *Silesaurus* as a muscle complex without distinguishing multiple heads (compare with Romer, 1944; Sullivan, 1962; Meers, 2003; Remes, 2008; Maidment & Barrett, 2011). The muscle originates on the subacromial depression of the scapula and extends on to the adjacent lateral surface of the coracoid, providing a clear broad, flat area on both bones (Figures 24A, 26, Table 7). The posteroventral extent of the m. supracoracoideus is delimited by a distinct bowed scar, which is clearly visible on specimens ZPAL AbIII/404/8, and 2634. Unfortunately, the dorsal range of the muscle attachment of this region is difficult to determine because of poor preservation in all specimens. The m. supracoracoideus inserted on the deltapectoral crest of the humerus. A small longitudinal depression located on the lateral surface of the deltopectoral crest in specimens ZPAL Ab III/1930, 452, 411/11 is consistent with this site of insertion and indicates the lateral extent of the insertion (Figures 27A, B, D, 28B, Table 7). The m. supracoracoideus acted as a protractor and abductor of the humerus (see Burch, 2014; Table 7).

M. supracoracoideus accessorius

I tentatively reconstruct the origin of this muscle on the subacromial depression of the scapula together with area for the m. supracoracoideus (compare with Burch, 2014; Figures 24A, 26, Table 7). The m. supracoracoideus accessorius inserted on the proximal part of the deltopectoral crest (anterior side) of *Silesaurus* and may be marked by a distinct semioval depression in ZPAL AbIII/1930 (Figures 27D, 28B, Table 7). The role of the muscle is the same as the previous one.

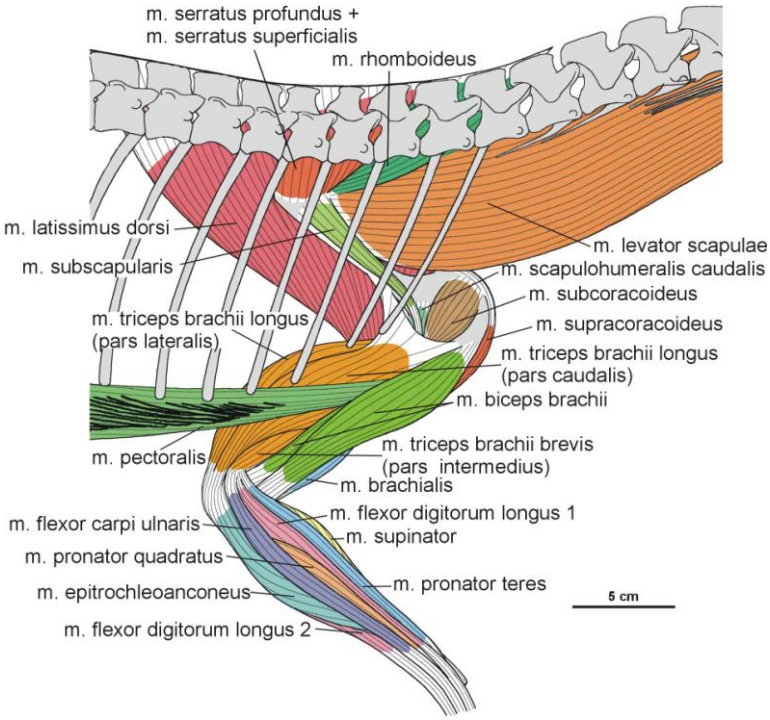

Figure 37. Muscle disposition on the forelimb of *Silesaurus opolensis* in medial view.

M. coracobrachialis brevis

The origin of the m. coracobrachialis brevis is unequivocally reconstructed here based on the origin of the crocodilian and ornithischian pars ventralis (compare with Romer, 1944; Sullivan, 1962; Meers, 2003; Maidment & Barrett, 2011; Burch, 2014). According to this, the muscle arises from the lateral aspect of the coracoids (Figure 24A, B, Table 7). A distinct fossa appears between the glenoid and the ventral process (ZPAL Ab III/2534 and 1203). The fossa is rugose and subdivided into two basins by an anteroposterior constriction. The ventral basin served for insertion of the m. costacoracoideus as proposed above. The dorsal basin belongs to the origin of the m. coracobrachialis brevis. Rugosities observed above this structure probably represent the extension of this origin (Figure 26). The insertion of this muscle is also phylogenetically unequivocal, situated on the broad, subtriangular depression that covers most of the anterior surface of the humerus (compare with Meers, 2003; Maidment & Barrett, 2011; Figure 27D, Table 7). In *Silesaurus*, this area is clearly visible on specimens ZPAL Ab III/452, and 411/11. Consistent with this morphology, the primary action of the m. coracobrachialis brevis would be protraction of the humerus (see Burch, 2014; Table 7).

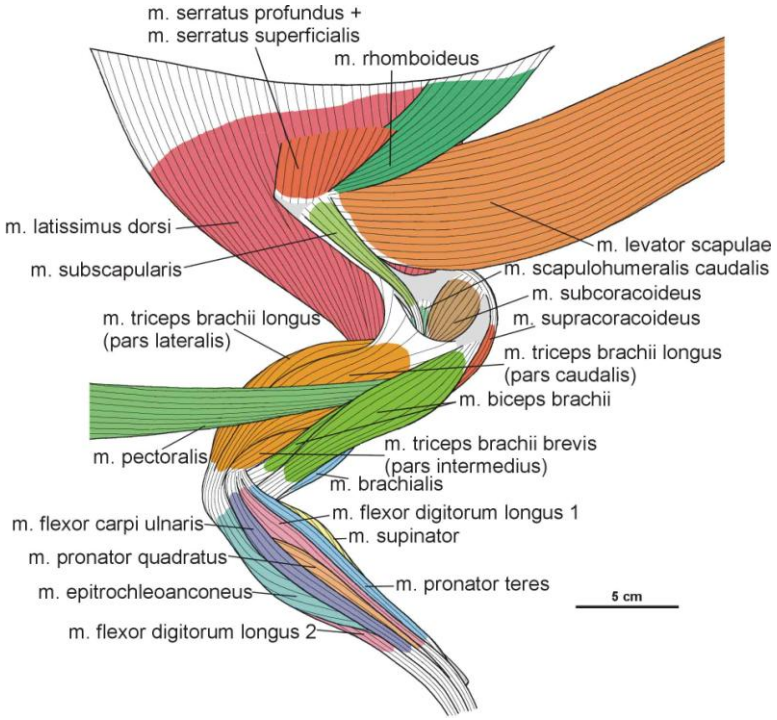

Figure 38. Muscle disposition on the forelimb of *Silesaurus opolensis* in medial view but without the axial skeleton.

M. coracobrachialis longus

Crocodilians lack the m. coracobranchialis longus making it phylogenetically equivocal (Burch, 2014). I opted not to reconstruct it in *Silesaurus* due to the lack of osteological correlates (Table 7).

M. scapulohumeralis caudalis

There is a distinct muscle scar next to glenoid on the medial side of the scapula in ZPAL AbIII/2534, 404/8, and 406/7. This rugose area is tear-shaped. There is also a distinct ridge on the ventral surface of the scapular blade just posteriorly to the scar. I identify these areas as the origin of the m. scapulohumeralis caudalis because it is in a location similar to that of crocodiles (compare with Romer, 1944; Meers, 2003; Burch, 2014; Figures 24, 25A, 26, Table 7). The insertion of the m. scapulohumeralis caudalis is located on the medial tuberosity of the humerus. Similar to that of some dromaeosaurids and *Tawa* (Burch, 2014; compare with George & Berger, 1966; Meers, 2003; Maidment & Barrett, 2011), the humerus of *Silesaurus* (ZPAL AbIII/452, 411/11, and 1930) has an oval depression on the posterior surface of the medial tuberosity that most probably corresponds to the insertion site of this muscle (Figures 27B, C, 32B, Table 7). The m. scapulohumeralis caudalis acted as a retractor of the humerus (see Burch, 2014; Table 7).

M. scapulohumeralis anterior

I failed to trace any insertion for the m. scapulohumeralis anterior in *Silesaurus*. The m. scapulohumeralis anterior is reconstructed in nonavian theropods by homology with birds and lepidosaurs. These dinosaurs bear a scar or a weak fossa on the posterior portion of the scapular blade, which marks the origin of the muscle. In contrast to birds, theropods have no trace of this muscle insertion on the humerus. The muscle is absent in crocodiles (see Burch, 2014; Table 7).

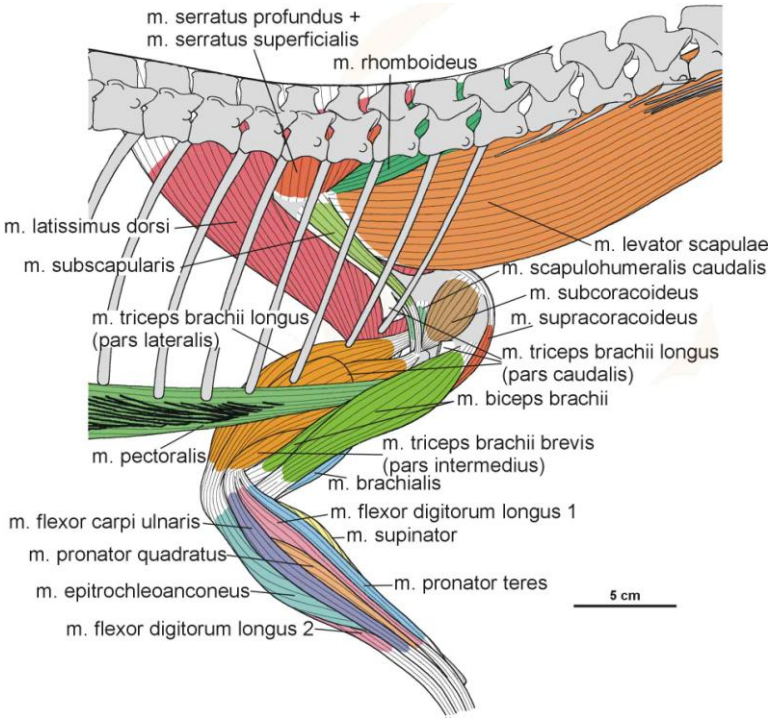

Figure 39. Muscle disposition on the forelimb of *Silesaurus opolensis* in medial view. Some muscles are removed.

M. deltoideus clavicularis

The origin of the m. deltoideus clavicularis is tentatively reconstructed here as a semilunar area restricted to the anterodorsal part of the lateral surface of the acromion process of the scapula (compare with Romer, 1944; Meers, 2003; Remes, 2008; Figure 24A, Table 7). The prominent acromial process of *Silesaurus* is similar in its development to that of ornithischians and crocodiles (Coombs, 1978; Norman, 1986; Johnson & Ostrom, 1995; Dilkes, 2000; Meers, 2003). The insertion of the m. deltoideus clavicularis is visible as a distinct longitudinal area on the lateral surface of the deltopectoral crest (compare with Sullivan, 1962; George & Berger, 1966; Dilkes, 2000; Meers, 2003; Burch, 2014; Figure 25). The m. deltoideus clavicularis would have abducted and slightly protracted the humerus (see Burch, 2014; Table 7).

M. deltoideus scapularis

In *Silesaurus*, the m. deltoideus scapularis probably originated on the lateral scapular blade which provides a large area of attachment (compare with Fürbringer, 1876; Romer, 1944, 1956; Remes, 2008; Sullivan, 1962; Meers, 2003; Maidment & Barrett, 2011; Figure 24A, B, Table 7). The muscle inserted on the posterolateral surface of the proximal humerus (compare with George & Berger, 1966; McGowan, 1982; Meers, 2003; Figure 27A, B, Table 7). There are subtle striations in this location (ZPAL AbIII/452) that likely represent a scar for this muscle (Figure 32B). The m. deltoideus scapularis would have abducted and retracted the humerus (see Burch, 2014; Table 7).

M. triceps brachii longus and brevis

In *Silesaurus*, clear striations appear on the lateroventral surface of the scapula just posterior to the scapular glenoid fossa, and form a distinct rugose tubercle. This can be easily homologized with the m. triceps branchii longus lateralis origin as it has the same location in crocodiles and birds (compare with Romer, 1944; George & Berger, 1966; Remes, 2008; Meers, 2003; Maidment & Barrett, 2011; Figures 24A, B, 26, Table 7). The tubercle is present in a similar location in the basal ornithischians *Heterodontosaurus* (Santa-Luca et al., 1976; Santa-Luca, 1980) and *Eocursor* (Butler, 2010). A rugosity in this area is variably developed across theropods (Burch, 2014). The m. triceps branchii longus caudalis origin is visible on the medial surface of the coracoid just anterior to the glenoid fossa, where the origin forms a distinct rugose concavity (Figures 24C, 25A, Table 7). Many authors recognized only one origin of the m. triceps on this bone in various early dinosaurs (Langer et al., 2007; Maidment & Barrett, 2011; Burch, 2014) as the second origin is equivocal and have no osteological correlates. However, Delcourt & Azevedo (2012) found a shallow pit on the medial portion of the scapular blade in *Saturnalia*. It has very similar form and position as the scapular attachment of m. triceps brachii longus in *Caiman brevirostris*. Based on that I tentatively reconstruct this attachment in *Silesaurus* (Figure 24, Table 7). The origins of the m. triceps brachii are also clearly visible on the humerus ZPAL AbIII/452, 411/11 of *Silesaurus*. In *Silesaurus*, the m. triceps brachii brevis caudalis occupied a distinct oval rugose surface. It is located in *Silesaurus* on the posterior side of the bone, just below the medial tuber (Figures 27B–D, 28A, Table 7). The m. triceps brachii brevis intermedius originated just distal to the pars caudalis and continued distally along the humeral shaft. The origin has

heart-like outline on the posterior side of the bone where it is expanded and bifurcated proximally (Figures 27A–C, 32B, Table 7). If present, the m. triceps brevis cranialis continued along the lateral border of the pars intermedius as a narrow strip. The common insertion of the m. triceps brachii is on the olecranon process of the ulna (compare with Meers, 2003; Remes, 2008; Maidment & Barrett, 2011; Burch, 2014; Figure 29B, C, Table 7). Although the *Silesaurus* olecranon is vestigial against many other Triassic Dinosauromorpha, it bears clear striations for this muscle in ZPAL AbIII/431/1, 459/3, and 407/3 (Figure 30C). The primary action of the m. triceps branchii would be in extending the antebranchium, as well as contributing to extension of the humerus (see Burch, 2014; Table 7).

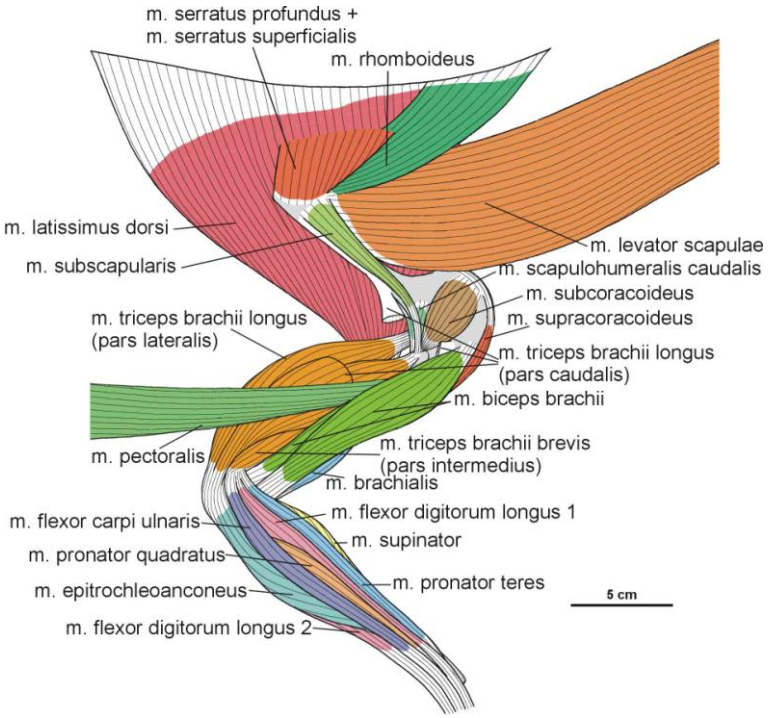

Figure 40. Muscle disposition on the forelimb of *Silesaurus opolensis* in medial view. Some muscles and the axial skeleton are removed.

M. biceps brachii

The origin of the m. biceps brachii is reconstructed here along the anterior edge of the coracoids (compare with Romer, 1944; Goslow, 1989; Meers, 2003; Remes, 2008; Maidment & Barrett, 2011; Burch, 2014; Fearon & Varricchio, 2016; Figure 24A, Table 7). Its ventral border is marked by a distinct biceps brachii tubercle (ZPAL AbIII/2534 and 1203; Figure 26). The tubercle appears anterior to the glenoid and dorsal to the ventral process of the coracoid. It is wider than high and directed anterolaterally. My reconstruction of the m. biceps brachii is in contrast to those proposed by some authors (Langer et al., 2007; Burch, 2014), which locate its origin on the 'elongated tuber' of the coracoid. However, I note that in extant archosaurs the origin of this muscle is on the acromial part of the coracoids (Meers, 2003), far

from the glenoid area. My interpretation is congruent with many others (i.e. Borsuk-Białynicka, 1977; Maidment & Barrett, 2011; Fearon and Varricchio, 2016). The humeral head of the m. biceps brachii is present only in birds among modern archosaurs (Vanden Berge & Zweers, 1993; Jasinoski et al., 2006; Remes, 2008) and is not reconstructed in non-theropod dinosaurs (i.a., Langer et al., 2007; Maidment & Barrett, 2011; Fearon & Varricchio, 2016). However, it is reconstructed even in the Triassic theropods (Burch, 2014). I observe an indistinct rugose surface in *Silesaurus* on the anteromedial aspect of the medial tuber that perhaps represents the biceps brachii humeral origin (Figure 27C, D). It is preserved only in ZPAL AbIII/411/11. As for the insertion, there is a distinct muscle scar on the anterior side of the ulna in *Silesaurus* (ZPAL AbIII/2538, 407/3, 407/12, 459/3, and 431/1) that corresponds with this attachment in extant taxa (Figures 29A, C, D, 30B, Table 7). It is located just distal to the articular surface and has a subtriangular outline that expands posterodistally. The radius (ZPAL AbIII/407/12) bears only delicate rugosities on its surface in an analogous area. The primary action of the m. biceps brachii would be flexion of the antebrachium (see Burch, 2014; Table 7).

M. humeroradialis

Because both origin and insertion of this muscle are indistinguishable in *Silesaurus*, its presence is inferred based on some theropods and crocodiles (compare with Fürbringer, 1876; Romer, 1944; Sullivan, 1962; Meers, 2003; Diogo & Abdala, 2010; Burch, 2014; Figures 27A, B, 29A, Table 7). The muscle lacks osteological correlates in any tetrapod group other than these two (Remes, 2008; Burch, 2014). The m. humeroradialis would have flexed the antebrachium (see Burch, 2014; Table 7).

M. brachialis

The origin of the m. brachialis of *Silesaurus* is located on the lateral humeral midshaft, distal to the deltopectoral crest (compare with Walker, 1973; Meers, 2003; Russell & Bauer, 2008; Maidment & Barrett, 2011; Figure 27D, Table 7), where an indistinct flat longitudinal surface is present. The surface is oriented proximo-distally along the humeral shaft. The separate insertion of the m. brachialis is reconstructed together with the origin of the m. biceps brachii on the proximal ends of the radius and ulna (compare with Remes, 2008; Figures 29A, D, 30B, Table 7). In *Silesaurus* material, the insertion area can be recognized in specimens ZPAL Ab III/2538, 459/3, 407/3, 12. A similar condition is present in crocodiles

and lepidosaurs. In birds it is restricted to the proximal ulna (Baumel et al., 1993). The m. brachialis would have flexed the forearm (see Burch, 2014; Table 7).

Antebrachial musculature

Muscles operating the forearm and wrist are mainly associated with extending, retracting and bending the limbs. As a result the forelimbs served as a support the body.

Table 8. Summary table of the antebrachial musculature in *Silesaurus opolensis*, listing their names, origins, insertions, and actions. Muscle attachments in bold are those that have visible osteological correlates.

Muscle name	Origin	Insertion	Proposed function	Level of inference
M. anconeus	Ectepicondyle of the humerus	**Lateral surface of the ulna**	Flexes the forearm	I
M. extensor carpi ulnaris	Ectepicondyle of the humerus	Manus	Extends and abducts the wrist, along with extension of the forearm	III
M. supinator	Ectepicondyle of the humerus	Anterolateral surface of the radius	Flexes and supinates the forearm	I
M. extensor carpi radialis	Ectepicondyle of the humerus	Manus	Extends and adducts the wrist, as well as contributing to flexion of the forearm	I
M. abductor radialis	Ectepicondyle of the humerus	Proximal half of the lateral surface of the radius	Abducts and slightly flexes the forearm	II
M. abductor pollicis longus	Facing surfaces of the radius and **ulna**	Manus	Extends and abducts the wrist, as well as abduction of digit I	I
M. extensor digitorum longus	Ectepicondyle of the humerus	Manus	Extends the wrist	I
M. pronator teres	Entepicondyle of the humerus	Anteromedial shaft of the radius	Flexes the forearm and pronates the antebrachium	I
M. pronator	Entepicondyle of the	Medial side of the	Flexes and pronates	II

accessorius	humerus	distal radius	the antebrachium	
M. pronator quadratus	**Medial side of the proximal ulna**	Posterior surface of the distal radius	Pronates the antebrachium and manus	I
M. epitrochleoanconeus	Entepicondyle of the humerus	**Medioventral surface of the proximal ulna**	Flexes the antebrachium	II
M. flexor carpi ulnaris	Entepicondyle of the humerus	Manus	Flexes and adduct the wrist	I
M. flexor digitorum longus	Entepicondyle of the humerus (flexor digitorum longus superficialis); **medioventral surface of the ulna (flexor digitorum longus profundus)**	Manus	Flexes the digits and the wrist	II

M. anconeus

The origin of the m. anconeus in *Silesaurus* is tentatively reconstructed here on the ectepicondyle of the humerus where it should share a tendon with the m. extensor carpi ulnaris (compare with Miner, 1925; Haines, 1939; Walker, 1973; Vanden Berge & Zweers, 1993; Meers, 2003; Russell & Bauer, 2008; Burch, 2014; Figure 27A, B, Table 8). The muscle insertion is reconstructed unequivocally on the lateral surface of the ulna, just behind the proximal articular surface of the bone and extending for most of its length (compare with Haines, 1939; Sullivan, 1962; Burch, 2014; Figure 29B, C, Table 8). It is marked by a relatively broad, longitudinal concavity on the lateral ulnar shaft (ZPAL Ab III/2538, 459/3,4, 4073, 407/12; Figure 30C). In *Silesaurus*, a prominent ridge begins at the ulnar midshaft and extends towards the distal end providing a distinct surface for the distal part of the m. anconeus and separating its insertion from the origin of the m. abductor pollicis longus. A similar condition in present in *Tawa* (Burch, 2014). The m. anconeus would have flexed the forearm (see Burch, 2014; Table 8).

M. extensor carpi ulnaris

The muscle is relatively conservative in non-archosaurian reptiles and birds (Burch, 2014). Therefore, this muscle was probably present in *Silesaurus*. The origin of the m. extensor carpi

ulnaris is tentatively reconstructed here on the ectepicondyle of the humerus, in the same place as the anconeus (Figure 27A, B, Table 8). Because the manus of *Silesaurus* is poorly known, the insertion of the m. extensor carpi ulnari cannot be reconstructed. M. extensor carpi ulnaris would have extended and abducted the wrist, along with extension of the forearm (see Burch, 2014; Table 8).

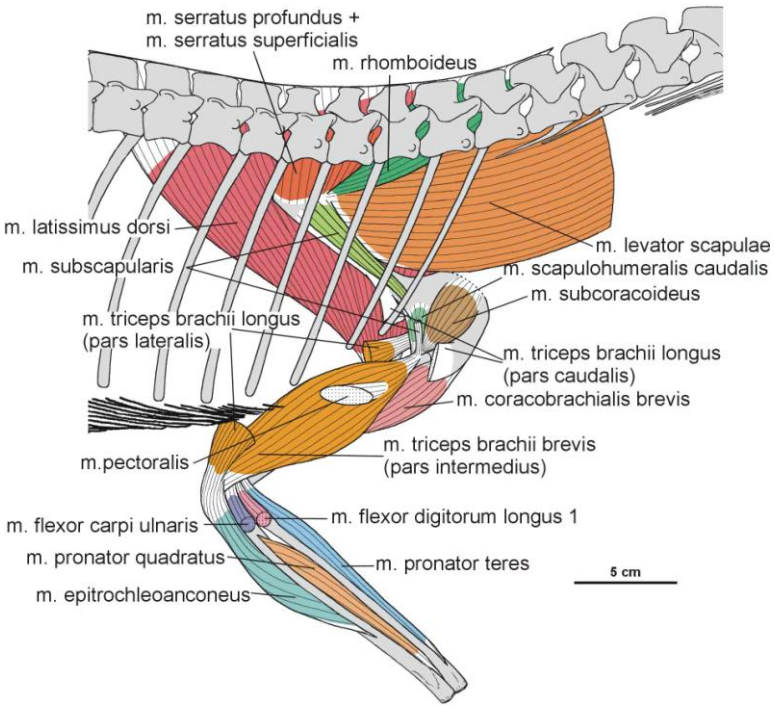

Figure 41. Muscle disposition on the forelimb of *Silesaurus opolensis* in medial view. Some muscles are removed.

M. supinator

Here I tentatively reconstruct the origin of m. supinator as the most proximal muscle attachment on the ectepicondyle in *Silesaurus*, just above origin of the m. extensor carpi radialis and close to that of the m. abductor radialis (compare with Haines, 1939; Remes, 2008; Russell & Bauer, 2008; Figure 27A, B, Table 8). The insertion of the m. supinator is located on the anterolateral surface of the radius behind the proximal articular surface and extending for most of its length (compare with Vanden Berge & Zweers, 1993; Vasques, 1994; Remes, 2008; Burch, 2014; Figure 29A, C, Table 8). The precise location of the insertion on the radial shaft is unclear in *Silesaurus*. The m. supinator would have flexed and supinated the forearm (see Burch, 2014; Table 8).

M. extensor carpi radialis

The origin of the m. extensor carpi radialis in *Silesaurus* is reconstructed on the ectepicondyle (compare with Haines, 1939; Baumel et al., 1993; Remes, 2008; Meers, 2003;

Russell & Bauer, 2008; Figure 27A, B, Table 8) in a location similar to that of crocodiles, lepidosaurs and turtles. The insertion (see Meers, 2003; Burch, 2014) cannot be reconstructed due to the incomplete manus. The m. extensor carpi radialis would have extended and adducted the wrist, as well as contributing to flexion of the forearm (see Burch, 2014; Table 8).

M. abductor radialis

The m. abductor radialis is reconstructed here as originating on the ectepicondyle, just proximal to the origin of both the m. anconeus and the m. extensor carpi ulnaris (compare with Haines, 1939; Remes, 2008; Russell & Bauer, 2008; Burch, 2014; Figure 27A, B, Table 8), as in crocodiles. I reconstruct its insertion on the proximal half of the lateral radial surface (compare with Meers, 2003; Remes, 2008; Burch, 2014; Figure 29C, Table 8). According to this interpretation, the m. abductor radialis would have abducted and slightly flexed the forearm (see Burch, 2014; Table 8).

M. abductor pollicis longus

The m. abductor pollicis longus originated unequivocally from the internal (interosseous) surfaces of the radius and ulna in *Silesaurus* (compare with Haines, 1939; Remes, 2008; Russell & Bauer, 2008; George & Berger, 1966; Burch, 2014; Figure 29A, C, D, Table 8). On the ulna, a distinct scar marks its distal extent (ZPAL Ab III/453, 459/3, 4; Figure 30B), with a faint ridge separating its proximal limit medially from the m. pronator quadratus on the same bone. It cannot be reconstructed because the adequate elements of the hand are not preserved. The m. abductor pollicis longus would have extended and abducted the wrist, as well as abducted digit I (see Burch, 2014; Table 8).

M. extensor digitorum longus

The m. extensor digitorum longus is reconstructed here as originating from approximately the middle of the ectepicondyle, between the origins of the m. extensor carpi ulnaris and the m. extensor carpi radialis or the m. supinator (compare with Burch, 2014; Figure 27A, B, Table 8), as in most living taxa. The insertion cannot be identified. M. extensor digitorum longus would have extended the wrist (see Burch, 2014; Table 8).

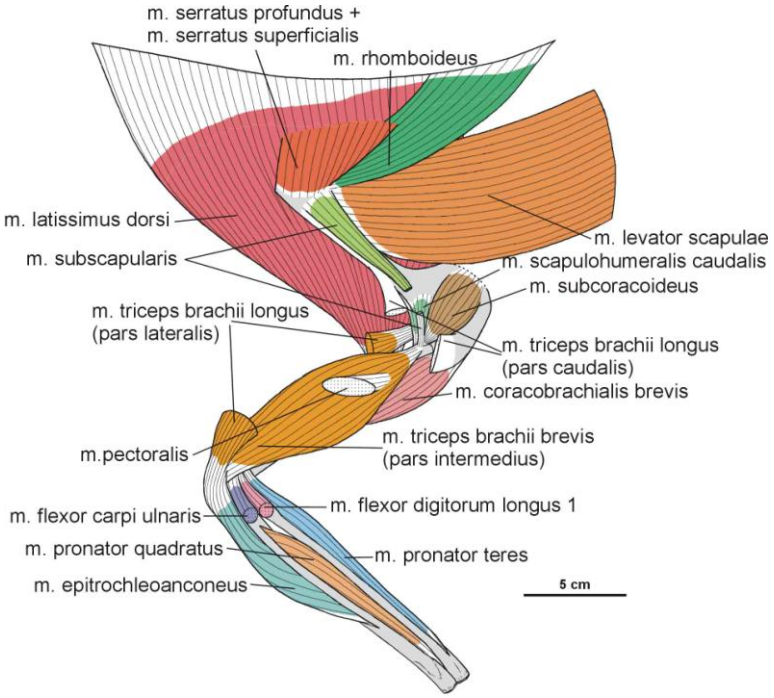

Figure 42. Muscle disposition on the forelimb of *Silesaurus opolensis* in medial view. Some muscles and the axial skeleton are removed.

M. pronator teres

Although the entepicondyle of *Silesaurus* lacks a distinct ridge or anterior projection, its proximal extension probably corresponds to the origin of the m. pronator teres (compare with Livezey, 1990; Remes, 2008; Figure 27B, C, Table 8). Based on *Tawa* (Burch, 2014), the muscle is reconstructed as inserting in a line along the anteromedial shaft of the radius for more than half of its overall length (compare with Straus, 1942; Haines, 1950; Remes, 2008; Russell & Bauer, 2008; Burch, 2014; Figure 29A, D, Table 8). M. pronator teres would have flexed the forearm and pronated the antebrachium (see Burch, 2014; Table 8).

M. pronator accessorius

After Burch (2014), the origin of the m. pronator accessorius of *Silesaurus* is reconstructed as being more distal than the origin of the m. pronator teres, at the distal end of the entepicondyle near to the origin of the m. flexor digitorum longus (Figure 27B–D, Table 8). I tentatively reconstruct the insertion of the m. pronator accessorius as running on the medial side of the distal radius of *Silesaurus* for slightly over half of its length (compare with Haines, 1950; George & Berger, 1966; Russell & Bauer, 2008; Burch, 2014; Figure 29D, Table 8). The m. pronator teres would have flexed and pronated the antebrachium (see Burch, 2014; Table 8).

M. pronator quadratus

Two faint ridges on the medial side of the proximal ulna are interpreted as delimiting the origin of the m. pronator quadratus in *Silesaurus* (ZPAL Ab III/453, 407/3, 459/3, 131/1), thus the muscle origin is reconstructed as covering most of the length of the bone (compare with Ribbing, 1907; Straus, 1942; Haines, 1950; Sullivan, 1962; George & Berger, 1966; Walker, 1973; Meers, 2003; Remes, 2008; Russell & Bauer, 2008; Figures 29A–C, 30B, Table 8), as in *Tawa* (Burch, 2014). The radial insertion of the m. pronator quadratus in *Silesaurus* is demarcated on the posterior surface of the AbIII 431/4 by a light narrow distal scar, suggesting a much shorter (Figure 29B, D, Table 8) insertion than that reconstructed for *Tawa* (Burch, 2014). The carpal attachment remains unknown. The primary action of the m. pronator quadratus would be pronation of the antebrachium and manus (see Burch, 2014; Table 8).

M. epitrochleoanconeus

The m. epitrochleoanoconeus is tentatively reconstructed in *Silesaurus* as originating between the origins of the m. flexor carpi ulnaris and the m. pronator accesorius on the entepicondyle (compare with George & Berger, 1966; Remes, 2008; Burch, 2014; Figure 27B, C, Table 8). Its insertion is defined by a distinct ridge on the ventromedial surface of the proximal ulna (compare with Miner, 1925; Remes, 2008; Burch, 2014; ZPAL Ab III/453, 407/3, 459/3, and 431/1), just behind the proximal articular surface and covering the medioventral surface of the bone, but restricted to its proximal half (Figures 29D, 30B, Table 8). The m. epitrochleoanoconeus would have flexed the antebrachium (see Burch, 2014; Table 8).

M. flexor carpi ulnaris

The m. flexor carpi ulnaris is reconstructed in *Silesaurus* as originating from a single tendon on the posterodistal aspect of the entepicondyle as in other diapsids (compare with Miner, 1925; Remes, 2008; Burch, 2014), just above the distal articular surface (Figure 27B, C, Table 8). The insertion cannot be reconstructed. The m. flexor carpi ulnaris would have flexed and adducted the wrist (see Burch, 2014; Table 8).

M. flexor digitorum longus

The origin of the m. flexor digitorum longus superficialis is reconstructed in *Silesaurus* in the same location on the humerus as in most modern taxa (Figure 27B, Table 8), and on the medioventral surface of the ulna, as is seen in crocodiles and lepidosaurs (compare with Straus, 1942; Fisher & Goodman, 1955; George & Berger, 1966; Fitzgerald, 1969; Cong et al., 1998; Meers, 2003; Russell & Bauer, 2008; Burch, 2014; Figures 29D, 30B, Table 8). The area is marked by two ridges (ZPAL Ab III/453, 407/3, 459/3, and 431/1), which separate it from the attachment site of the m. pronator quadratus anteriorly and the m. epitrochleoanoconeus posteriorly. The insertion cannot be identified. The function of the m. flexor digitorum longus is to flex the digits and the wrist (see Burch, 2014; Table 8).

Chapter 7. Skeleton of pelvic girdle and hindlimb[7]

The anatomy of pelvic girdle in *Silesaurus* is characterized by a relatively wide lateral inclination of the iliac blade with downward directed acetabulum. In result, both legs were under the trunk.

Pelvis

The sacrum of *Silesaurus* consist of four fused sacrals (Dzik & Sulej, 2007), which contact the ilium by three strong ribs. The ribs are attached between the centra (Dzik, 2003).

Ilium

The ilium of *Silesaurus* is as long as the four sacral vertebrae in ZPAL Ab III/362 (that is longer than restored by Dzik, 2003; Figure 43A, B). The bone was inclined at about 30° to the vertical plane, more than in the original reconstruction (Figure 43B, D). The acetabulum faced more ventrally than laterally. The articulation surfaces for the pubis and ischium were not in the same line. The latter was parasagittal, while the former was inclined laterally (Figure 43D, E).

The best preserved ilia of *Silesaurus*, ZPAL Ab III/361, 362, 363, and 404/2, show an extremely thin, almost vertical (contra Dzik, 2003) iliac blade, inclined towards wing-like apophyses of the sacral vertebrae (Dzik, 2003). Specimens ZPAL Ab III/361 and 362 show how the ilium articulated the sacrum. Unfortunately, this specimen is crooked and accurate geometry of the pelvis is difficult to determine (Figures 44, 45A, B). The blade (Figures 43A, C, 44, 46B, C) formed a saddle-like structure between the anterior and postacetabular processes of the ilium, and seems to have been originally in contact with apophyses of the sacrals (Dzik, 2003). The medial surface of the ilium bears facets for three sacral ribs.

The relatively short anterior process projects anterodorsally and curves laterally (Dzik, 2003). Its distal surface was covered originally by cartilage. This structure has a very variable outline in population from Krasiejów (Piechowski et al., 2014). A distinct tear-shaped scar is marked on the ventrolateral side of the anterior process (Figure 45C).

[7] Part of this chapter was published in:
Piechowski, R., Tałanda, M. & Dzik, J. 2014. Skeletal variation and ontogeny of the Late Triassic dinosauriform *Silesaurus opolensis*. *Journal of Vertebrate Paleontology* **34**, 1383–1393.
Piechowski, R. & Tałanda. M. 2020. The locomotor musculature and posture of the early dinosauriform *Silesaurus opolensis* provides a new look into the evolution of Dinosauromorpha. *Journal of Anatomy* DOI: 10.1111/joa.13155

The postacetabular process of the iliac blade is the strongest and most prominent part of the ilium, giving its posterior margin a semicircular curvature (Dzik, 2003). The apical surface of the process is mostly roughened analogously to the anterior one, which is better expressed in adult specimens. A prominent, posteroventrally oriented ridge (brevis shelf) separates two longitudinal areas for muscle attachments on the postacetabular process.

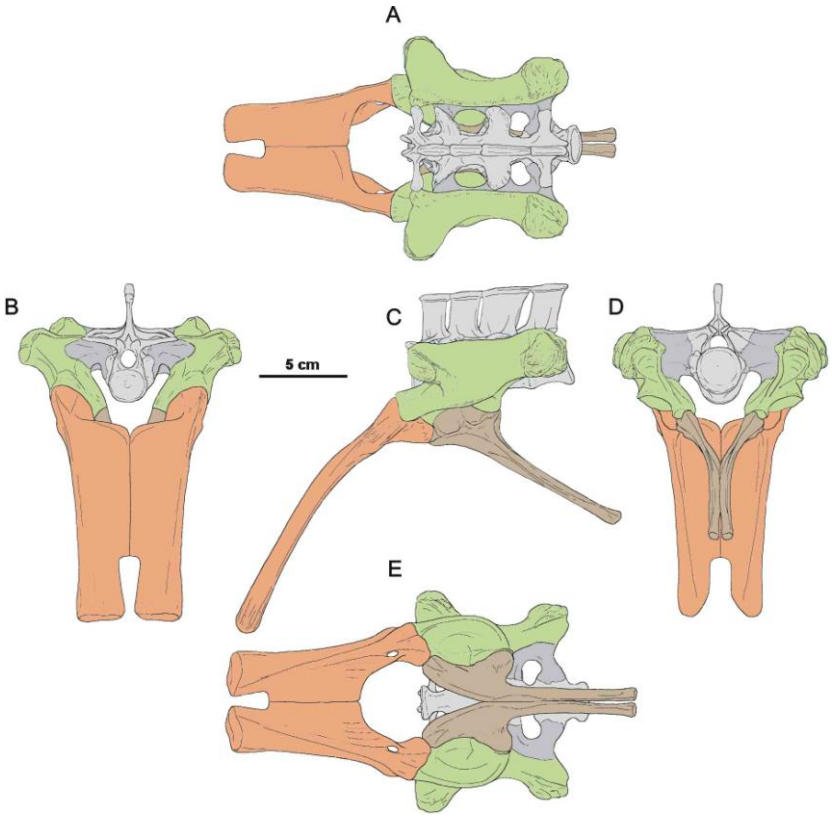

Figure 43. Restoration of pelvis and sacrum of *Silesaurus opolensis* based mostly on ZPAL AbIII/362, 925, 404/2, 404/5, and 411/1. **A**, dorsal view; **B**, anterior view; **C**, lateral view; **D**, posterior view; **E**, ventral view.

The acetabulum (Figure 43C, E) is large relative to the head of the femur. A strong semicircular supra-actetabular crest overhangs the acetabulum, obscuring the dorsal part of the fossa. The most prominent section of the crest is located in the middle. The ilium contributes to the two-thirds of the acetabular wall. The acetabulum is not opened and the iliac wall shows an extensive ventral contact with other pelvic bones. The surface of the antitrochanter rises relatively to the anterior portion of the acetabulum.

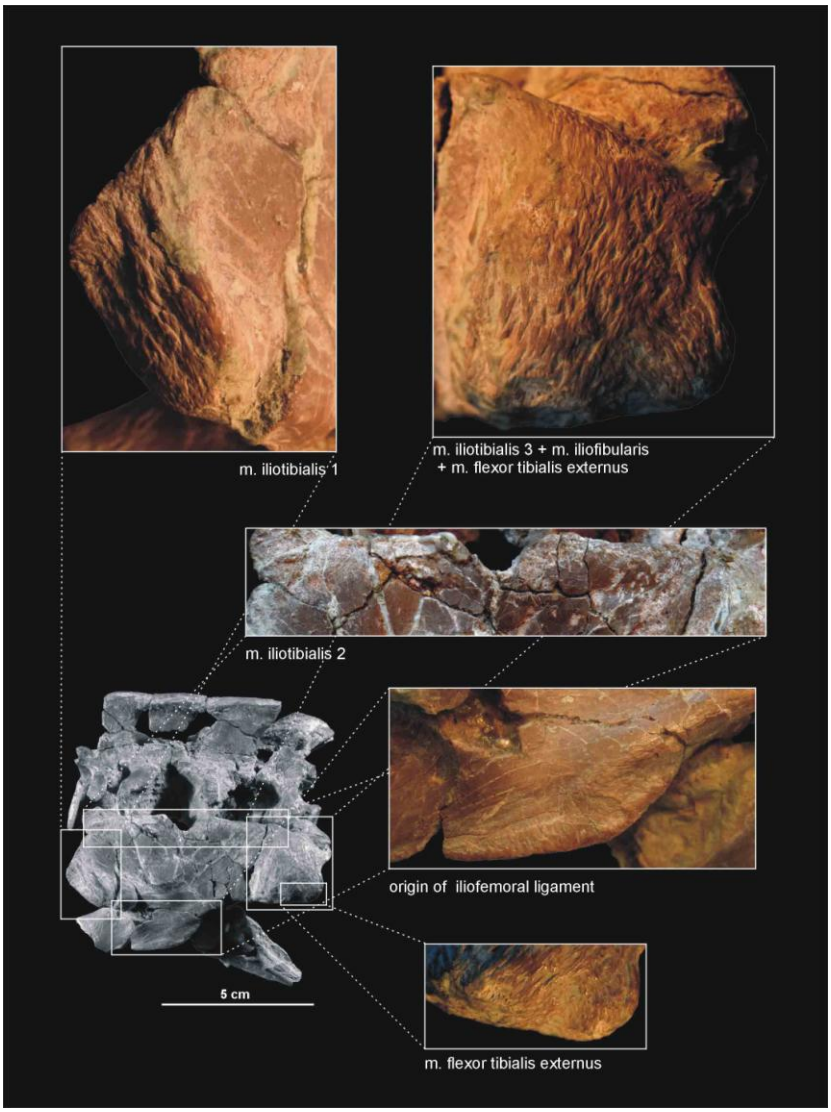

Figure 44. Muscle scars visible on the lateral aspect of the ilium of *Silesaurus opolensis* and pelvis in lateral view. All photographs of ZPAL AbIII/362 (mirrored).

Pubis

The pubis occupies a broader space than the ischium (Figure 43B, D, E). The obturator plate flares medially, thus the obturator foramen was visible in anterior view. The pubic bones have an almost straight shaft in anterior view (not slightly bent as proposed by Dzik, 2003). The shafts contact each other by a thin medial blade that is broader proximally than distally because the shafts are oriented ventromedially.

The pubis is preserved in articulation with the ilium in ZPAL Ab III/361 (Dzik, 2003). Unfortunately, the extremely thin medial blade is incomplete in all isolated specimens (Dzik, 2003). The best preserved of these is ZPAL Ab III 404/5, however, the actual extent of the blade is traceable on the basis of partially articulated specimen ZPAL Ab III/363 (Dzik, 2003). The pubis of *Silesaurus* is very long, only slightly shorter than the femur and considerably longer than the ilium (Figure 47B). The pubis is curved and expands

anteroventrally in the lateral view. The two pubes are joined for much of their length by a strong plate-like structure, with comma-shaped (Dzik, 2003) cross section. Their transverse width decreases slightly from the proximal to distal ends in the anterior view. The proximal end of each pubis shows two robust articulations. The pubes diverge from each other at about third of their length dorsally, and each bone extends upward and slightly laterally to articulation with the ilium. As a consequence, there is an anterior opening in the pelvis. The articulation with the ischium is oriented directly posteriorly. The medium obturator foramen appears close to this articulation. The pubes are separated distally for a short distance down to their tips. The distal ends of the pubis are slightly rounded, covered originally by cartilage.

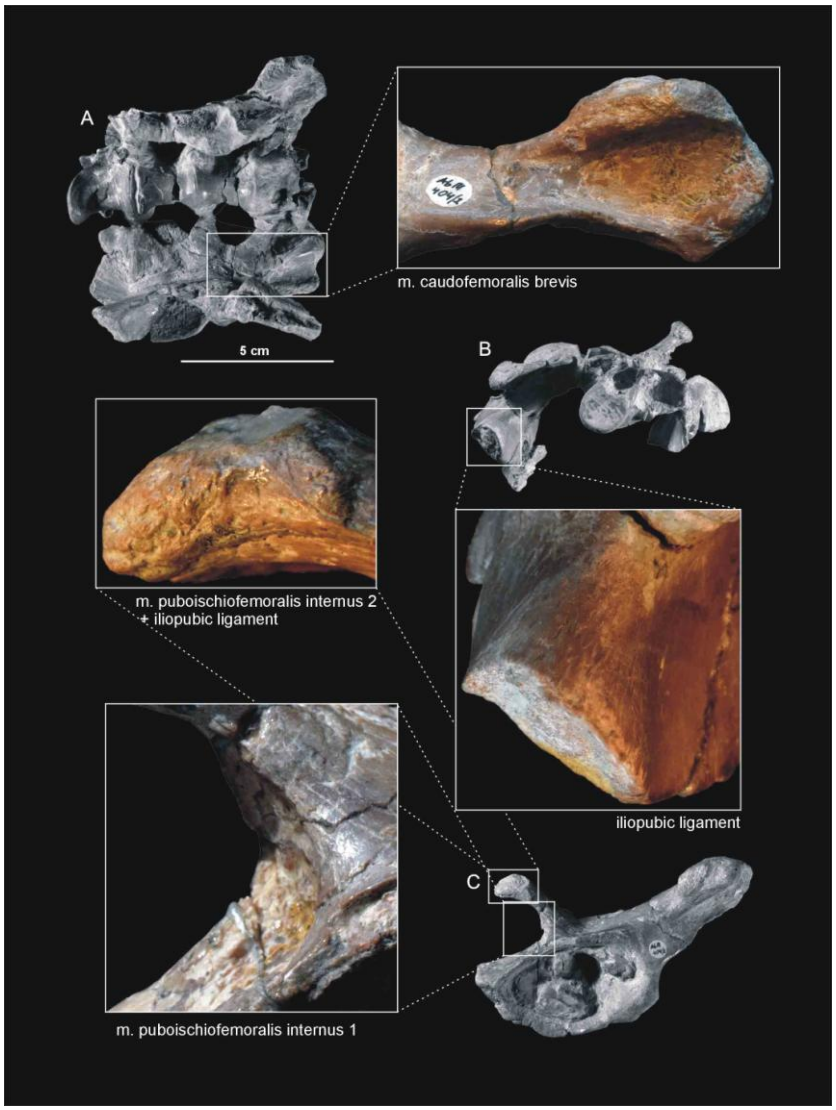

Figure 45. Muscle and ligament scars visible on the ventral and anterior aspects of the ilium of *Silesaurus opolensis*. **A**, crushed pelvis of ZPAL AbIII/362 in ventral view; **B**, same in anterior view; **C**, left ilium ZPAL AbIII/404/2 in ventrolateral view.

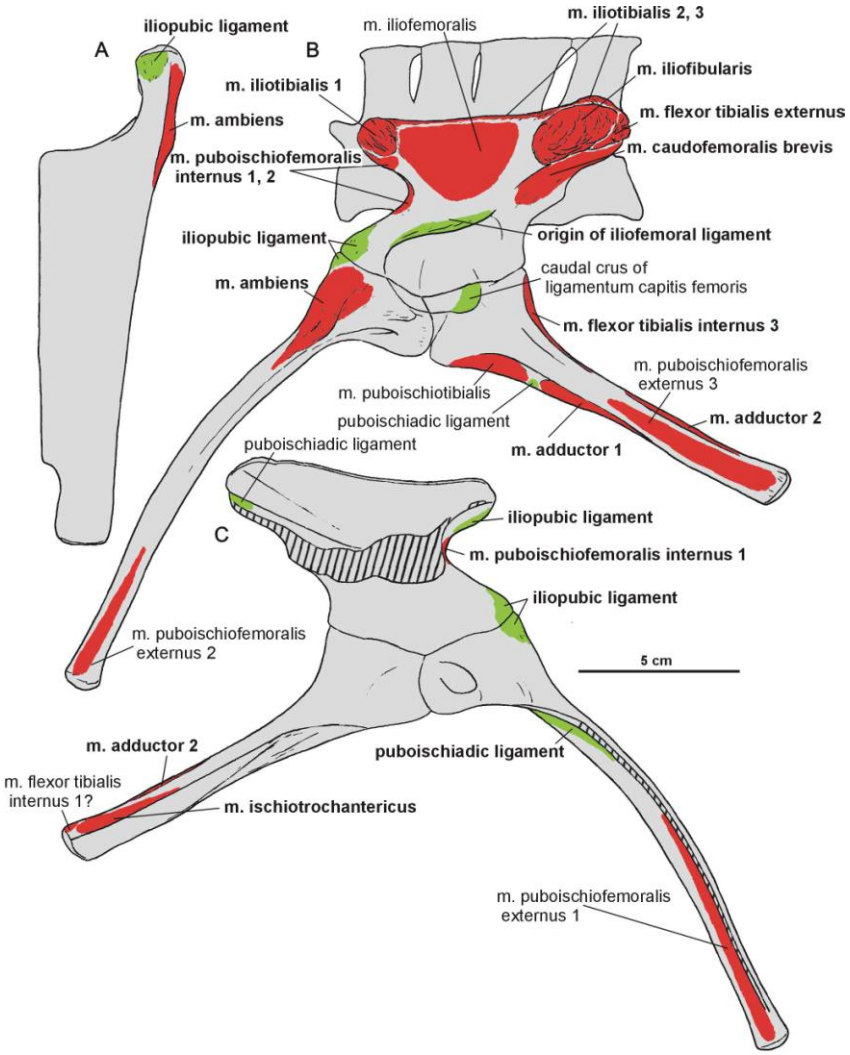

Figure 46. Attachments of muscles and ligaments on the left pelvis of *Silesaurus opolensis* based mostly on the holotype. Origins are in red, ligaments are in green. Muscle and ligament attachments in bold are those that have visible osteological correlates. **A**, anterodorsal view of pubis; **B**, ventrolateral view of pelvis; **C**, dorsomedial view of pelvis.

Ischium

Dzik (2003) reconstructed the pelvis of *Silesaurus* with ischia meeting each other only at their distalmost end. This was because the pubis is lateromedially broad, while the ischia have only a slight curvature at their proximal ends, requiring a narrow space between them to be able to meet. However, Nesbitt (2011) noticed that isolated ischia of *Silesaurus* bear a symphysis throughout most of the anteromedial margins. My observations confirm this (Figure 43D, E). The ilium was inclined medially, so the proximal parts of the ischia were close to each other. The symphysis between the ischia appears just below the contact with the ilium, and continues along the shaft to the distal end.

Almost all ischia are more or less disarticulated. This bone is also elongated, being about two-thirds of the length of the femur. Proximally, the ischium branches dorsally to meet the ischial peduncle and anteriorly to articulate with the pubis. Distally, the ischiatic shaft is laterally compressed, with slightly expanded end, originally covered by cartilage. Isolated specimens ZPAL Ab III/404/1, 404/7, 925 shows a ‘symphysis’ throughout the anteromedial

margins. The ischia connected each other probably by ligament, which remained as a rough, flat, symphyseal-like, medial surface.

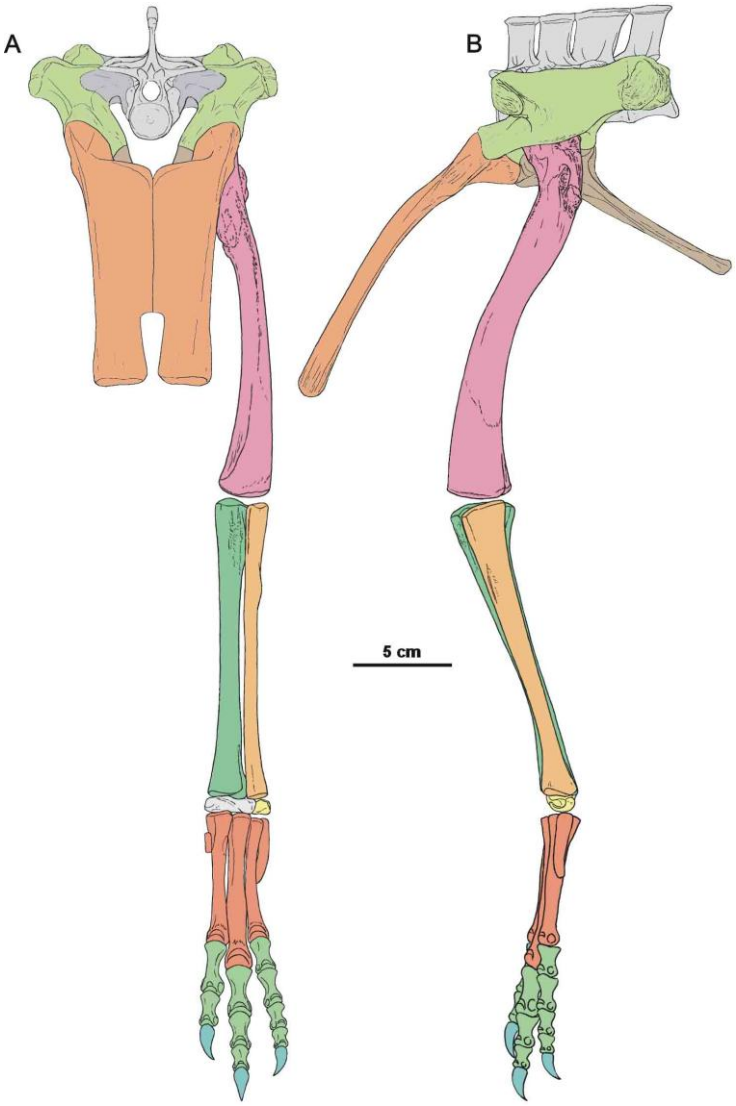

Figure 47. Restoration of pelvis, sacrum and hidlimb of *Silesaurus opolensis* in anterior (**A**) and lateral view (**B**).

Femur

The femur is the longest hindlimb bone. It is proportionally longer in larger specimens (Piechowski et al., 2014; Figure 47, Table 6). The proximal head is not rotated medially as in typical dinosaurs. However, as seen in anterior view the bone is slightly curved medially in its proximal half. As a result, the proximal articular surface is not parallel to the distal one. Furthermore, the distal half of the bone was oriented at right angles to the ground, while the proximal half was inclined to meet the acetabulum.

The femur (Figures 47–51) is semitriangular in the proximal view, with the broader margin facing the acetabulum. A straight groove passes through most of the articular surface on the

proximal head. In some cases, the proximal articular surface forms a gentle overhang posteriorly (Piechowski et al., 2014). The proximal head is poorly defined without recognizable neck between the femoral head and shaft.

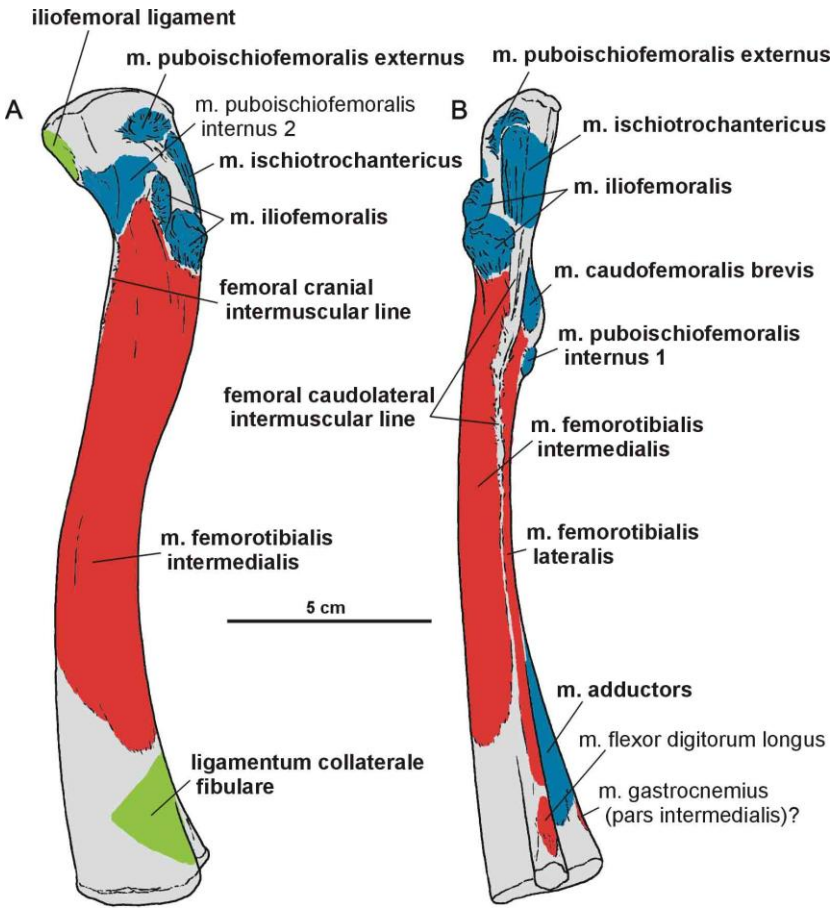

Figure 48. Attachments of muscles and ligaments on the left femur of *Silesaurus opolensis*. Origins are in red, insertions are in blue, ligaments are in green. Muscle, intermuscular lines and ligament attachments in bold are those that have visible osteological correlates. **A**, lateral view; **B**, posterior view.

The greater trochanter is marked by an indistinct ridge (Dzik, 2003) on the posterolateral side of the head. In *Silesaurus*, the anterior (lesser) trochanter is very prominent, as a longitudinal ridge on the anterolateral surface, below the head. This ridge is stronger and more pointed in proximal aspect. The trochanteric shelf (= the lateral ossification of Piechowski et al. 2014) extends posteriorly along the entire posterolateral surface of the bone from the base of anterior trochanter, but only in some specimens. An additional tuberosity, the dorsolateral ossification (Piechowski et al., 2014) is present above the anterior trochanter, on the head in some specimens. Posteriorly to them, a longitudinal ridge, the dorsolateral trochanter continues down to the trochanteric shelf level.

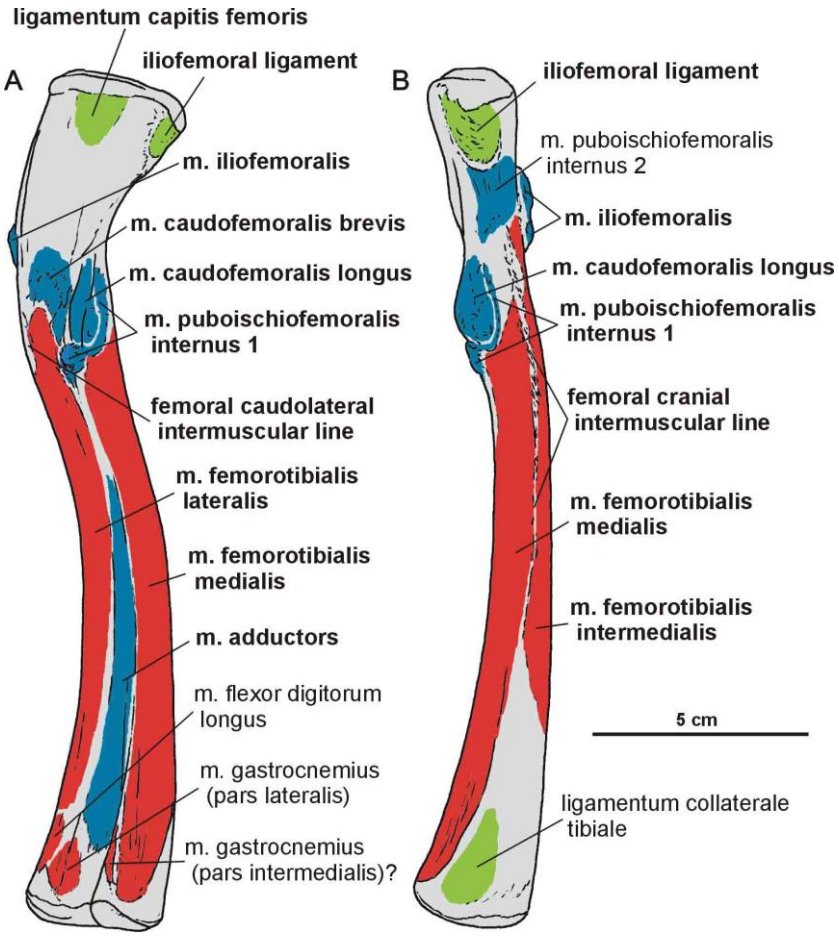

Figure 49. Attachments of muscles and ligaments on the left femur of *Silesaurus opolensis*. Origins are in red, insertions are in blue, ligaments are in green. Muscle, intermuscular lines and ligament attachments in bold are those that have visible osteological correlates. **A**, medial view; **B**, anterior view.

The fourth trochanter form an elongated ridge on the medial surface of the bone. It is located nearly at one third of the length of the femur from its proximal end. It curvature is different from the proximal curvature of the femoral shaft. This ridge is occupies by a small ossification, but only in some specimens (Piechowski et al., 2014). The proximal and distal margins of the fourth trochanter run at nearly equal, low angles to the femoral shaft. A round indistinct depression is present next to the anterior border of the trochanter. In the femur of *Silesaurus*, the dorsolateral ossification always coexists with the lateral ossification, 'overhang calcification' and ossification of the fourth trochanter (Piechowski et al., 2014).

A clear femoral cranial intermuscular line (Figures 48A, 49B, 50A) appears on the anterodorsal surface of the bone just behind the neck. A prominent femoral caudolateral intermuscularis line (Figures 48B, 49A, 50B) extends distally between the lateral ossification and fourth trochanter on the posterior surface of the shaft.

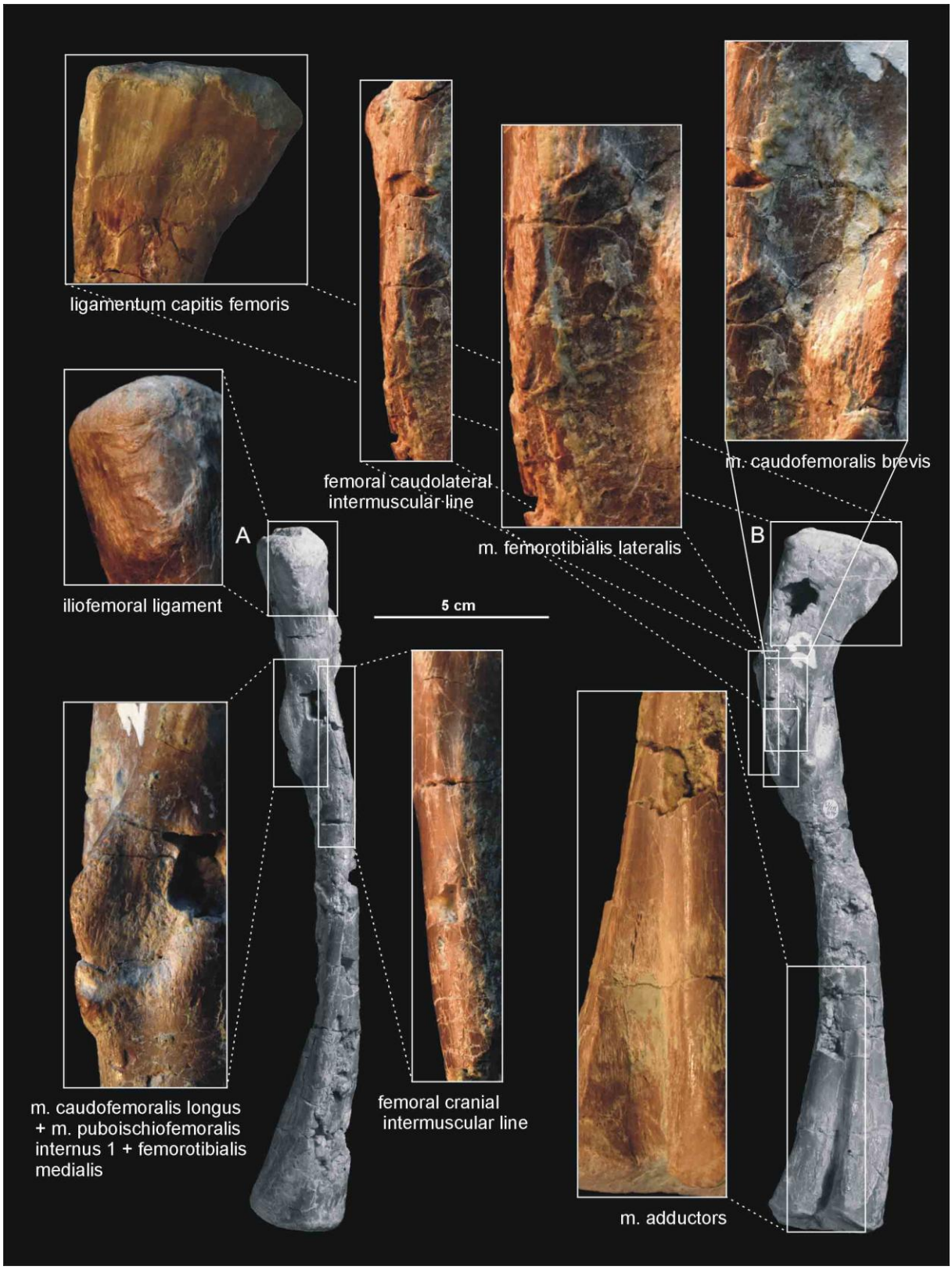

Figure 50. Muscle and ligament scars visible on the anterior and medial aspect of the femur of *Silesaurus opolensis*. Upper photograph of ligament from ZPAL AbIII/457, the surrounding two photographs are from ZPAL AbIII/361/21, the rest from 361/23. **A**, left femur in anterior view; **B**, same in medial view.

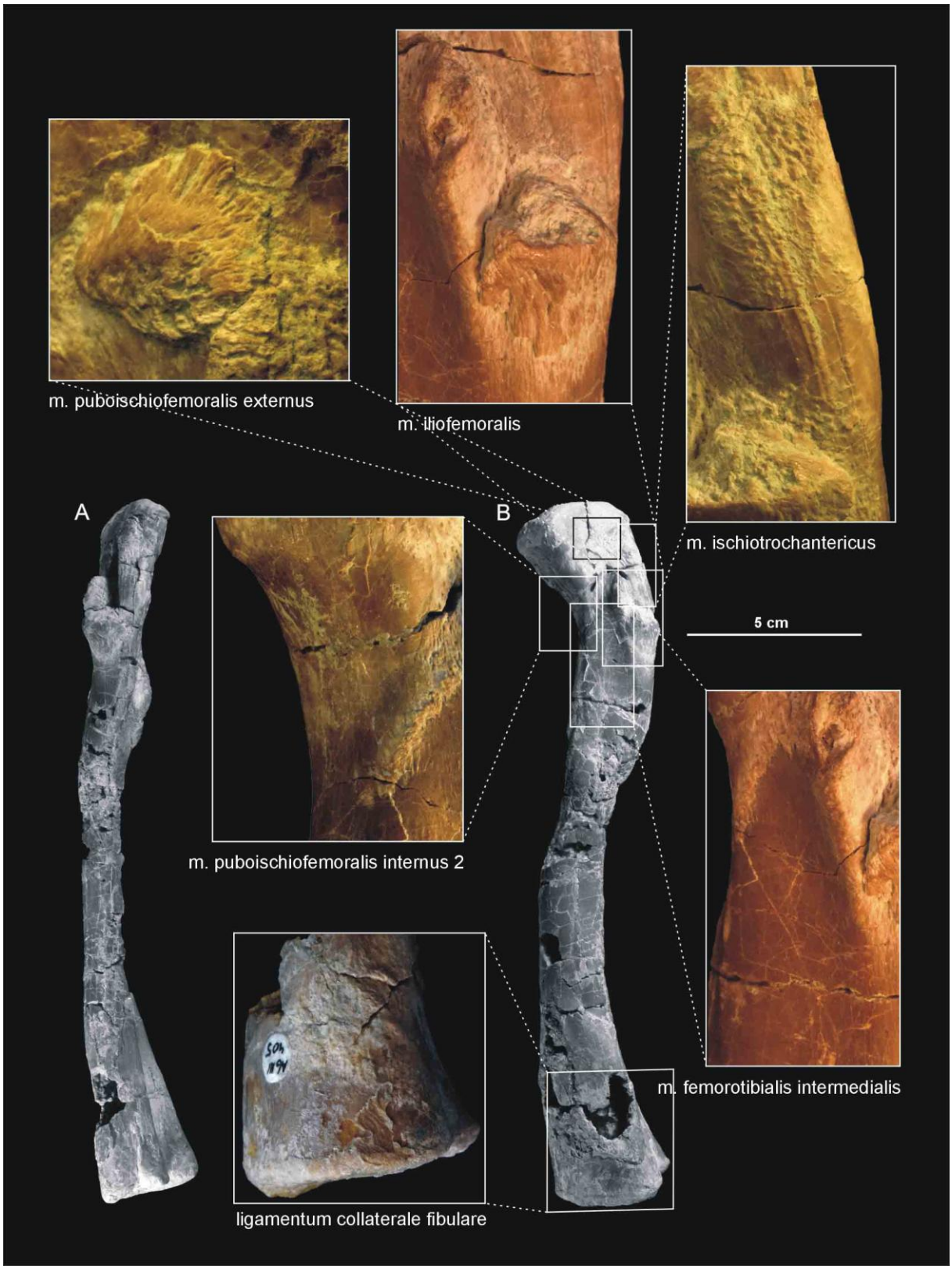

Figure 51. Muscle and ligament scars visible on the lateral aspect of the femur of *Silesaurus opolensis*. Muscle scars in ZPAL AbIII/361/21, ligament scar in 405, complete bone in 361/23. **A**, left femur in posterior view; **B**, same in lateral view.

The distal end of femur is oriented posteriorly and its articular surface bears two conjoined condyles: a larger one for articulation with the tibia (the lateral condyle) and the smaller one with the fibula (the fibular condyle). A third distinct condyle (the medial condyle) is located in opposition to them. Posteriorly, the articular surface bears a depression, with divides the distal head into medial and lateral areas.

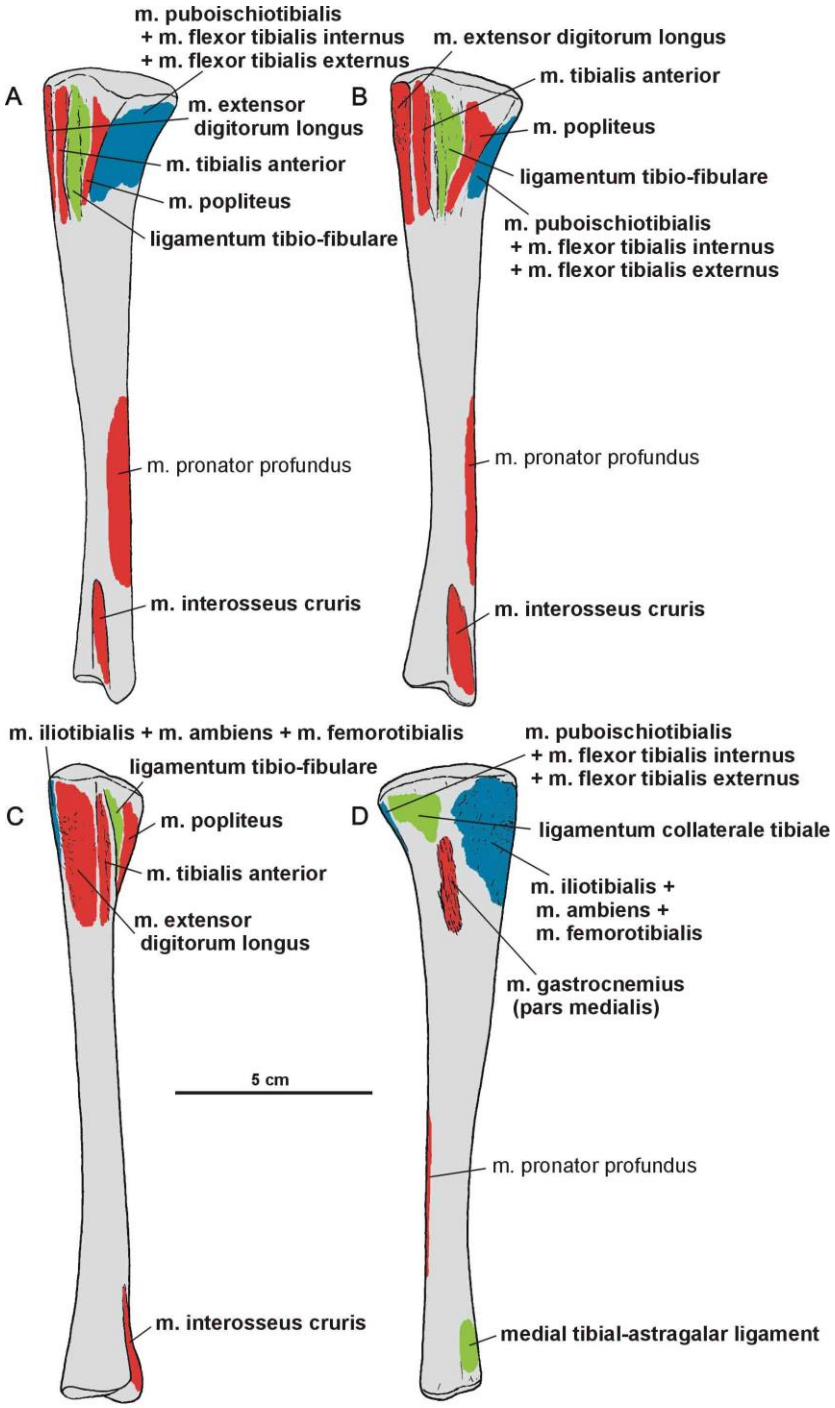

Figure 52. Attachments of muscles and ligaments on the left tibia of *Silesaurus opolensis*. Origins are in red, insertions are in blue, ligaments are in green. Muscle and ligament attachments in bold are those that have visible osteological correlates. **A**, posterolateral view; **B**, lateral view; **C**, anterior view; **D**, medial view.

Shank

Both epipodials are represented as articulated in the specimens ZPAL Ab III/361/8, 364, 1930, and 362. The tibia (Figures 47 and 52–54) is a robust, straight bone that is shorter in length than the femur. The proximal end of tibia is subtriangular, with an anteroposterior elongation. It is much stronger than its distal end. The proximal articulation surface shows well developed internal and fibular condyles, on the posteromedial and posterior side, respectively. A straight cnemial crest appears on the anterior side. A low fibular flange (Dzik, 2003) occurs proximally on the lateral surface of the tibia. The shaft of the tibia is robust.

The distal end of tibia is slightly broader than longer anteroposteriorly, because its distal articular surface is oriented in a transverse plane. Its articular surface has a rounded anteromedial corner with a prominent astragalar overhang. The distal lateral end of tibia forms a wall-like descending process (Figure 53A). It overlaps the posterior surface of the astragalar ascending process. A gentle vertical groove on the lateral surface of the tibia separates its descending process from the articular surface for the ascending process of the astragalus. The groove terminates distally as a shallow notch in the distal articular surface, which is large and broader than the descending process.

The fibula (Figures 47, 53B, 54B, 55, 56) is more slender than the tibia. The fibula is closely attached to the tibia proximally and distally, but separated throughout rest of its length. As a result, there is a narrow gap between them. The proximal end of fibula is anteroposteriorly expanded, and its central portion articulates with the fibular condyle of the tibia. The fibular shaft is straight. The spiral ridge (Dzik, 2003) is developed as a low crest on the anterior margin of it proximal part.

The fibula continues distally slightly more than the tibia. Its articular surface is elliptical in the distal view, with oblique medioanterior to lateroposterior orientation. The lateral part of the articular surface meet the calcaneum, while its medioanterior and medial edges articulate distally with the astragalus.

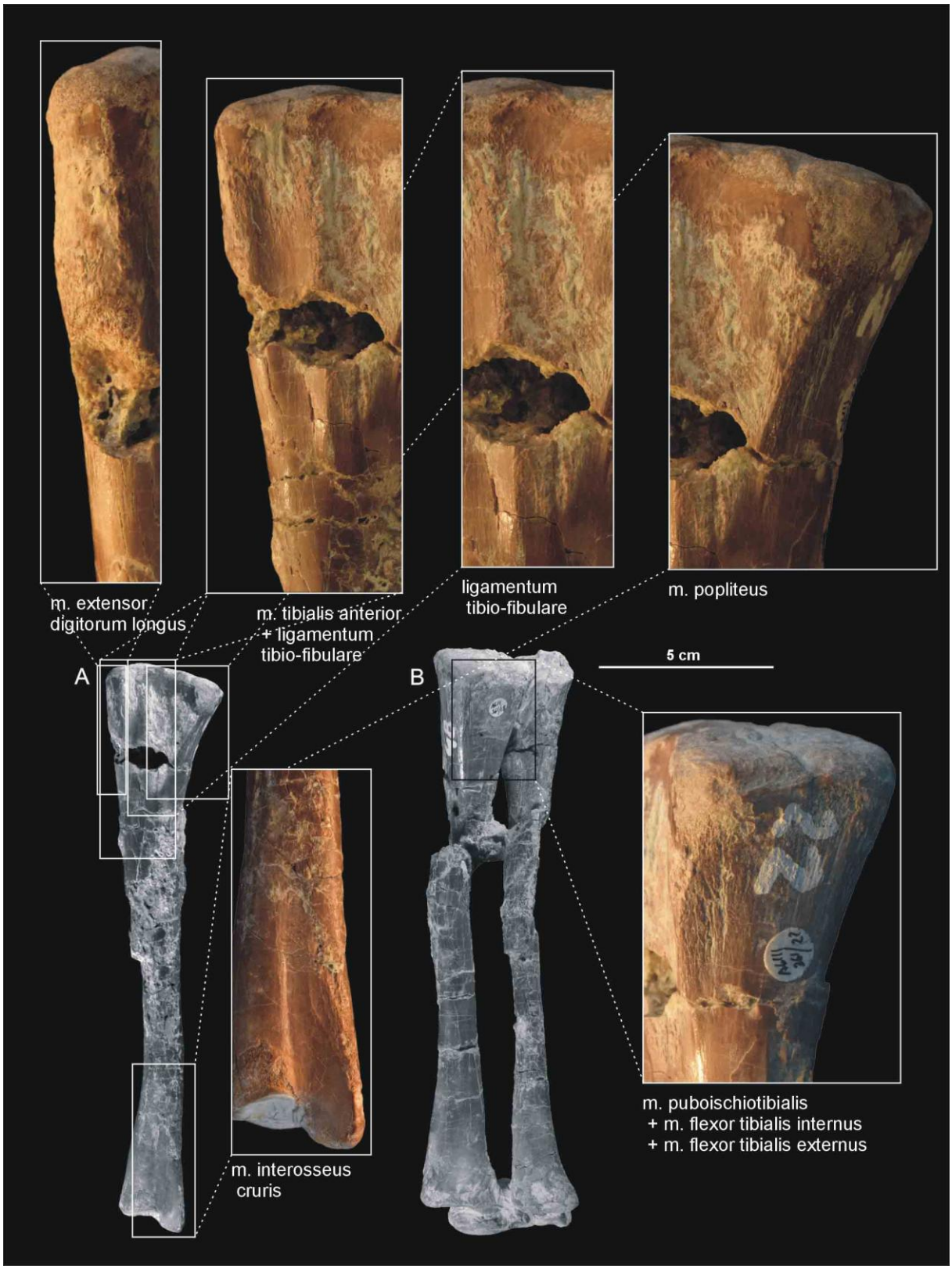

Figure 53. Muscle and ligament scars visible on the lateral aspect of the tibia of *Silesaurus opolensis*. All scars are from ZPAL AbIII/361/22. **A**, left tibia from the same specimen in lateral view; **B**, right shank and astragalocalcaneum ZPAL AbIII/361/48 in posterior view.

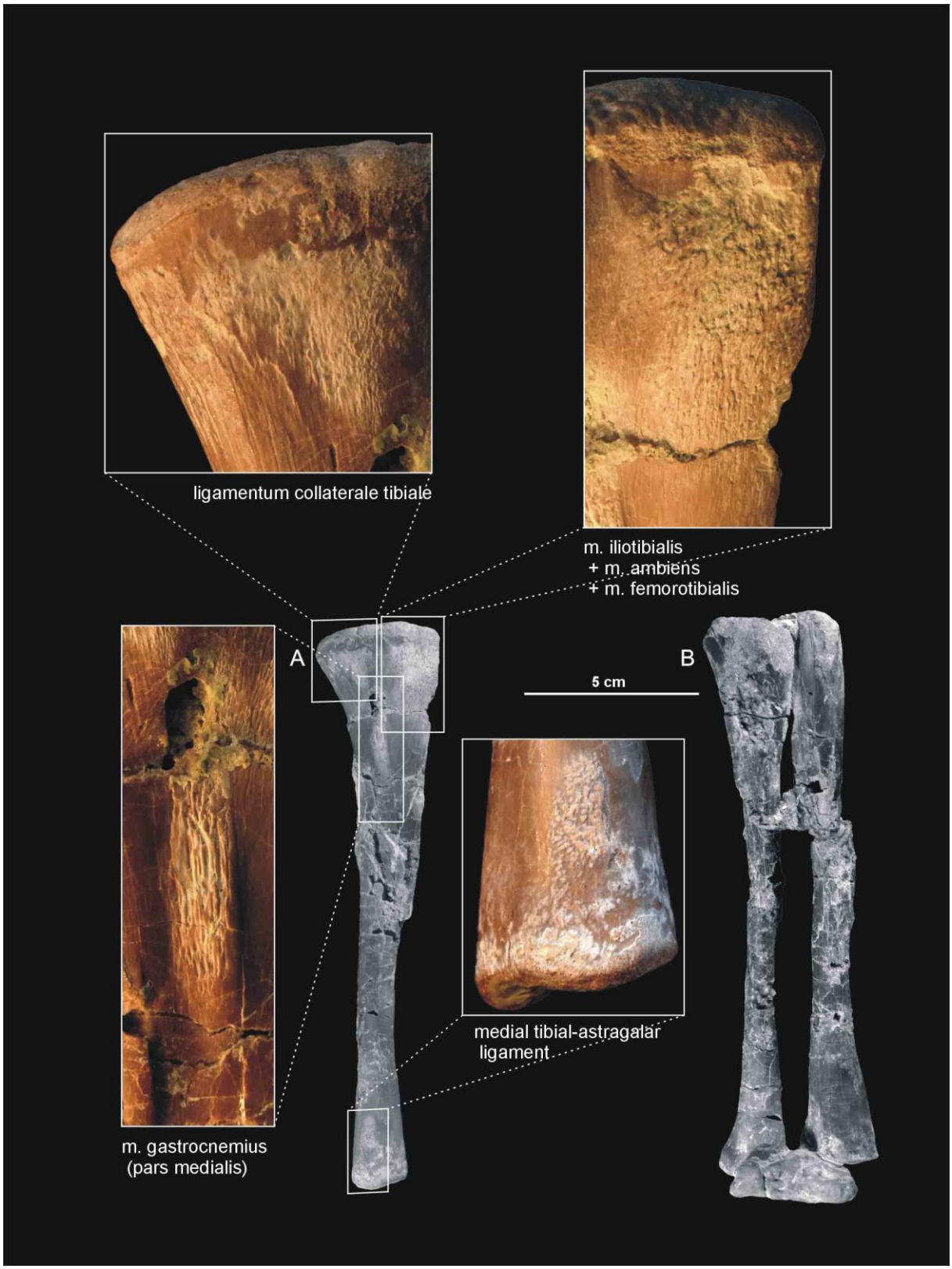

Figure 54. Muscle and ligament scars visible on the medial aspect of the tibia of *Silesaurus opolensis*. All scars are on ZPAL AbIII/361/22. **A**, left tibia from the same specimen in medial view; **B**, right shank and astragalocalcaneum ZPAL AbIII/361/48 in anterior view.

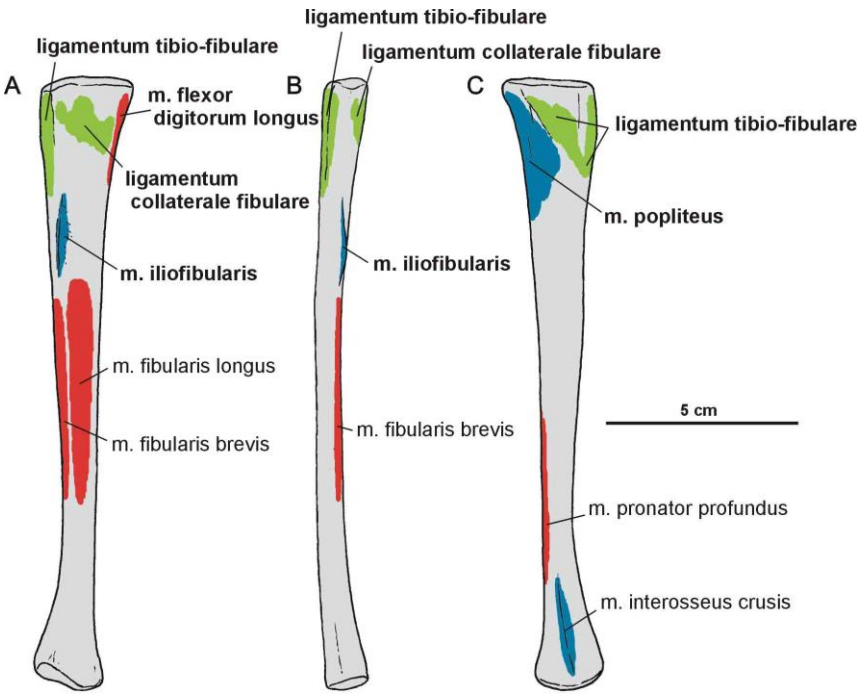

Figure 55. Attachments of muscles and ligaments on the left fibula of *Silesaurus opolensis*. Origins are in red, insertions are in blue, ligaments are in green. Muscle and ligament attachments in bold are those that have visible osteological correlates. **A**, lateral view; **B**, anterior view; **C**, medial view.

Ankle joint

In *Silesaurus*, like in dinosaurs, the midtarsal joint is well developed. Two conjoined bones, astragalus and calcaneum, connected the epipodials with the rest of the pes. In all retained specimens the astragalus and calcaneum are tightly connected (Figures 47, 57A, 58D), with the oblique straight suture between them (Dzik, 2003).

The astragalus is a strong, transversely elongated bone. A vertical, nonarticular surface separates the dorsal and ventral articular facets in the anterior view. A shallow depression occurs on the anterior surface of the astragalus. The posterior side of the astragalus has a similar, but gently convex nonarticular surface. A roughly horizontal groove is visible on the medial side.

The astragalus is almost trapezoidal in the dorsal view, with anteriorly expanded medial part. The uneven tibial facet is separated from the fibular one by a pyramidal crest of the ascending process. Three broad concavities extend through its surface. The anterior margin of the ascending process continues on the rest of the surface. Posteriorly, the ascending process borders with the dorsal basin, which articulates with the descending process of the tibia. The ascending process bears posteromedial ridge, which demarcates the dorsal basin from the medial articular surface of the astragalus. The lower posterior part of the ascending process articulates with a notch on the distal end of the tibia. Lateral to the ascending process, the bone is low in dorsoventral aspects and shows an oblique straight suture to border the tight

articulation with the calcaneum. The concave lateral surface exposes the fibular facet of the astragalus. The fibula articulates with this articular surface, as well as with the lateral surface of the ascending process. The ventral articular surface of the astragalus articulates with the proximal ends of the first to third metatarsals. Although this facet shows a slight mediolaterally concave curvature, the articular surface is anteroposteriorly convex.

Figure 56. Muscle and ligament scars visible on the lateral and medial aspects of the fibula of *Silesaurus opolensis*. All scars are on ZPAL AbIII/361/24 except that of m. iliofibularis (ZPAL AbIII/416). **A**, left fibula ZPAL AbIII/361/48 in lateral view; **B**, same in medial view.

The calcaneum is a relatively small subtrapezoidal bone, with lateroproximal expanded rim. In result, the calcaneal tuberosity projects lateroposteriorly. The dorsal articular surface for the fibula meets medially with the articular surface of the astragalus. In ventral view, the calcaneum shows a convex elliptical surface for articulation with the fourth metatarsus. Laterally, a distinct notch extends anteriorly on a short distance. The astragalus and

calcaneum belong functionally to the epipodials, while the bones of proximal tarsus constitute a functional part of the pes.

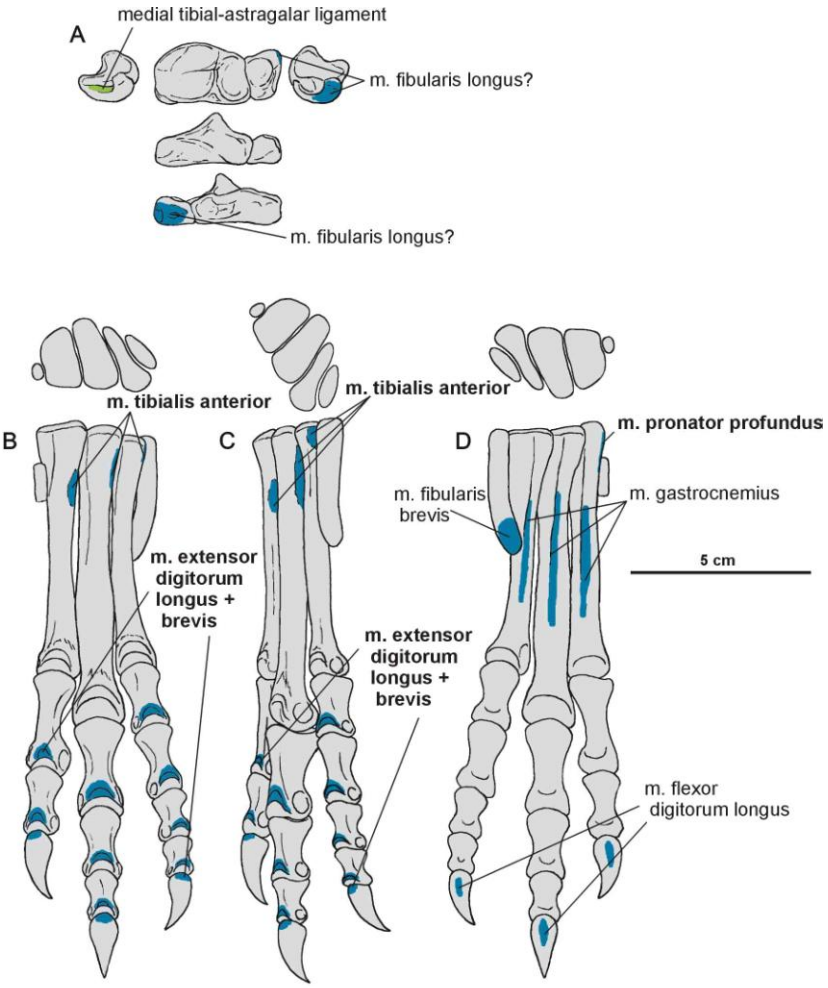

Figure 57. Attachments of muscles and ligaments on the left pes of *Silesaurus opolensis*. Insertions are in blue, ligaments are in green. Muscle attachments in bold are those that have visible osteological correlates. **A**, astragalocalcaneum in medial, dorsal, lateral, anterior, and posterior views; **B**, metatarsals and digits in dorsal and anterior view; **C**, same in dorsal and lateral view; **D**, same in dorsal and medial view.

Pes

Articulated metatarsals are known from specimen ZPAL Ab III/364. Dzik (2003) reconstructed them as contacting each other parallel to the long axis of the leg. However, my inspection of the specimen revealed that they overlap each other as in modern crocodiles and many other taxa. As a result, their proximal heads were rotated medially in relation to the rest of the bone (Figure 57B–D).

Metatarsals show much variability in shape of their proximal ends (Dzik, 2003). The proximal ends of the second and third metatarsals are in almost horizontal alignment with the proximal end of the fourth metatarsal. Their articular surfaces, are slightly concave, to accommodate the distal surface of the astragalus and calcaneum. In the dorsal view, the second metatarsal is trapezoidal, third metatarsal is usually parallelogram, and fourth metatarsal shows a comma-like surface, which fits the oval fifth metatarsal. The shafts of the

second to fourth metatarsal are straight and closely appressed throughout most of their lengths. The third metatarsal is the most robust and longest in the series. The second and fourth are somewhat shorter than the third, but are equal to each other in length. Although the specimens are usually twisted by deformations, the central parts of the metatarsals show variability corresponding with their proximal ends. Metatarsals II—IV have well-developed distal articular surfaces that contacted the proximal phalanges. The distal ends of the metatarsals have dorsal extensor depressions for intercondylar processes of their respective proximal phalanges. Pits for the collateral ligaments are also present in the metatarsals. In addition, scars for the insertion of the collateral ligaments are present on the proximal end of bones. The fifth digit is represented only by the metatarsal, which angles mediodistally across the posterior side of the metatarsus. The possible first digit is a narrow rib-like bone attached to the right metatarsal second in the specimen ZPAL Ab III/364 (Dzik, 2003).

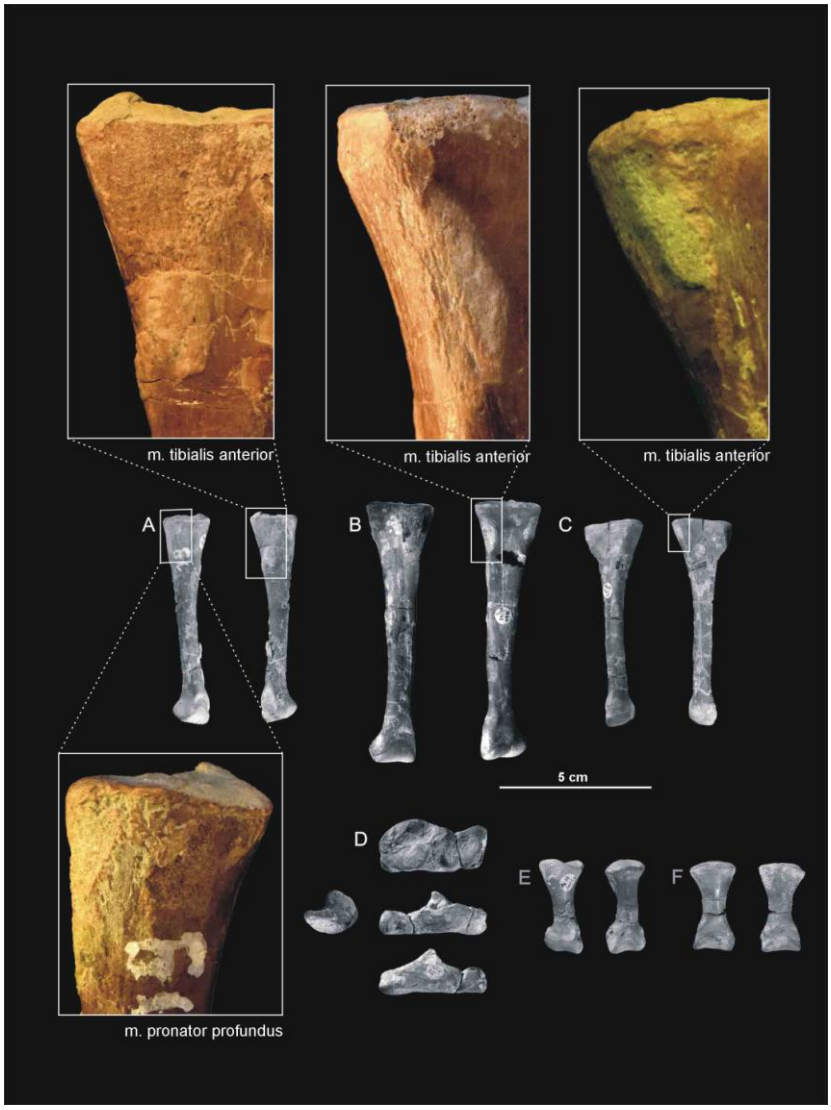

Figure 58. Muscle scars visible on the pes of *Silesaurus opolensis*. **A**, left metatarsal II from ZPAL AbIII/361/19 in medial and lateral views; **B**, right metatarsal III from ZPAL AbIII/361/14 in dorsal and ventral views; **C**, left metatarsal IV from ZPAL AbIII/361/2 in dorsal and ventral views; **D**, left astragalocalcaneum ZPAL AbIII/361/20 in medial, dorsal, anterior and posterior views; **E**, first phalanx of the digit II from the right pes ZPAL AbIII/361/13 in ventral and dorsal views; **F**, proximal phalanx of digit III from ZPAL AbIII/1930 in ventral and dorsal views.

Table 9. Length measurements of the pes bones of *Silesaurus opolensis* ZPAL AbIII/364 (in mm).

	I	II	III	IV	V
Metatarsals	?	64	77	63	33
Phalanx 1		23	25	19	
Phalanx 2		16	19	~14	
Phalanx 3			14	~10	
Phalanx 4				~9	
Unguals		16	?	10	

Description of the pedal phalanges (Figures 57B–D, 58E–F, Table 9) is based mostly on the articulated specimen ZPAL Ab III/364. Individual morphology of particular phalanges is supported by the isolated specimens ZPAL Ab III/361/13, 32, and 1930. The pedal phalangeal formula of *Silesaurus* is 0 – 3 – 4 – 5 – 0. The phalanges have distally rounded articular surface, which corresponds to concave surfaces on the proximal ends of the succeeding phalanges. This proximal surface presents a dorsoproximal prong. The distal articular surface of most nonungual phalanges bear well-developed pits for the extensor ligaments. Distinct pits for the collateral ligaments are present on all nonungual phalanges. They are approximately of the same depth on both sides of the bones.

The unguals (Figure 57B–D, Table 9) are subtriangular in cross-section and curved, each with a convex dorsal and concave ventral edge. Their proximal articular surfaces are similar to proximal ones of preceding phalanges. The dorsal surface of unguals bears scars for the extensor attachment. The unguals are elongated and they possess a sharp point.

Variability of femora and ilia

The the variation among *Silesaurus* femora and ilia was described by Piechowski et al. (2014) based on thirty-three more-or-less complete femora, and twenty ilia which were available for measurements (Figures 4 and 59–60, Tables 2–3 and 10).

Eight factors were identified in the matrix of 38 femur measurements, and five factors were identified in the matrix of 34 ilium measurements. The obtained first PCA plot shows the dominance of ontogenetic variability, which obliterates other factors. Apparently, the linear dimensions of bones express both population variability and directional ontogenetic change, whereas coefficients reflect only variability at each ontogenetic stage. To remove this bias, I created a covariance matrix of 15 iliac variables and 24 femoral variables, which are not directly dependent on size. These are mainly angles between bone structures, the presence

or absence of various features, and surface area or linear measurements in relation to specimen size (Figure 4, Tables 2 and 3). They were used in the second PCA and Student's t-tests. Size dependence has ceased in the second data set and new significant factors emerge. Four factors appear essential for the femur and two factors for the ilium.

Because of bone incompleteness the data matrix includes many missing measurements. Substitution of a missing measurements based on the coefficient of relative specimen size (explained above in Chapter 1) enabled use of incomplete specimens in the PCA, but this has resulted in an artificial clustering of such specimens in the center of the plots (Figures 59, 60).

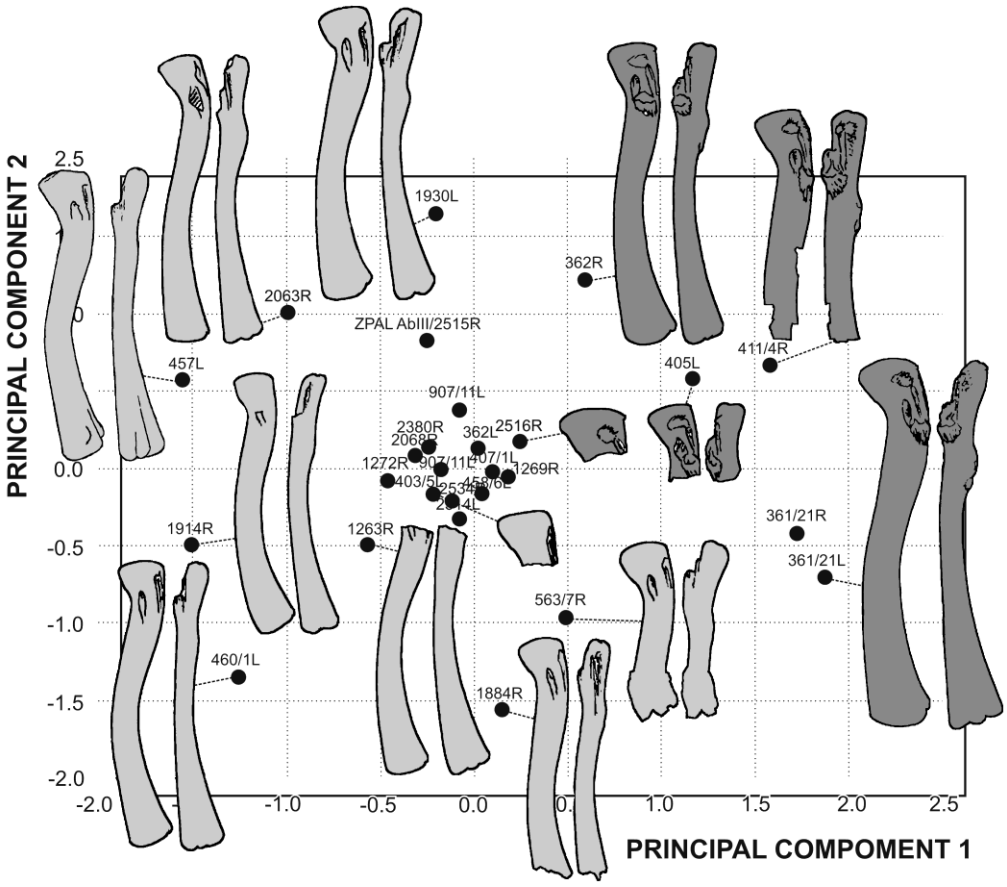

Figure 59. Principal component analysis plot for femora. The difference between any two animals is expressed by the root of the sum of squared differences among each of 24 different parameters. The total stress (sum of squared differences between the predefined distances and those that go on the chart) amounts to 37.069. The cluster of specimens in the centre of the plot is an artifact of the method of supplementing missing data used in this study (see Chapter 1). Darker color marks femora with ossifications.

More complete specimens of femora form a ring around the central cluster of points (Figure 59). Main characters (factor 1) responsible for the distribution of femoral in the PCA plot were linked to additional ossifications (Table 2, nos. 16, 17, 18, and 24). Other factors

were connected with fourth trochanter variability, femoral head curvature, and femoral shaft compression (Table 2, nos. 4, 5, 8, 20, 21, 22, and 23).

The distribution of ilia on the PCA plot is more uniform (Figure 60). The shallow ilia group at the bottom of the scattergram; small and high ones are above them. The total stress is also low. This shows that intraspecific variation dominates over ontogenetic differences. Main characters (factor 1) responsible for the distribution of the ilia were linked to the position of the brevis shelf, bone thickness, and width (Table 3, nos. 7, 9, 13, and 14). Other factors were connected with ischiadic process length, the angle between the anterior and preacetabular processes, anteroposterior iliac blade extent, and iliac height (Table 3, nos. 4, 6, 8, and 11).

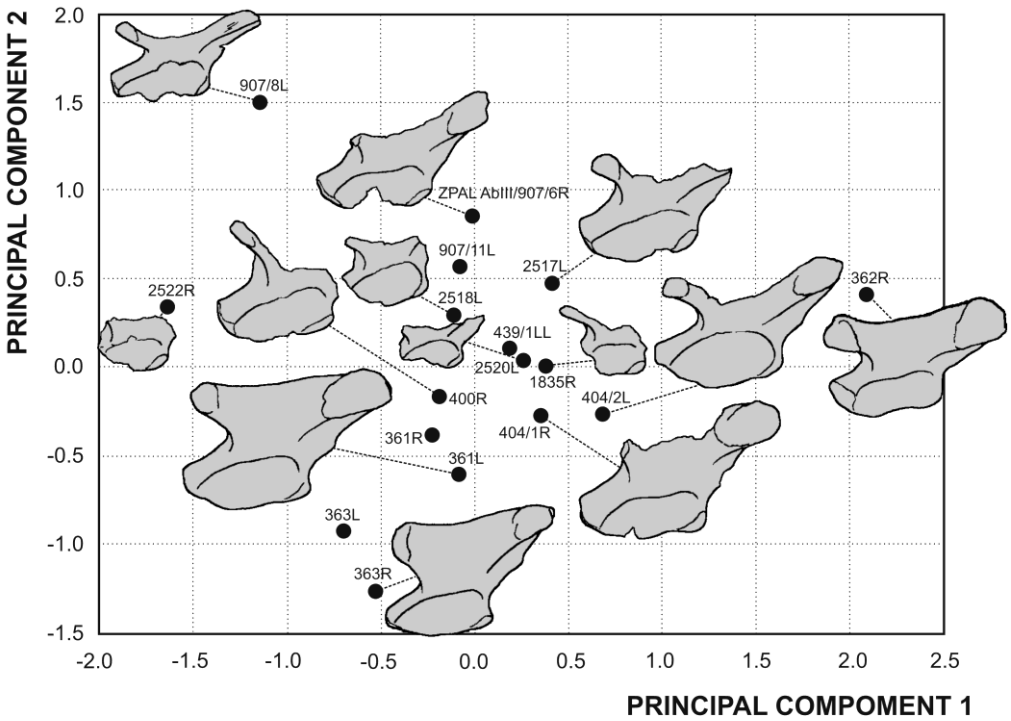

Figure 60. Principal component analysis plot for ilia. The difference between any two animals is expressed by the root of the sum of squared differences among each of 15 different parameters. The total stress (sum of squared differences between the predefined distances and those that go on the chart) is 4.612.

Student's t-Test

The two recognized groups of femora (those with or without ossifications) significantly differ in a number of other variables (Table 10). This clearly shows that the ossifications developed with age, together with changing compression and curvature of the femur. Specimens with the overhang structure are statistically larger and bear extra ossifications.

However, there are no grounds to reject the null hypothesis of no difference for the other variables between groups with and without the overhang structure, and excluding the relative specimen size from the analysis did not change the results significantly.

TABLE 10. Results of Student's t-tests.

Character	Group without the overhang structure	Group with the overhang structure	t	P
The index of size	1.065	0.946	t(21) = 3.12	0.005
The lower edge of femoral head compression	1.996	1.798	t(23) = 2.12	0.045
The level of femoral shaft curvature angle	–147.51	–145.44	t(23) = 2.2	0.038
The distance from dorsolateral trochanter to proximal end	0.3396	0.3126	t(23) = 2.29	0.031
The lateral ossification size	–0.82	0.37	t(11.08) = 0.52	0.009
The distance from proximal edge of lateral ossification to proximal end	0.2192	0.2322	t(9.20) = 0.01	0.018
The distance from distal edge of lateral ossification to proximal end	0.2602	0.2756	t(9.28) = 0.01	0.015

Ontogenetic change

In statistical analyses relative specimen size is usually used as an ontogenetic proxy. Size is not strictly correlated with ontogenetic age but approximates some trends. The small number of specimens means I are unable to obtain significant results for some trends on the bivariate plots.

The position of the dorsolateral trochanter (Figures 4A, 61A, B) differs in larger and smaller individuals ($r = 0.8052$, $P = 0.0005$, $r_s = 0.7379$, $P = 0.0026$). Its distance from the posterior edge of the femur ranges from 6 to 13 mm (Figure 61A), being located more anteriorly in larger individuals. The specimens with additional ossifications have the dorsolateral trochanter positioned distinctly further from the posterior edge of femur (8–13 mm). In contrast, femora without additional ossifications have this structure 6–9 mm from the posterior edge of the bone (Figure 61A). Treating these two groups separately, trends are less visible: $r = 0.8024$, $P = 0.1023$, $r_s = 0.9$, $P = 0.0167$ and $r = 0.7195$, $P = 0.0289$, $r_s = 0.3347$, $P = 0.3747$, respectively. The distance from the dorsolateral trochanter to the end of the

proximal femur ranges from 10 to 19 mm (Figure 61B). Again, specimens with additional ossifications show a notably larger distance from the femoral edge to this structure (14–19 mm). There is also a positive relationship between the specimen size and this distance: r = 0.6168, P = 0.0143, r_s = 0.6673, P = 0.0066. However, no trends are visible in these separate groups alone: r = 0.4614, P = 0.4341, r_s = 0.2052, P = 0.7333 and r = 0.2665, P = 0.4567, r_s = 0.3404, P = 0.3358, respectively.

The femoral shaft angle (Figure 61C) seems to be greater in larger individuals, but the trend is insignificant: r = 0.7032, P = 0.1191, r_s = 0.7714, P = 0.1029. It ranges from 139° to 151°. In contrast, the angle between femoral head and shaft (Figure 61D) seems to be lower in larger specimens, but the trend is also insignificant: r = –0.3187, P = 0.3395, r_s = 0.2145, P = 0.5265. No positive or negative trend (r = –0.0911, P D 0.8301, r_s = 0.0952, P = 0.8401) can be observed from the fourth trochanter angle (Figure 61E). All three angles (Figure 4A) have notable variation but are not dependant on size (Figure 61C–E).

The ratio between femoral shaft length and width (measurement 32 and 31 in Figure 4A) is larger in larger individuals (Figure 61F). In the smallest specimen, this ratio is less than 1.2, whereas in the largest it is almost 1.6. Again, the change is insignificant probably due to small sample size: r = 0.6577, P = 0.1084, r_s = 0.7143, P = 0.0881.

Despite small number of specimens, I observed some possible ontogenetic changes. The femoral shaft changes its cross-sectional shape (Figure 61F). It is circular and disproportionally narrower in small individuals and wide anteroposteriorly in larger specimens, which makes its cross-section more ovate. Also, the angle between the femoral shaft and the head changed during ontogeny (Figure 61D). Heads are more erect in smaller individuals. The proximal part of femur is more curved in larger specimens (Figures 5, 60), and they also have a larger fourth trochanter, but the angle between the fourth trochanter and the femoral shaft is variable (Figure 61E). In smaller individuals, the femoral shaft is strongly curved, and it straightens in larger ones (Figures 5, 59, 61C). The posteromedial tuber on the proximal femur head (tuberosity of Ezcurra, 2006) usually disappears with growth (Figure 64), but it is retained in large femora without ossifications (unfortunately, this feature is not well preserved in several specimens).

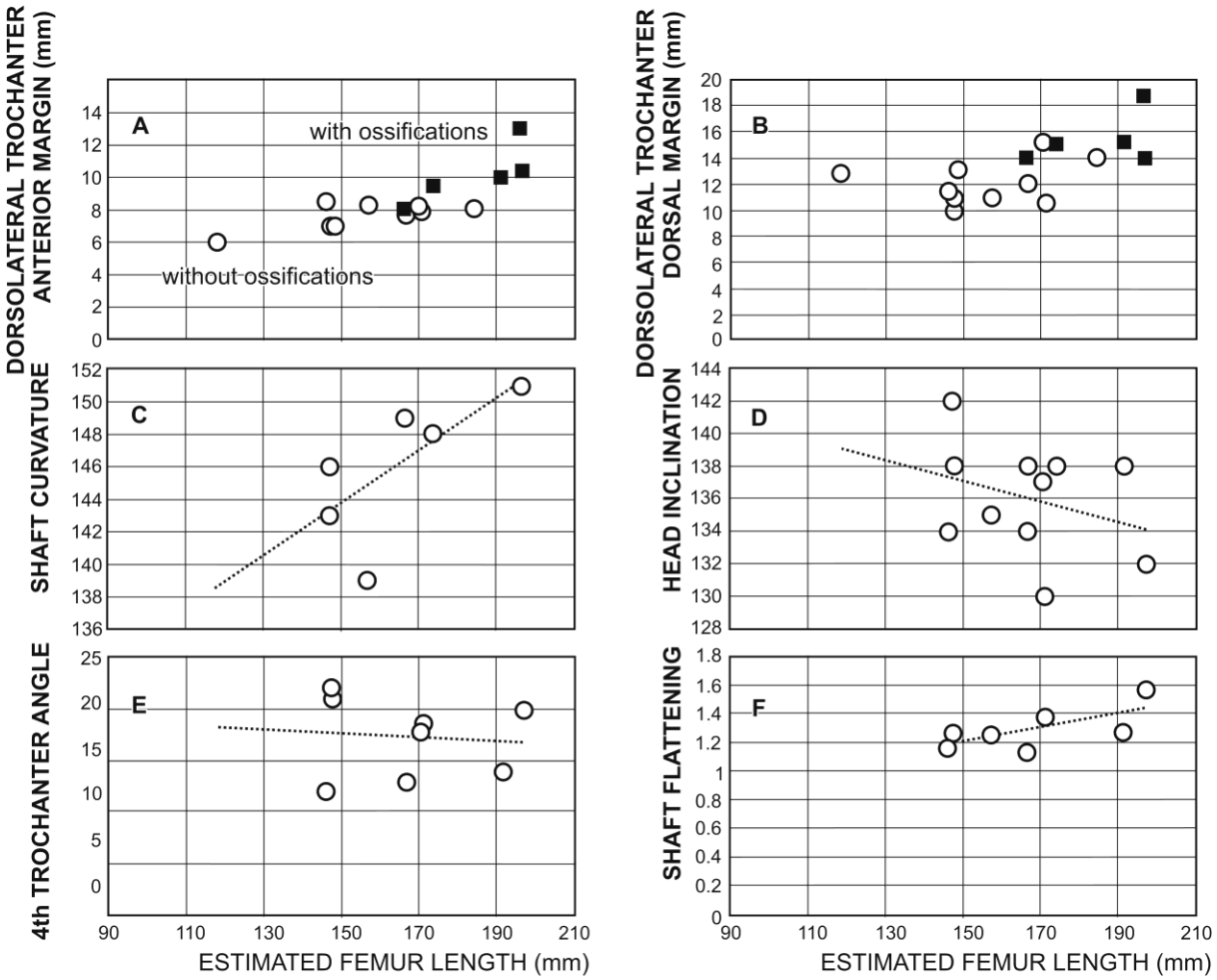

Figure 61. Ontogeny of femora. **A**, anterior dorsolateral trochanter location (measurement 10 on Fig. 1A) plotted against specimen size as a measure of ontogenetic stage (r = 0.8052, P = 0.0005, r_s = 0.7379, P = 0.0026); **B**, distance from the dorsolateral trochanter to proximal femur end (measurement 8 on Fig. 1A) plotted against specimen size (r = 0.6168, P = 0.0143, r_s = 0.6672, P = 0.0066); **C**, femoral shaft curvature (measurement 38 on Fig. 1A) plotted against specimen size (r = 0.7032, P = 0.1191, r_s = 0.7714, P = 0.1028); **D**, angle between femoral head and shaft curvature (measurement 36 on Fig. 1A) plotted against specimen size (r = -0.3187, P = 0.3395, r_s = 0.2145, P = 0.5264); **E**, angle between fourth trochanter and femoral shaft (measurement 37 on Fig. 1A) plotted against specimen size (r = -0.0911, P = 0.8301, r_s = 0.0952, P = 0.8401); **F**, femoral shaft flattening (the ratio of measurement 32 and 31 on Fig. 1A) plotted against specimen size (r = 0.6577, P = 0.1084, r_s = 0.7143, P = 0.0881).

The length and shape of muscle attachments on the anterior and posterior iliac processes (Figures 4B, 60, 62A) are variable, and they are usually disproportionally longer in larger specimens (r = 0.7816, P = 0.0379, r_s = 0.8469, P = 0.0246 and r = 0.6948, P = 0.0558, r_s = –0.0793, P = 0.8540, respectively). In particular, the posterior iliac process is larger and reaches a length of almost 30 mm in the largest individual.

The distance between the ischiadic process and the attachment of the third sacral rib (Figure 62B) is disproportionally greater in larger specimens: r = 0.7495, P = 0.0126, but r_s = 0.6159, P = 0.0580. The distance ranges from 11 to 26 mm.

The length of the iliac blade as well as the length of the lower part of the ilium (Figure 62C) increase disproportionally in larger individuals: r = 0.9778, P = 0.00002, r_s = 0.8434, P = 0.0137 and r = 0.9058, P = 0.00005, r_s = 0.8443, P = 0.0005, respectively. The iliac blade is relatively longer in the largest specimens compared with the lower part of the ilium. Variation among individuals of similar size is low (Figure 62C).

The height of the anterior iliac process and the whole ilium (Figure 62D) has slightly different proportions in small and large individuals: r = –0.4982, P = 0.2089, r_s = 0.0482, P = 0.9181 and r = 0.4885, P = 0.1821, r_s = 0.1958, P = 0.6123, respectively. The height of the whole ilium increases slightly more than the height of the anterior iliac process, but the trend is insignificant.

The lengths of particular sacral rib attachments and their proportions are very variable (Figure 63) and appear to be not related with specimen size.

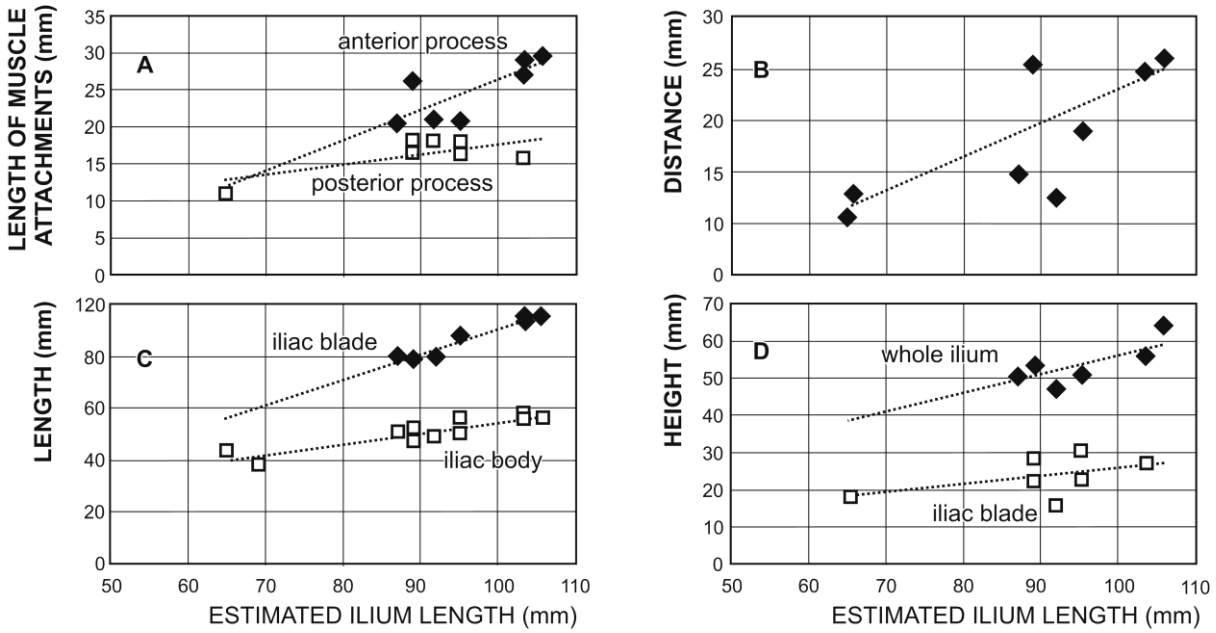

Figure 62. Ontogeny of ilia. **A**, length of muscle attachments on anterior and posterior iliac processes (measurement 30 and 31 on Fig. 1B) plotted against the specimen size (measurement 30: *r* = 0.7816, *P* = 0.0379, r_s = 0.8469, *P* = 0.0246; measurement 31: *r* = 0.6948, *P* = 0.0558, r_s = 0.0793, *P* = 0.8540); **B**, distance between the ischiadic process and the attachment of the third sacral rib (measurement 32 on Fig. 1B) (*r* = 0.7495, *P* = 0.0379, r_s = 0.6159, *P* = 0.0580); **C**, length of iliac blade (measurement 5 on Fig. 1B) and the length of the ventral part of ilium (measurement 7 on Fig. 1B) (measurement 5: *r* = 0.9778, *P* = 0.00002, r_s = 0.8434, *P* = 0.0137; measurement 7: *r* = 0.9058, *P* = 0.00005, r_s = 0.8443, *P*= 0.0005); **D**, height of the anterior iliac process

(measurement 15 on Fig. 1B) and ilium (measurement 11 on Fig. 1B) (measurement 11: r = -0.4982, P = 0.2089, r_s = 0.0482, P = 0.9181; measurement 15: r = 0.4885, P = 0.1821, r_s = 0.1958, P = 0.6123).

Smaller ilia have prominent anterior and postacetabular processes. In larger individuals, these processes are proportionally longer. In contrast, the lower part of the bone grew proportionally slower during ontogeny (Figure 62C). The muscle attachments grew faster on the anterior iliac process than on the posterior iliac process (Figure 62A), but their shape is variable. The acetabulum depth increases with respect to the whole bone size. Small ilia are robust and their thickness increased slightly during growth, as did the height of ilium. The distance between the ischiadic process and the attachment of third sacral rib is variable (Figure 62B).

Histological sections of femora ZPAL AbIII/2380, 411, and 405 imply that they were probably skeletally mature (Fostowicz- Frelik & Sulej, 2010). Similar size and complete coossification of the vertebral centra suggest that all examined individuals of *Silesaurus* from Krasiejów were adult or close to maturity (Brochu, 1996; Irmis, 2007). Smaller femora are not represented in the sample, so only changes in late ontogeny can be traced. An inference on earlier stages of ontogeny is possible only by extrapolation of trends recognizable in the variability of medium- and large-sized specimens. These specimens differ significantly in size and thus, presumably, in their ontogenetic age. The ilia show a somewhat wider size distribution and presumably a larger span of ontogeny.

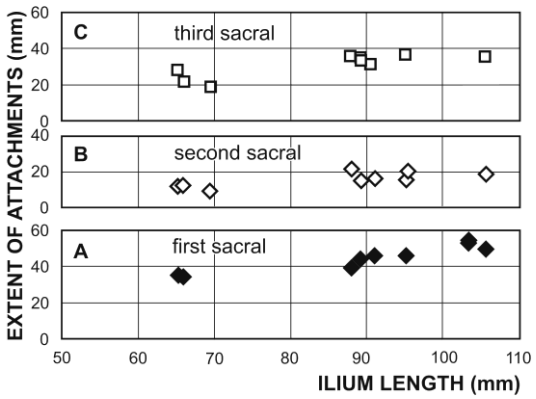

Figure 63. Length of sacral rib attachments to ilia of different size.

The femoral shaft widens anteroposteriorly and becomes oval in cross-section during the ontogeny of *Silesaurus* (Figure 61F). A similar change was observed in the ontogeny of *Allosaurus* by Foster and Chure (2006). Presumably, juveniles had a more multidirectional load and stress on the hind limb because of their more agile running (Foster & Chure, 2006). However, data on bird locomotion suggest that there is no direct correlation between femoral

shaft geometry and appendage movements (Habib & Ruff, 2008; Farke & Alicea, 2009). The femoral shaft of *Silesaurus* also became increasingly straight (Figure 61C), as in *Coelophysis* (Colbert, 1989). The femoral head is more curved anteriorly in larger specimens (Figure 61D), and the fourth trochanter is higher. The depth of the acetabulum also increased slightly. All these changes may reflect adaptation to carrying a heavier body more efficiently and may also be a compensation for disproportionally shorter tibia, as a kind of trade-off.

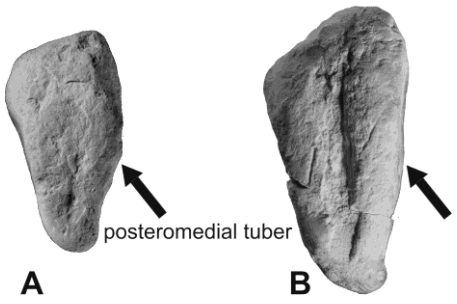

Figure 64. The proximal end of femora. **A**, small individual ZPAL AbIII/457L with posteromedial tuber (arrow); **B**, large individual ZPAL AbIII/361/23 without posteromedial tuber (arrow).

Body proportions changed during the growth of *Silesaurus*, as suggested by the only two specimens preserved completely enough to offer a femur/tibia ratio. In specimen ZPAL AbIII/1930, the ratio is 1.13 (femur 16.0 cm, tibia 14.2 cm). In the larger individual ZPAL AbIII/361, the same ratio is 1.25 (femur 20.0 cm, tibia 16.0 cm). This suggests that the femur grew faster than the tibia and that smaller individuals might have run relatively fast for their size (Foster & Chure, 2006), but inferring cursoriality from bone proportions is a complex problem in extinct animals (Farlow et al., 2000). This suggestion may be supported by the fact that smaller individuals are generally subjected to greater predatory pressures (Pounds et al., 1983), because relatively few carnivores are able to attack larger prey. Having a longer femur with respect to the tibia enables carrying a heavier body mass (Fechner, 2009). However, these two specimens were found in different layers and may represent morphologically different populations.

The question emerges whether changes in bone proportions modified the body posture in *Silesaurus* (discussed more extensively below). Generally, a straight femoral shaft follows the achievement of bipedal locomotion in the evolution of early dinosauromorphs (Fechner, 2009). However, in larger individuals of *Silesaurus*, ilia are disproportionally shorter than in smaller ones. This might suggest that older individuals had reduced abilities for bipedal locomotion. Fechner (2009) argued that *Silesaurus* was quadrupedal based on limb and trunk proportions. Indeed, this species has a long trunk (Piechowski & Dzik, 2010) as compared with the hind limbs and long (but disproportionally gracile) forelimbs. These proportions are

known only for large individuals. However, body posture depends also on location of the center of gravity of the body. Piechowski & Dzik (2010) posited that center of gravity of the body was near sacrum in *Silesaurus*. This implies that it was able to stand on two limbs, even if quadrupedal posture dominated in large individuals.

The fast rate of growth of young individuals of *Silesaurus* is a typical archosaurian pattern (Fostowicz-Frelik & Sulej, 2010). Selection pressure was focused on the hind limbs, which were the main locomotory organ. The intraspecific variability of *Silesaurus* ilia is higher than of femora, especially regarding sacral rib attachments (Figure 63). Apparently, the functional aspects of femoral morphology were more important for survival.

Tendon ossification

A peculiar aspect of femoral variability in *Silesaurus* is the presence of additional bony structures (Figure 5). The osseous structures of irregular rosette shape have distinct sharp margins and a fissure separating them from the bone proper at least near their margins. Their central elevated areas are truncated, and they represent the basal parts of muscle tendons, which sometimes ossify in vertebrates (Hutchinson, 2002). They are located on the muscle attachment site near to, or on, the trochanters (Figure 5). In some smaller individuals, the bone surface on which such ossifications develop is marked by a rough area.

Incipient ossification of tendon heads cannot be confirmed in the material because the calcified parts apparently detached during decay. They remained attached only after the ossification had resulted in unification of the ossified tendon with the femur surface. This result suggests that ossification of the tendons was rapid. Hence, there are only two classes of specimens: those lacking ossifications and those with ossifications already well developed. I propose that the dorsolateral, lateral, and fourth trochanter ossifications probably appeared simultaneously in ontogeny (Figure 5). Specimens with tendon ossifications have also developed a characteristic ‘overhang structure’ on the proximal femoral head (Figure 5A) that is interpreted as a calcification of the articular cartilage (see Holliday et al., 2010).

In dinosaurs, tendon ossifications develop mostly in the tail, and I have not been able to trace in the literature any mention of these kinds of separate ossifications associated with hind limbs, although such structures are common in birds (e.g., Hutchinson, 2002). Their histology is similar to that of regular bone (Moodie, 1928; Organ & Adams, 2005; Zhou et al., 2010). It is possible that the trochanteric shelf in some dinosaurs is of such origin (Raath, 1990; Nesbitt et al., 2009). Griffin & Nesbitt (2016) interpreted similar structures on the *Asilisaurus* femur

as muscle scars. They are clearly separated from the compact or calcareous bone (Griffin & Nesbitt, 2016, fig. 10A, B) that allows to reject the muscle scars interpretation.

Ossifications of tendons on the femur developed late in ontogeny and simultaneously in different locations (Figure 65). Presumably, as suggested by the rough surface of muscle attachment area, in smaller individuals a layer of cartilaginous tissue was developed there, such as on the epiphyses of crocodiles (Suzuki et al., 2003).

Calcified tendon attachments (Figure 5) and articular cartilage (overhang structure) are associated with the lack of a posteromedial tuber (Figure 64B) and a dorsolateral trochanter positioned relatively far from the bone margins (Figure 61A, B). The posteromedial tuber is present in specimens lacking any additional ossifications, and these specimens have a dorsolateral trochanter positioned relatively close to the bone margin. As supported by t-tests, femora with ossifications are generally larger than those without them (Figure 59). It would therefore seem apparent that femora with ossifications represent a later ontogenetic stage. Calcification of cartilaginous elements is induced by calcitonin in all vertebrates (Sasayama, 1999; Lyritis & Boscainos, 2001). In fishes (salmon), an increase of calcitonin level marks puberty in both sexes (Fouchereau-Peron et al., 1990). Secretion of this hormone is influenced by sex hormones: estrogens and androgens (Dacke et al., 1976).

Possible sexual dimorphism

In birds, ossifications in larger individuals are connected with a high level of calcitonin. In the Japanese quail (*Coturnix coturnix japonica*), castration of male birds considerably reduces the calcitonin level. This therefore indicates a relationship between calcitonin and gonadal hormone activity (Dacke et al., 1976) and that the possibly dimorphic pattern of ossification in *Silesaurus* may be an ancestral archosaur feature. As observed in *C. coturnix*, the females exhibit a three-fold increase in plasma calcitonin levels shortly before maturity, whereas males have more stable levels (Dacke et al., 1976). It is suggested that this surge in plasma calcitonin levels might be associated with the appearance of additional ossifications in the *Silesaurus* femora.

Size ranges of *Silesaurus* femora with and without ossifications overlap strongly (Figure 65). Moreover, the range of variability in this respect seems to be largest among specimens of sizes close to the mean of the sample (Figure 65; admittedly, the sample size is too small to prove this statistically). This may be an expression of limited correspondence between size and age (Brochu, 1996) or low precision of hormonal control of ossification. However, the

largest specimen without ossification, ZPAL AbIII/1930, seems to belong to a series with a different trajectory of ontogenetic change than specimens of similar size with welldeveloped ossifications (Figures 61A, B, 65). Two classes are recognizable at this stage of growth: the specimens with and without a posteromedial tuber. Again, the sample size is inconveniently low, but an appealing alternative to population variability is sexual dimorphism. Large specimens without additional ossifications (including a trochanteric shelf) and preserving the posteromedial tuber would then belong to males and specimens with additional ossifications to females (see Chinsamy, 1990; Raath, 1990). Also, the position and shape of the dorsolateral trochanter would be sex related. The distance between the dorsolateral trochanter and proximal end of femur and location of the anterior margin of dorsolateral trochanter are higher in the proposed females (Figure 61A,B). The high value of this trait in ZPAL AbIII/563/7R may indicate that it belonged to an immature female (Figure 59). This refers also to the posteromedial tuber (Figure 64). A similar pattern was observed and interpreted as sexual dimorphism in *Megapnosaurus* (Raath, 1990), with two morphotypes differing in size, presence or absence of the trochanteric shelf, and other ossified muscle insertions. The additional ossifications of these fossil forms appeared during maturity (Raath, 1990). This may correspond with an increase in calcitonin levels shortly before maturity, because it is observed in modern quail females (Dacke et al., 1976).

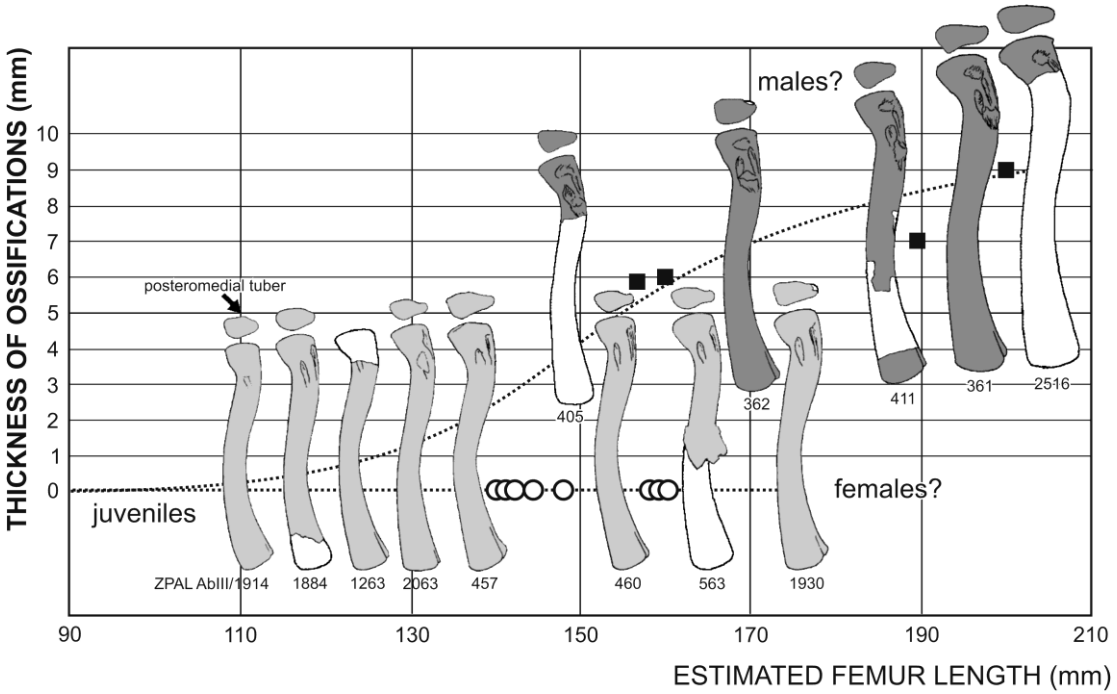

Figure 65. Proposed interpretation of the variability of *Silesaurus opolensis* femora as being an expression of sexual dimorphism. Males would be significantly smaller than females.

On the ilium, the anterior and postacetabular iliac processes grew proportionally faster than the acetabulum region (Figure 62C). However, the difference is moderate. At the same time, the anterior and postacetabular iliac processeses became wider and more massive. Muscle attachments become more distinct, presumably as a result of ossification of tendon attachment sites on the bone (Figures 6, 62A). This may have also resulted from increased body mass. Perhaps the height of ilia is related to sex or intraspecific variation.

Taxonomic implications

Intraspecific variation is often underestimated in taxonomic studies of silesaurids. For example Peecook et al. (2013) diagnosed *Lutungutali* based on the height of the iliac blade but the ilia of *Silesaurus* are variable in this aspect (Piechowski et al., 2014), and the condition found in *Lutungutali* falls within the range of this variation. Barrett et al. (2015) described a large silesaurid femur from the Manda Beds, which they considered to be either a second species or a very large individual of *Asilisaurus*. Griffin & Nesbitt (2016) stated that 'To date, *Asilisaurus* is the only species-level taxon of silesaurid known from the Manda Beds, and all evidence available to us indicates that there is not more than one species-level taxon of silesaurid'. A few limb bone fragments of a large silesaurid-like dinosauriform have also been found in Krasiejów in association with *Silesaurus* (Niedźwiedzki, 2015). The specimens analyzed by Griffin & Nesbitt (2016) did not show any LAGs in the outer cortices (Petermann et al., 2017) and were much smaller than the largest femora of *Silesaurus* found. The Manda Beds specimens probably represent individuals of *Asilisaurus* far from their growth limits.

The differences between individuals of *Silesaurus* that appear to result from ontogenetic changes have been used to discriminate species in early dinosauromorphs (i.e., Ezcurra, 2006; Ferigolo & Langer, 2006). A distinct tuberosity on the proximal femoral head, and lack of a trochanteric shelf and other ossifications (Ezcurra, 2006; Ferigolo & Langer, 2006), suggests that fossils of *Eucoelophysis* and *Sacisaurus* represent juvenile or male forms. The condition of *Eucoelophysis* (allegedly more basal than *Silesaurus*), *Diodorus*, or *Sacisaurus* (Kammerer et al., 2012) is in conflict with their younger geologic age (Norian). Similarly, the isolated femur from Woźniki (Sulej et al., 2011) may represent a juvenile individual or a male. The anterior trochanter is prominent during the whole known ontogeny of *Silesaurus* in both sexes. Surprisingly, young individuals of *Dromomeron gregorii* lack this feature (Nesbitt et al., 2009). It is therefore possible that this is an expression of their early ontogenetic stage.

I applied PCA to the measurable morphological traits of ilia and femora to test a possibility that two species are represented in the *Silesaurus* material from Krasiejów. As mentioned above, the plot of femora forms a ring surrounding the specimens in the center with incomplete data sets. The right half of the ring (Figure 59) is composed of specimens with additional ossifications. As shown by Student's t-tests, specimens without ossifications on the left are usually smaller (Figure 59). There is a continuity between these groups because the distinguishing characters develop gradually during ontogeny (Figure 65). It cannot be asserted, based on the morphology of femur alone, whether these groups represent separate sexes (as proposed here) or species. The variance of ilia is more uniform, but it is dominated by intraspecific variation, with no signs of a bimodal frequency distribution (Figure 60). The highly specific morphology of associated jaws of *Silesaurus* (Dzik, 2003; Kubo & Kubo, 2014) suggests that not more than one morphospecies is represented in the material.

Taking all the available evidence together, it seems likely that the material studied here probably represents one biological species with dimorphic femora developing in late ontogeny. Most of the morphological characteristics show wide intraspecific variability. There are few data regarding intraspecific variability in other closely related taxa to compare with *Silesaurus*. The presence of a trochanteric shelf in *Saturnalia* (Nesbitt et al., 2009) and *Megapnosaurus* (Raath, 1990) varies within these species, which is observed also in *Silesaurus*. This calls for caution while using such characters in phylogenetic studies. It appears that the most variable characters within species are the shape and position of the dorsolateral trochanter, the contact of the ilium with the sacral ribs, the angle of the fourth trochanter, and the distance between the ischiadic process and the edge of fourth sacral rib articulation area. Also, the muscle attachments on the anterior and posterior iliac processes are variable in shape (more or less ossified). The presence of a lateral ossification fused with the femur shaft (trochanteric shelf) may be an aspect of late ontogenetic age (Nesbitt et al., 2009) or sexual dimorphism, as discussed above. This may explain the chaotic distribution of this character among dinosauromorphs (see Langer & Benton, 2006).

Evolutionary implications

Most *Silesaurus* material comes from a single lens of mudstone in the upper part of the Krasiejów clay-pit (Dzik, 2003; Dzik & Sulej, 2007; Piechowski & Dzik, 2010). Only a few specimens were collected from the lower fossiliferous horizon. Among them, ZPAL AbIII/1930 is the most complete, with preserved femora. There is no doubt that it represents

an older population belonging to the same local continuum. The difference in age is difficult to estimate, but the sedimentation rate of the fluvial deposits in Krasiejów was probable high (Gruszka & Zieliński, 2008). It cannot be excluded that only thousands of years separate the two horizons.

The femur of the most complete specimen ZPAL AbIII/1930 from the lacustrine lower horizon is located on the margin of the PCA plot (Figure 59A). It is relatively large, but lacks the ossifications observed in other large individuals. Despite that it is very robust. It may represent a male individual, according to the interpretation proposed above.

Ilia are not preserved in ZPAL AbIII/1930, but other bones, including vertebrae, scapulocoracoids, the humerus, and dentary, seem to differ slightly in morphology and proportions from the specimens most common in the upper horizon. Such differences might be a result of microevolutionary changes, but the morphological distance is not large enough to preclude this single individual belonging to a population with the same range of variability.

Differences between populations of different geologic age may be influenced by directional evolution. If precise stratigraphic control is lacking, it is difficult to distinguish such differences from sexual dimorphism. Possibly, bimodal distribution of variables in *Kentrosaurus* (Barden & Maidment, 2011) may have resulted from differences between populations. However, the disparity in prominence of the greater trochanter supports the sexual dimorphism interpretation.

Chapter 8. Musculature of pelvic girdle and hind limb[8]

Pelvic myology of *Silesaurus* indicates a decrease in the importance of the m. ilifemoralis, which dominates in the dinosaur pelvis. Instead, there are extensive attachments of knee flexors and extensors.

Table 11. Summary of the pelvic and leg musculature in *Silesaurus opolensis*, listing their names, origins, insertions, and actions. Muscle attachments in bold are those which have visible osteological correlates.

Muscle name	Origin	Insertion	Proposed function	Level of inference
M. iliotibialis	**Dorsal border of the iliac blade**	**Cnemial crest of the tibia**	Flexes, extends, and abducts the hip, as well as extending the knee	I
M. ambiens	**Pubic tubercle**	**Cnemial crest of the tibia**	Flexes the hip and extends the knee	I
M. femorotibialis	**Femoral shaft**	**Cnemial crest of the tibia**	Extends the knee	I
M. iliofibularis	**Dorsolateral surface of the postacetabular process of the ilium**	**Spiral ridge of the fibula**	Extends and abducts the hip, as well as flexes the knee	I
M. iliofemoralis	Lateral surface of the ilium	**Anterior trochanter and the trochanteric shelf of the femur**	Abducts the hip	I
M. puboischiofemoralis internus (pifi)	**Anterior aspect of the ilium (pifi 1); lateroventral aspect of the anterior process of the ilium (pifi 2)**	**Femoral shaft, anterior to the fourth trochanter (pifi 1);** anterolateral aspect of the femoral neck (pifi 2)	Flexes the hip	I
M. puboischiotibialis	Obturator plate of the ischium	**Posteromedial aspect of the proximal tibia**	Abducts and extends the hip, as well as flexes the	II

[8] Part of this chapter was published in:
Piechowski, R. & Tałanda. M. 2020. The locomotor musculature and posture of the early dinosauriform *Silesaurus opolensis* provides a new look into the evolution of Dinosauromorpha. *Journal of Anatomy* DOI: 10.1111/joa.13155

			knee	
M. pubotibialis	Not reconstructed			
M. flexor tibialis internus	Distalmost ischium ? (flexor tibialis internus 1); **distinct, rugose ridge on the proximodorsal part of the ischium, posterior to the acetabulum (flexor tibialis internus 3)**	**Posteromedial aspect of the proximal tibia**	Adducts and extends the hip, as well as flexes the knee	II
M. flexor tibialis externus	**Postacetabular process of the ilium**	**Posteromedial aspect of the proximal tibia**	Extends and adducts the hip, as well as flexes the knee	I
M. adductors	**Ventral portion of the ischial body (adductor 1); dorsal margin of the posterior ischium (adductor 2)**	**Femoral shaft, between the medial and lateral condyle**	Adducts the hip	I
M. puboischiofemoralis externus (pife)	Medial surface of the distal half of the pubic shaft (pife 1); lateral surface of the distal pubic shaft (pife 2); lateral ischial shaft (pife 3)	**Dorsolateral ossification of the femur**	Flexes and adducts the hip	II
M. ischiotrochantericus	**Dorsomedial surface of the distal ischium**	**Dorsolateral trochanter of the femur**	Lateral rotation (supination), and retraction of the hip	I
M. caudofemoralis brevis	**Brevis fossa of the ilium**	**Femoral shaft, just posteriorly to the fourth trochanter**	Extend and adduct the hip	I
M. caudofemoralis longus	Bodies of a varying number of caudal vertebrae and ventral surfaces of their transverse process	**Oval concavity, anteromedial to the fourth trochanter of the femur;** posterior aspect of the proximal fibula (secondary	Extends and adducts the hip	I

tendon)

M. triceps femoris

The term ‘triceps femoris’ is used in a wider context, subsuming three distinct muscles: the m. iliotibialis, the m. ambiens, and the m. femorotibialis. In all extant taxa, these three divisions coalesce into a common femoropatellar tendon that inserts on the cnemial crest of the tibia. The primary action of the m. triceps femoris would be in flexing the hip and extending the knee (after Schachner et al., 2011; Table 11).

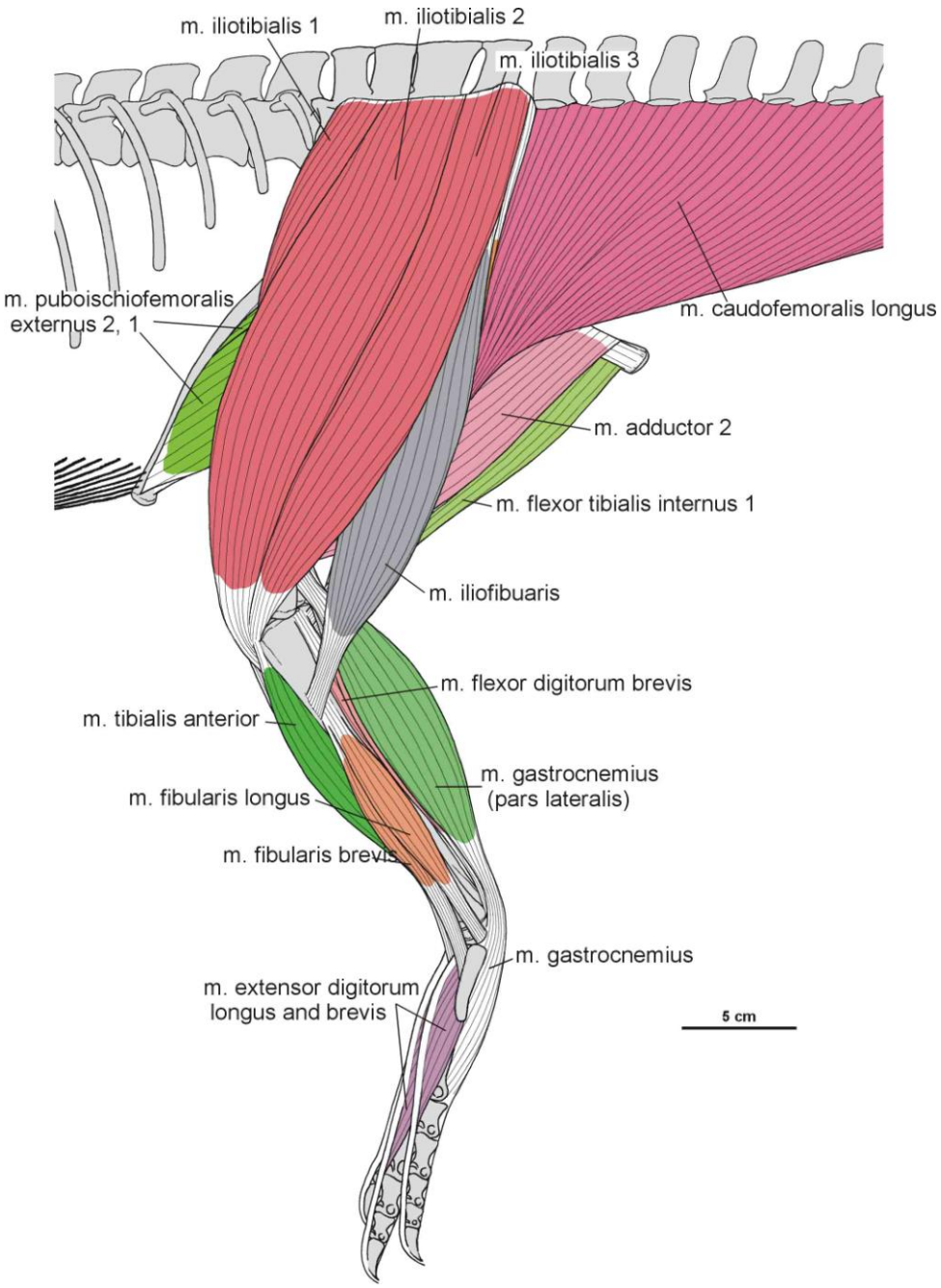

Figure 66. Muscle disposition on the hind limb of *Silesaurus opolensis* in lateral view.

M. iliotibialis

In specimens ZPAL Ab III/361, 362, and 404/1, 2 the origin of the m. iliotibialis is marked by a distinct longitudinal narrow rugosity along the dorsal border of the iliac blade (compare with Vanden Berge & Zweers, 1993; Carrano & Hutchinson, 2002; Fechner, 2009; Schachner et al., 2011; Liparini & Schultz, 2013; Figures 44, 46B, Table 11). The rugosity expands onto the anterior process, covering its anterolateral surface. It is very broad there and has a rounded lateroventral margin. The part situated on the iliac blade expands posteriorly to cover the dorsalmost part of the postacetabular process. It is difficult to determine the exact boundaries between the different parts of the m. iliotibialis. The presence of the anteriorly straight cnemial crest indicates that the m. iliotibialis of *Silesaurus* attached to the anteromedial aspect of the crest (compare with Romer, 1923b; Maidment & Barrett, 2011; Figures 52C, D, 54A, Table 11). In the *Silesaurus* material, the insertion area can be recognized in specimens ZPAL Ab III/361, 403, 414, 2539, 1245, 1246, 1930, and 404/10. There is a large, distinct scar, marking the position of the common insertion for three muscles (m. iliotibialis, m. ambiens, and m. femorotibialis).

M. ambiens

The different origination patterns of the m. ambiens in modern diapsids make reconstructions in extinct taxa difficult. Phylogenetic bracketing indicates that the double-headed m. ambiens is a derived feature of crocodiles (Maidment & Barrett, 2011). However, it is possible that the second head evolved earlier and was secondarily lost in advanced dinosaurs (Langer, 2003). I reconstruct the origin of the m. ambiens as lying laterally on the pubic tubercle in *Silesaurus* (Figure 46A, B, Table 11), as in lepidosaurs and basal archosaurs (compare with Romer, 1923b, 1927b; George & Berger, 1966; Vanden Berge & Zweers, 1993; Fechner, 2009; Schachner et al., 2011; Liparini & Schultz, 2013). This position is supported by a large scar that covers whole anterior surface of the tubercle and extends craniodorsally to the dorsal rim of the pubis and also ventrally (ZPAL Ab III/361, 363, 404/5, 1930, 3339, and 3340; Figure 33B). In most dinosaurs, the dorsal rim of the pubis is somewhat protruding, while the pubic tubercle is absent (Langer, 2003). This led various authors to locate the ambiens origin dorsally near proximal end of the pubis, as in crocodiles (Romer, 1923a; Romer, 1927b; Borsuk-Białynicka, 1977; Dilkes, 2000; Langer, 2003). The m. ambiens had a common insertion with the m. iliotibialis and the m. femorotibialis (compare with Liparini & Schultz, 2013; Figures 52C, D, 54A, Table 11). It is impossible to

determine whether a secondary tendon crossed the knee extensor tendon and inserted on the m. gastrocnemius lateralis as in extant archosaurs.

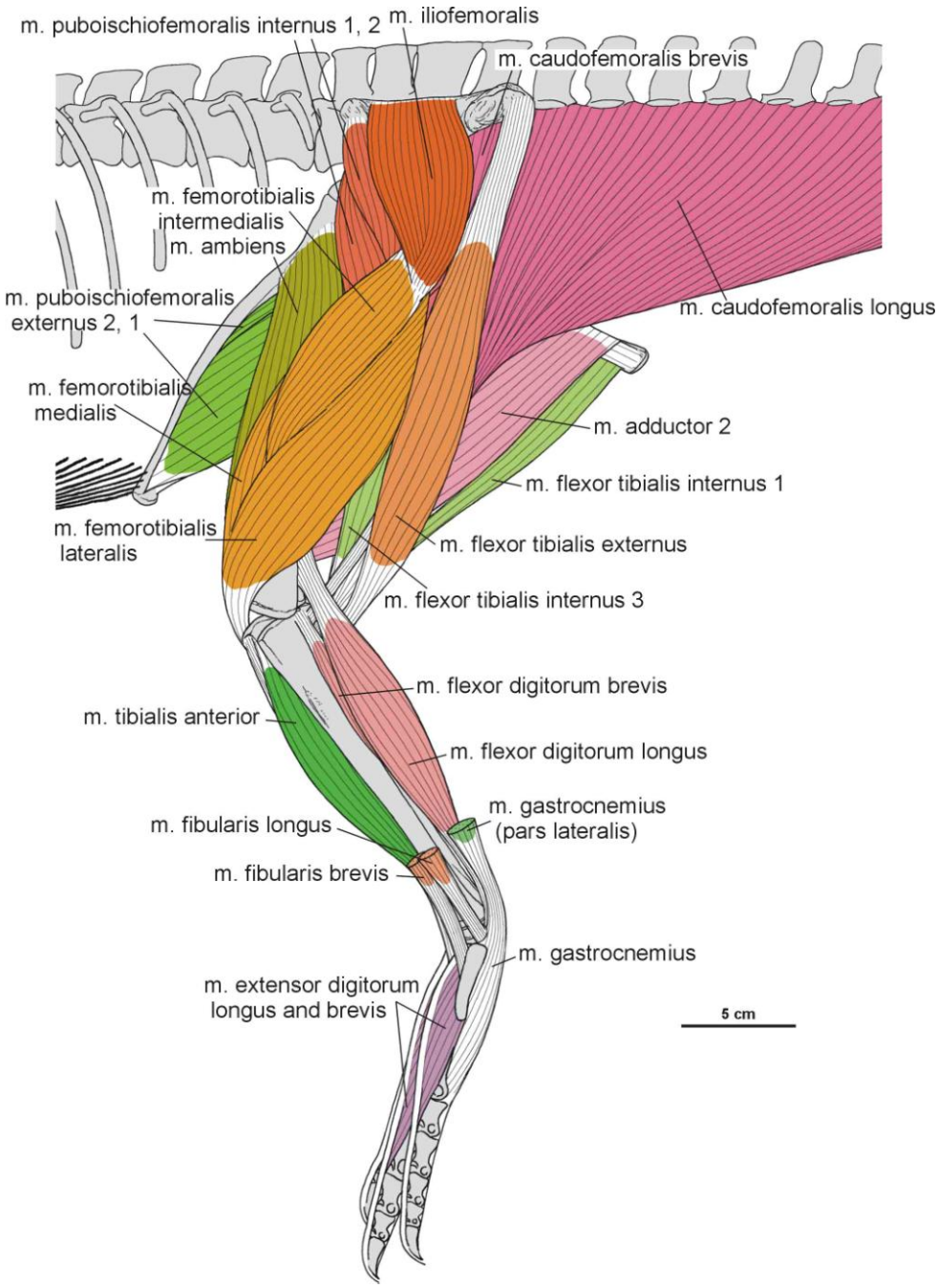

Figure 67. Muscle disposition on the hind limb of *Silesaurus opolensis* in lateral view. Some muscles are removed.

M. femorotibialis

I reconstructed three parts for the m. femorotibialis in *Silesaurus*, as in birds and non-avian dinosaurs (Langer, 2003; Fechner, 2009); contra Carrano & Hutchinson (2002) and Maidment & Barrett (2011). On the femur, a proximodistally oriented cranial intermuscular line (Figures 48A, 49B, 53A) clearly separates the origins of the m intermedialis and medialis, whereas a caudolateral intermuscular line (Figures 48B, 49A, 50B) separates the origins of the m.

intermedialis and lateralis. As a result, intermedialis part covers most of the anterolateral surface of the femoral shaft (Figure 48, Table 11). A distinct scar at approximately the mid-level of the anterior trochanter marks the proximal limit of the origin (Figure 51B). Distally, the scar is very faint but it is possible to recognize its posterolateral elevation. The origin of the m. femorotibialis medialis surrounds the depression marking the caudofemoralis longus origin proximally (Figures 49, 50A, Table 11), whereas the distal limit is marked by a clear rounded scar. The proximal scar for the m. femorotibialis lateralis origin is pointed and located posterior to the fourth trochanter (Figures 48B, 49A, 50B, Table 11). The distal limit of this origin is marked by a rounded scar on the lateral condyle. In *Silesaurus* material, the area of origin is visible in specimens ZPAL Ab III/361, 405, and 1263. The m. femorotibialis inserts in the same place as the previous two muscles.

M. iliofibularis

Despite the relatively smooth surface of the dinosaurian ilium, the postacetabular process of *Silesaurus* has a raised and rugose dorsolateral surface that probably marks the origin of m. iliofibularis (compare with Romer, 1923b; Gangl et al., 2004; Maidment & Barrett, 2011; Schachner et al., 2011). It is the largest rugose surface on the ilium (Figure 46B, Table 11) and, in *Silesaurus* material, is visible in specimens ZPAL Ab III/361, 362, 404/1,2 (Figure 44). The insertion is marked by a spiral ridge (Dzik, 2003) less than one-third of the way down the anterolateral surface of the fibular shaft (compare with Fechner, 2009; Schachner et al., 2011; Figure 55A, B, Table 11). The ridge is visible in specimens ZPAL Ab III/361, 416, and 3342 (Figure 56A). The primary action of the m. iliofibularis would be to extend and abduct the hip, as well as flexing the knee (see Schachner et al., 2011; Table 11).

M. iliofemoralis

The lateral surface of the ilium of *Silesaurus* presents a marked, smooth concavity above the acetabulum that is probably related to the origin of the m. iliofemoralis, (Figure 46B, Table 11) based on comparison with crocodilians (compare with Romer, 1923b; Rowe, 1986; Hutchinson, 2002; Fechner, 2009; Maidment & Barrett, 2011; Schachner et al., 2011;). However, *Silesaurus* lacks a ridge on the iliac blade making it difficult to judge if the m. iliofemoralis was divided into the m. iliotrochantericus caudalis and the m. iliofemoralis externus as in birds (compare with Osborn & Mook, 1916; Romer, 1927b; George & Berger, 1966; Osmólska et al., 1972; Bonaparte, 1986; Barsbold & Maryańska, Rowe, 1986; 1990;

Hutchinson, 2001b; Carrano & Hutchinson, 2002; Langer, 2003; Maidment & Barrett, 2011; Schachner et al., 2011). However, the anterior trochanter and the trochanteric shelf (= lateral ossification Piechowski et al. 2014) of *Silesaurus* might correspond respectively to the insertion of those two muscles (Figures 48, 49, Table 11). In *Silesaurus* material, the insertion area is visible in ZPAL Ab III/361, 405, 457, 1930, 460/1, and 411/4 (compare with Fechner, 2009; Schachner et al., 2011; Figure 51B). The m. iliofemoralis abducted the hip (see Schachner et al., 2011; Table 11).

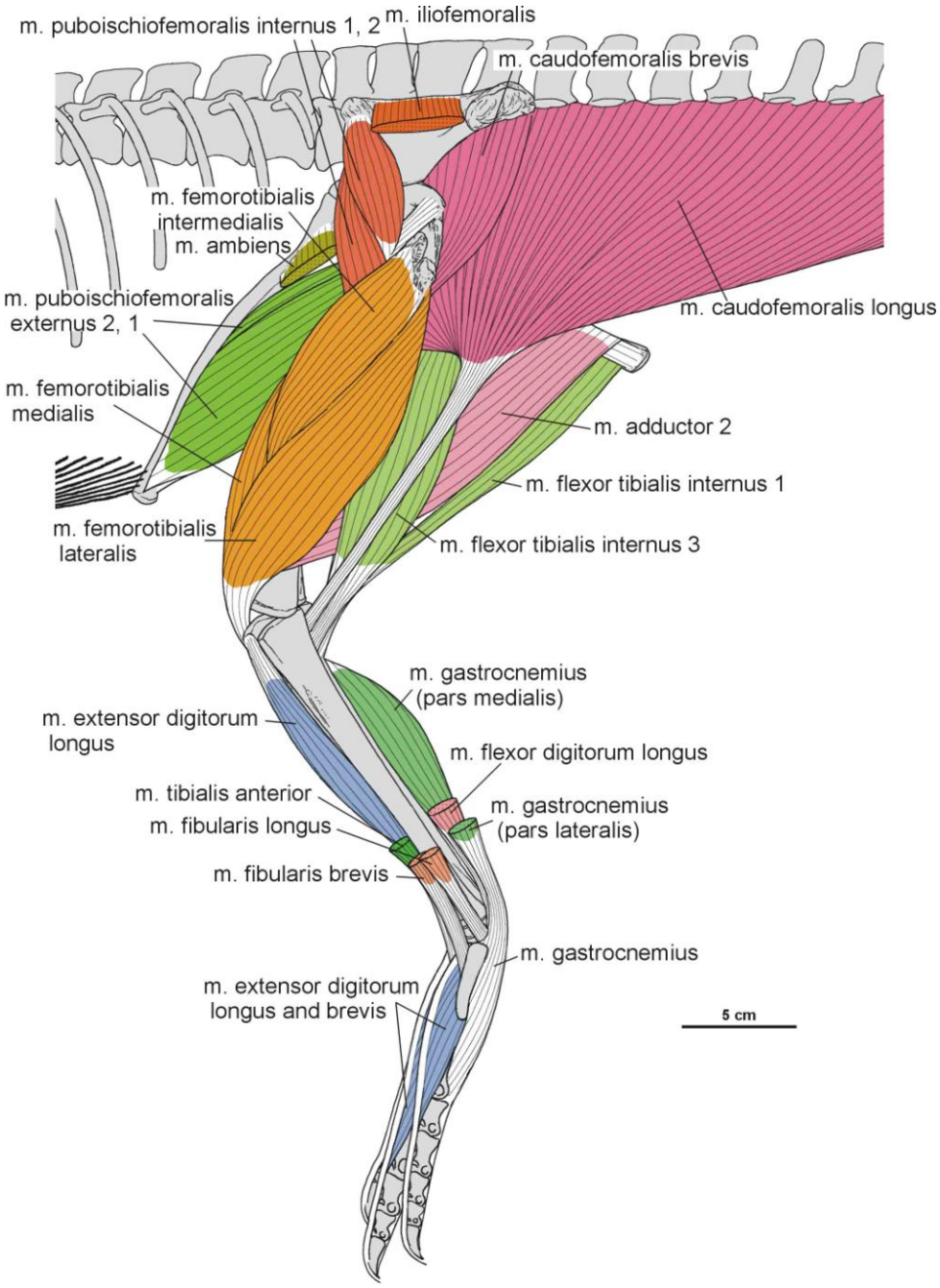

Figure 68. Muscle disposition on the hind limb of *Silesaurus opolensis* in lateral view. Some muscles are removed.

M. puboischiofemoralis internus

The m. puboischiofemoralis internus 1 is reconstructed here as arising from a distinct fossa on the anterior aspect of the ilium (ZPAL Ab III/361, 362, 404/1, 2), located exactly between the pubic peduncle and the anterior process (compare with Romer, 1927b; Fechner, 2009; Maidment & Barrett, 2011; Schachner et al., 2011; Figures 45C, 46B, C, Table 11). The fossa has an elliptical outline. The area of origin of the m. puboischiofemoralis internus 2 in *Silesaurus* could be on the lateroventral aspect of the anterior process similar to the position in birds (compare with Romer, 1927b; Rowe, 1986; Carrano & Hutchinson, 2002; Fechner, 2009; Schachner et al., 2011; Figures 45C, 46B, Table 11). There is a small tubercle next to the lateral extremity of the m. iliotibialis 1 that continues ventrally as a small ridge anterodorsal to the m. puboischiofemoralis internus 1. The insertion of the m. puboischiofemoralis internus 1 in *Silesaurus* apparently retained the crocodilian condition (compare with Romer, 1923b; George & Berger, 1966; Hutchinson, 2001b; Fechner, 2009; Maidment & Barrett, 2011; Figures 48B, 49, Table 11). It forms an arch along a low ridge that surrounds the semioval depression for the m. caudofemoralis longus mediodistally (Figure 50A). The insertion site extends on to the distalmost part of the fourth trochanter, the ossification of which reflects this attachment (Piechowski et al., 2014). The m. puboischiofemoralis internus 2 insertion occupies the anterolateral aspect of the femoral neck (compare with Fechner, 2009; Maidment & Barrett, 2011; Figures 48A, 49B). A distinct scar bounds the attachment area anteriorly, extended over the anterior trochanter (ZPAL Ab III/361; Figure 51B), but its medial outline is difficult to determine. This muscle would have flexed the hip (see Schachner et al., 2011; Table 11).

M. puboischiotibialis

The reconstruction of the m. puboischiotibialis in *Silesaurus* is equivocal (see Walker, 1973; Fechner, 2009; Liparini & Schultz, 2013). The muscle usually originates from the obturator plate of the ischium (Fechner, 2009; Schachner et al., 2011). A lateral depression on the proximoventral ischium, slightly separated from the reconstructed origin of the adductor muscles, was interpreted by some authors as a site of origin of the m. puboischiotibialis (Schachner et al., 2011; Liparini & Schultz, 2013). If present, the m. puboischiotibialis of *Silesaurus* may have arisen from a similar position (Figure 46B, Table 11) and inserted on the posteromedial surface of the proximal tibia (Figure 52A, B, D, Table 11). The rugose,

common insertion area for the pubotibialis, flexor tibialis internus and externus is visible in specimens ZPAL Ab III/361, 403, 414, 1246, 1930, 460/3, 411/2, and 1239 (compare with Schachner et al., 2011; Figure 53B). The m. puboischiotibialis would have abducted and extended the hip, as well as flexed the knee (see Schachner et al., 2011; Table 11).

M. pubotibialis

I am not able to identify any osteological correlate for the m. pubotibialis in *Silesaurus* and do not attempt to reconstruct it (Table 11).

M. flexor tibialis internus

This muscle is variously reconstructed in fossil tetrapods (compare with Romer, 1923b; George & Berger, 1966; Borsuk-Bialynicka, 1977; Dilkes, 2000; Hutchinson, 2001a; Langer, 2003; Gangl et al., 2004; Fechner, 2009; Maidment & Barrett, 2011; Schachner et al., 2011; Liparini & Schultz, 2013) due to the differences between modern birds and crocodiles. I provisionally follow the crocodilian arrangement because *Silesaurus* has similar distribution of rugosities on the ischium. However, I only reconstructed two parts, one of which is uncertain. A distinct rugose ridge on the proximodorsal part of the ischium posterior to the acetabulum is attributed to the origin of m. flexor tibialis internus 3 (Figure 46B, Table 11). This ridge is proximodistally elongated and runs parallel to the bone axis. It has convex surface facing laterally and tapers distally along approximately one third of the bone (ZPAL Ab III/361, 362, 925, 1228, 3226, and 404/1; Figure 34A). The m. flexor tibialis internus 1 may have originated from the dorsal part of the distalmost ischium (Figure 46C, Table 11), where an indistinct surface can be seen on some specimens (i.e. ZPAL AbIII/3288; Figure 34D). The insertion was probably on the posteromedial surface of the proximal tibia, together with m. puboischiotibialis and m. flexor tibialis externus (Figure 52A, B, D, Table 11). In *Silesaurus* material, the insertion area is visible in ZPAL Ab III/361, 403, 414, 1246, 1930, 460/3, 411/2, and 1239 (compare with Fechner, 2009; Schachner et al., 2011; Figure 53B). The action of the m. flexor tibialis internus would have been adduction and extension of the hip, as well as flexion of the knee (see Schachner et al., 2011; Table 11).

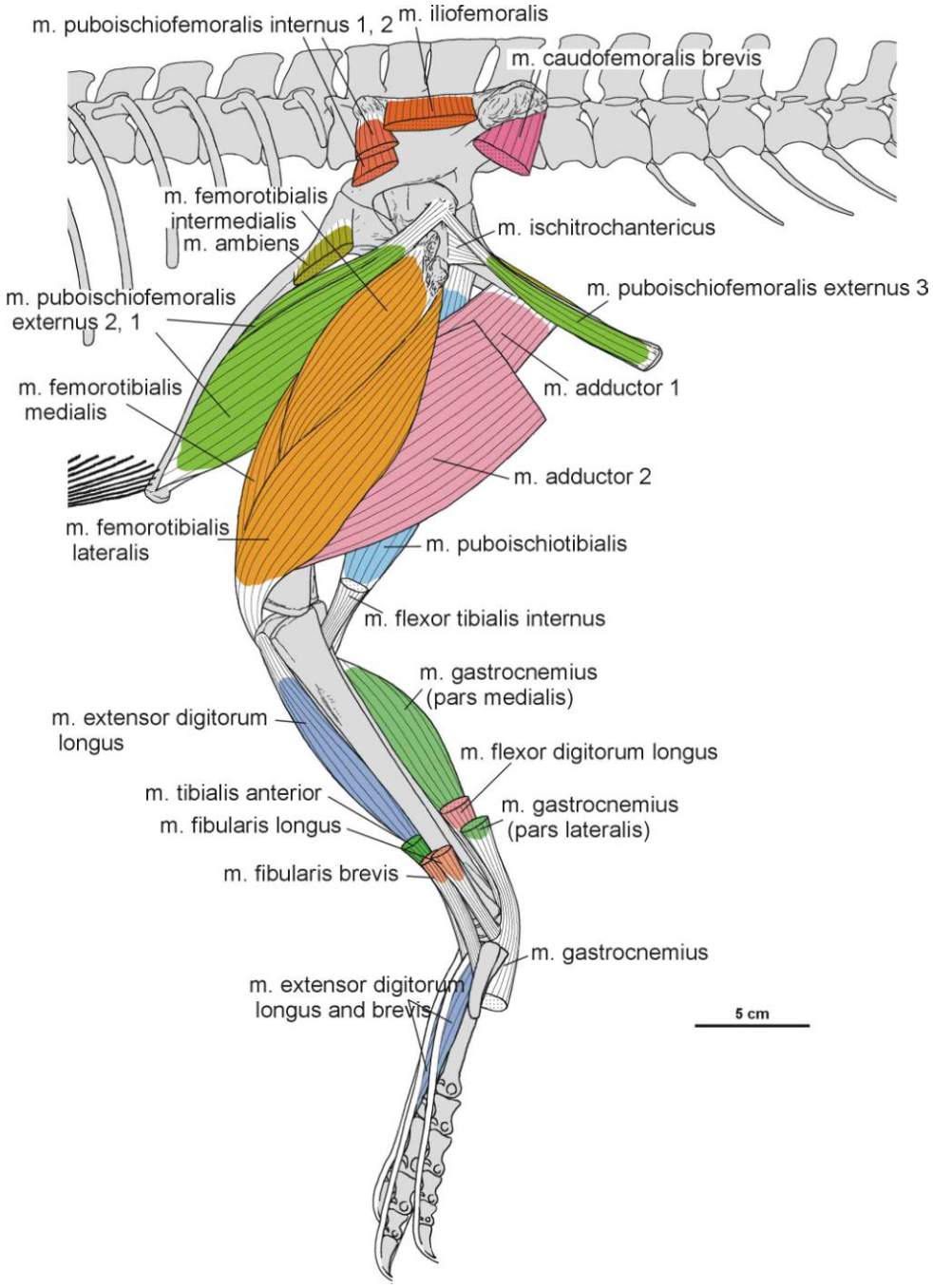

Figure 69. Muscle disposition on the hind limb of *Silesaurus opolensis* in lateral view. Some muscles are removed.

M. flexor tibialis externus

In *Silesaurus*, the m. flexor tibialis externus originates from the posterior iliac crest (compare with Romer, 1923b; George & Berger, 1966; Gangl et al. 2004; Schachner et al., 2011). A rugose tuberosity on the postacetabular process is divided into two distinct portions. The largest marks the origin of the m. iliofibularis, while the smaller marks the origin of the m. flexor tibialis externus. The latter is located more posteroventrally (Figures 44, 46B, Table 11). The insertion of the m. flexor tibialis externus is reconstructed here on the posteromedial surface of the proximal tibia (ZPAL Ab III/361, 403, 414, 1246, 1930, 460/3, 411/2, and 1239), together with the insertions of m. flexor tibialis internus and m. puboischiotibialis

(compare with Schachner et al., 2011; Figures 52A, B, D, 53B, Table 11). The m. flexor tibialis externus would have extended and adducted the hip as well as flexed the knee (see Schachner et al., 2011; Table 11).

M. adductors

Silesaurus is interpreted as having two parts to the m. adductors, both originating from the lateral side of the ischium (ZPAL Ab III/361, 925, 404/7) as evidenced by the presence of two clear longitudinal scars. The first scar runs along the dorsal margin of the posterior ischium, proximolateral to the m. ischiotrochantericus origin. The second scar is on the ventral portion of the ischial body, distal to the origin of the m. puboischiotibialis (compare with Romer, 1923b; Hutchinson, 2001b; Fechner, 2009; Schachner et al., 2011; Figure 46B, C, Table 11). The insertion of the m. adductors is clearly visible (ZPAL Ab III/361, 1914, and 460/1) as a distinct scar between the medial and lateral femoral condyles (compare with Romer, 1923b; Fechner, 2009; Maidment & Barrett, 2011; Figures 48B, 49A, 50B, Table 11). The scar is rounded and marks the distalmost extremity of this muscle attachment. Its proximal limit is difficult to trace. The action of the m. adductors would be adduction and extension of the hip (see Schachner et al., 2011; Table 11).

M. puboischiofemoralis externus

The orientation of the pubis and ischium remains plesiomorphic in *Silesaurus*. For that reason, the m. puboischiofemoralis externus is reconstructed in three parts (compare with Fechner, 2009; Hutchinson, 2001b; Figure 46B, C, Table 11). It was the main muscle attached to the pubic shaft. M. puboischiofemoralis externus 1 probably originated from the medial surface of the distal half of the shaft, but my reconstruction should be treated as tentative because this area is not well preserved in available specimens. M. puboischiofemoralis externus 2 is reconstructed as originating on the lateral surface of the distal pubic shaft, with an indistinct scar marking its distal limit (compare with Fechner, 2009: Hutchinson & Gatesy, 2000, Hutchinson 2001a). The m. puboischiofemoralis externus 3 probably occupied the lateral ischial shaft distally between the sites of origin of the m. adductors, as seen in crocodiles (compare with Gadow, 1882; Romer, 1923b; Fechner, 2009). Some longitudinal striations close to distal end of the bone may indicate its presence. All parts of the muscle inserted on a dorsolateral ossification (‘anterolateral scar’ Griffin & Nesbitt, 2016; e.g., ZPAL Ab III/361, 405, and 411/4; Figure 51B) or rugose scar (e.g., ZPAL Ab III/457, 460/1, 1930,

2063, and 563/7) on the femoral head (compare with Gadow, 1882; Romer, 1923a; George & Berger, 1966; Hutchinson, 2001b; Fechner, 2009; Maidment & Barrett, 2011; Figure 48, Table 11). The m. puboischiofemoralis externus would have flexed and adducted the hip (see Schachner et al., 2011; Table 11).

M. ischiotrochantericus

The m. ischiotrochantericus is reconstructed here as originating from the dorsomedial surface of the distal ischium (compare with Romer, 1923b; Gangl et al., 2004; Fechner, 2009; Maidment & Barrett, 2011; Liparini & Schultz, 2013; Figure 46C, Table 11), marked by a proximodistally elongated rugose scar (ZPAL Ab III/3223, 925, and 404/7; Figure 34B). Its site of insertion is located on the dorsolateral trochanter (= 'greater trochanter' Griffin & Nesbitt, 2016), as indicated by a prominent scar in some specimens (Figures 48, 40B, Table 11). Proximally, this insertion lies next to that of the m. puboischiofemoralis externus as in modern archosaurs (Fechner, 2009; Hutchinson, 2001b; Maidment & Barrett, 2011). In *Silesaurus* material, the insertional area is visible in specimens ZPAL Ab III/361, 405, 457, 1930, 460/1, and 411/4. The m. ischiotrochantericus would have laterally rotated (supination) and retracted the hip (see Schachner et al., 2011; Table 11).

M. caudofemoralis brevis

In *Silesaurus*, a large ventrally concave surface on the anteroventral portion of the postacetabular ala (Figure 46B, Table 11) — the brevis fossa (Novas, 1996) — marks the origin of the m. caudofemoralis brevis. It is visible in ZPAL Ab III/361, 362, and 404/1,2 (compare with Romer, 1923b; Gauthier, 1986; Fechner, 2009; Schachner et al., 2011; Figure 45A). The fourth trochanter of *Silesaurus* bears an extensive scarring on its posteromedial surface, marking the insertion of the muscle (Figures 48B, 49A, Table 11). The insertional area is relatively wide in the middle but tapers proximally and distally. It is visible in ZPAL Ab III/361 and 1914 (compare with George & Berger, 1966; Gangl et al., 2004; Maidment & Barrett, 2011; Figure 50B). The m. caudofemoralis brevis would have extended and adducted the hip (see Schachner et al., 2011; Table 11).

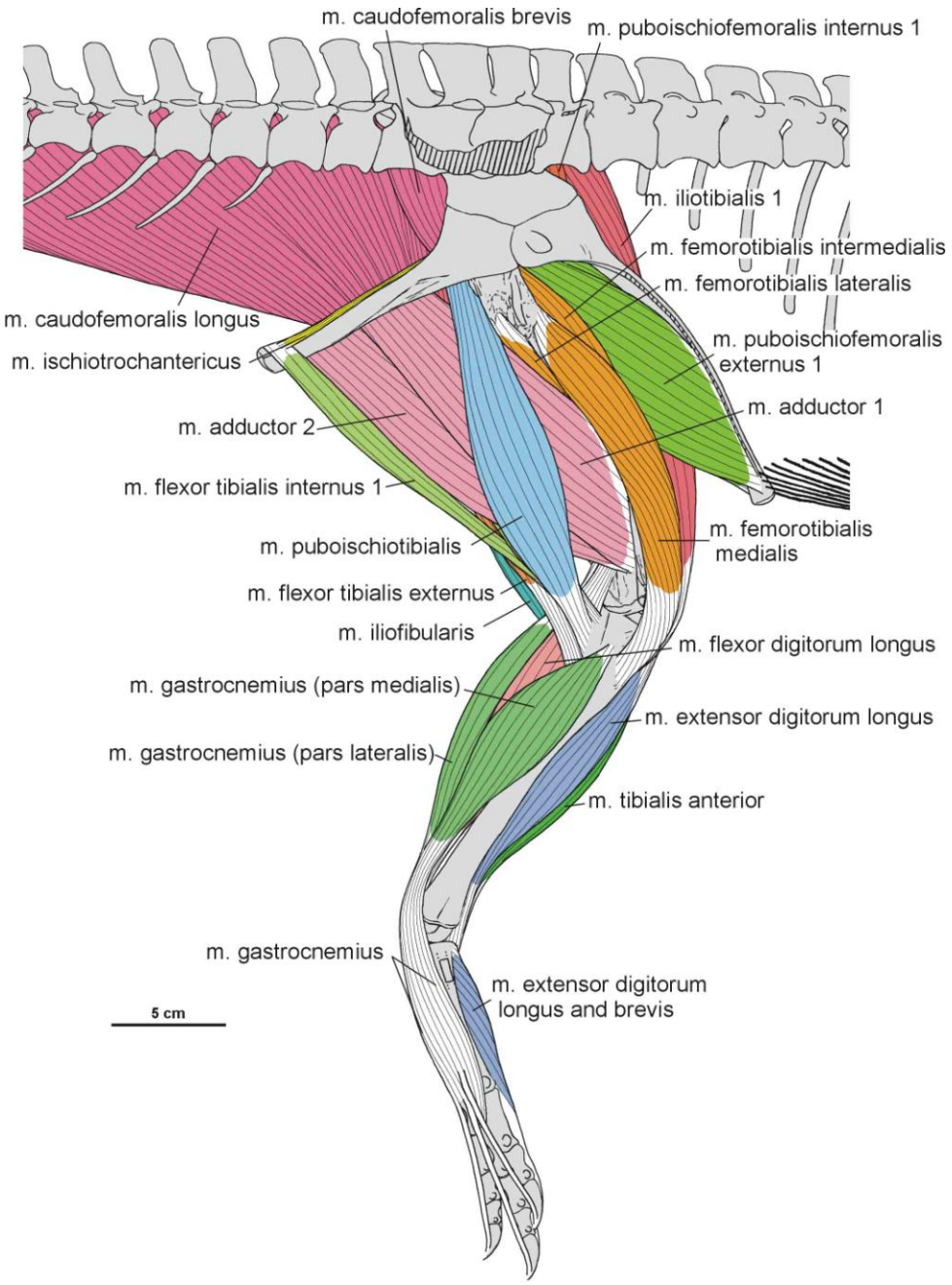

Figure 70. Muscle disposition on the hind limb of *Silesaurus opolensis* in medial view.

M. caudofemoralis longus

Silesaurus had a long, strong tail (Piechowski & Dzik, 2010) so it is likely that the origin of the m. caudofemoralis longus resembled that of crocodiles (compare with Romer, 1923a; Fechner, 2009; Schachner et al., 2011, contra Gatesy, 1990; Gangl et al., 2004; Maidment & Barrett, 2011), with an insertion on the femur marked by an oval concavity anteromedial to the fourth trochanter (Langer, 2003; Figure 49, Table 11). The insertion area can be seen in ZPAL Ab III/361, 1930, 1914, 2063, and 411/4 (compare with Fechner, 2009; Maidment & Barrett, 2011; Schachner et al., 2011; Figure 50A, Table 11). There may have been a second

insertion behind the knee (see Liparini & Schultz, 2013). The m. caudofemoralis longus would have extended and adducted the hip (see Schachner et al., 2011; Table 11).

Muscles to the pes

Muscles operating the pes in *Silesaurus* are limited mainly to three walking fingers.

Table 12. Summary of the pes musculature in *Silesaurus opolensis*, listing the names, origins, insertions, and actions. Muscle attachments in bold are those that have visible osteological correlates.

Muscle name	Origin	Insertion	Proposed function	Level of inference
M. gastrocnemius	Lateral femoral condyle (gastrocnemius pars lateralis); **medial aspect of the proximal tibia (gastrocnemius pars medialis);** posteromedial aspect of the femoral medial condyle? (gastrocnemius pars intermedius)	Ventral aspect of the metatarsals II-IV	Flexes the knee, and extends the ankle joint	I
M. tibialis anterior	**Anterolateral side of the proximal tibia**	**Lateral surfaces of the proximal metatarsals II – IV**	Flexes the ankle joint	I
M. popliteus	**Posteromedial side of the proximal tibia**	**Facing side of the fibula**	Rotates the fibula	I
M. interosseus cruris	**Posteromedial aspect of the distal tibia**	Facing side of the fibula	Flexes the ankle joint	II
M. pronator profundus	Posterior or posteromedial portion of the fibula and the lateral side of tibia	**Ventromedial basis of the proximal metatarsal II**	Flexes the ankle joint	II
M. fibularis longus and brevis	Lateral surface of the fibula	Ventral aspect of the calcaneum? (fibularis longus); ventral surface of the distal end of the metatarsal	Flexes the ankle joint	I

		V (fibularis brevis)		
M. extensor digitorum longus and brevis	**Cnemial crest of the tibia (extensor digitorum longus); dorsal aspect of the proximal tarsals? (extensor digitorum brevis)**	**Dorsal surface of the phalanges,** and the dorsal aspects of the unguals	Flexes the ankle joint, and extend the pedal digits	I, II
M. flexor digitorum longus and brevis	Femoral lateral condyle, and **posterolateral aspect of the proximal fibula (flexor digitorum longus);** plantar aponeurosis? (flexor digitorum brevis)	Ventral surface of the unguals of digits II – IV (flexor digitorum longus); basis of the phalanges of digits II – IV? (flexor digitorum brevis)	Extends the ankle joint, and flexes the digits	I, II
M. extensor hallucis longus	Probably lost			
M. flexor hallucis longus	Probably lost			

M. gastrocnemius

Based on the phylogenetic bracket, *Silesaurus* probably had at least two parts of the m. gastrocnemius (compare with Fechner, 2009; Schachner et al., 2011; Hutchinson, 2002). As reconstructed, its pars lateralis arose from a rugose area on the lateral femoral condyle, just distal to the insertion of the m. adductors (Figure 49A, Table 12), whereas the pars medialis originated from the medial aspect of the proximal tibia (Figure 52D, Table 12). The area displays distinct longitudinal scarring (ZPAL Ab III/361, 403, 414, 1245, 1246, and 2539; Figure 54A). It is difficult to judge whether *Silesaurus* had the avian pars intermedius. If it was present, it could have arisen from the posteromedial aspect of the femoral medial condyle between the m. adductors and the m. femorotibialis pars medialis. Langer (2003) after Romer, (1927b), suggested that the m. gastrocnemius originated from the distal inflection of the fourth trochanter of *Saturnalia*. However, this is not supported by the anatomy of extant archosaurs (Fechner, 2009; Schachner et al., 2011). In *Silesaurus*, all divisions of the m. gastrocnemius probably merged into common tendon that ran distal to the calcaneum and inserted along the ventral aspect of metatarsals II-IV (compare with Gadow, 1882; Hudson et

al., 1969; McGowan, 1979; Nickel et al., 2003; Gangl et al., 2004; Fechner, 2009; Schachner et al., 2011; Figure 57D, Table 12). The m. gastrocnemius would have flexed the knee and extended the ankle joint (see Schachner et al., 2011; Table 12).

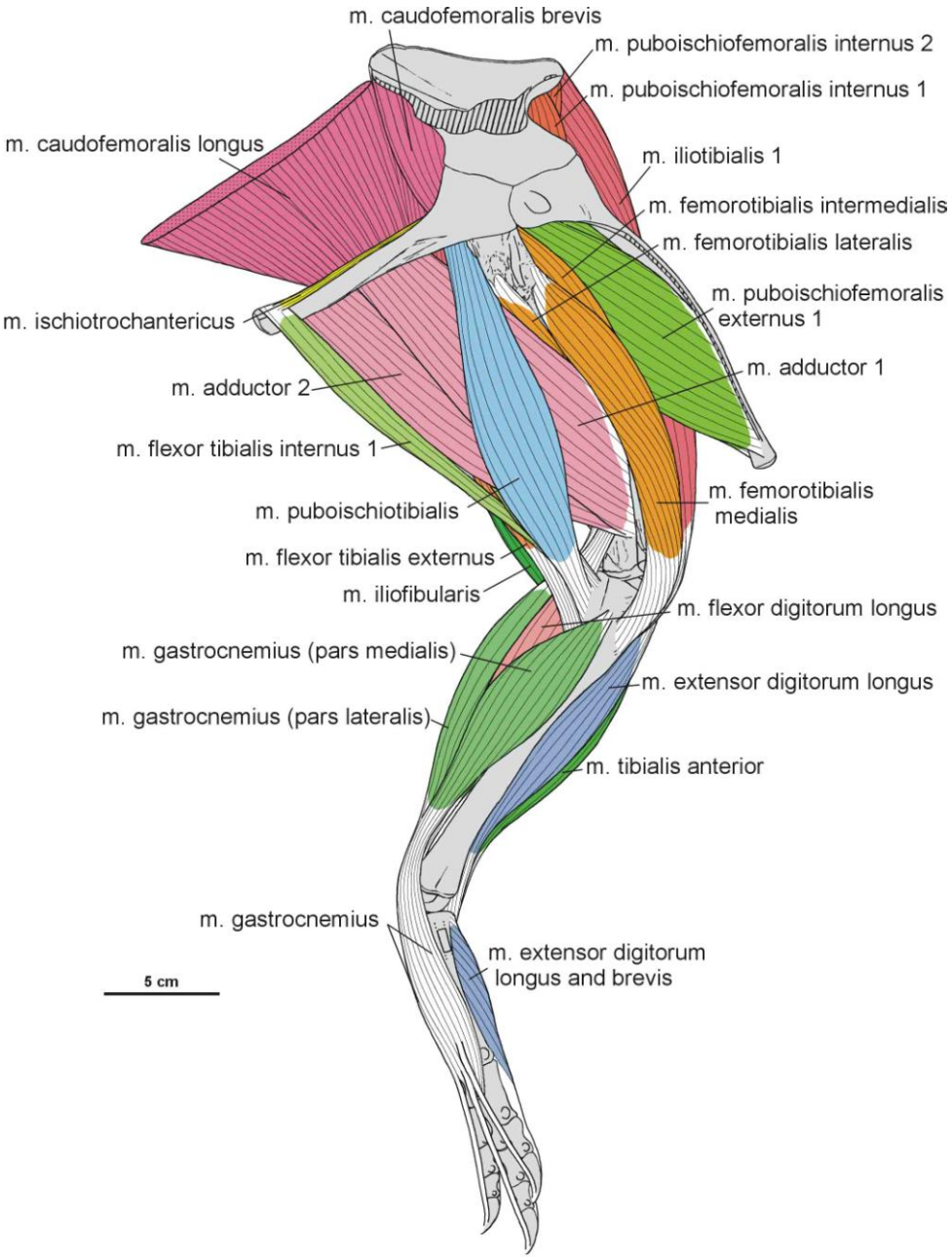

Figure 71. Muscle disposition on the hind limb of *Silesaurus opolensis* in lateral view. The axial skeleton is removed.

M. tibialis anterior

In *Silesaurus*, the m. tibialis anterior clearly originated from the lateral side of the tibial cnemial crest (Langer, 2003), as evidenced by scars for muscle attachment (compare with Dilkes, 2000; Fechner, 2009; Gadow, 1882; Schachner et al., 2011; ZPAL Ab III/361, 403, 414, 1930, and 2539; Figures 52A–C, 53A, Table 12). The presence of a second head in *Silesaurus* is uncertain, as there is no obvious attachment surface on the femur (compare with

Hudson et al., 1969; McGowan, 1979; Nickel et al., 2003; Gangl et al., 2004; Fechner, 2009; Schachner et al., 2011). Distinct muscle insertions are visible on the proximolateral surfaces of metatarsals II–IV in ZPAL Ab III/361 and 439/2 (compare with Hudson et al., 1969; McGowan, 1979; Dilkes, 2000; Nickel et al., 2003; Gangl et al., 2004; Fechner, 2009; Schachner et al., 2011; Figures 57B, C, 58E–G, Table 12). The insertion on metatarsal II is located further distally than others and is relatively short, whereas that on metatarsal III slightly more proximal and twice as long and that on metatarsal IV lies at the proximal end of the bone, and is short and wide. The m. tibialis anterior would have flexed the ankle joint (see Schachner et al., 2011; Table 12).

M. popliteus

The reconstruction of the m. popliteus in *Silesaurus* is unequivocal, with an attachment to the facing (interosseal) surfaces of the proximal fibula and tibia where both bones display clear longitudinal concavities (compare with Osawa, 1898; Romer, 1922; Hudson et al., 1969; McGowan, 1979; Nickel et al., 2003; Gangl et al., 2004; Fechner, 2009; Schachner et al., 2011; Figures 52A–C, 57C, Table 12). In *Silesaurus* material, the area of origin area is visible in specimens ZPAL Ab III/361, 403, 414, 1245, and 1930 (Figures 53A, 56B), and the insertion site is visible on ZPAL Ab III/361 and 416. The m. popliteus would have rotated the fibula (see Schachner et al., 2011; Table 12).

M. interosseus cruris

Reconstruction of the m. interosseus cruris in *Silesaurus* is unequivocal as the distal fibula is not reduced and therefore the muscle would have attached to the facing surfaces of the tibia and fibula (compare with Gadow, 1882; Kriegler, 1961; Vanden Berge & Zweers, 1993; Carrano & Hutchinson, 2002; Hutchinson & Garcia, 2002; Fechner, 2009; Figure 55C, Table 12). The tibia bears a distinct groove that may mark the attachment (ZPAL Ab III/ 361, 403/3, 411/2, 1225, 1930, and 1248; Figure 53A) whereas the distal fibula has a small ridge in that area (ZPAL Ab III/361). The m. interosseus cruris would have flexed the ankle joint (Table 12).

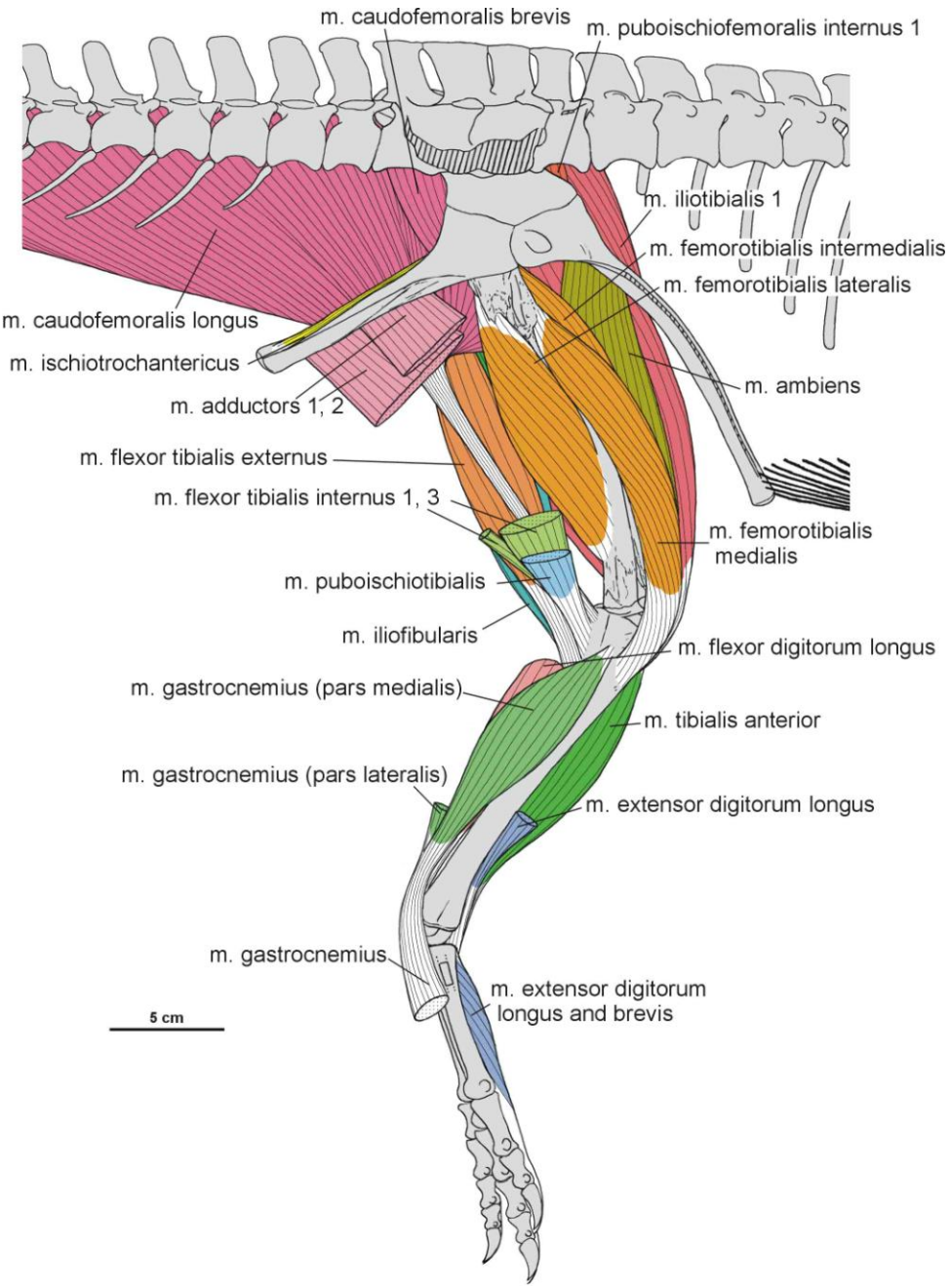

Figure 72. Muscle disposition on the hind limb of *Silesaurus opolensis* in medial view. Some muscles are cut off.

M. pronator profundus

The fibula of *Silesaurus* is not reduced, so I reconstructed the m. pronator profundus like that of a crocodile. It originated unequivocally on the posterior or posteromedial portion of the fibula and the lateral side of the tibia (compare with Gadow, 1882; Tarsitano, 1981; Hutchinson & Garcia, 2002; Fechner, 2009; Figures 52A, B, D, 55C, Table 12), and inserted on the ventromedial surface of the base of metatarsal II, due to reduction of metatarsal I (compare with Gadow, 1882; Kriegler, 1961; Fechner, 2009; Figure 57D, Table 12). The bone has a clearly visible scar in that area (Figure 58A). The m. pronator profundus would have flexed the ankle joint (Table 12).

M. fibularis longus and brevis

Silesaurus lacks any osteological correlates for the m. fibularis. However, it probably retained a fibular origin for both muscle heads because its fibula is not reduced and the tibia lacks cristae like those that serve for the m. fibularis longus attachment in birds (compare with Fechner, 2009; Schachner et al., 2011; Figure 55A, B, Table 12). The calcaneum of *Silesaurus* lacks a calcaneal tuber (Nesbitt, 2011; Figure 57A, Table 12), so the m. fibularis longus could have inserted elsewhere, as in birds. The m. fibularis brevis probably inserted on the distoventral surface of metatarsal V (compare with Hudson et al., 1969; McGowan, 1979; Nickel et al., 2003; Gangl et al., 2004; Fechner, 2009; Schachner et al., 2011; Figure 57D, Table 12). The m. fibularis would have flexed the ankle joint (see Schachner et al., 2011; Table 12).

M. extensor digitorum longus and brevis

Reconstruction of the m. extensor digitorum longus in *Silesaurus* was difficult. I correlated a shift in its origin from femur to tibia with the appearance of a cnemial crest (ZPAL Ab III/361, 2539, 1930, and 403/3,4). Thus the muscle may have originated from the anterior face of the cnemial crest as in birds (compare with Gadow, 1882; 1882; Kriegler, 1961; Hudson et al., 1969; McGowan, 1979; Tarsitano, 1981; Dilkes, 2000; Nickel et al., 2003; Gangl et al., 2004; Fechner, 2009; Schachner et al., 2011; Figures 52A–C, 53A, Table 12). One specimen (ZPAL AbIII/361/22) bears a distinct oval tuberosity distal to the origin. It could be interpreted as a distal extension of the origin but is probably some kind of pathology as it is absent in other specimens. The insertion site is equivocal due to the differences in extant archosaurs (see above). As *Silesaurus* was digitigrade with partially integrated metatarsals, it may have approached the avian in which the m. extensor digitorum longus and brevis could already be fused (Hutchinson & Garcia, 2002), with a single insertion on the dorsal surface of the phalanges and on the proximodorsal aspects of the unguals (compare with Gadow, 1882; Hudson et al., 1969; McGowan, 1979; Tarsitano, 1981; Vanden Berge & Zweers, 1993; Carrano & Hutchinson, 2002; Nickel et al., 2003; Fechner, 2009; Schachner et al., 2011; Figure 57B, C, Table 12) as seen in ZPAL Ab III/361. Both the m. extensor digitorum longus and brevis would have flexed the ankle joint and extended the pedal digits (see Schachner et al., 2011; Table 12).

M. flexor digitorum longus and brevis

In *Silesaurus* the origin of the m. flexor digitorum longus is marked by a clear tear-shaped region on the femoral lateral condyle, distal to the origin of the m. femorotibialis lateralis (compare with Dilkes, 2000; Fechner, 2009; Schachner et al., 2011; Figures 48B, 49A, Table 12). A slightly rugose surface on the posterolateral aspect of the proximal fibula is interpreted as an origin site of the second head (compare with Hudson et al., 1969; McGowan, 1979; Nickel et al., 2003; Gangl et al., 2004; Fechner, 2009; Schachner et al., 2011; Figures 55A, 56A, Table 12). The muscle would have been inserted on the ventral surface of the unguals of digits II–IV (compare with Hudson et al., 1969; Kriegler, 1961; McGowan, 1979; Tarsitano, 1981; Dilkes, 2000; Nickel et al., 2003; Gangl et al., 2004; Fechner, 2009; Schachner et al., 2011; Figure 57D, Table 12).

The m. flexor digitorum brevis not reconstructed for *Silesaurus* as its presence is uncertain, given its absence in birds (see Gadow, 1882; Kriegler, 1961; Vanden Berge & Zweers, 1993; Dilkes, 2000; Fechner, 2009). If present it would have originated from the plantar aponeurosis and inserted on the bases of the phalanges of digits II–IV. Both the m. flexor digitorum longus and brevis would have extended the ankle joint and flexed the digits (see Schachner et al., 2011; Table 12).

M. extensor hallucis longus

In *Silesaurus*, in which is observed a reduction of digit I, the m. extensor hallucis longus was probably lost together as in some modern ratites (McGowan, 1979; compare with Gadow, 1882; McGowan, 1979; Carrano & Hutchinson, 2002; Nickel et al., 2003; Fechner, 2009; Schachner et al., 2011; Table 12).

M. flexor hallucis longus

The muscle was probably lost in *Silesaurus* together with digit I (compare with Carrano & Hutchinson, 2002; Fechner, 2009; Schachner et al., 2011; Table 12).

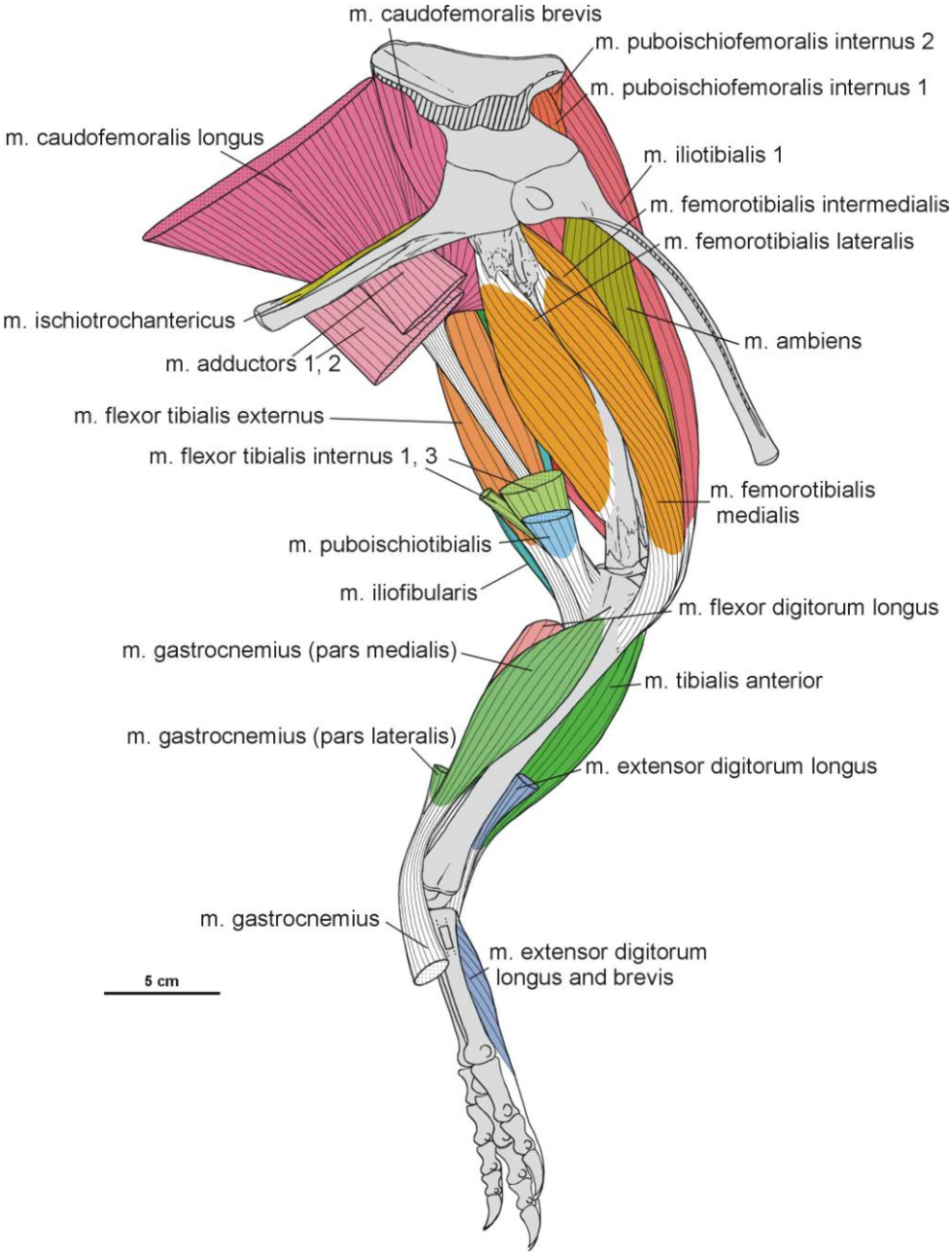

Figure 73. Muscle disposition on the hind limb of *Silesaurus opolensis* in medial view. Some muscles and the axial skeleton is removed.

Ligaments

In this section I describe ligaments that left a trace on the appendicular skeleton of *Silesaurus*. This description is far from exhaustive as I focused only on ligament attachments that could be confused with muscle attachments. At least two ligaments left distinct scars on the anterior and the posterior aspects of the distalmost ulna (Figures 29, 30A). Their surface is more rugose than muscle scars preserved in the same specimens.

The pelvis of lepidosaurs and crocodiles is associated with series of ligaments that act as structural supports and attachment sites for the pelvic muscles (Schachner et al., 2011). Hutchinson (2001a) argued that the primary semicircular ilio- and ischiopubic ligaments of birds are probably homologous to those of extant crocodilians.

Ligamentum iliopubicum

In the above taxa, this ligament or its homologues (Hutchinson, 2001a) generally runs from the preacetabular ilium to the pubic tubercle, and serves as a site of origin for some of the hypaxial musculature (Schachner et al., 2011). The attachment areas of the iliopubic ligament in *Silesaurus* resemble those in *Poposaurus* (Schachner et al., 2011). The ligament arose from the ventral surface of the preacetabular process of the ilium (Figures 45C, 46C), as indicated by a longitudinal groove just medial to the origin of the m. puboischiofemoralis internus 2. The insertion is clearly visible as a rugose area on the medial side of the iliopubic articulation (Figures 33A, 45B, 46). The attachments of the iliopubic ligament are visible in ZPAL Ab III/2517, 404/1, 2, 5, and 462.

Ligamentum puboischiadicum

In extant archosaurs, the puboischiadic ligament originates on the caudoproximal aspect of the pubis and inserts on the proximal ischium (Hutchinson, 2001a; Schachner et al., 2011). Distinct striations on ventral pubis of *Silesaurus* (ZPAL Ab III/404/5) may represent an origin site for this ligament (Figures 33C, 46C), whereas the ischial insertion may have been between the origins of the m. puboischiotibialis and the m. adductor 1, at the ventral margin of the bone (Figure 46B).

Ligamentum ilioischiadicum

The ilioischiadic membrane of Neornithes and the dense fascia in crocodiles are probably homologues of the ilioischiadic ligament of lepidosaurs (Hutchinson, 2001a; Schachner et al., 2011). I follow the reconstruction of *Poposaurus* (Schachner et al., 2011), where the ligament was reconstructing as arising from a distal pit on the ventral surface of the postacetabular process. The ilium of *Silesaurus* has a clear rugosity in the same position in ZPAL Ab III/362 and 404/1, 2 (Figure 46C). As in *Poposaurus*, the ischial attachment site is unclear.

Ligamentum capitis femoris

In crocodiles, this ligament has two crura that originate from the pelvis and merge into a single attachment on the femur. The caudal crus originates from the acetabular part of the pubic peduncle of the ischium, and the condition in *Silesaurus* was probably similar as the ischium bears a rugose attachment area (Figure 46B). The rostral crus in crocodiles is a

continuation of the deep meniscus (Tsai & Holliday, 2015). The two crura join and insert on the surface of the posteromedial tuber (Figure 49A), which is variably developed in *Silesaurus* (Piechowski et al., 2014). The attachment site of the ligamentum capitis femoris is visible in ZPAL Ab III/361, 405, and 411/4 (Figure 50B).

Ligamentum iliofemorale

In crocodiles, the iliofemoral ligament originates dorsally on the acetabular labrum of the acetabular crest (Tsai & Holliday, 2015). The area is greatly expanded in *Silesaurus*, forming a distinct supra-acetabular crest that creates a roof for the acetabulum and bears clear rugosities along its margin (Figures 44, 46B). The insertion site of the iliofemoral ligament in *Silesaurus* is identified as a large, rounded area on the anteromedial aspect of the femoral head limited distally by a semilunate scar (Figures 48A, 49). The attachments of the iliofemoral ligament are visible in ZPAL Ab III/361, 362, 404/2, and 407/6 (Figure 50A).

Ligamentum collaterale tibiale

The ligament covered the medial side of the knee joint and connected the distal femur with proximal tibia (Haines, 1942). *Silesaurus* has a weak scar for this ligament on the medial surface of the medial femoral condyle (Figure 49B) and the proximal head of the tibia bears a clear irregular scar posteromedially (Figure 52D). The attachments of the ligamentum collateral tibiale are visible in ZPAL Ab III/361, 403, 416, and 2539 (Figure 54A).

Ligamentum collaterale fibulare

This ligament connects the distal femur with the proximal fibula, on the lateral side of the knee joint (Haines, 1942). *Silesaurus* bears large scars for this ligament. The lateral condyle of femur bears semitriangular rugose area on its lateral surface (Figure 48A). It is visible on ZPAL AbIII/361, 363, 1263, 1914, and 403/5 (Figure 51B). The insertion covers most of the lateral surface of the proximal fibular head (Figure 55A,B), as evidenced by extensive but irregular scarring, especially visible on ZPAL AbIII/361/24 (Figure 56A).

Ligamentum tibio-fibulare

This ligament connects the tibia and fibula anteriorly, below the knee joint in crocodiles (Haines, 1942). Intensive scarring on the anterior surface of the proximal fibula of *Silesaurus* marks the presence of this ligament (Figure 55A, B), as may further intensive scarring on the

medial concavity of the fibular head and on the fibular articular facet on the lateral aspect of the tibia (Figures 52A–C, 55C). The attachments of the ligamentum tibio-fibulare are visible in ZPAL Ab III/361 and 416 (Figures 53A, 56).

Ligamentum mediale tibialo-astragalare

This is one of the ligaments connecting the tibia and astragalus of crocodiles (Brinkman, 1980). It limits rotation between the two bones (Brinkman, 1980). In *Silesaurus* (ZPAL Ab III/361, 403/1, 411/2, and 1247: Figure 54A), the distal tibia bears a tongue-shaped scar on its medial aspect (Figure 52D). The ligament probably inserted on the medial aspect of the astragalus (Figure 57A) that bears a distinct semihorizontal groove in that area.

Comparison with extant archosaurs

The derived condition of extant crocodiles and birds makes interpretation of primitive archosaurian musculature difficult. *Silesaurus* is one of the earliest members of the dinosaur-line archosaurs. Given its geological age and phylogenetic position, it may help us to understand the polarity of archosaurian characters. The pectoral musculature of *Silesaurus* (Figures 24 and 35–41) was obviously more crocodile-like than bird-like because birds have highly modified forelimbs for flight. The scapular blade of *Silesaurus* and crocodiles has a machete-like shape (Figures 23, 24A, C), whereas in birds it is narrow and sabre-like. A prominent acromial process contributes to a large area for attachment of the supracoracoideus, which protracts, retracts, and abducts the humerus in crocodiles and thus also *Silesaurus* (Figures 23, 24A, C and 35–41). Birds reduced this process in association with changes in the musculature. Birds and crocodiles convergently expanded the coracoid toward the sternum. Triassic archosaurs including *Silesaurus* restrict this part of the coracoid to a small tuber (Figs. 23; 24). The complex architecture of this tuber in *Silesaurus* probably reflects attachments of various muscles (m. costocoracoideus, m. triceps, and m. coracobrachialis) grouped on a small area (Figures 24 and 35–41), and may represent the plesiomorphic archosaurian condition. The anatomy of the forelimb is simplified in *Silesaurus* by comparison to *Euparkeria* and *Osmolskina*, so the typical archosaurian condition should not be expected in its brachial musculature.

Intermuscular lines on the femur of *Silesaurus* indicate that the m. femorotibialis had three distinct parts, as in birds, although crocodiles have only two (Figures 48, 49, and 67–72). It remains unknown whether the ancestor of the dinosaur-bird clade gained the third part or the

common ancestors of archosaurs already had it. In the latter scenario crocodiles secondarily lost the third part. As in crocodiles, osteological correlates are present for only two heads of the m. puboischiofemoralis internus in *Silesaurus* (Figures 46B, C and 67–72). The insertion sites for this muscle on the femur of *Silesaurus* are similar to those in crocodiles. If this identification is correct, the muscle originated from the well-developed anterior process of the ilium, which would approach the bird condition (Hutchinson & Gatesy, 2000). Because more derived archosaurs on the lineage to birds expanded the process further anteriorly, this change would be homologous with the condition found in Aves. The obturator plate is reduced in *Silesaurus*, so the m. puboischiotibialis was also reduced in size (Figures 46B, C, 52A, B, D and 69–72; it is absent in birds). The ischium of *Silesaurus* has a scar in the same place as the crocodilian pit for the m. flexor tibialis internus 3, suggesting this is the primitive condition (Figures 46B, C and 67–72). The ischium of *Silesaurus* has more posterior orientation than that of crocodiles but the position of the m. adductors origin on that bone is homologous (Figures 46B, C and 67–72). The development of the cnemial crest is probably correlated with the more proximal position of origins of the m. tibialis anterior and the m. extensor digitorum longus (Figures 52A–C and 67–72) but insertions of the m. tibialis anterior are primitive (crocodilian-like) due to the separated metatarsals. Insertions of the m. extensor digitorum longus are difficult to determine (Figure 57B, C). The well-developed distal part of fibula and the scaring on the distal tibia and fibula suggest a primitive condition for the m. interosseus cruris (Figure 52A–C), and also for the m. pronator profundus, the m. fibularis longus and brevis, and the m. popliteus (Hutchinson, 2002; Figures 52, 55, and 66–69). The femur of *Silesaurus* retained a tear-shaped scar for the m. flexor digitorum longus (Figures 48B, 49A), while in birds the origin had shifted to the tibia.

Chapter 9. Locomotion of *Silesaurus opolensis*[9]

The posture of *Silesaurus* was discussed for the first time by Dzik (2003). Subsequently, additional information about the *Silesaurus* posture has been offered i.a. by Langer (2003), Dzik & Sulej (2007), Langer et al. (2007), Fechner (2009), Nesbitt (2011), Kubo & Kubo (2012), Langer et al. (2013), Piechowski et al. (2014), Nesbitt et al. (2017), Piechowski & Tałanda (2020). The atypical limb proportions of *Silesaurus* have elicited discussion among researchers about locomotion of this animal. Dzik (2003) reconstructed *Silesaurus* in a quadrupedal stance, and Fechner (2009), as well as Kubo & Kubo (2012) concluded that *Silesaurus* was a slow, obligate quadruped based on its body proportions. Later, Piechowski & Dzik (2010) also agreed that *Silesaurus* evolved toward quadrupedality (Figure 74). However, they suggested that the gracile forelimbs and large counterbalancing tail might indicate an ability to run bipedally at speed (Figure 75). Otero et al. (2019) pointed out that relative development of the tail and neck plays a more important role in supporting bipedal locomotion than influence of hindlimb/forelimb lengths.

The hind limb to trunk length ratio of *Silesaurus* is 0.79, which is similar to obligate quadrupeds (Remes, 2008). The antebrachium is similar in length to the humerus in *Silesaurus* (1.1), a very high value compared to that of basal dinosaurs and *Euparkeria* in which the antebrachium ranges from 0.62 to 0.84 of humeral length (Remes, 2008). It means that elongation of the forelimb of *Silesaurus* was achieved mainly by prolonging the antebrachium. In sum, short hindlimbs (relative to the trunk) and elongated forelimbs supports previous hypotheses that *Silesaurus* was an obligate quadruped (Figure 74).

It is interesting in this context that I found many similarities between the forelimbs of *Silesaurus* and those of non-neosauropod non-mamenchisaurid sauropods like *Patagosaurus* and *Cetiosaurus*. These are: 1) weakly expanded distal end of scapula; 2) long, slender and straight scapular blade; 3) convex anterior (dorsal) margin of scapula; 4) deep scapular head occupied by large oval fossa; 5) slightly expanded humeral heads relative to the shaft; 6) subtriangular proximal half of humerus in anterior view; 7) indistinct torsion of humeral heads; 8) reduced deltopectoral crest; 9) distal humeral head narrower than the proximal one; 10) relatively slender radius and ulna; 11) reduced olecranon process.

[9] Part of this chapter was published in:
Piechowski, R. & Tałanda. M. 2020. The locomotor musculature and posture of the early dinosauriform *Silesaurus opolensis* provides a new look into the evolution of Dinosauromorpha. *Journal of Anatomy* DOI: 10.1111/joa.13155

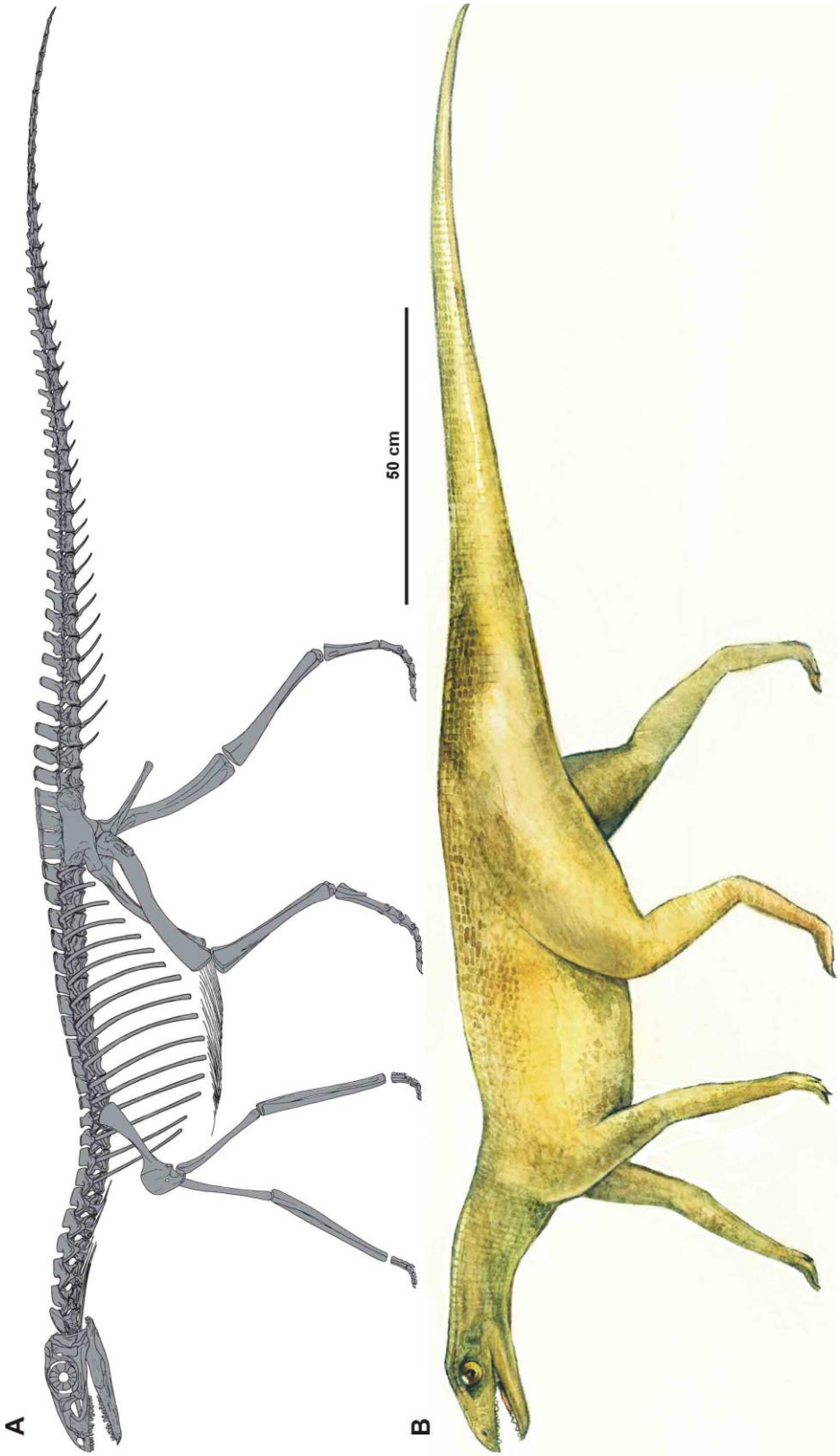

Figure 74. Restoration of *Silesaurus opolensis* in a quadrupedal pose. **A**, skeletal reconstruction in lateral view; **B**, body reconstruction in lateral view (drawing by Małgorzata Czaja).

The obvious difference between *Silesaurus* and early sauropods is the robustness of the forelimb elements, which is a consequence of size and weight in these animals. The common characters of the scapula are not restricted to *Silesaurus* and sauropods. They rather represent the primitive condition and function. However, the anatomy of the humerus, ulna, and radius is derived in early sauropods compared to prosauropods. The same situation is with *Silesaurus* compared to *Teleocrater*, *Osmolskina* or *Euparkeria*. Reduction of deltopectoral crest marks a decreasing role of m. pectoralis and m. deltoideus clavicularis (Figures 27D and 35–41). Remes (2008) correlates this with the vertical orientation of the humerus in sauropods. The same may apply to *Silesaurus* (Figures 23, 76), which also had reduced humeral protractors. Protraction of humerus was limited by the position of the coracoids (Remes, 2008). The tightly spaced distal condyles of the humerus indicate reduced rotation capabilities in this joint (Remes, 2008; Figures 23, 27). The olecranon process works as a lever for m. triceps brachii. Reduction of this structure lead to less effective extension movements of the forelimb in *Silesaurus* and early sauropods (Figures 23, 76). It also indicates columnar alignment of the elbow joint (Wilson, 2005). Furthermore, these reptiles reduced rotation of humerus, while the ulna is rotated laterally and the radius anteriorly, modifications that enabled effective and permanent pronation of the manus.

In conclusion, *Silesaurus* and early sauropods achieved a fully quadrupedal stance through analogous joint and muscle modifications. However, they faced the problem of limited forelimb pronation (Bonnan & Yates, 2007). The erect humerus is blocked anteriorly by the coracoidal part of the glenoid (Remes, 2008). The forelimb can make only short steps, prohibiting fast locomotion (Remes, 2008). Large herbivores like sauropods were slow animals. In the case of *Silesaurus*, Langer et al. (2013) concluded that the simple rounded proximal articular surfaces of the ulna and radius enabled pronation (Figure 23). Thus, the unusually elongated antebrachium of *Silesaurus* could have been an adaptation to allow greater range of protraction, extending the step length and improving locomotion speed.

In contrast, the hind limb seems to have been capable of greater speed. Fechner (2009) and Tsai et al. (2018) pointed out several features indicating erect hindlimb posture in *Silesaurus*. It lacks only a perforated acetabulum (Figure 46B, C). However, Tsai et al. (2018) concluded that *Silesaurus* had a greater range of hindlimb abduction and axial rotation than was inferred by previous studies. They argued that the femoral epiphysis articulated dorsally with the supraacetabular labrum during parasagittal limb movement. This was based on an incorrect orientation (Dzik, 2003) of the pelvis. The acetabular wall was inclined 30° dorsoventral to the sagittal plane, as in the ilium as a whole. The supra-acetabular crest of *Silesaurus* was

lateroventrally, not laterally, oriented (Figures 43B–D, 47). As a consequence, it could not articulate with a dorsomedially oriented femoral head. Instead, it probably restricted femoral abduction and rotation (Bates & Schachner, 2012; Hutchinson & Gatesy, 2000; Tsai et al., 2018). The femoral epiphysis entered the deep acetabulum and articulated with the ilium at the junction of the supra-acetabular crest and the acetabular wall. This means that *Silesaurus* obtained a pillar-erect hindlimb posture similar to that of some pseudosuchians (Benton & Clark, 1988; Bates & Schachner, 2012; Figure 47A). This is a novel insight as ornithodirans were considered to have only buttress-erect limb posture (Sullivan, 2015).

Reduced muscular abduction-adduction of the femur is congruent with my reconstruction of *Silesaurus*. The iliofemoralis (abductor) is altered in comparison with more primitive archosaurs. Its origin (Figure 46B, C) is not discernable on the iliac blade and the bone is very thin and delicate in that area. The insertion is marked by well-developed anterior trochanter and trochanteric shelf (Figures 48, 49), but this insertion is located much further proximally than in crocodiles and Lagerpetidae (Fechner, 2009; Figure 77), closer to bird condition (Hutchinson & Garcia, 2002). This might reflect a change of activity of this muscle related with increasing bipedal abilities. This is reflected in shift of the muscle activity from swing phase to stance phase abduction and gave rise to an iliofemoralis capable of medial femoral rotation (Hutchinson & Gatesy, 2000). The reduced obturator plate and delicate ischium (Figure 46B, C) without distinct scarring, indicate a decreased role for the hip adductors compared to non-dinosauriform archosaurs. This suggests that adductor-controlled postural support was no longer required by *Silesaurus*. In contrast to the adductors, the muscles involved in flexing and extending the knee have large tuberosities or scars marking their attachment areas (mm. iliotibialis, ambiens, femorotibialis, iliofibularis, flexor tibialis internus and externus; Figures 46, 48, 49, 52, 55A, B, Table 11). *Silesaurus* had narrow ischia connected through most of their length (Figure 43A, D, E), resulting in a decreased interacetabular distance, a condition necessary to reduce the lever arm of the ground reaction force, an adaptation observed in obligate bipedal dinosaurs (Fechner, 2009).

To sum up, *Silesaurus* had simplified, fully erect forelimbs capable of parasagittal movements and permanent pronation of the manus. This position resembles that of early sauropods, suggesting that both groups used the forelimb in a similar manner, mainly to support the anterior part of the body during slow quadrupedal locomotion (Figure 76). However, *Silesaurus* had a shorter humerus and a more elongated antebrachium (Figure 23), probably to increase the range of pronation. As a consequence, *Silesaurus* could make longer steps and gain greater speed than early sauropods.

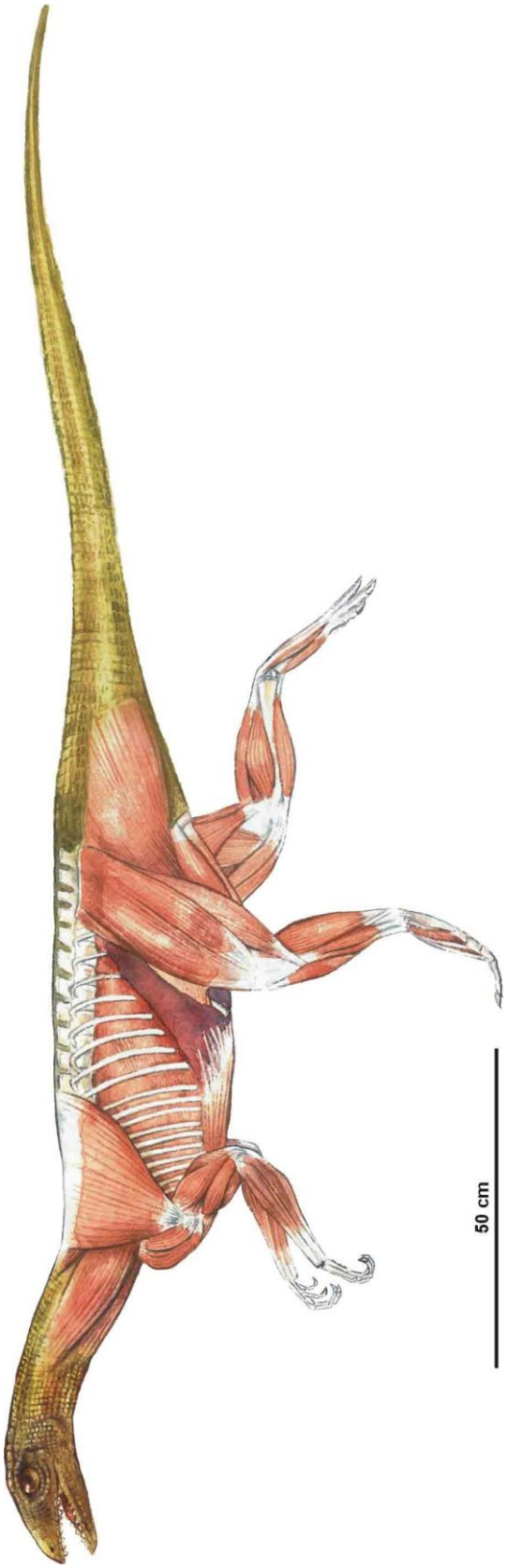

Figure 75. Restoration of muscles in *Silesaurus opolensis* in a facultative bipedal running pose. Note that muscles are slightly separated from each other for greater visibility. (drawing by Małgorzata Czaja).

The hindlimbs of *Silesaurus* were also fully erect but in contrast to sauropods and other dinosaurs, the acetabulum was directed ventrolaterally, not laterally (Figures 43B–D, 47). This pillar-erected hip joint was previously known only in some pseudosuchians. Reduction of adductors, modification of abductor m. iliofemoralis, strong flexors and extensors of the knee, supraacetabular crest limiting femoral abduction and rotation, mesaxonic pes – all these features suggest a narrow parasagittal gait. Some modern lizards are able to run bipedally to avoid danger (Persons & Curie, 2017). Fossil evidence suggests that lagerpetids could also run bipedally at higher speeds (Fechner, 2009). *Silesaurus* has a much more efficient locomotor apparatus than these two groups because its joints were aligned closer to the vector of the ground reaction force, therefore less muscle energy was involved in limb posture control. This locomotor morphology could be explained as an adaptation to greater body mass (Fechner, 2009), as some bones belonged to individuals of at least three meters in length (personal observation). Alternatively, it could be related to a greater capacity for facultative bipedal running (Piechowski & Dzik, 2010; Figure 75), as this animal had no clear adaptations to avoid predators other than running. Of course, both hypotheses are not mutually exclusive.

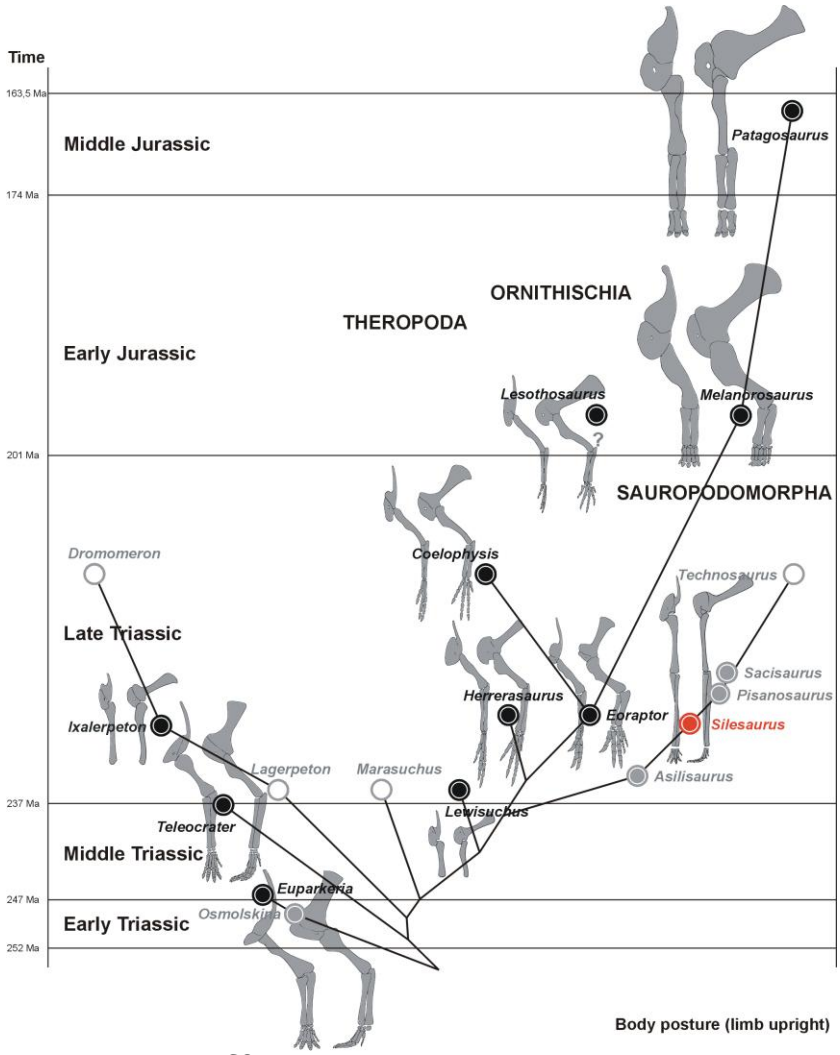

Figure 76. Evolution of forelimb skeleton and its posture in selected early dinosaurs and their predecessors. Black dots represent illustrated taxa. Grey dots are unillustrated taxa having some forelimb bones known. White dots are unillustrated taxa with no forelimb material known. *Silesaurus* has a red dot. The topology of the tree follows Müller et al. (2018) with the addition of *Osmolskina*, *Melanorosaurus*, and *Patagosaurus*. Closely related taxa from different time horizons are illustrated as one lineage for clarity of the figure.

My reconstruction of locomotion and posture of *Silesaurus* is congruent with the ichnological record. Skeletal remains of a silesaurid co-occur with tracks left by this medium-sized quadrupedal animal at the Woźniki locality (Sulej et al. 2011). The manus imprints are small, digitigrade, and consist of three to four digits. They are oriented parallel to the walk direction and close to the trackway axis. This suggests that the track-maker had fully erected forelimbs that acted in a parasagittal plane just like the forelimbs of *Silesaurus* (Figures 23, 31). Similar trace fossils widely occurring in the Mid-Late Triassic strata match the skeletal reconstructions of the Silesauridae anatomically and stratigraphically (Olsen & Baird, 1986; Haubold & Klein, 2000; Safran & Rainforth, 2004; Porchetti et al., 2008). The pes is mesaxonic, tulip-shaped, and has three functional digits as in *Silesaurus* (Porchetti et al. 2008). The hallux is not preserved even in very deep tracks (Olsen & Baird, 1986). The phalangeal formula reconstructed by Olsen & Baird (1986) matches that of *Silesaurus*. The gait is narrow and the pedes are parasagittaly oriented. Again, this reflects my reconstruction of *Silesaurus*. The trackway YPM 9962 named Atreipus milfordensis by Olsen & Baird, (1986) shows an ability for facultative bipedality.

Evolution of limb postures

The common ancestors of pseudosuchians and dinosaurs had already semi-erect limbs, which could be pulled beneath the body, resulting in a narrower gait. However, they had a primitive "crocodile-normal" ankle joint and adductor-based postural support (Hutchinson, 2006; Fechner, 2009). Most authors agree that *Euparkeria* and *Osmolskina* are anatomically similar to the ancestral form (Figures 76, 78). A large, shallow acetabulum permitted a wide range of femoral abduction and rotation. They were quadrupedal animals with poor, if any, bipedal capabilities. *Euparkeria* had a pectoral girdle that was as wide as it was high, with a vertically oriented scapular blade and a horizontal coracoid. As a result, the humerus was oriented laterally, generating a sprawling posture (Remes, 2008). The well developed deltopectoral crest in *Euparkeria* and *Osmolskina* (Borsuk-Białynicka & Sennikow, 2009) indicates strong humeral retractors (Remes, 2008), whereas the olecranon process (triceps brachii insertion) was moderately developed. These reptiles probably still used a sprawled forelimb in propulsion.

These primitive features were largely inherited by *Teleocrater* from the earliest Carnian (Nesbitt et al., 2017; Figures 76, 78). Its larger size is probably an independent advancement as lagerpetids *Marasuchus* and, most importantly, Early–Mid Triassic dinosauromorph tracks

are much smaller (Fechner, 2009; Brusatte et al., 2011; Niedźwiedzki et al., 2013). The dinosauromorph lineage achieved digitigrady (Hutchinson, 2006) early and reorganized their digits, as shown by Early and Mid Triassic tracks (Brusatte et al., 2011; Niedźwiedzki et al., 2013). An advanced mesotarsal joint and a more parasagittal gait probably evolved during that time.

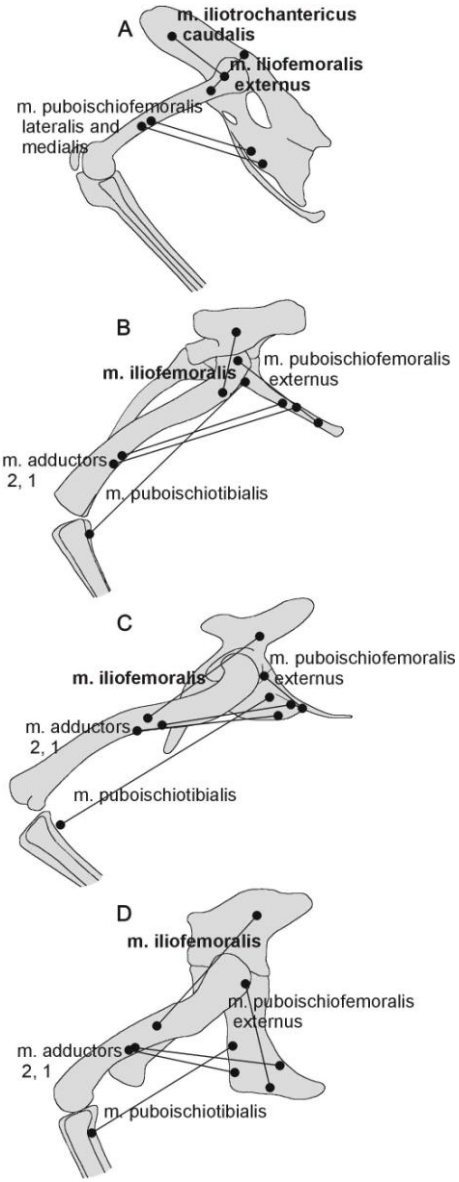

Figure 77. Comparison of the adductor and abductor musculature of extant and extinct archosaurs. **A**, *Gallus* (based on Fechner 2009); **B**, *Silesaurus* (this study); **C**, *Lagerpeton* (based on Fechner 2009); **D**, *Alligator* (based on Fechner 2009).

Lagerpetids (Figure 78) possess a well developed anterior process of the ilium and more cursorial hindlimb proportions (Sereno & Arcucci, 1994; Fechner, 2009; Hutchinson, 2006). They were predominantly quadrupedal but were capable of bipedal running at higher speeds (Fechner, 2009). Despite these advancements, they retain a large obturator plate, a large, shallow acetabulum, and an asymmetric pes. These features imply a high degree of hindlimb

rotation and abduction, and a primitive adductor-controlled postural support (Fechner, 2009) resulting in a semierect posture. Until recently, our knowledge about their forelimb was restricted only to manus imprints. Based on those, it is apparent that the forelimb had a narrower gait than the hindlimb; it moved parasagittally, and produced relatively short steps (Fechner, 2009). Because of the latter, it was inferred that lagerpetids had short forelimbs (Fechner, 2009; Brusatte et al., 2011), but recently the humerus and scapula of a late Carnian lagerpetid were discovered (Cabreira et al., 2016; Müller et al., 2018). They show surprising similarities to the corresponding elements of the early dinosauriforms *Asilisaurus* (Nesbitt et al., 2010), *Lewisuchus* (Remes, 2008), and *Silesaurus* (Dzik, 2003) in having a long, slender scapular blade, low humeral deltopectoral crest, a weakly expanded distal humeral head, and low torsion of the humeral shaft. This suggests that the forelimb locomotor characteristics of *Silesaurus* and their resemblance to those of early sauropods were not restricted to this taxon but represent the primitive condition of all dinosauromorphs. This group fully erected their forelimbs resulting in a narrow and parasagittal gait (Figure 76). The forelimbs predominantly supported the body while propulsion was generated mainly by the hindlimbs. If my hypothesis is correct, than the short step of lagerpetids was a result of restricted humeral pronation, not short forelimbs. I predict that forelimb proportions were similar in lagerpetids, silesaurids and *Lewisuchus* (Figure 76).

Fully erect hindlimbs evolved later. *Marasuchus* from the early Carnian represents this transition (Sereno & Arcucci, 1994; Figure 78). The obturator plate is smaller, the acetabulum is deeper with a more developed supraacetabular crest, and the pes is more symmetrical than that of lagerpetids. These features implies a lesser role for the adductors in limb posture, and more erect hindlimbs that moved almost parasagittally with only three functional digits.

The process was complete when a deep acetabulum fully encompassed the femoral head. This resulted in the pillar-erected hindlimb of *Silesaurus*. This pseudosuchian-like construction was possible because the femoral head was not rotated medially, whereas the acetabulum and supraacetabular crest were oriented ventrolaterally, not laterally as in previous reconstructions. It is unclear when this orientation of the acetabulum appeared in the evolution of Dinosauromorpha. There are two possibilities. The condition could be an autapomorphy of *Silesaurus*, or a pillar-erected hindlimb was a necessary step before the femoral head rotated medially and the acetabulum became open in the buttress-erected limb posture of dinosaurs. If the second hypothesis is correct then condition in *Silesaurus* represents a transition toward the improved locomotion of typical dinosaurs.

Primitive dinosaurs still retain a closed acetabulum but their femoral head is rotated medially. The ilium is anteroposteriorly short in *Herrerasaurus* and moderately elongated in *Saturnalia*. More advanced dinosaurs have a fully opened acetabulum and an anteroposteriorly expanded ilium for an enlarged iliofemoralis, a key muscle in an abductor-controlled limb. There is growing evidence that this process of pelvic modification occurred in parallel in different dinosaur lineages (Tsai et al., 2018).

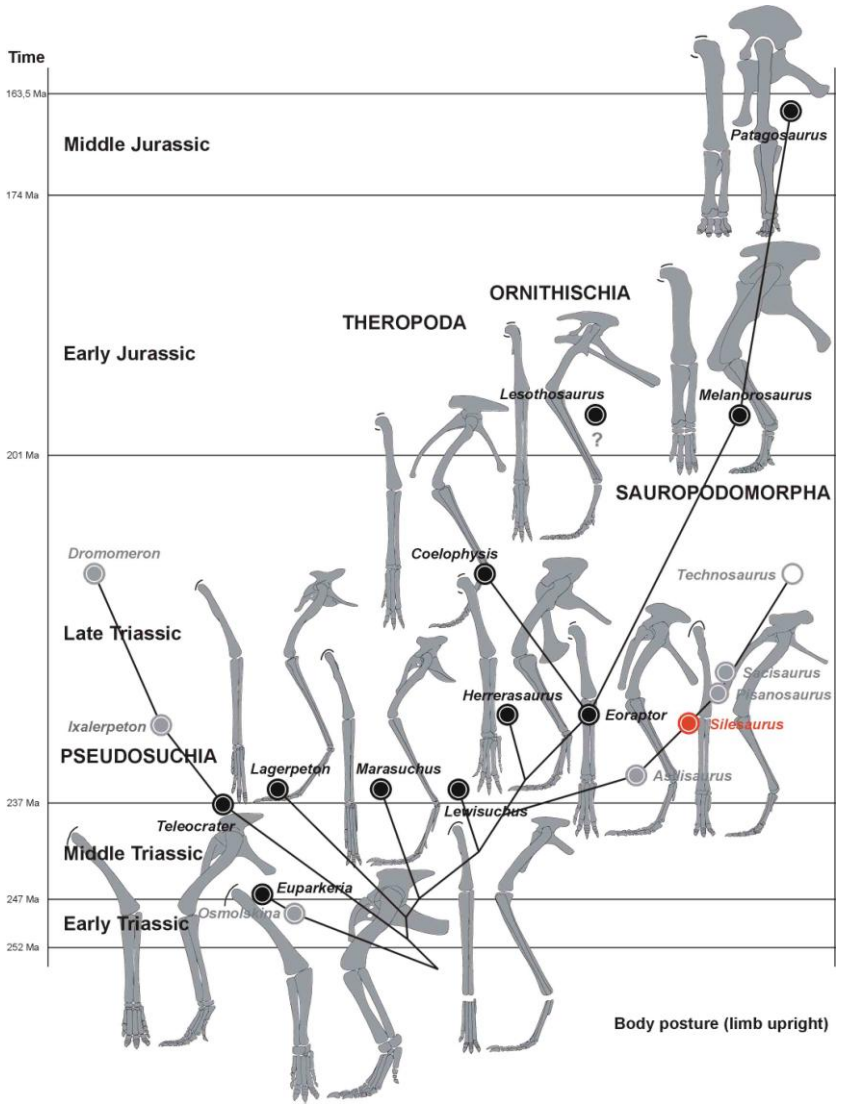

Figure 78. Evolution of hindlimb skeleton and its posture in selected early dinosaurs and their predecessors. Black dots represent illustrated taxa. Grey dots are unillustrated taxa having some forelimb bones known. White dots are unillustrated taxa with no forelimb material known. *Silesaurus* has a red dot. The topology of the tree follows Müller et al. (2018) with addition of *Osmolskina*, *Melanorosaurus*, and *Patagosaurus*. Closely related taxa from different time horizons are illustrated as one lineage for clarity of the figure.

The same probably applies to the forelimb of early dinosaurs. According to my results, dinosaurs re-developed a large deltopectoral crest on the humerus and some convergently to each other acquired a large olecranon process on the ulna. These changes show an increasing role of humeral protractors and forelimb extension. It is not easy to determine which early dinosaurs were fully bipedal and which were not (Remes, 2008; Fechner, 2009), but with

increasing bipedal abilities, the forelimb was shortened and could be engaged in new functions.

Conclusions

This study suggests that the available material of *Silesaurus* represents populations of a single dimorphic species. Ontogeny was the main factor influencing variation in the sample. Presence or absence of tendinous ossifications on the femora may have been determined by the maturity and sex of individuals. The ossifications developed simultaneously and may have been controlled by raised levels of calcitonin during puberty in females (or by their ageing). Therefore, specimens with enlarged trochanteric shelves, and tendon ossification at this and other muscle attachments, are interpreted as mature females that were significantly larger than males. Specimens without ossifications belong to males and immature females. Femoral variations are more dependent on ontogeny than iliac variations. This is presumably because femoral morphology was more important for efficient locomotion and survival. Ontogenetic changes were influenced by the disproportionate increase of body mass and slightly different ecology of older individuals. Ilia show higher intrapopulation variability than femora. It remains a possibility that the population from the lower horizon within the Krasiejów exposure represents a different stage in the evolution of the species than that from the upper horizon.

I confirm the presence of recesses on the ventral and lateral surface of the parabasisphenoid, and find that both may be homologous to those of early dinosaurs. There are also several similarities between the braincase of *Silesaurus* and other early dinosauriforms (e.g., *Lewisuchus, Marasuchus*). Some variations of the *Silesaurus* braincase are not individual/size dependent, but are rather linked specifically to the development of the craniocervical musculature. Braincase sizes do not correlate with the lengths of the long bones. The analyzed braincase traits are more vulnerable to intra-population variation. The ventral deflection of the paroccipital processes resulted in a rearrangement of neck muscles related to feeding behaviour, as observed in modern birds.

New data on the vertebral column of *Silesaurus* provide some insight into the early evolution of this skeletal system within the dinosauromorph lineage. *Silesaurus* is one of the most completely known and important basal dinosauromorphs from anywhere in the world. The geological age of *Silesaurus* has been determined, based on associated fauna and flora, as

late Carnian (Dzik & Sulej, 2007). Late Carnian strata in Italy, biostratigraphically correlated with Krasiejów, have yielded a radioisotopic age of 230.91 ± 0.33 Ma (Furin et al., 2006b). The Ischiqualasto Formation, from which most information on probable early dinosaurs come, is radioisotopically dated at 227.8 ± 0.3 Ma (Rogers et al., 1993; but 230.3-231.4 according to Furin et al., 2006b, p. 1011). *Silesaurus* is thus coeval with, possibly even slightly older than, the oldest known predatory and herbivorous dinosaurs but only the significantly younger *Coelophysis* is represented by skeletons preserved well enough to provide comparable information on the axial skeleton (Colbert, 1989).

This makes it difficult to decide whether the peculiar disparity between the structural and functional neck-thorax transition in *Silesaurus* is a primitive or derived feature. More apparent is the meaning of the rather smooth gradient in functional aspects of the vertebrae, consistent with elongation of the forelimbs and the presence of three sacrals firmly connected by their ribs with the ilium. All these aspects of the skeleton suggest mainly quadrupedal stance and gait. The long tail of *Silesaurus*, providing a counterbalance to the weight of the body in front of the pelvis, as well as the disproportionally gracile forelimbs, suggest that *Silesaurus* had the ability for fast bipedal running.

Unfortunately, published data on species that might be closely related to *Silesaurus* are extremely scarce. Until additional reliable evidence is available, the exact phylogenetic position of *Silesaurus* must remain unresolved.

Musculoskeletal reconstruction of *Silesaurus* presented here, provides a good fit for the Mid–Late Triassic tracks called Atreipus. This animal was mainly quadrupedal. It used forelimbs mainly for support, whereas propulsion was generated mainly by the hindlimbs. The forelimbs were fully erect and moved mainly in a parasagittal plane. This resulted in reduction of several muscle attachment sites related to sprawling posture. That is why *Silesaurus* shows surprising similarities to primitive sauropods in its forelimbs.

The ilium of *Silesaurus* was inclined about 30° dorsomedially. As a consequence the acetabulum and supraacetabular crest fully encompassed the femoral head resulting in pillar-erected hindlimbs like some pseudosuchians. The ischia were in contact through most of their length. As a result, the pelvis of *Silesaurus* was wide dorsally and narrow ventrally and had a short interacetabular distance. This improvement probably enabled a more efficient bipedal run.

At the beginning of their evolution, Dinosauromorpha acquired fully erect, elongated and simplified forelimbs like *Silesaurus* while retaining a primitive adductor-controlled hindlimb posture. Early dinosauriforms fully erected their hindlimbs by deepening the acetabulum and

developing a supraacetabular crest above the femur. This pillar-erected limb posture was probably necessary before the femur of early dinosaurs rotated medially to meet the laterally directed acetabulum. After obtaining full bipedality, the forelimb of early dinosaurs redeveloped attachment sites for retractors, flexors and extensors to meet functions other than support of the body. My results agree with those of Persons & Currie (2017) that obligatory bipedality was a response to increasing cursorial abilities, while the change in forelimb function was secondary.

References

Aerts, P., Van Damme, R., D'Aout, K. & Van Hooydonck, B. 2003. Bipedalism in lizards: whole-body modelling reveals a possible spandrel. *Philosophical Transactions of the Royal Society of London B* **358**, 525-1533.

Arcucci, A. 1986. Nuevos materiales y reinterpretation de *Lagerprton chanarensis* Romer (Thecodontia, Lagerpetontidae nov.) del Triasico medio de La Rioja, Argentina. *Ameghiniana* **23**, 233–242.

Ashmore, C. R., Addis, P. B., Doerr, L. & Stokes, H. 1973. Development of muscle fibers in the complexus muscle of normal and dystrophic chicks. *Journal Histochemistry and Cytochemistry* **21**, 266–278.

Baier, D. B. & Gatesy, S. M. 2013. Three dimensional skeletal kinematics of the shoulder girdle and forelimb in walking *Alligator*. *Journal of Anatomy* **223**, 462-473.

Bakker, R. T. 2000. Brontosaur killers: Late Jurassic allosaurids as sabretooth cat analogues. *Gaia* **15**, 145–158.

Bates, K. T. & Schachner, E. R. 2012. Disparity and convergence in bipedal archosaur locomotion. *Journal of the Royal Society Interface* **9**, 1339-1353.

Barden, H. E. & Maidment, S. C. R. 2011. Evidence for sexual dimorphism in the stegosaurian dinosaur *Kentrosaurus aethiopicus* from the Upper Jurassic of Tanzania. *Journal of Vertebrate Paleontology* **31**, 641–651.

Barrett, P. M., Nesbitt, S. J. & Peecook, B. R. 2015. A large-bodied silesaurid from the Lifua Member of the Manda beds (Middle Triassic) of Tanzania and its implications for body-size evolution in Dinosauromorpha. *Gondwana Research* **27**, 925–931.

Barsbold, R. & Maryańska, T. 1990. Segnosauria. In: D. B. Weishampel, P. Dodson & H. Osmólska (eds) *The Dinosauria* 408–415. Berkeley: University of California Press.

Baumel, J. J. & Raikow, R. J. 1993. In: J. J. Baumel, A. S. King, J. E. Breazile, H. E. Evans, J. C. Vanden Berge (eds) *Handbook of Avian Anatomy: Nomina Anatomica Avium* 45–132. Cambridge (MA): Nuttall Ornithological Club.

Baumel, J. J., King, A. S. Breazile, J. E., Evans, H. E. & Vanden Berge, J. C. 1993. In: J. J. Baumel, A. S. King, J. E.Breazile, H. E. Evans, J. C. Vanden Berge (eds) *Handbook of Avian Anatomy: Nomina Anatomica Avium* 45–132. Cambridge (MA): Nuttall Ornithological Club.

Baumel, J. J. & Witmer, L. M. 1993. Osteologia. In: J. J. Baumel, A. S. King, J. E.Breazile, H. E. Evans, J. C. Vanden Berge (eds) *Handbook of Avian Anatomy: Nomina Anatomica Avium* 45–132. Cambridge (MA): Nuttall Ornithological Club.

Benton, M. J. & Clark, J. M. 1988. Archosaur phylogeny and the relationships of the Crocodylia. *The Phylogeny and Classification of the Tetrapods* **1**, 295–338.

Benton, M. J. & D. J. Gower. 1997. Richard Owen's giant Triassic frogs: Archosaurs from the Middle Triassic of England. *Journal of Vertebrate Paleontology* **17**, 74–88.

Benton, M. J., Juul, L., Storrs, G. W. & Galton, P. M. 2000. Anatomy and systematic of the prosauropod dinosaur *Thecodontosaurus antiquus* from the Upper Triassic of southwest England. *Journal of Vertebrate Paleontology* **20**, 77–108.

Bittencourt, J. S., Arcucci, A. B., Marsicano, C. A. & Langer, M. C. 2015. Osteology of the Middle Triassic archosaur *Lewisuchus admixtus* Romer (Chañares Formation, Argentina), its inclusivity, and relationships amongst early dinosauromorphs. *Journal of Systematic Palaeontology* **13**, 189–219.

Bodzioch, A. & Kowal-Linka, M. 2012. Unraveling the origin of the Late Triassic multitaxic bone accumulation at Krasiejów (S Poland) by diagenetic analysis. *Palaeogeography, Palaeoclimatology, Palaeoecology* **346–347**, 25–36.

Borsuk-Białynicka, M. & Evans, S. E. 2009. Cranial and mandibular osteology of the Early Triassic archosauriform *Osmolskina czatkowicensis* from Poland. *Palaeontologia Polonica* **65**, 235–281.

Brusatte, S. L., Niedźwiedzki, G. & Butler, R. J. 2011. Footprints pull origin and diversification of dinosaur stem lineage deep into Early Triassic. *Proceedings of the Royal Society B Biological Sciences* **278**, 1107–1113.

Bonaparte, J. F. 1972. Los tetrápodos del sector superior de la Formacion Los Colorados, La Rioja, Argentina (Triássico Superior). *Opera Lilloana* **22**, 1–183.

Bonaparte, J. F. 1975. Nuevos materiales de *Lagosuchus talampayensis* Romer (Thecodontia – Pseudosuchia) y su significado en el origin de los Saurischia. Chañarense inferior, Triasico Medio de Argentina. *Acta Geologica Lilloana* **13**, 5–90.

Bonaparte, J. F. 1984. Locomotion in rauisuchid thecodonts. *Journal of Vertebrate Paleontology* **3**, 210-218.

Bonaparte, J. F. 1986. Les Dinosaures (Carnosaures, Allosauridés, Sauropodes, Cétiosauridés) du Jurassique moyen de Cerro Cóndor (Chubut, Argentine). *Annales de Paléontologie* **72**, 247–289.

Bonaparte, J. F. 1999. Evolución de las vértebras presacras en Sauropodomorpha. *Ameghiniana* **36**, 115–187.

Bonaparte, J. F., Novas, F. E. & Coria, R. A. 1990. *Carnotaurus sastrei* Bonaparte, the horned, lightly built carnosaur from the Middle Cretaceous of Patagonia. *Natural History Museum of Los Angeles County, Contributions in Science* **411**, 1–42.

Bonaparte, J. F., Ferigolo J. & Ribeiro, A. M. 1999. A new early Late Triassic saurischian dinosaur from Rio Grande do Sul State, Brazil. *National Science Museum Monographs* **15**, 9–109.

Bonnan, M. F. & Yates, A. M. 2007. A new description of the forelimb of the basal sauropodomorph *Melanorosaurus*: implication for the evolution of pronation, manus shape and quadrupedalism in sauropod dinosaurs. *Evolution and Palaeobiology of Early Sauropodomorph Dinosaurs* **77**, 139–155.

Borsuk-Bialynicka, M. 1977. A new camarasaurid sauropod *Opisthocoelicaudia skarzynskii* gen. n., sp. n. from the Upper Cretaceous of Mongolia. *Palaeontologia Polonica* **37**, 5–64.

Borsuk-Białynicka, M. & Sennikov, A. G. 2009. Archosauriform postcranial remains from the Early Triassic karst deposits of southern Poland. *Palaeontologia Polonica* **65**, 283–328.

Brinkman, D. 1980. The hind limb step cycle of *Caiman sclerops* and the mechanics of the crocodile tarsus and metatarsus. *Canadian Journal of Zoology* **58**, 2187–2200.

Brítt, B. B. 1993. *Pneumatic postcranial bones in dinosaurs and other archosaurs*. 383 pp. PhD Dissertation. University of Calgary, Alberta.

Brochu, C. A. 1996. Closure of neurocentral sutures during crocodilian ontogeny: implications for maturity assessment in fossil archosaurs. *Journal of Vertebrate Paleontology* **16**, 49–62.

Brusatte, S. L., Benton, M. J., Ruta, M. & Lioyd, T. 2008. Superiority, competition, and opportunism in the evolutionary radiation of dinosaurs. *Science* **302**, 1485–1488.

Brusatte, S. L, Niedźwiedzki, G. & Butler, R. J. 2011. Footprints pull origin and diversification of dinosaur stem lineage deep into Early Triassic. *Proceedings of the Royal Society B Biological Sciences* **278**, 1107–1113.

Butler, R. J., Barret, P. M. & Gower, D. J. 2009. Postcranial skeletal pneumaticity and air-sacs in the earliest pterosaurs. *Biology Letters* **5**, 557–560.

Butler, R. J. 2010. The anatomy of the basal ornithischian dinosaur *Eocursor parvus* from the lower Elliot Formation (Late Triassic) of South Africa. *Zoological Journal of the Linnean Society* **160**, 648–684.

Burch, S. H. 2014. Complete forelimb myology of the basal theropod dinosaur *Tawa hallae* on a novel robust muscle reconstruction method. *Journal of Anatomy* **225**, 271–297.

Cabreira, S. F., Kellner, A. W. A., Dias-da-Silva, S., da Silva, L. R., Bronzati, M., de Almeida Marsola, J. C., Müller, R. T., de Souza Bittencourt, J., Batista, B. J., Raugust, T., Carrilho, R., Brodt, A. & Langer, M. C. 2016. A unique Late Triassic dinosauromorph assemblage reveals dinosaur ancestral anatomy and diet. *Current Biology* **26**, 3090–3095.

Carrano, M. T. 1998. Locomotion in non-avian dinosaurs: integrating data from hindlimb kinematics, in vivo strains and bone morphology. *Paleobiology* **24**, 450–469.

Carrano, M. T. & Hutchinson, J. R. 2002. Pelvic and hindlimb musculature of *Tyrannosaurus rex* (Dinosauria: Theropoda). *Journal of Morphology* **253**, 207–228.

Carter, D. R., Mikie, B. & Padian, K. 1998. Epigenetic mechanical factors in the evolution of long bone epiphyses. *Zoological Journal of the Linnean Society* **123**, 163–178.

Chatterjie, S. 1978. A primitive parasauchid (phytosaur) reptile from the Upper Triassic Maleri Formation of India. *Paleobiology* **21**, 83–127.

Chinsamy, A. 1990. Physiological implications of the bone histology of *Syntarsus rhodesiensis* (Saurischia: Theropoda). *Paleontologia Africana* **27**, 77–82.

Colbert, E. 1989. The Triassic dinosaur *Coelophysis*. *Museum of Northern Arizona Bulletin* **57**, 1–160.

Christian, A. & Preuschoft, H. 1996. Deducing the body posture of extinct large vertebrates from the shape of the vertebral column. *Palaeontology* **39**, 801–812.

Cong, L., Hou, L., Wu, X-C. & Hou, J. F. 1998. The gross anatomy of *Alligator sinensis* Fauvel (in Chinese). *China Forestry Publishing House, Beijing* **338,** 271–290.

Colbert, E. H. 1989. The Triassic dinosaur *Coelophysis*. *Museum of Northern Arizona Bulletin* **57**, 1–160.

Coombs, W. P. 1978. Forelimb muscles of the Ankylosauria (Reptilia, Ornithischia). *Journal of Paleontology* **52**, 642–657.

Cooper, M. R. 1981. The prosauropod dinosaur *Massospondylus caritanus* Owen from Zimbabwe: its biology, mode of life and phylogenetic significance. *Occasional Papers of the National Museums and Monuments of Rhodesia, series B, Natural Sciences* **6**, 689–840.

Currie, P. J. & Zhao, X. J. 1994. A new carnosaur (Dinosauria, Treropoda) from the Jurassic of Xinjiang, People's Republic of China. *Canadian Journal of Earth Sciences* **30**, 2037–2081.

Dacke, C. G., Furr, B. J., Boelkins, J. N. & Kenny, A. D. 1976. Sexually related changes in plasma calcitonin levels in Japanese quail. *Comparative Biochemistry and Physiology, Part A: Comparative Physiology* **55**, 341–344.

Delcourt, R. & Azevedo, S. A. K. 2012. New information on the scapular musculature of *Saturnalia tupiniquim* (Dinosauria, Saurischia). *Gaea — Journal of Geoscience* **8.1**, 1–5.

Dilkes, D. W. 2000. Appendicular myology of the hadrosaurian dinosaurs *Maiasauria peeblesorum* from the Late Cretaceous (Campanian) of Montana. *Transactions of the Royal Society of Edinburgh, Earth Sciences* **90**, 87–125.

Diogo, R. & Abdala, V. 2010. *Muscles of Vertebrates: Comparative Anatomy, Evolution, Homologies, and Development*. CRC Press.

Dzik, J. 2001. A new *Paleorhinus* fauna in the early Late Triassic of Poland. *Journal of Vertebrate Paleontology* **21**, 625–627.

Dzik, J. 2003. A beaked herbivorous archosaur with dinosaur affinities from the early Late Triassic of Poland. *Journal of Vertebrate Paleontology* **23**, 556–574.

Dzik, J. & Sulej, T. 2007. A review of the early Late Triassic Krasiejów biota from Silesia, Poland. *Palaeontologia Polonica* **64**, 1–27.

Dzik, J. & Sulej, T. 2016. An early Late Triassic long-necked reptile with a bony pectoral shield and gracile appendages. *Palaeontologia Polonica* **61**, 805–823.

Evans, S. E. 1986. The braincase of *Prolacerta broomi* (Reptilia, Triassic). *Neues Jahrbuch für Geologie und Paläontologie, Abhandlungen* **173**, 181–200.

Ewer, R. F. 1965. The anatomy of the thecodont reptile *Euparkeria capensis* Broom. *Philosophical Transactions of the Royal Society of London. Series B, Biological Sciences* **248**, 379–435.

Ezcurra, M. D. 2006. A review of the systematic position of the dinosauriform archosaur *Eucoelophysis baldwini* Sullivan & Lucas, 1999 from the Upper Triassic of New Mexico, USA. *Geodiversitas* **28**, 649–684.

Farke, A. A. & Alicea, J. 2009. Femoral strength and posture in terrestrial birds and non-avian theropods. *The Anatomical Record* **292**, 1406–1411.

Farlow, J. O., Gatesy, S. M., Holtz Jr., T. R., Hutchinson, J. R. & Robinson, J. M. 2000. Theropod locomotion. *American Zoologist* **40**, 640–663.

Fearon, J. L. & Varricchio, D. J. 2016. Reconstruction of the forelimb musculature of the Cretaceous ornithopod dinosaur *Oryctodromeus cubicularis*: implications for digging. *Journal of Vertebrate Paleontology* **36**, e1078341.

Fechner, R. 2009. *Morphofunctional Evolution of the Pelvic Girdle and Hindlimb of Dinosauromorpha on the Lineage to Sauropoda*. PhD Dissertation. Fakultät für Geowissenschaften, Ludwig-Maximilians-Universität, Munich.

Ferigolo, J. & Langer, M. C. 2007. A Late Triassic dinosauriform from south Brazil and the origin of the ornithischian predentary bone. *Historical Biology* **19**, 23–33.

Fisher, H. I. & Goodman D. C. 1955 The myology of the Whooping Crane, *Grus americana*. *Illinois Biological Monographs* **24**, 1–127.

Fitzgerald, T. C. 1969. The Coturnix Quail. *Iowa State University Press, Ames* **221**, 258–260.

Forster, C. T. 1990. The postcranial skeleton of the ornithopod dinosaur *Tenontosaurus tilletti*. *Journal of Vertebrate Paleontology* **10**, 273–294.

Foster, J. R. & Chure, D. J. 2006. Hindlimb allometry in the Late Jurassic theropod dinosaur *Allosaurus*, with comments on its abundance and distribution. *New Mexico Museum of Natural History and Science Bulletin* **36**, 57–65.

Fostowicz-Frelik, Ł. & Sulej, T. 2010. Bone histology of *Silesaurus opolensis* Dzik, 2003 from the Late Triassic of Poland. *Lethaia* **43**, 137–148.

Fouchereau-Peron, M., Arlot-Bonnemains, Y., Taboulet, J., Milhaud, G. & Moukhtar, M. S. 1990. Distribution of calcitonin gene-related peptide and calcitonin-like immunoreactivity in trout. *Regulatory Peptides* **27**, 171–179.

Fraser, N. C., Padian, K., Walkden, G. M. & Davis, A. L. M. 2002. Basal dinosauriform remains from Britain and the diagnosis of the Dinosauria. *Palaeontology* **45**, 79-95.

Furin, S., Preto, N., Rigo, M., Roghi, G., Gianolla, P., Crowley, J. L. & Bowring, S. A. 2006. High-precision U-Pb zircon age from the Triassic of Italy: Implications for the Triassic time scale and the Carnian origin of calcareous nannoplankton and dinosaurs. *Geology* **34**, 1009–1012.

Fürbringer, M. 1876. Zur vergleichenden Anatomie des Schultermuskeln – 3. Teil: Capitel IV: Saurier und Crocodile. *Gegenbaurs morphologisches Jahrbuch* **1**, 636–816.

Fürbringer, M. 1888. Untersuchungen zur Morphologie und Systematik der Vögel, zugleich ein Beitrag zur Anatomie der Stütz-und Bewegungsorgane. *Bijdragen tot de Dierkunde* **15**, 1–834.

Fürbringer, M. 1900. Zur vergleichenden Anatomie des Brustschulterapparates und der Schultermuskeln, IV. Teil: Reptilien. *Jenaische Zeitschrift für Naturwissenschaft* **36**, 215–712.

Fürbringer, M. 1902. Zur vergleichenden Anatomie des Brustschulterapparates und der Schultermuskeln, V. Teil: Vögel. *Jenaische Zeitschrift für Naturwissenschaft* **36**, 289–736.

Gadow, H. 1882. Beiträge zur Myologie der hinteren Extremität der Reptilien. *Morphologisches Jahrbuch* **7**, 329–466.

Galton, P. M. 1974. The ornithischian dinosaur *Hypsilophodon* from the Wealden of the Isle of Wight. *Bulletin of the British Museum of Natural History (Geology)* **25**, 1–152.

Galton, P. M. 1976. Prosauropod dinosaur (Reptilia: Saurischia) of North America. *Postilla* **169**, 1–98.

Galton, P. M. 1977. On *Staurikosaurus pricei*, an early saurischian dinosaur from the Triassic of Brazil, with notes on the Herrerasauridae and Poposauridae. *Paläontologische Zeitschrift* **51**, 234–245.

Galton, P. M. & Powell, H. P. 1980. The ornithischians dinosaur *Camptosaurus prestwichii* from the Upper Jurassic of England. *Palaeontology* **23**, 411–443.

Galton, P. M. & Walker, A. D. 1996. *Bromsgroveia* from the Middle Triassic of England, the earliest record of a poposaurid thecodontian reptile (Archosauria: Rauisuchia). *Neues Jahrbuch für Geologie und Paläontologie, Abhandlungen* **201**, 303–325.

Galton, P. M. & Kermack D. 2010. The anatomy of *Pantydraco caducus*, a very basal sauropodomorph dinosaur from the Rhaetian (Upper Triassic) of South Wales, UK. *Revue de Paléobiologie* **29**, 341–404.

Gangl, D., Weissengruber, G. E., Egerbacher, M. & Forstenpointner, G. 2004. Anatomical description of the muscles of the pelvis limb in the Ostrich (*Struthio camelus*). *Anatomy, Histology, Embryology* **33**, 100–114.

Gardner, N. M., Holliday, C. M. & O'Keefe, F. R. 2010. The braincase of *Youngina capensis* (Reptilia, Diapsida): new insights from high resolution CT scanning of the holotype. *Palaeontologia Electronica* **13**, 19.

Gatesy, S. M. 1990. Caudofemoral musculature and the evolution of theropod locomotion. *Paleobiology* **16**, 170–186.

Gatesy, S. M. 1995. Functional evolution of the hindlimb and tail from basal theropods to birds. In: J. J. Thomason (ed.) *Functional Morphology in Vertebrate Palaeontology* 219–234. Cambridge: Cambridge University Press.

Gauthier, J. 1986. Saurischian monophyly and the origin of birds. *Memoirs of the California Academy of Sciences* **8**, 1–55.

George, J. C. & Berger, A. J. 1966. *Avian Myology*. 500 pp. New York: Academic Press.

Gold, M. E. L., Brochu, C. A. & Norell, M. A. 2014. An expanded combined evidence approach to the *Gavialis* problem using geometric morphometric data from crocodylian braincases and Eustachian systems. *PLoS ONE* **9**, e105793.

Goslow, G. E., Dial, K. P. & Jenkins, F. A. 1989. The avian shoulder: an experimental approach. *American Zoologist* **29**, 287–301.

Gow, C. E. 1990. Morphology and growth of the *Massospondylus* braincase (Dinosauria, Prosauropoda). *Palaeontologia Africana* **27**, 59–75.

Gower, D. J. 1997. The braincase of the early archosaurian reptile *Erythrosuchus africanus*. *Journal of Zoology* **242**, 557–576.

Gower, D. J. 2001. Possible postcranial pneumaticity in the last common ancestor of bidrs and crocodilians: evidence from *Erythrosuchus* and other Mesozoic archosaurs. *Naturwissenschaften* **88**, 119–121.

Gower, D. J. & Sennikov, A. G. 1996. Morphology and phylogenetic informativeness of early archosaur braincases. *Palaeontology* **39**, 883–906.

Gower, D. J. & Sennikov, A. G. 1996. Endocranial casts of early archosaurian reptiles. *Paläontologisches Zeitschrift* **70**, 579–589.

Gower, D. J., Hancox, P. J., Botha-Brink, J., Sennikov, A. G. & Butler, R. J. 2014. A new species of *Garjainia* Ochev, 1958 (Diapsida: Archosauriformes: Erythrosuchidae) from the Early Triassic of South Africa. *PLoS ONE* **9**, e111154.

Gower, D. J. & Weber, E. 1998. The braincase of *Euparkeria*, and the evolutionary relationships of birds and crocodilians. *Biological Reviews* **73**, 367–411.

Griffin, C. T. & Nesbitt, S. J. 2016. The femoral ontogeny and long bone histology of the Middle Triassic (? late Anisian) dinosauriform *Asilisaurus kongwe* and implications for the growth of early dinosaurs. *Journal of Vertebrate Paleontology* **36**, e1111224.

Griffin, C. T., Bano, L. S., Turner, A. H., Smith, N. D., Irmis, R. B. & Nesbitt, S. J. 2019. Integrating gross morphology and bone histology to assess skeletal maturity in early dinosauromorphs: new insights from *Dromomeron* (Archosauria: Dinosauromorpha). *PeerJ* **7**, e6331.

Gross, G. H. & Oppenheim, R. W. 1985. Novel sources of descending input to the spinal cord of the hatchling chick. *Journal of Comparative Neurology* **232**, 162–179.

Gruszka, B. & Zieliński, T. 2008. Evidence for a very low-energy fluvial system: a study from the dinosaur-bearing Upper Triassic rocks of southern Poland. *Geological Quarterly* **52**, 239–252.

Habib, M. B. & C. B. Ruff. 2008. The effects of locomotion on the structural characteristics of avian limb bones. *Zoological Journal of the Linnean Society* **153**, 601–624.

Haines, R. W. 1939. A revision of the extensor muscles of the forearm in tetrapods. *Journal of Anatomy* **73**, 211–233.

Haines, R. W. 1942. The tetrapod knee joint. *Journal of Anatomy* **76**, 270–301.

Haines, R. W. 1950. The flexor muscles of the forearm and hand in lizard and mammals. *Journal of Anatomy* **84**, 12–29.

Harris, J. D. 1998. A reanalysis of *Acrocanthosaurus atokensis*, its phylogenetic status, and paleobiogeographic implications, based on a new specimen from Texas. *Bulletin of the New Mexico Museum of Natural History and Science* **13**, 1–75.

Haubold, H. & Klein, H. 2000. Die dinosauroiden Fährten *Parachirotherium–Atreipus–Grallator* aus dem unteren Mittelkeuper (Obere Trias: Ladin, Karn, ?Nor) in Franken. *Hallesches Jahrbuch für Geowissenschaften B* **22**, 59–85.

He, X., Li, K. & Cai, K. 1988. *The Middle Jurassic Dinosaurian Fauna from Dashanpu, Zigong, Sichuan: Sauropod Dinosaurs (2)* Omeisaurus tanfuensis. 145 pp. Chengdo: Sichuan Scientific and Technological Publishing House.

Heaton, M. J. 1979. Cranial anatomy of primitive captorhinid reptiles from the late Pennsylvanian and Early Permian of Oklahoma and Texas. *Oklahoma Geological Survey Bulletin* **127**, 1–81.

Herring, S. W. 1993. Epigenetic and functional influences on skull growth. In: J. Hanken & B. K. Hall (eds) *The Skull. Vol. 1*. 153–206. Chicago: University of Chicago Press.

Holliday, C. M. 2009. New insights into dinosaur jaw muscle anatomy. *Anatomical Record* **292**, 1246–1265.

Holliday, C. M., Ridgely, R. C., Sedlmayr, J. C. & Witmer, L. M. 2010. Cartilaginous epiphyses in extant archosaurs and their implications for reconstructing limb function in dinosaurs. *PLoS ONE* **5**, e13120.

Hudson, G. E, Hoff, K. M., Berge, J. V. & Trivette, E. C. 1969. A numerical study of the wing and leg muscles of Lari and Alcae. *Ibis* **111**, 459–524.

Hunt, A. P., Heckert, A. B., Sullivan, R. M. & Lockley, M. G. 1998. Late Triassic dinosaurs from the western United States. *Geobios* **31**, 511–531.

Hutchinson, J. R. 2001. *The Evolution of Hindlimb Anatomy and Function in Theropod Dinosaurs*. PhD Dissertation, University of California, Berkeley.

Hutchinson, J. R. 2001. The evolution of the femoral osteology and soft tissues on the line to extant birds (Neornithes). *Zoological Journal of the Linnean Society* **131**, 169–197.

Hutchinson, J. R. 2002. The evolution of hindlimb tendons and muscles on the line to crown-group birds. *Comparative Biochemistry and Physiology Part A* **133**, 1051–1086.

Hutchinson, J. R. 2004. Biomechanical modeling and sensitivy analysis of bipedal running ability. II. Extinct taxa. *Journal of Morphology* **262**, 441–461.

Hutchinson, J. R. 2006. The evolution of locomotion in archosaurs. *Comptes Rendus Palevol* **5**, 519–530.

Hutchinson, J. R. & Garcia, M. 2002. *Tyrannosaurus* was not a fast runner. *Nature* **415**, 1018–1021.

Hutchinson, J. R. & Gatesy, S. M. 2000 Adductors, abductors, and the evolution of archosaur locomotion. *Paleobiology* **26**, 734–751.

Hutchinson, J. R., Anderson, F. C., Blemker, S. S. & Delp, S. L. 2005. Analysis hindlimb muscle moment arms in *Tyrannosaurus rex* using a three-dimensional musculoskeletal computer model: implications for stance, gait, and speed. *Paleobiology* **31**, 676–701.

Hutchinson, J. R., Miller, C., Fritsch, G. & Hildebrandt, T. 2008. The anatomical foundation for multidisciplinary studies of animal limb function: examples from dinosaur and elephant limb imaging studies. In: H. Endo & R. Frey (eds) *Anatomical Imaging Techniques: Towards a New Morphology* 23–38, Springer-Verlag, Berlin.

Hutson, J. D. & Hutson, K. N. 2015. An examination of forearm bone mobility in *Alligator mississipiensis* (Daulin, 1802) and *Struthio came*lus Linnaeus, 1758 reveals that *Archaeopteryx* and dromaeosaurus shared an adaptation for gliding and/or flapping. *Geodiversitas* **37**, 325–344.

Hutson, J. D. & Hutson, K. N. 2017. An investigation of the locomotor function of therian forearm pronation provides renewed support for an arboreal, chameleon-like evolutionary stage. *Journal of Mammalian Evolution* **24**, 195–177.

Irmis, R. B., Nesbitt, S. J., Padian, K., Smith, N. D., Turner, A. H., Woody, D., & Downs, A. 2007. A late Triassic dinosauromorph assemblage from New Mexico and the rise of dinosaurs. *Science* **317**, 358–361.

Irmis, R. B., Parker, W. G., Nesbitt, S. J., & Jun, L. 2007. Early ornitischian dinosaurs: the Triassic record. *Historical Biology* **19**, 3–22.

Irmis, R. B. 2007. Axial skeleton ontogeny in the Parasuchia (Archosauria: Pseudosuchia) and its implications for ontogenetic determination in archosaurs. *Journal of Vertebrate Paleontology* **27**, 350–361.

Jackson, J. E. 1991. *A User's Guide to Principal Components*. 575 pp. New York: Wiley-Interscience.

Jasinoski, S. C., Russel, A. P. & Currie, P. J. 2006. An integrative phylogenetic and extrapolary approach to the reconstruction of dromaeosaur (Theropoda: Eomaniraptora) shoulder musculature. *Zoological Journal of Linnean Society* **146**, 301–344.

Jewuła, K., Matysik, M., Paszkowski, M. & Szulc, J. 2019. The late Triassic development of playa, gilgai floodplain, and fluvial environments from Upper Silesia, southern Poland. *Sedimentary Geology* **379**, 25–45.

Johnson, R. E. & Ostrom, J. H. 1995. The forelimb of *Torosaurus* and an analysis of the posture and gait of ceratopsian dinosaurs. In: J. J. Thomason (ed.) *Functional Morphology in Vertebrate Paleontology* 205–218. Cambridge: Cambridge University Press.

Kammerer, C. F, Nesbitt, S. J. & Shubin, N. H. 2012. The first basal dinosauriform (Silesauridae) from the Late Triassic of Morocco. *Acta Palaeontologica Polonica* **57**, 277–284.

Klein, N. & Sander, M. 2008. Ontogenetic stages in the long bone histology of sauropod dinosaurs. *Paleobiology* **34**, 247–263.

Kozur, H. W. & Weems, R. E. (2010). The biostratigraphic importance of conchostracans in the continental Triassic of the northern hemisphere. *Geological Society, London, Special Publications* **334**, 315–417.

Kriegler, W. 1961. Zur Myologie des Beckens und der Hinterextremität der Reptilien. *Morphologisches Jahrbuch* **101**, 541–625.

Kubo, T. & Kubo, M. O. 2012. Associated evolution of bipedality and cursoriality among Triassic archosaurs: a phylogenetically controlled evaluation. *Paleobiology* **38**, 474–485.

Kubo, T. & Kubo, M. O. 2014. Dental microwear of a Late Triassic dinosauriform, *Silesaurus opolensis*. *Acta Palaeontologica Polonica* **59**, 305–312.

Kundrat, M. 2009. Primary chondrification foci in the wing basipodium of *Struthio camelus* with comments on interpretation of autopodial elements in Crocodilia and Aves. *Journal of Experimental Zoology Part B: Molecular and Developmental Evolution* **312**, 30–41.

Landsmeer, J. M. F. 1983. The mechanism of forearm rotation in *Varanus exanthematicus*. *Journal of Morphology* **175**, 119–130.

Langer, M. C. 2003. The pelvic and hind limb anatomy of the stem-sauropodomorph *Saturnalia tupiniquim* (Late Triassic, Brazil). *Paleobios* **23**, 1–40.

Langer, M. C. 2014. The origins of Dinosauria: much ado about nothing. *Palaeontology* **57**, 469–478.

Langer, M. C. & Benton, M. J. 2006. Early dinosaurs: a phylogenetic study. *Journal of Systematic Palaeontology* **4**, 309–358.

Langer, M. C., Ezcurra, M. D., Bittencourt, J. S. & Novas, F. E. 2009. The origin and early evolution of dinosaurs. *Biological Reviews* **84**, 1–56.

Langer, M. C., França, M. A. G. & Gabriel, S. 2007. The pectoral girdle and forelimb anatomy of the stem-sauropodomorph *Saturnalia tupiniquim* (Upper Triassic, Brazil). *Special Papers in Palaeontology* **77**, 113–137.

Langer, M. C. & Ferigolo, J. 2013. The Late Triassic dinosauromorph *Sacisaurus agudoensis* (Caturrita Formation; Rio Grande do Sul, Brazil): anatomy and affinities. In: S. J. Nesbitt, J. B. Desojo & R. B. Irmis (eds). *Anatomy, Phylogeny and Palaeobiology of Early Archosaurs and their Kin. Geological Society of London Special Publications* **379**, 353–392.

Langer, M. C., Nesbitt, S. J., Bittencourt, J. S. & Irmis, R. B. 2013. Non-dinosaurian Dinosauromorpha. In: S. J. Nesbitt, J. B. Desojo & R. B. Irmis (eds). *Anatomy, Phylogeny and Palaeobiology of Early Archosaurs and their Kin. Geological Society of London Special Publications* **379**, 157–186.

Liparini, A. & Schultz, C. L. 2013. A reconstruction of the thigh musculature of the extinct pseudosuchian *Prestosuchus chiniquensis* from the *Dinodontosaurus* Assemblage Zone (Middle Triassic Epoch), Santa Maria 1 Sequence, southern Brasil. In: S. J. Nesbitt, J. B. Desojo & R. B. Irmis (eds). *Anatomy, Phylogeny and Palaeobiology of Early Archosaurs and their Kin. Geological Society of London Special Publications* **379**, 441–468.

Livezey, B. C. 1990. Evolutionary morphology of flightlessness in the Aukland Islands teal. *Condor* **92**, 639–673.

Long, R. A. & Murry, P. A. 1995. Late Triassic (Carnian and Norian) tetrapods from the southwestern United States. *New Mexico Museum of Natural History and Science Bulletin* **4**, 1–254.

Lucas, S. G. 2015. Age and correlation of Late Triassic tetrapods from southern Poland. *Annales Societatis Geologorum Poloniae* **85**, 627–635.

Marpmann, J. S., Carballido, J. L, Sander, P. M. & Knötschke, N. 2014. Cranial anatomy of the Late Jurassic dwarf sauropod *Europasaurus holgeri* (Dinosauria, Camarasauromorpha): ontogenetic changes and size dimorphism. *Journal of Systematic Palaeontology* **3**, 221–263.

Lyritis, G. & P. J. Boscainos. 2001. Calcitonin effects on cartilage and fracture healing. *Journal of Musculoskeleton Neuronal Interactions* **2**, 137–142.

Madsen, J. H. 1976. *Allosaurus fragilis*: a revised osteology. *Utah Geological Survey Bulletin* **109**, 3–163.

Madsen, J. H. J. & Welles, S. P. 2000. *Ceratosaurus* (Dinosauria, Theropoda). A revised osteology. *Utah Geological Survey Miscellaneous Publication* **2**, 1–80.

Maidment, S. C. R. & Barrett, P. M. 2011. The locomotor musculature of basal ornithischian dinosaurs. *Journal of Vertebrate Paleontology* **31**, 1265–1291.

Martin, J., Martin-Rolland, V. & Frey, E. 1998. Not cranes or masts, but beams: The biomechanics of sauropod necks. *Oryctos* **1**, 113–120.

Martínez, R. N., Sereno P. C. & Alcober, O. A. 2008. A new basal theropod from the Ischigualasto Formation of San Juan Province, Argentina. *Libro de Resúmenes, III Congreso Latinoamericano de Paleontología de Vertebrados, Neuquén, Patagonia, Argentina*, p. 153.

Martinez, R.N. & Alcober, O. A. 2009. A basal sauropodomorph (Dinosauria: Saurischia) from the Ischigualasto Formation (Triassic, Carnian) and the early evolution of Sauropodomorpha. *PLoS ONE* **4**, e4397.

Martinez, R. N., Haro, J. A. & Apaldetti, C. 2013. Braincase of *Panphagia protos* (Dinosauria, Sauropodomorpha). *Journal of Vertebrate Paleontology* **32**(supplement), 70–82.

Martinez, R. N., Sereno, P. C., Alcober, O. A, Colombi, C. E., Renne, P. R., Montanez, I. P. & Currie, B. S. 2011. A basal dinosaur from the dawn of the dinosaur era in southwestern Pangaea. *Science* **331**, 206–210.

Mazurek, D. & Słowiak, J. 2009. Silezaur dinozaurem? *Przegląd Geologiczny* **57**, 569–571.

McGowan, C. 1979. The hind limb musculature of the Brown Kiwi, *Apteryx australis mantelli*. *Journal of Morphology* **160**, 33–74.

McGowan, C. 1982. The wing musculature of the Brown Kiwi, *Apteryx australis mantelli* and its bearing on ratite affinities. *Journal of Zoology* **197**, 173–219.

McIntosh, J. S. 1989. The sauropod dinosaurs: a brief survey. In: K. Padian & D. J. Chure (eds) *The Age of Dinosaurs. Short courses in Paleontology Number 2*. 85–99. University of Tennessee, Knoxville.

Meers, M. B. 2003. Crocodilian forelimb musculature and its relevance to Archosauria. The *Anatomical Record Part A* **274**, 891–916.

Miner, R. W. 1925. The pectoral limb of *Eryops* and other primitive tetrapods. *Bulletin of the American Museum of Natural History* **51**, 145–312.

Monteiro, L. R. & Abe, A. S. 1997. Allometry and morphological integration in the skull of *Tupinambis merianae* (Lacertilia: Teiidae). *Amphibia-Reptilia* **18**, 397–405.

Moodie, R. L. 1928. The histological nature of ossified tendons found in dinosaurs. *American Museum Novitates* **311**, 1–15.

Munter, R. C. & Clark, J. M. 2006. Theropod dinosaurs from the Early Jurassic of Huizachal Canyon, Mexico. In: M. T. Carrano, T. J. Gaudin, R. W. Blob & R. J. Wible (eds) *Amniote Paleobiology: Perspectives on the Evolution of Mammals, Birds, and Reptiles* 53–75. Chicago: University of Chicago Press.

Müller, R. T., Langer, M. C. & Dias-Da-Silva, S. 2018. Ingroup relationships of Lagerpetidae (Avemetatarsalia: Dinosauromorpha): a further phylogenetic investigation on the understanding of dinosaur relatives. *Zootaxa* **4392**, 149–158.

Nawrocki, J., Jewuła, K., Stachowska, A. & Szulc, J. 2015. Magnetic polarity of Upper Triassic sediments of the Germanic Basin In Poland. *Annales Societatis Geologorum Poloniae* **85**, 663–674.

Nesbitt, S. J. 2005. The osteology of the pseudosuchian *Arizonasaurus babbitti*. *Historical Biology* **17**, 19–47.

Nesbitt, S. J., 2007. The anatomy of *Effigia okeeffeae* (Archosauria, Suchia), theropod-like convergance, and the distribution of related taxa. *Bulletin of the American Museum of Natural History* **302**, 1–84.

Nesbitt, S. J. 2011. The early evolution of archosaurs: relationships and the origin of major clades. *Bulletin of the American Museum of Natural History* **352**, 1–292.

Nesbitt, S. J., Irmis, R. B., Parker, W. G., Smith, N. D., Turner, A. H. & Rowe, T. 2009. Hind limb osteology and distribution of basal dinosauromorphs from the Late Triassic of North America. *Journal of Vertebrate Paleontology* **29**, 498–516.

Nesbitt, S. J., Barrett, P. M., Werning, S., Sidor, C. A. & Charig, A. J. 2013. The oldest dinosaur? A Middle Triassic dinosauriform from Tanzania. *Biology Letters* **9**, 20120949.

Nesbitt, S. J., Butler, R. J, Ezcurra, M. D., Barrett, P. M., Stocker, M. R., Angielczyk, K. D., Smith, R. M. H., Sidor, C. A., Niedźwiedzki, G., Sennikov, A. G. & Charig, A. J. 2017. The earliest bird-line archosaurs and the assembly of the dinosaur body plan. *Nature* **544**, 484–487.

Nesbitt, S. J., Irmis, R. B. & Parker, W. G. 2007. A critical re-evaluation of the Late Triassic dinosaur taxa of North America. *Journal of Systematic Palaeontology* **5**, 209–243.

Nesbitt, S. J., Butler, R. J., Ezcurra, M. D., Charig, A. J. & Barrett, P. M. 2017. The anatomy of *Teleocrater rhadinus*, an early avemetatarsalian from the lower portion of the Lifua Member of the Manda Beds (Middle Triassic). *Journal of Vertebrate Paleontology* **37**(supplement 1), 142–177.

Nesbitt, S. J., Sidor, C. A., Irmis, R. B., Angielczyk, K. D., Smith. R. M. & Tsuji, L. A. 2010. Ecologically distinct dinosaurian sister group shows early diversification of Ornithodira. *Nature* **464**, 95–98.

Nickel, R., Schummer, A., Seiferle, E. E. 2003. *Lehrbuch der Anatomie der Haustiere I: Bewegungsapparat: Bd I*. Stuttgart: Parey Verlag.

Niedźwiedzki, G. 2015. New finds of dinosauromorphs and dinosauriforms from the Middle and Upper Triassic of Poland. *13th Annual Meeting of the European Association of Vertebrate Palaeontologists, Opole, Poland; Jul 8–12. Abstracts*, p. 84.

Niedźwiedzki, G., Brusatte, S. L. & Butler, R. J. 2013. *Prorotodactylus* and *Rotodactylus* tracks: an ichnological record of dinosauromorphs from the Early–Middle Triassic of Poland. *Geological Society, London, Special Publications* **379**, 319–351.

Niedźwiedzki, G., Piechowski, R. & Sulej, T. 2009. New data on the anatomy and phylogenetic position of *Silesaurus opolensis* from the late Carnian of Poland. *Journal of Vertebrate Paleontology* **29**(supplement), 155A.

Niedźwiedzki, G., Sennikov, A. G. & Brusatte, S. L. 2016. The osteology and systematic position of *Dongusuchus efremovi* Sennikov, 1988 from the Anisian (Middle Triassic) of Russia. *Historical Biology* **28**, 550–570.

Niedźwiedzki, G., Sulej, T. & Dzik, J. 2012. A large predatory archosaur from the Late Triassic of Poland. *Acta Palaeontologica Polonica* **57**, 267–276.

Norman, D. B. 1980. On the ornithischian dinosaur *Iguanodon bernissartensis* from the Lower Cretaceous of Bernissart (Belgium). *Institute Royale de Sciences Naturelles de Belgique Mémoire* **178**, 1-103.

Norman, D. B. 1986. On the anatomy of *Iguanodon athierfieldensis* (Ornithischia, Ornithopoda). *Bulletin de L`Institut Royal des Sciences Naturelle de Belgique: Sciences de la Terre* **56**, 281–372.

Novas, F. E. 1996. Dinosaur monophyly. *Journal of Vertebrate Paleontology* **16**, 723–741.

O'Connor, P. 2006. Postcranial pneumaticity: an evaluation of soft-tissue influences on the postcranial skeleton and the reconstruction of pulmonary anatomy in archosaurs. *Journal of Morphology* **267**, 1199–1226.

O'Connor, P. & Claessens, L. 2005. Basic avian pulmonary design and flow-through ventilation in non-avian theropod dinosaurs. *Nature* **436**, 253–256.

Oelrich, T. M. 1956. The anatomy of the head of *Ctenosaura pectinata* (Iguanidae). *Miscellaneous Publications Museum of Zoology University of Michigan* **94**, 1–122.

Olempska E. 2004. Late Triassic spinicaudatan crustaceans from SW Poland. *Acta Palaeontologica Polonica* **49**, 429–442.

Olsen, P. E. & Baird, D. 1986. The ichnogenus *Atreipus* and its significance for Triassic biostratigraphy. *The Beginning of the Age of Dinosaurs.* 61–87. Cambridge: Cambridge University Press.

Organ, C. L. & Adams, J. 2005. The histology of ossified tendon in dinosaurs. *Journal of Vertebrate Paleontology* **25**, 602–613.

Osawa, C. 1898. Beiträge zur Anatomie von *Hatteria punctata*. *Archiv für mikroskopische Anatomie und Entwicklungsgeschichte* **51**, 548–675.

Osborn, H. F. & Mook, C. C. 1916. Skeletal adaptations of *Ornitholestes, Struthiomimus, Tyrannosaurus*. *Bulletin of the American Museum of Natural History* **35**, 733–771.

Osmólska, H., Maryanska, T. & Barsbold, R. 1972. A new dinosaur, *Gallimimus bullatus* n. gen., n. sp. (Ornithomimidae) from the Upper Cretaceous of Mongolia. *Palaeontologica Polonica* **27**, 103–143.

Ostrom, J. H. 1978. The osteology of *Compsognathus longipes* Wagner. *Zitteliana* **4**, 73–118.

Ostrom, J. H. & McIntosh, J. S. 1966. *Marsh's Dinosaurs*. 388 pp. New Haven: Yale University Press.

Otero, A,, Gallina, P. A. & Herrera, Y. 2010. Pelvic musculature and function of *Caiman latirostis*. *Herpetological Journal* **20**, 173–184.

Otero, A., Allen, V., Pol, D. & Hutchonson, J. R. 2017. Forelimb muscle and joint actions in Archosauria: insights from *Crocodylus johnstoni* (Pseudosuchia) and *Mussaurus patagonicus* (Sauropodomorpha). *PeerJ* **5**, e3976.

Otero, A. 2018. Forelimb musculature and osteological correlates in Sauropodomorpha (Dinosauria, Saurischia). *PLoS ONE* **13**, e0198988.

Otero, A., Cuff, A. R., Allen, V., Sumner-Rooney, L., Pol, D. & Hutchinson, J. R. 2019. Ontogenetic changes in the body plan of the sauropodomorph dinosaur *Mussaurus patagonicus* reveal shifts of locomotor stance during growth. *Scientific Reports* **9**, 7614.

Pacyna, G. 2014. Plant remains from the Polish Triassic. Present knowledge and future prospects. *Acta Palaeobotanica* **54**, 3–33.

Pacyna, G. 2019. Sphenopsid and fern remains from the Upper Triassic of Krasiejów (SW Poland). *Annales Societatis Geologorum Poloniae* **89**, 307–316.

Padian, K. 2004. Basal Avialae. In: D. B. Weishampel, P. Dodson & H. Osmólska (eds) *The Dinosauria, 2nd edn*. 210–231. Berkeley: University of California Press.

Parker, W. G. 2008. Description of new material of the aetosaur *Desmatosuchus spuriensis*. *PaleoBios* **28**, 1–40.

Parker, W. G., Irmis, R. B., Nesbitt, S. J., Martz, J. W., & Browne, L. S. 2005. The Late Triassic pseudosuchian *Revueltosaurus callenderi* and its implications for the diversity of early ornithischian dinosaurs. *Proceedings of the Royal Society of London Series B* **272**, 963–969.

Parrish, J. M. 1993. Phylogeny of the Crocodylotarsi, with reference to archosaurian and crurotarsan monophyly. *Journal of Vertebrate Paleontology* **13**, 287–308.

Peecook, B. R., Sidor, C. A., Nesbitt, S. J., Smith, R. M., Steyer, J. S. & Angielczyk, K. D. 2013. A new silesaurid from the Upper Ntawere Formation of Zambia (Middle Triassic) demonstrates the rapid diversification of Silesauridae (Avemetatarsalia, Dinosauriformes). *Journal of Vertebrate Paleontol*ogy **33**, 1127–1137.

Perle, A. 1985. Comparative myology of the pelvic-femoral region in the bipedal dinosaurs. *Paleontological Journal* **19**, 105–109.

Persons, W. S. & Currie, P. J. 2017. The functional origin of dinosaur bipedalism: Cumulative evidence from bipedally inclined reptiles and disinclined mammals. *Journal of Theoretical Biology* **420**, 1–7.

Petermann, H., Koch, N. M. & Gauthier, J. A. 2017. Osteohistology and sequence of suture fusion reveal complex environmentally influenced growth in the teiid lizard *Aspidoscelis tigris* implications for fossil squamates. *Palaeogeography Palaeoclimatology Palaeoecology* **475**, 12–22.

Piechowski, R. & Dzik, J. 2010. The axial skeleton of *Silesaurus opolensis*. *Journal of Vertebrate Paleontology* **30**, 1127–1141.

Piechowski, R., Tałanda, M. & Dzik, J. 2014. Skeletal variation and ontogeny of the Late Triassic dinosauriform *Silesaurus opolensis*. *Journal of Vertebrate Paleontology* **34**, 1383–1393.

Piechowski, R., Niedźwiedzki, G. & Tałanda, M. 2015. New data on skull anatomy of *Silesaurus opolensis*. *13th Annual Meeting of the European Association of Vertebrate Palaeontologists, Opole, Poland; Jul 8–12. Abstracts*, p. 143.

Piechowski, R., Tałanda, M, and G. Niedźwiedzki. 2018. Unexpected bird-like features and high intraspecific variation in the braincase of the Triassic relative to dinosaurs. *Historical Biology* https://doi.org/10.1080/08912963.2017.1418339

Piechowski, R. & Tałanda. M. 2020. The locomotor musculature and posture of the early dinosauriform *Silesaurus opolensis* provides a new look into the evolution of Dinosauromorpha. *Journal of Anatomy* DOI: 10.1111/joa.13155

Porchetti, S. D., Nicosia, U., Mietto, P. Petti, F. M. & Avanzini, M. 2008. Atreipus-like footprints and their co-occurrence with Evazoum from the upper Carnian (Tuvalian) of Trentino-Alto Adige. *Studi Trentini di Scienze Naturali: Acta Geologica* **83**, 277–287.

Pounds, A. J., Jackson, J. K., & Shively, S. H. 1983. Allometric growth of the hind limbs of some terrestrial iguanid lizards. *American Midland Naturalist* **110**, 201–206.

Prieto-Márquez, A. & Norell, M. A. 2011. Redescription of a nearly complete skull of *Plateosaurus* (Dinosauria: Sauropodomorpha) from the Late Triassic of Trossingen (Germany). *American Museum Novitates* **3727**, 1–58.

Raath, M. A. 1969. A new coelurosaurian dinosaur from the Forest Sandstone of Rhodesia. *Arnoldia* **4**, 1–25.

Raath, M. 1990. Morphological variation in small theropods and its meaning in systematics: evidence from *Syntarsus rhodesiensis*. In: K. Carpenter & P. J. Currie (eds) *Dinosaur Systematics* 91–105. Cambridge: Cambridge University Press.

Rauhut, O. W. M. 2003. The interrelationships and evolution of basal theropod dinosaurs. *Special Papers in Palaeontology* **69**, 1–215.

Remes, K. 2008. *Evolution of the Pectoral Girdle and Forelimb in Sauropodomorpha (Dinosauria, Saurischia): Osteology, Myology, and Function*. PhD Dissertation, Ludwig-Maximilians-Universität, Munich.

Ribbing, L. 1907. Die distale Armmuskulatur der Amphibien, Reptilien und Säugetiere. *Zoologische Jahrbucher. Abteilung für Anatomie und Ontogenie der Tiere* **23**, 587–682.

Rinehart, L. F., Lucas, S. G., Heckert, A. B., Spielmann, J. A. & Celesky, M. D. 2009. The paleobiology of *Coelophysis bauri* (Cope) from the Upper Triassic (Apachean) Whitaker

quarry, New Mexico, with detailed analysis of a single quarry block. *New Mexico Museum of Natural History and Science Bulletin* **45**, 1–260.

Rogers, R. R., Swisher, C. III, Sereno, P. C., Monetta, A. M., Forster, C. A., & Martínez, R. N. 1993. The Ischigualasto tetrapod assemblage (Late Triassic, Argentina) and $^{40}Ar/^{39}Ar$ dating of dinosaur origins. *Science* **260**, 794-797.

Romer, A. S. 1922. The locomotor apparatus of certain primitive and mammal-like reptiles. *Bulletin of the American Museum of Natural History* **46**, 517–606.

Romer, A. S. 1923. Crocodilian pelvic muscles and their avian and reptilian homologues. *Bulletin of the American Museum of Natural History* **48**, 533–552.

Romer, A. S. 1923. The ilium in dinosaurs and birds. *Bulletin of the American Museum of Natural History* **48**, 141–145.

Romer, A. S. 1927 The pelvic musculature of the ornithischian dinosaurs. *Acta Zoologica* **8**, 225–275.

Romer, A. S. 1944. The development of tetrapod limb musculature—the shoulder region of *Lacerta*. *Journal of Morphology* **74**, 1–41.

Romer, A. S. 1956. The osteology of the reptiles. Chicago: The Uniwersity of Chicago Press.

Rowe, T. 1986. Homology and evolution of the deep dorsal thigh musculature in birds and other Reptilia. *Journal of Morphology* **189**, 327–346.

Rowe, T. 1989. A new species of the theropod dinosaur *Syntarsus* from the Early Jurassic Kayenta Formation of Arizona. *Journal of Vertebrate Paleontology* **9**, 125–136.

Russell, A. P. & Bauer, A. M. 2008. The appendicular locomotor apparatus of *Sphenodon* and normal-limbed squamates. In: C. Gans, A. S. Gaunt & K. Adler (eds) *Biology of the Reptilia 24, Morphology 1*. 1–466, Ithaca, NY: Society for the Study of Amphibians and Reptiles.

Safran, J. & Rainforth, E. C. 2004. Distinguishing the tridactyl dinosaurian ichnogenera *Atreipus* and *Grallator*: where are the latest Triassic Ornithischia in the Newark Supergroup. *Geological Society of America Abstracts and Programs* **36**, 2, p. 96.

Sampson, S. D. & Witmer, L. M. 2007. Craniofacial anatomy of *Majungasaurus crenatissimus* (Theropoda: Abelisauridae) from the Late Cretaceous of Madagascar. *Journal of Vertebrate Paleontology* **8**, 32–102.

Santa-Luca, A. P., Crompton, A. W. & Charig, A. J. 1976. A complete skeleton of the Late Triassic ornithischian *Heterodontosaurus tucki*. *Nature* **264**, 324–328.

Santa-Luca, A. P. 1980. The postcranial skeleton of *Heterodontosaurus tucki* (Reptilia, Ornithischia) from the Stromberg of South Africa. *Annals of the South African Museum* **79**, 159–211.

Sasayama, Y. 1999. Hormonal control of Ca homeostasis in lower vertebrates: Considering the evolution. *Zoological Science* **16**, 857–869.

Schachner, E. R., Manning, P. L. & Dodson, P. 2011. Pelvic and hindlimb myology of the basal archosaur *Poposaurus gracilis* (Archosauria: Poposauroidea). *Journal of Morphology* **272**, 1464–1491.

Schmidt, M. & Fischer, M. S. 2009. Morphological integration in mammalian limb proportions: Dissociation between function and development. *Evolution* **63**, 749–766.

Schwabl, H. & Lipar, J. 2007. Hormonal regulation of begging behaviour. In: J. Wright & M. L. Leonard (eds) *The Evolution of Begging* 221–244. Amsterdam: Springer.

Schwarz, D., Frey, E. & Meyer, C. A. 2007. Pneumaticity and soft-tissue reconstructions in the neck of diplodocid and dicraeosaurid sauropods. *Acta Palaeontologica Polonica* **52**, 167–188.

Sellers, W. L. & Manning, P. L. 2007. Estimating dinosaur maximum running speeds using evolutionary robotics. *Proceedings of the Royal Society of London, Series B* **274**, 2711–2716.

Sereno, P. C. 1991. *Lesothosaurus*, "fabrosaurids", and the early evolution of Ornithischia. *Journal of Vertebrate Paleontology* **11**, 168–197.

Sereno, P. C. & Novas, F. E. 1994. The skull and neck of the basal theropod *Herrerasaurus ischiqualastensis*. *Journal of Vertebrate Paleontology* **13**, 451–476.

Sereno, P. C., Forster, C. A., Rogers, R. R., & Monetta, A. M. 1993. Primitive dinosaur skeleton from Argentina and the early evolution of Dinosauria. *Nature* **361**, 64–66.

Sereno, P. C. & Arcucci, A. B. 1994. Dinosaurian precursors from the Middle Triassic of Argentina: *Marasuchus lilloensis*, n. gen. *Journal of Vertebrate Paleontology* **14**, 53–73.

Sereno, P. C., Martinez, R. N. & Alcober, A. O. 2012. Osteology of *Eoraptor lunensis* (Dinosauria: Sauropodomorpha). *Journal of Vertebrate Paleontology* **32** (supplement 1), 81–177.

Shah, R. V. & Patel, V. B. 1964. Myology of the chelonian pectoral appendage. *Journal of Animal Morphology and Physiology* **11**, 58–84.

Skawiński, T., Ziegler, M., Czepiński, Ł., Szermański, M., Tałanda, M., Surmik, D. & Niedźwiedzki, G. 2017. A re-evaluation of the historical 'dinosaur' remains from the Middle-Upper Triassic of Poland. *Historical Biology* **29**, 442–472.

Smith, D. K. 2015. Craniocervical myology and functional morphology of the small-headed Therizinosaurian Theropods *Falcarius utahensis* and *Nothronychus mckinleyi*. *PLoS ONE* **10**, e0117281.

Smith, N. D., Makovicky, P. J., Hammer, E. R. & Currie, P. J. 2007. Osteology of *Cryolophosaurus ellioti* (Dinosauria: Theropoda) from the Early Jurassic of Antarctica and implications for early theropod evolution. *Zoological Journal of the Linnean Society* **151**, 377–421.

Snively, E. & Russell, A. P. 2007. Functional variation of neck muscles and their relation to feeding style in Tyrannosauridae and other large theropod dinosaurs. *Anatomical Record* **290**, 934–957.

Snively, E. & Russell, A. P. 2007. Functional morphology of neck musculature in the Tyrannosauridae (Dinosauria, Theropoda) as determined via a hierarchical inferential approach. *Zoological Journal of the Linnean Society* **151**, 759–808.

Snyder, R. C. 1954.The anatomy and function of the pelvic girdle and hindlimb in lizard locomotion. *American Journal of Anatomy* **95**, 1–14.

Sobral, G., Sookias, R. B., Bhullar, B-AS., Smith, R., Butler, R. J. & Müller, J. 2016. New information on the braincase and inner ear of *Euparkeria capensis* Broom: implications for diapsid and archosaur evolution. *Royal Society Open Science* **3**, 160072.

Straus, W. L. 1942. The homologies of the forearm flexors: urodeles, lizards, mammals. *American Journal of Anatomy* **70**, 281–316.

Sulej, T. 2007. A new rauisuchian reptile (Diapsida: Archosauria) from the Late Triassic of Poland. *Journal of Vertebrate Paleontology* **25**, 78–86.

Sulej, T., Bronowicz, R., Tałanda, M. & Niedźwiedzki, G. 2011. A new dicynodont-archosaur assemblage from the Late Triassic (Carnian) of Poland. *Earth and Enviromental Science of the Royal Society of Edinburgh* **101**, 261–269.

Sullivan, G. E. 1962. Anatomy and embryology of the wing musculature of the domestic flow (*Gallus). Australian Journal of Zoology* **10**, 458–518.

Sullivan, C. 2015. Evolution of hind limb posture in Triassic archosauriforms. In: K. P. Dial, N. Shubin & E. L. Brainerd (eds) *Great Transformations in Vertebrate Evolution* 107–124. Chicago: University of Chicago Press.

Suzuki, D., Murakami, G. & Minoura, N. 2003. Crocodilian bone-tendon and bone-ligament interfaces. *Annals of Anatomy* **185**, 425–433.

Szulc, J., Racki, G. & Jewuła, K. 2015. Key aspects of the biostratigraphy of the Upper Silesian middle Keuper, southern Poland. *Annales Societatis Geologorum Poloniae* **85**, 557–686.

Tarsitano, S. F. 1981. *Pelvic and Hindlimb Musculature of Archosaurian Reptiles*. PhD Dissertation. City University, New York.

Tsai, H. P. & Holliday, C. M. 2015. Articular soft tissue anatomy of the archosaur hip joint: structural homology and functional implications. *Journal of Morphology* **276**, 601–630.

Tsai, H. P., Middleton, K. M., Hutchinson, J. R. & Holliday, C. M. 2018. Hip joint articular soft tissues of non-dinosaurian Dinosauromorpha and early Dinosauria: evolutionary and biomechanical implications for Saurischia. *Journal of Vertebrate Paleontology* **38**, e1427593.

Tsuihiji, T. 2005. Homologies of transversospinalis muscles in the anterior presacral region of Saurian (crown Diapsida). *Journal of Morphology* **263**, 151–178.

Tsuihiji, T. 2007. Homologies of longissimus, iliocostalis, and hypaxial muscles in the anterior presacral region of extant Diapsida. *Journal of Morphology* **268**, 986–1020.

Tsuihiji, T. 2010. Reconstructions of the axial muscle insertions in the occipital region of dinosaurs: evaluations of past hypotheses on Marginocephalia and Tyrannosauridae using the extant phylogenetic bracket approach. *Anatomical Record* **293**, 1360–1386.

Tsuihiji, K., Witmer, L. M., Watabe, M., Barsbold, R., Tsogtbaatar, K., Suzuki, S. & Khatanbaatar, P. 2017. New information on the cranial morphology of *Avimimus* (Theropoda: Oviraptorosauria). *Journal of Vertebrate Paleontology* **37**, e1347177.

Tykoski, R. S. 1998. *The Osteology of* Syntarsus kayentakatae *and its Implications for Ceratosaurid Phylogeny*. MSc thesis. University of Texas at Austin.

Vanden Berge, J. C. & Zweers, G. A. 1993. Myologia. In: J. J. Baumel, A. S. King, J. C. Breazile, H. E. Evans & J. C. Vanden Berge (eds) *Handbook of Avian Anatomy: Nomina Anatomica Avium* 189–247. Cambridge MA: Nuttall Ornithological Club.

Vazques, R. J. 1994. The automating skeletal and muscular mechanism of the avian wing (Aves). *Zoomorphology* **114**, 59–71.

Walker, A. D. 1961. Triassic reptiles from the Elgin area: *Stagonolepis*, *Dasygnathus* and their allies. *Philosophical Transactions of the Royal Society of London B* **244**, 103–204.

Walker, A. D. 1977. Evolution of the pelvis in birds and dinosaurs. In: S. M. Andrew, R. S. Miles & A. D. Walker (eds) *Problems in Vertebrate Evolution* 319–358. Linnean Society Symposium Series.

Walker, J. W. F. 1973. The locomotor apparatus of testudines. In: C. Gans & T. S. Parsons (eds). *Biology of the Reptilia 4* 1–100. New York: Academic Press.

Walker, A. D. 1990. A revision of *Sphenosuchus acutus* Haughton, crocodylomorph reptile from the Elliot Formation (Late Triassic or Early Jurassic) of South Africa. *Philosophical Transactions of the Royal Society London B* **330**, 1–120.

Welman J. 1995. *Euparkeria* and the origin of birds. *South African Journal of Science* **91**, 533–537.

Welles, S. P. 1984. *Dilophosaurus wetherilli* (Dinosauria, Theropoda), osteology and comparisons. *Palaeontographica A* **185**, 85–180.

Wedel, M. 2007. What pneumaticity tells us about 'popsauropods', and vice versa. *Special Papers in Paleontology* **77**, 207–222.

Wedel, M. 2009. Evidence for bird-like air-sacs in saurischian dinosaur. *Journal of Experimental Zoology Part A: Ecological Genetics and Physiology* **311.8**, 611–628.

Weinbaum, J. C. & Hungerbühler, A. 2007. A revision of *Poposaurus gracilis* (Archosauria, Suchia) based on two new specimens from the Late Triassic of the southwestern U.S.A. *Paläontologische Zeitschrift* **81**, 131–145.

Wilson, J. A. 1999. A nomenclature for vertebral laminae in sauropods and other saurischian dinosaurs. *Journal of Vertebrate Paleontology* **19**, 639–653.

Wilson, J. A. 2005. Integrating ichnofossil and body fossil records to estimate locomotor posture and spatiotemporal distribution of early sauropod dinosaurs: a stratocladistic approach. *Paleobiology* **31**, 511–518.

Witmer, L. M. 1995. The extant phylogenetic bracket and the importance of reconstructing soft tissues in fossils. In: J. J. Thomason (ed.) *Functional Morphology in Vertebrate Paleontology* 19–33. Cambridge: Cambridge University Press.

Witmer, L. M. 1997. Craniofacial air sinus systems. In: P. J. Currie & K. Padian (eds) *Encyclopedia of Dinosaurs* 151–159. New York: Academic Press.

Witmer, L. M. & Ridgely, R. C. 2009. New insights into the brain, braincase, and ear region of tyrannosaurs, with implications for sensory organization and behavior. *Anatomical Record* **292**, 1266–1296.

von Huene, F. 1926. Vollstandige Osteologie eines Plateosauriden aus dem schwabischen Keuper. *Geologische und Paläontologische Abhandlungen, Neue Folge* **15(2)**, 139–179.

Xing, L. 2012. Sinosaurus *from southwestern China*. MSc thesis, University of Alberta, Edmonton.

Yates, A. M. 2003. A new species of the primitive dinosaur *Thecodontosaurus* (Saurischia: Sauropodomorpha) and its implications for the systematics of early dinosaurs. *Journal of Systematic Palaeontology* **1**, 1–42.

Zatoń, M. & Piechota, A. 2003. Carnian (Late Triassic) charophyte flora of the *Paleorhinus* biochron at Krasiejów (SW Poland). *Freiberger Forschungshefte C 499: Paläontologie, Stratigraphie, Fazies* **11**, 43–51.

Zatoń, M., Piechota, A. & Sienkiewicz, E. 2005. Late Triassic charophytes around the bone-bearing bed at Krasiejów (SW Poland) – palaeoecological and environmental remarks. *Acta Geologica Polonica* **55**, 283–293.

Zhang, Y. 1988. The Middle Jurassic dinosaur fauna from Dashanpu, Zigong, Sichuan. *Journal of the Chengdu College of Geology* **3**, 1–87.

Zhou, C.-F., Gao, K.-Q. & Fox, R. C. 2010. Morphology and histology of lattice-like ossified epaxial tendons in *Psittacosaurus* (Dinosauria: Ceratopsia). *Acta Geologica Sinica (English edition)* **84**, 463–471.